Development of inhibitors of alternative splicing events crucial to HIV-1 replication: A new anti-HIV/AIDS strategy targeting the host cell machinery

by

Laura Elizabeth Bandy

B.Sc., Ball State University, 2008

A THESIS SUBMITTED IN PARTIAL FULFILLMENT OF THE REQUIREMENTS FOR THE DEGREE OF

MASTER OF SCIENCE

in

THE FACULTY OF GRADUATE STUDIES

(Pharmaceutical Sciences)

THE UNIVERSITY OF BRITISH COLUMBIA

(Vancouver)

April 2012

Abstract

Introduction: HIV infects over 35 million people worldwide. Since the introduction of HAART the survival rate for HIV/AIDS patients has increased exponentially. HAART, although effective, does have long term limitations resulting from cross resistance to certain drugs of the same class, compliance, and side effects; therefore, investigating alternative avenues and targets for therapeutic treatment is vital. Through compound library screening, IDC16, a tetracyclic indole compound, has been identified as an inhibitor of SR protein splicing factor 1 (SRSF1). This protein plays a redundant role in human splicing but is specifically used in HIV-1 infected cell alternative splicing. Blocking HIV-1 alternative splicing through inhibition of SRSF1 function may establish a novel strategy for HIV/AIDS therapy and is advantageous because it *(i) targets a protein that is essential to HIV replication, (ii) targets a human protein potentially eliminating the chances of mutation and subsequent resistance to drug therapy*. Although IDC16 displays cytotoxicity, the design of mimics of IDC16 could allow for the discovery of an equally or more potent compound which eliminates the cytotoxic effects.

Hypothesis: The synthesis of appropriately functionalized and conformationally mobile ring opened mimics of IDC16 will lead to the identification of new HIV replication inhibitors that: target SRSF1; are not cytotoxic; do not intercalate DNA; and retain similar or superior anti-HIV activity when compared to IDC16.

Objectives: The synthesis and evaluation of the anti-HIV activity of a library of IDC16 mimics corresponding to different structural types from a common 2-pyridinone scaffold: 1) bisheterocyclic amides, 2) bisheterocyclic oxadiazoles, 3) fused bisheterocyclic isoxazolidin-7-ones, 4) fused bisheterocyclic 5-arylpyrazolidin-7-ones and 5) C-4 (hetero)aryl substituted 2-pyridinones.

Results: Our effort to synthesize inhibitors of HIV-1 by creating a library of IDC16 mimics led to the discovery of DGPS39/LB-45. This compound was 90% as effective as the HAART drug AZT in blocking HIV-1 replication.

Significance: Creating a non-cytotoxic IDC16 mimic with the same or greater affinity for the target protein SRSF1 will allow for further investigation into a novel treatment of HIV/AIDS; which has the potential to circumvent the problems with viral resistance experienced with HAART.

Table of Contents

List of Tables

List of Figures

List of Schemes

List of Abbreviations

3'ss	3' Splice site
5'ss	5' Splice site
7-AAD	7-Aminoactinomycin D
AIDS	Acquired immunodeficiency syndrome
A	Adenosine
ATP	Adenosine triphosphate
Annexin V-PE	Annexin V conjugated to phycoerythrin
R	Arginine
Ar	Aryl
AZT	Azidothymidine
bp	Base pairs
BOP-Cl	Bis(2-oxo-3-oxazolidinyl)phosphonic chloride
BBP	Branch point binding protein
BPS	Branch point sequence
Br	Bromine
BuLi	Butyllithium
CaMK11δ	Ca^{2+}/calmodulin-dependent kinase
Clk/Sty	Cdc 2-like kinase/serine threonine tyrosine
Cs_2CO_3	Cesium carbonate
CsF	Cesium fluoride
Cl	Chlorine
cDNA	Complimentary deoxyribonucleic acid
Cu	Copper
CuI	Copper iodide
DENV	Dengue virus
DNA	Deoxyribonucleic acid
DHA	Di(hetero)aryl amide
DCM	Dichloromethane
DIPEA	Diisopropylethylamine
DMF	Dimethylformamide
DMSO	Dimethylsulfoxide
ESE	Exonic splicing enhancer
ESS	Exonic splicing silencer
IGHD II	Familial isolated growth hormone deficiency type II
G	Guanine
hnRNP	Heterogeneous ribonuclear proteins
HMDS	Hexamethyldisilane
HAART	Highly active anti-retroviral therapy
HIV	Human immunodeficiency virus
HPV	Human papilloma virus
HCl	Hydrochloric acid
NH_2OH-HCl	Hydroxylamine hydrochloride
pp-SRSF1	Hyper-phosphorylated SRSF1
p-SRSF1	Hypo-phosphorylated SRSF1

IDC16	Indole compound 16
IGC	Interchromatin granule clusters
ISS	Intronic splicing silencer
kDa	Kilodalton
LDA	Lithium diisopropylamide
LiOH	Lithium hydroxide
mTOR	Mammalian target of rapamycin
MNK2	MAP kinase-interacting serine/threonine-protein kinase 2
mRNA	Messenger ribonucleic acid
MeOH	Methanol
MLV	Murine leukemia virus
DM	Myotonic dystrophy
nm	Nanometre
N_2	Nitrogen gas
NNRTI	Non-nucleoside analogue reverse transcriptase inhibitor
NMD	Nonsense-mediated decay
NES	Nuclear export signal
NMR	Nuclear magnetic resonance
NRTI	Nucleoside analogue reverse transcriptase inhibitor
nt	Nucleotide
Pd	Palladium
Log p	Partition coefficient
ppm	Parts per million
PBMC	Peripheral blood mononuclear cells
PIFA	Phenyliodine(III)bis-(trifluoroacetate)
PS	Phosphatidylserine
$POCl_3$	Phosphorous oxychloride
PPT	Polypyrimidine tract
$KHCO_3$	Potassium bicarbonate
K_2CO_3	Potassium carbonate
KCN	Potassium cyanide
K^tOBu	Potassium tert-butoxide
PTC	Premature termination codons
R_f	Retention factor
RRE	Rev response element
RT	Reverse transcriptase
RNP	Ribonucleoprotein
RBD	RNA binding domain
RRM	RNA recognition motif
RRMH	RRM homolog
S	Serine
SRSF1	Serine and arginine protein splicing factor 1
snRNP	Small nuclear ribonucleoprotein
NaN_3	Sodium azide
$NHCO_3$	Sodium bicarbonate

NaH	Sodium hydride
NaOH	Sodium hydroxide
SMA	Spinal muscular atrophy
SRPK1/2	SR protein kinase 1/2
SAR	Structure activity relationship
SMN1	Survival motor neuron
SELEX	Systematic evolution of ligands by exponential enrichment
THF	Tetrahydrofuran
TLC	Thin layer chromatography
$SOCl_2$	Thionyl chloride
TAP/NFX1	Tip-associated protein/nuclear transcription factor X I
Topo	Topoisomerase
TAR	Transactivation response element
Et_3N	Triethylamine
$Et_3NH^+Cl^-$	Triethylammonium chloride
TFA	Trifluoroacetic acid
TMSCl	Trimethylsilylchloride
TMSOTf	Trimethylsilyltriflate

Acknowledgements

I would like to thank my supervisor, Dr. Grierson, for his guidance and patience. Most of all I would like to thank him for giving me the opportunity to work on such a fascinating and innovative project, I have truly enjoyed my experience. I would also like to thank the members of the Grierson lab, both past and present. I am grateful for your support, guidance and assistance; especially Maryam, who has not only been a colleague, but a wonderful friend. I would like to thank the members of my committee, including my chair Dr. Rigs, for their guidance and support especially through my unique circumstances. I would also like to thank the Faculty of Pharmaceutical Sciences for everything they do for their grad students. I am thankful for the opportunities I have been given to contribute to the graduate student community. It is important to also give recognition to Dr. Markus Heller from the CDRD for running all my NMR samples and Andras Szeitz for his assistance with mass spectroscopy. Finally, and most importantly, I would like to thank my family and James for their continual support; it never goes unnoticed.

To my parents

1. Introduction

"Medicinal chemistry covers all aspects of the conception, design and synthesis of biologically active compounds with the objective of developing such molecules as therapeutic agents for the treatment of disease, physical injury and other conditions that impair normal human activity. In practice, medicinal chemistry relates the structure of a molecule to its potential to be a drug. This is a highly interdisciplinary [science] that combines expertise in synthetic and physical chemistry with biochemistry, pharmacology-toxicology, structural and molecular biology, computational sciences, formulation and delivery technologies, and pharmacognosy. It is not surprising, therefore, that medicinal chemistry plays a major role in essentially all phases of drug discovery leading up to the identification of clinical candidate drugs."[1] In the context of drug discovery, medicinal chemistry can be looked upon as a companion discipline to pharmacology-toxicology.

In our modern era, structure-based drug design is made possible by increasingly ready access to structural data for pharmacologically important proteins. Knowing the structure of a protein gives the design and synthesis of molecules to target the protein more direction. This is important because amino acid residues within the binding site can be identified and molecules can be designed to target and interact with them. However, there are still many drug targets for which specific structural data is not available. Homology modeling is one solution that has been developed to overcome this problem. It involves developing a three-dimensional model of an unknown protein from its amino acid sequence based on the known structures of homologous proteins.[2] The G protein-coupled receptor rhodopsin model is an example where homology modeling has been used successfully. However, there are many complex proteins and protein systems for which no structural data or related structural data is available; the spliceosome is a pertinent example.

The spliceosome is a large, dynamic, multi-component complex that effects intron removal from a transcribed pre-mRNA (messenger ribonucleic acid) and re-connects the exons to produce a mature mRNA which serves as the precursor for the translation of a protein. Splicing allows for one gene to produce more than one protein since the pre-mRNA transcript can be alternatively spliced. In alternative splicing, exons are arranged in different combinations to produce different mature mRNAs which each produce a distinct protein. Alternative splicing

has evolved as an economic and rapid mechanism to generate the diversity of proteins found in the cell from a minimal set of genes. In humans, about 95% of pre-mRNAs undergo alternative splicing.[3]

Alternative splicing has significant implications in physiology with respect to proper cell development and function and in pathophysiology, as aberrant splicing can lead to disease. Additionally, various viruses, upon infection, use the human splicing machinery to replicate. Therefore, there is a need to find molecules and biologics that inhibit or control events orchestrated by the spliceosome.

The global mechanism of splicing and alternative splicing is known, however there is no specific structural data for the individual components of the spliceosome or the interaction between these components. Thus, developing small molecule based drugs targeting the spliceosome is challenging. As there is limited molecular and structural data on the spliceosome, the only solution for identifying alternative splicing inhibitors is through the use of compound library screening. This is essentially a "blind" process that has been successfully used in the discovery of many active molecules.

In the context of the work presented in this thesis, the compound library screening approach was used (collaboration between David Grierson while at the Curie Institute in Paris, and the RNA biology group led by Pr. Jamal Tazi in Montpellier, France) to identify small molecules with the ability to inhibit alternative splicing events. Specifically, the collaboration was seeking to identify molecules that inhibit the activity of a particular serine arginine rich (SR) protein, SRSF1 (previously known as ASF/SF2). Of all the indoles screened, one molecule was identified as being the most active, IDC16 (indole compound 16). It was shown that IDC16 interferes with binding to the unorganized, highly polar RS (arginine serine rich) domain of SRSF1 and not to the ribonucleotide binding domain (RBD). Considering the RS domain of SRSF1 is important for interactions with components of the spliceosome, it was suggested that the IDC16 works through the disruption of protein-protein interactions. This molecule has the potential to be a valuable tool to study the spliceosome.

SR proteins play a redundant role in human cellular splicing and alternative splicing but have a specific role in HIV-1 protein synthesis in infected cells. IDC16 was found to be essentially equipotent to the nucleoside analogue reverse transcriptase inhibitor (NRTI) azidothymidine (AZT). It was further demonstrated that IDC16 stops HIV-1 replication in blood

isolates from HIV-1 patients no longer responding to highly active anti-retroviral therapy (HAART). Additionally, the compound was not toxic at the concentrations used in the studies.

As IDC16 is a flat molecule, it can intercalate DNA, which means it is mildly cytotoxic and not an ideal drug candidate. Knowing the limitations of IDC16, our strategy is to synthesize compounds which are ring opened conformationally flexible mimics of IDC16. It is intended that such molecules will retain the interactions that IDC16 has with the SR protein target which are crucial for inhibition, but that the cytotoxicity properties associated with its planar structure will be eliminated. The development of IDC16 mimics based on the use of the 2-pyridinone scaffold as the starting point in library synthesis is the subject of my thesis. The following sections will describe splicing, HIV biology, the objectives of my work and the discovery of DGPS39/LB-45, a pyridinone derivative that, in cell based assays, is 90% as active as AZT in blocking HIV-1 replication.

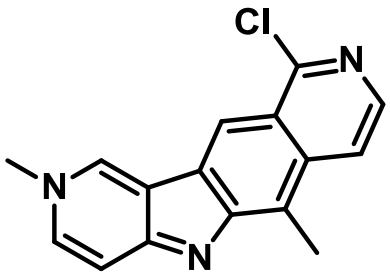

Figure 1: IDC16. The molecule found through compound library screening to have anti-HIV-1 activity.

1.1 HIV/AIDS: The Human Immunodeficiency Virus (HIV) affects approximately 33 million people worldwide, with two thirds of those infected living in Sub-Saharan Africa. HIV is the causative agent of the Acquired Immunodeficiency Syndrome (AIDS), a condition where selective invasion of helper T cells ($CD4^+$T cells) by the virus leads to progressive destruction of the immune system, leaving the victim vulnerable to life threatening opportunistic infections. About 1.8 million people die per year due to AIDS, and until the mid-1990s, the life expectancy for patients with AIDS was one to two years.[4] However, with access to Highly Active Anti-Retroviral Therapy (HAART), otherwise known as drug combination therapy, the situation has dramatically changed. By simultaneously taking several drugs that target the viral entry and/or the viral enzymes reverse transcriptase (RT), integrase and protease, viral loads are reduced to

undetectable levels. In this context, in developed countries HIV is treated as a chronic infection, rather than a life threatening illness.

In common with other viruses, HIV cannot ensure its own replication. Therefore, upon entry into the host cell it must take control of the cell machinery in order to replicate. Schematically, (**figure 2**) the virus first binds to the host cell through interactions with the CCR5 and CXCR4 receptors and this is followed by virus-cell fusion. The viral capsid is released into the cytoplasm of the host cell where it is uncoated, releasing the viral enzymes and viral RNA. The single stranded viral RNA is then converted to a double stranded complimentary viral DNA (cDNA) by the viral enzyme RT. The cDNA is translocated to the nucleus where it is incorporated into the host DNA; this step is facilitated by the viral enzyme integrase. To produce new viral particles the integrated viral DNA must be first transcribed into mRNA in the nucleus and then translated into the viral protein Gag-Pol, in the cytoplasm. Gag-Pol is then cleaved by the viral enzyme protease into gag, gag-pol and env. Further processing by protease yields the remaining essential, structural HIV-1 proteins. The viral proteins then assemble at the cell membrane and bud off as a new immature virus.

The three key enzymes, RT, integrase and protease, in the HIV replication cycle are the major targets against which anti-HIV/AIDS drugs have been developed.[5] **Table 1** highlights where each drug targets the HIV life cycle. Currently, 29 RT and protease inhibitors and the integrase inhibitor Raltegravir[6] are being used in anti-HIV/AIDS therapy in HAART. They inhibit the viral enzymes from performing their vital roles in the HIV-1 replication cycle. There are also 2 entry inhibitors (Maraviroc[7] and Enfuvirtide[8]) used in HAART which interfere with the binding, fusion and entry of HIV into a cell.[9] It is important to note that the selection of drugs in a combination therapy as well as the dosing regimen for each drug is tailored to the individual patient because the combination of drugs must block replication of all HIV variants present. Treatment is also guided by an individual's viral load and CD4 counts. Unfortunately, long term use of HAART is limited by issues of drug compliance, toxic side effects and drug resistance.[10] This reality underscores the continuing need for new and accessible drugs, and in particular, those acting through new, and as of yet unexplored, mechanisms of action.

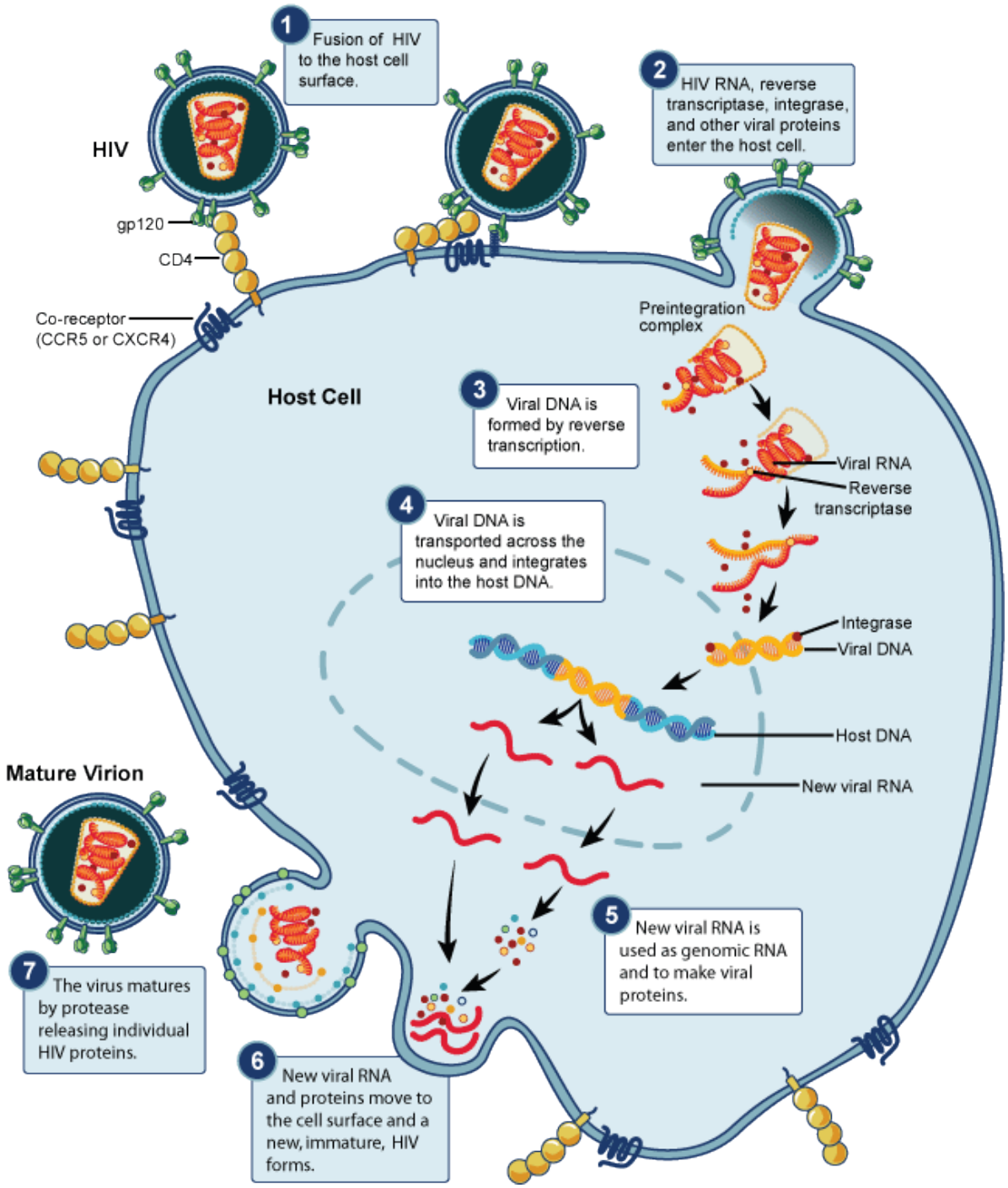

Figure 2: HIV-1 life cycle. 1. The virus binds and fuses to the host cell. 2. The contents of the viral capsid are released into the cytoplasm (HIV enzymes protease, integrase and reverse transcriptase, viral RNA and viral proteins. 3. The viral DNA is formed from viral RNA by viral reverse transcriptase. 4. The viral DNA moves into the nucleus and using viral integrase is inserted into the host cell's genome. 5. New viral proteins are produced though transcription of viral DNA and translation of mRNA. 6. The new viral particles assemble at the cell surface to form new, immature HIV. 7. The virus buds off from the host cell and in order to become a mature virus, through the action of protease. Courtesy: National Institute of Allergy and Infectious Diseases. Adapted from 'HIV Replication Cycle'.
http://www.niaid.nih.gov/topics/HIVAIDS/Understanding/Biology/pages/hivreplicationcycle.aspx **(accessed 11/22, 2011).**

Table 1: HIV drugs and their site of action.

Site of Inhibition	Current Drugs
Entry	Maraviroc, Enfuvirtide
Reverse Transcriptase (RT)	- Nucleoside reverse transcriptase inhibitor (NRTI) = Zidovudine, Didanosine, Zalcitabine, Stavudine, Abacavir, Emtricitabine, Entecavir, Apricitabine - Nucleotide reverse transcriptase inhibitor (NtRTI) = Tenofovir, Adefovir - Non-nucleoside reverse transcriptase inhibitor (NNRTI) = Efavirenz, Nevirapine, Delavirdine, Etravirine, Rilpivirine
Integrase	Raltegravir
Protease	Saquinavir, Ritonavir, Indinavir, Nelfinavir, Amprenavir

In addition to the HAART approach, there are other, less studied strategies to block HIV replication, including, inhibition of the regulatory (tat, rev) and accessory (nef) viral proteins; thereby preventing them from performing their vital roles in viral replication. Exploration of this avenue has resulted in the discovery of active molecules, several of which are depicted in **figure 3**.

Tat is a regulatory protein that stimulates transcriptional elongation by interacting with the transactivation response (TAR) RNA element; it is crucial for viral replication.[11] Durhamycin A is a natural product which has been shown to inhibit tat transactivation and tat-dependent *in vitro* transcription.[12,13] In the body, the half-life for HIV-infected T-cells is less than 48 hours, whereas in the lab, the HIV-1 infected cells survive for a much longer period. Prior to 2005, the assays used to identify tat inhibitors, measured the cumulative effect produced by the molecules over 4-5 days. For many of the compounds studied, inhibition of HIV replication was only observed after the third day, the consequence being that these compounds correspond to "false positives." For this reason, the large majority of the tat inhibitors identified in the early 2000's have not been developed further.[14,15]

The role of Nef in HIV-1 infection has not been fully characterized however it is known to be essential in the propagation and maintenance of viral loads.[16] A library of guanidine alkaloid analogs was screened because these types of molecules are known to play a role in the inhibition of HIV-1 cell fusion by disrupting protein-protein interactions. Three molecules were found to be potent inhibitors of nef activity (molecule A-C, shown in **figure 3**). These compounds inhibited vital Nef-ligand interactions with p53, actin and $p56^{lck}$ required for proper virus propagation.[17]

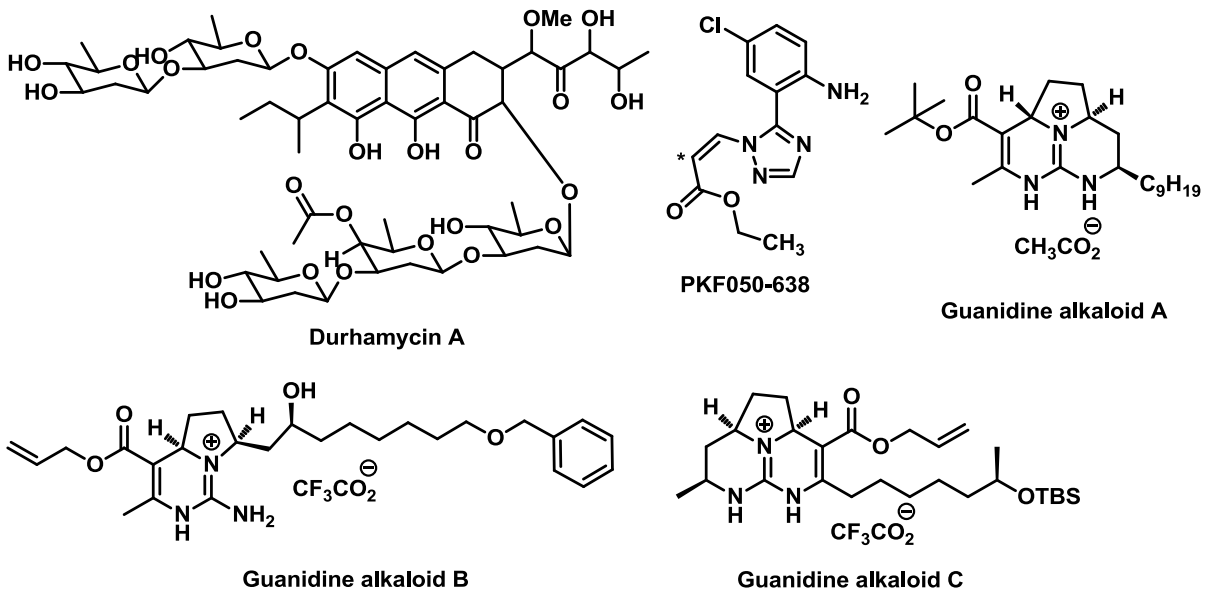

Figure 3: Tat, rev and nef inhibitors: Durhamycin A, PKF050-638, and Guanidine Alkaloid A-C, respectively.

Rev is instrumental in spliced and incompletely spliced mRNA export because of the presence of an arginine-rich binding motif known as the Rev Response element (RRE). mRNA export is mediated by the RRE and a leucine-rich nuclear export signal (NES) binding to an export receptor known at CRM1.[127] PKF050-638 inhibits CRM1-mediated Rev nuclear export by disrupting the CRM1-NES interaction through direct binding to Cys-539 on CRM1.[18] Note that for both nef and rev inhibitors cytotoxicity is a persistent issue, necessitating further research to develop safe drugs.

The identification of tat, nef and rev inhibitors is still an active area of antiviral research. However, as for the already established targets, drug resistance resulting from point mutations in these proteins is again an important issue. An alternative strategy, which we are exploring, is to target the synthesis of these regulatory HIV-1 proteins. In order to do this, we are targeting a human cellular entity, the spliceosome, and thus inhibiting the splicing and alternative splicing pathway required for the production of HIV-1 proteins. By targeting a human factor, instead of a viral factor, these types of drugs have the potential to avoid viral resistance.

1.2 Splicing and alternative splicing: To produce cellular proteins, genes are first transcribed in the nucleus of the cell to produce mRNA, and this mRNA is subsequently transported to the cytoplasm and used as a template to initiate protein synthesis. A newly

transcribed mRNA is known as an immature pre-mRNA, consisting of exons (coding regions) and introns (non-coding regions) (**figure 4a**). Production of a mature mRNA from this pre-mRNA requires that the introns be removed and the exons reconnected. Introns are hundreds or thousands of base pairs (bp) long, whereas, exons are short, usually 50-250 bp; therefore, greater than 90% of the pre-mRNA must be removed before the mature mRNA can be used in translation.[19]

Splicing is the process whereby the introns in a pre-mRNA are excised and the exons are rejoined. **Figure 4** illustrates how alternative splicing results in the exons being joined in different arrangements. After alternative splicing, each distinctly different mature mRNA will be translated into a unique protein;[19] thus, one gene can produce multiple proteins (**figure 4b**).[20]

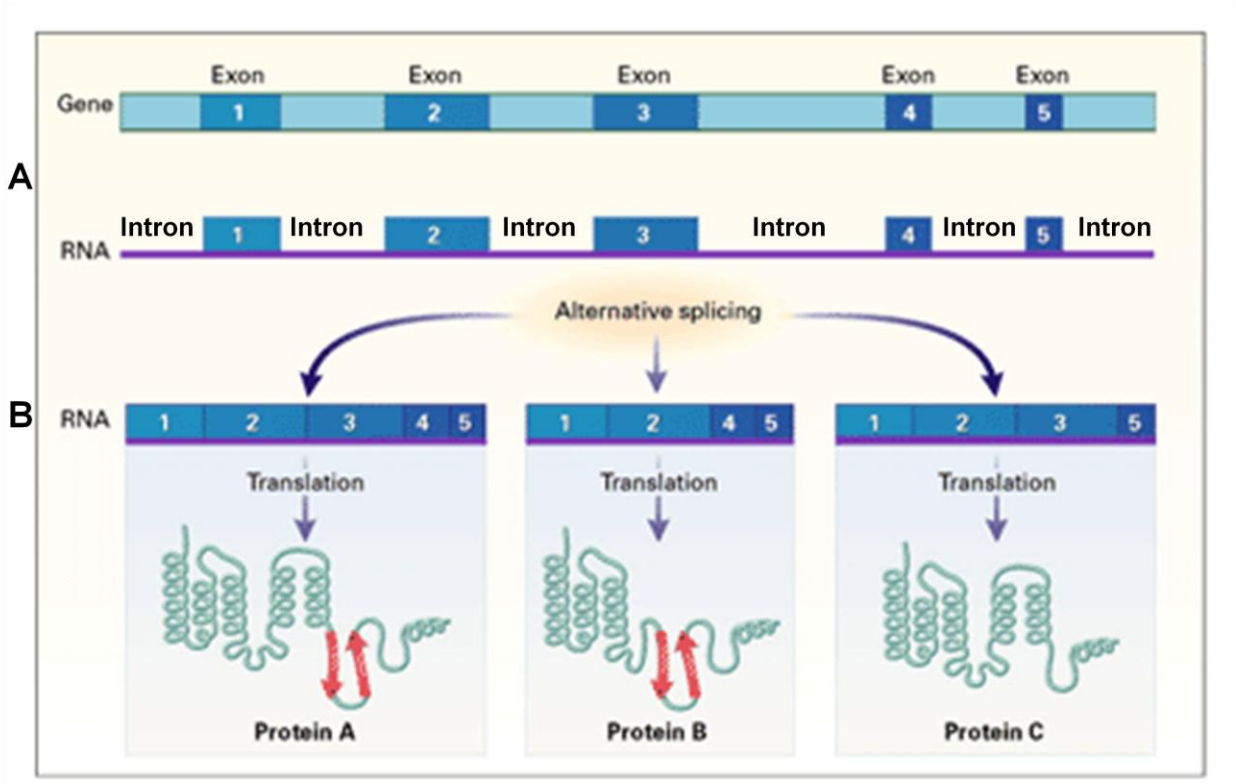

Figure 4. Alternative splicing. A. The structure of a pre-mRNA, made up of exons and introns. B. In alternative splicing exons are arranged in different ways to produce different proteins. Adapted with permission from "Genomic medicine - A primer", by Guttmacher, A. E., & Collins, F. S., 2002, New. Engl. J. Med. 347, p. 1516.

1.2.1 The spliceosome: Splicing and alternative splicing is carried out in the nucleus by the spliceosome. The spliceosome is a large, multicomponent machine consisting of specialized RNAs and more than 150 proteins that come together in different combinations at the different steps in the splicing process (complexes A-E). There are five specialized RNA structures, U1,

U2, U4, U5, and U6, known as small nuclear ribonucleoproteins (snRNP), these form the catalytic core of the spliceosome. Mechanistically, splicing is a complex process. In short, the spliceosome binds the pre-mRNA, forms a lariat structure composed of the intron and then cuts the lariat out of the pre-mRNA and rejoins the two exons on either side of it. [21]

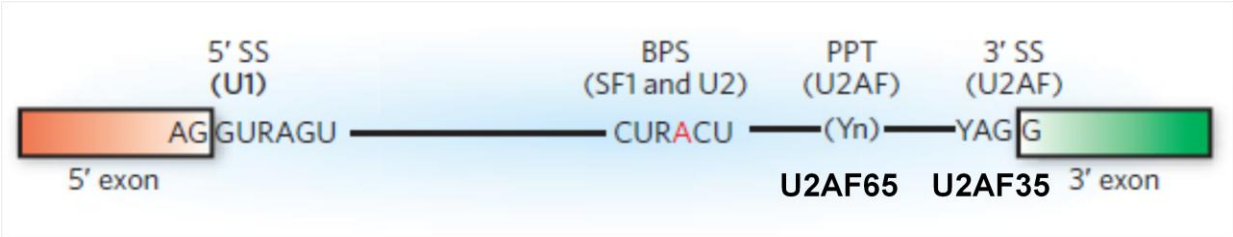

Figure 5: Initiation step of spliceosome assembly. Initiation requires the 5'ss, the branch point sequence (BPS), the polypyrimidine tract (PPT) and the 3'ss. A = adenine, G = guanine, U = uracil, C = cytosine, R = any purine, Y = any pyrimidine, n = any nucleobase. Reprinted by permission from Macmillan Publishers Ltd: Nat Chem Biol. Schneider-Poetsch, T., et al. 'Garbled messages and corrupted translations.' Vol 6, p. 191, copyright 2010.

Splicing starts with the initiation step which requires a 5' splice site (5'ss), a 3' splice site (3'ss) and a branch point sequence (BPS) (**figure 5**). The 5'ss and 3'ss are found at the 5' and 3' ends of the intron being removed and are also known as the splice donor and splice acceptor site, respectively. These splice sites define the region where the spliceosomal machinery will bind. In the initiation step, the 5'ss binds U1 snRNP and the 3'ss binds U2AF. The 3'ss includes a polypyrimidine tract (PPT) and a conserved AG sequence. U2AF is made up of 2 subunits: U2AF65, which binds to the PPT and U2AF35 which binds to the AG sequence. The 3'ss and 5'ss can be defined as "strong" or "weak" depending on the extent of homology of the consensus splice site. The BPS has a loose consensus sequence and is bound by BP binding protein (SF1/BBP) early in spliceosome assembly.[22]

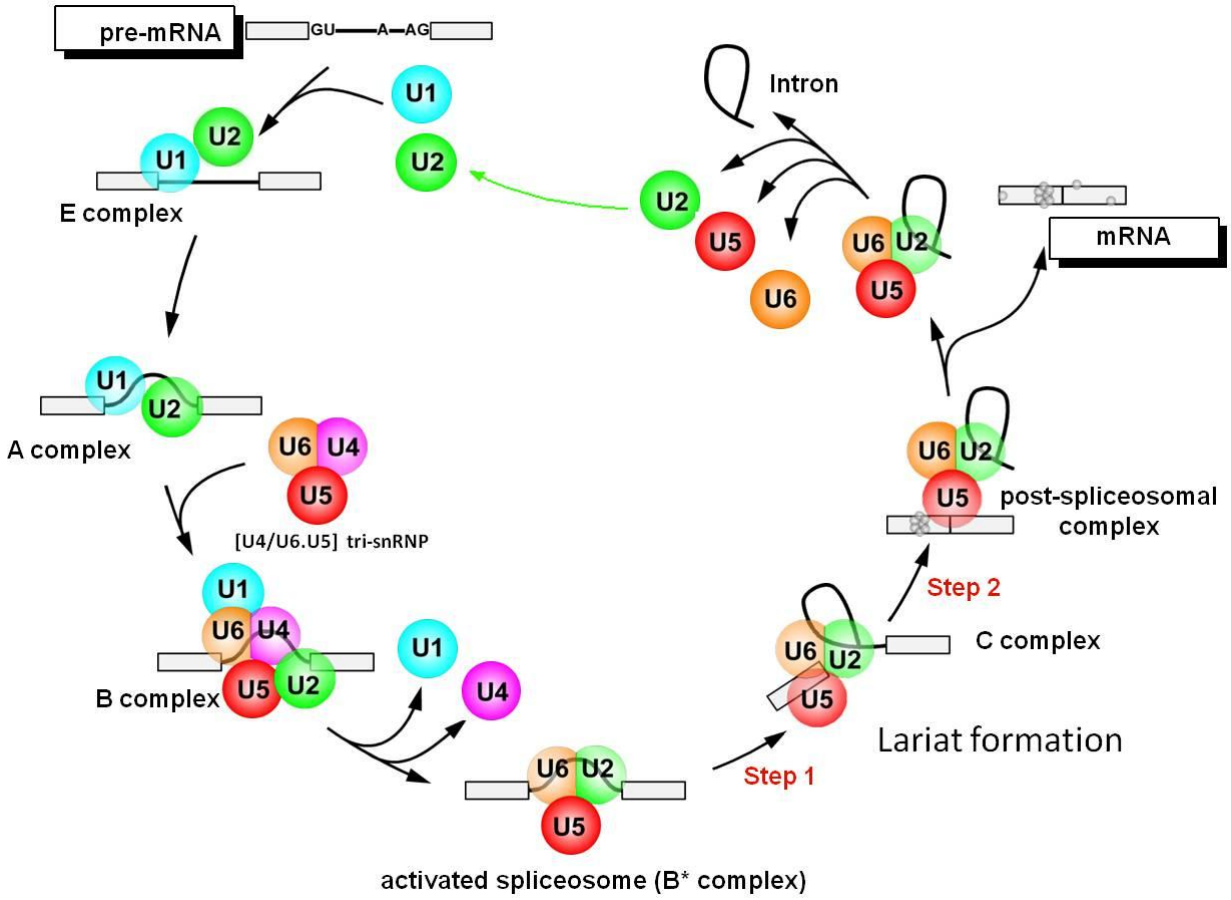

Figure 6: Splicing mechanism. E complex forms when U1 binds to the 5'ss. A complex forms when U2 binds to the intron. B complex forms when the U4/U6-U5 tri-snRNP binds to the intron. The complex is activated to B* complex when U4 and U1 are released. The first phosphodiester bond forms creating a lariat structure and forming the C complex. The second phosphodiester bond forms which removes the intron and the exons are then joined together. The snRNPs are recycled and the lariat intron is degraded.

Structurally, the spliceosome is assembled from its different components and functions in a stepwise fashion (**figure 6** and **7**). First, the E complex forms. This is characterized by the U1 snRNP binding to the 5'ss of the intron. Meanwhile, the SR protein SF1 (splicing factor 1) binds to the BPS on the intron and U2AF binds the PPT between the BPS and 3'ss. The BPS contains a conserved adenosine required for this first step of splicing. The A complex forms when U2 displaces SF1 with the help of ATP. At this point, the U4/U6-U5 tri-snRNP integrates in, forming the B complex which is activated (B* complex) following the release of U1 and U4 from the splicing complex. As shown in **figure 7B**, the splicing reaction involves the reaction of the 2'-hydroxyl group oxygen on the branch site A (adenosine) with the 5' end phosphate on G (guanine) to form a 2',5'-phosphodiester linkage; this forms a lariat structure. Then, as illustrated in **figure 7C**, the 3'-hydroxyl group oxygen of the upstream exon (G) captures the 3' end

phosphate of the intron by forming a second phosphodiester bond. This results in the splicing products shown in **figures 7D** and **6**; the post spliceosomal complex consists of two exons which are joined together with the help of U5[16] and a free intron in lariat form. The lariat is subsequently removed, the matured mRNA is released, and the snRNP complexes are recycled.[21,23]

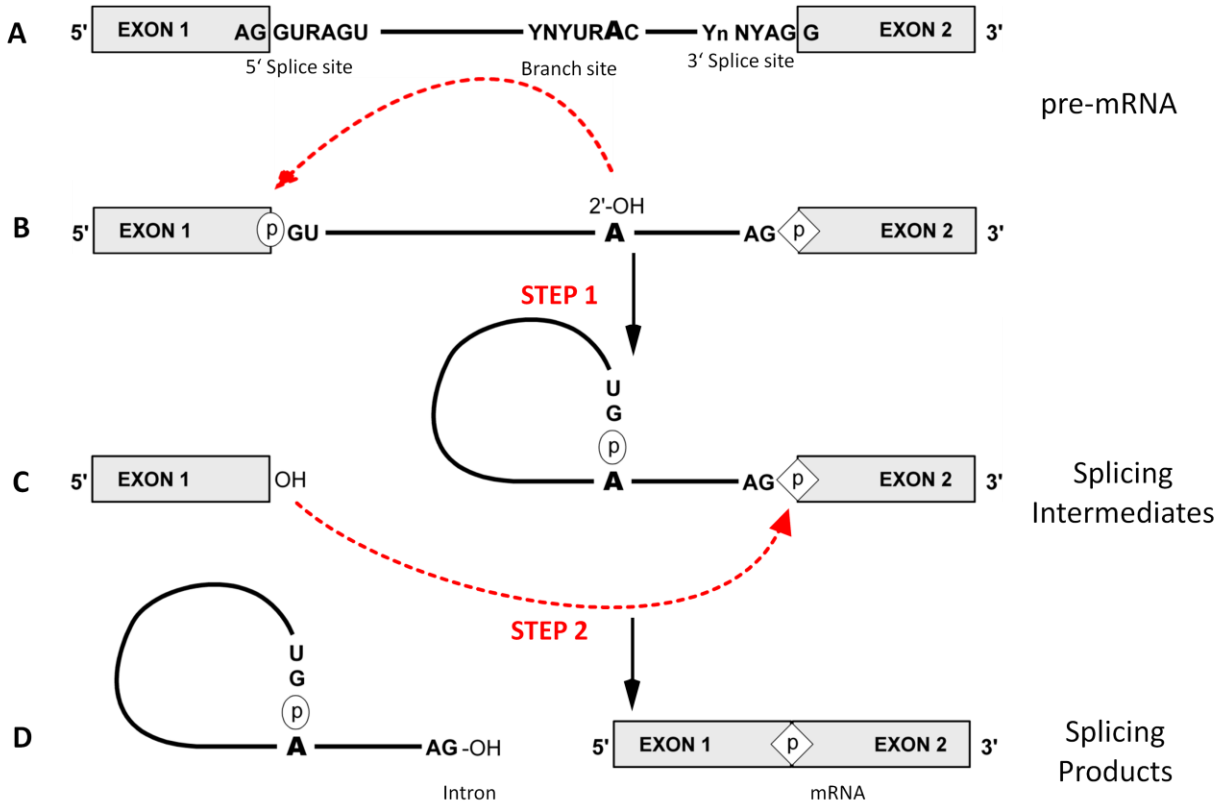

Figure 7: Two step mechanism of pre-mRNA splicing. A. The pre-mRNA consists of a 5'ss, 3'ss, PPT, and BPS. B. In step 1 the 2' OH of the adenosine on the BPS attacks the phosphate on the 3' guanine forming the first phosphodiester bond. C. In step 2 the 5' OH attacks the 3' phosphate forming a second phosphodiester bond. D. The splicing products are the intron in a lariat form and the joined exons. A = Adenine, G = guanine, U = uracil, N = any nucleobase, R = any purine, Y = any pyrimidine.

1.2.2 Regulation of splicing and alternative splicing: As mentioned, within the intron, a 3'ss, a 5'ss, and a BPS are required for splicing (**figure 5**). These elements, together with intronic splicing silencers (ISS), exonic splicing silencers (ESS) and exonic splicing enhancers (ESE), ensure proper recognition of exonic and intronic sequences and regulation of splicing.[24] Splicing silencers and enhancers are considered c*is*-acting sequences and together with cellular splicing factors are responsible for the regulation of alternative splicing.[25] Cis-acting sequences

are regions in DNA or RNA which regulate the expression of genes on the same molecule of DNA/RNA (usually a chromosome). Trans-acting elements regulate gene expression but are not directly located on the same chromosome and are usually splicing factors. Splicing silencers and enhancers are usually 6 to 13 nucleotides (nt) in length, with multiple GAR sequence repeats, where R is a purine (either guanine or adenine).[26]

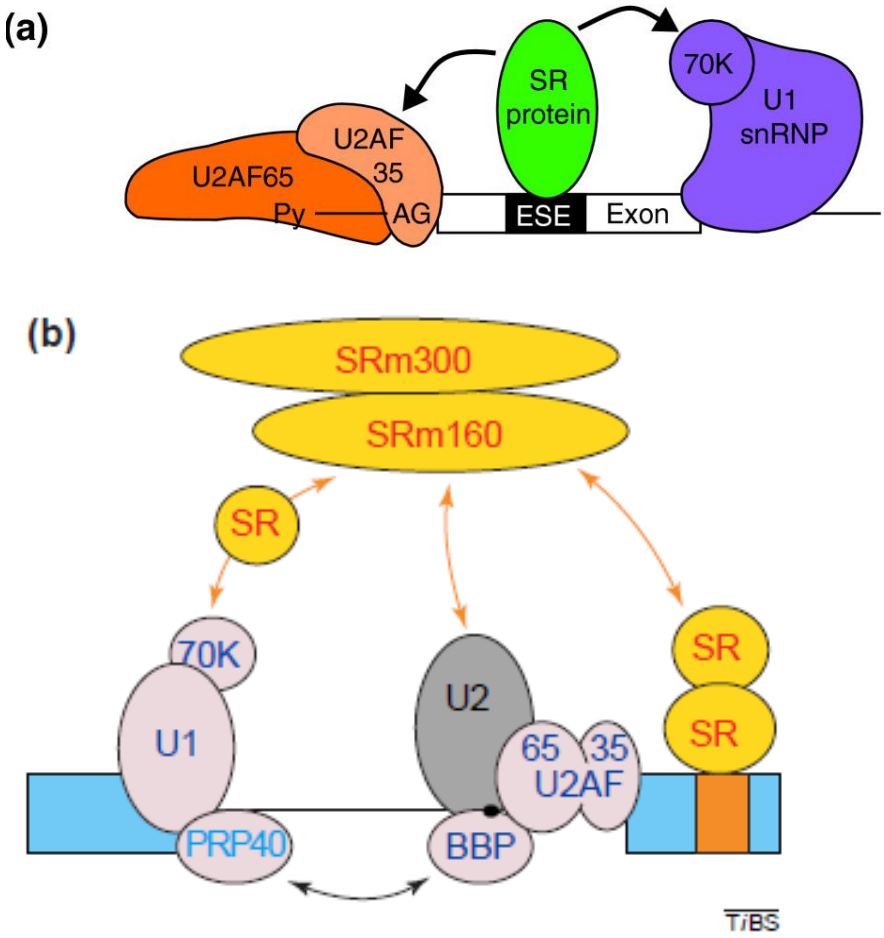

Figure 8: Interactions between SR proteins and the splicing machinery. A. The SR protein communicates directly to the splicing factors, snRNPs. B. The SR proteins communicate to the spliceosome snRNPs through the 'bridging protein' SRM160/300. Adapted with permission from: Shepard, P.J., Hertel, K.J. "The SR protein family." Genome Biol. 10:242, p. 6. Copyright 2009 BioMed Central Ltd. Reprinted from Trends Biochem Sci, 25, Blencowe, B.J., "Exonic splicing enhancers: mechanism of action, diversity and role in human genetic diseases." p. 108, Copyright 2000, with permission from Elsevier.

ESEs are short (5-7nt), highly degenerate consensus sequences which bind SR proteins and SR-related proteins and promote splicing. SELEX (systematic evolution of ligands by exponential enrichment) experiments concluded that ESEs are comprised of a diverse spectrum

of sequences.[27,28] However, among the best characterized ESEs are purine-rich sequences that recruit members of the SR family of splicing activators. When SR proteins or SR-related proteins bind to an ESE they promote splicing by facilitating, for example, the binding of U2AF65 to PPT through an interaction mediated by U2AF35 (**figure 8a**). Additionally, SRm160/300 is known to be a splicing coactivator in ESE function. SRm160/300 is a complex of two SR-related nuclear matrix proteins made of 160 kilodaltons (kDa) and 300kDa respectively. These proteins facilitate communications with components of the spliceosome by acting as a bridge between ESE-bound SR proteins and spliceosome components (specifically, snRNPs) (**figure 8b**).[29]

ESS's bind splicing inhibitory proteins, usually cellular heterogeneous ribonuclear proteins (hnRNP), which repress exon definition (**figure 9**) and are different than snRNPs Suppressing splicing, like splicing enhancing, is achieved through protein-protein interactions of ESS and ISS bound proteins and the splicing machinery, usually snRNPs.

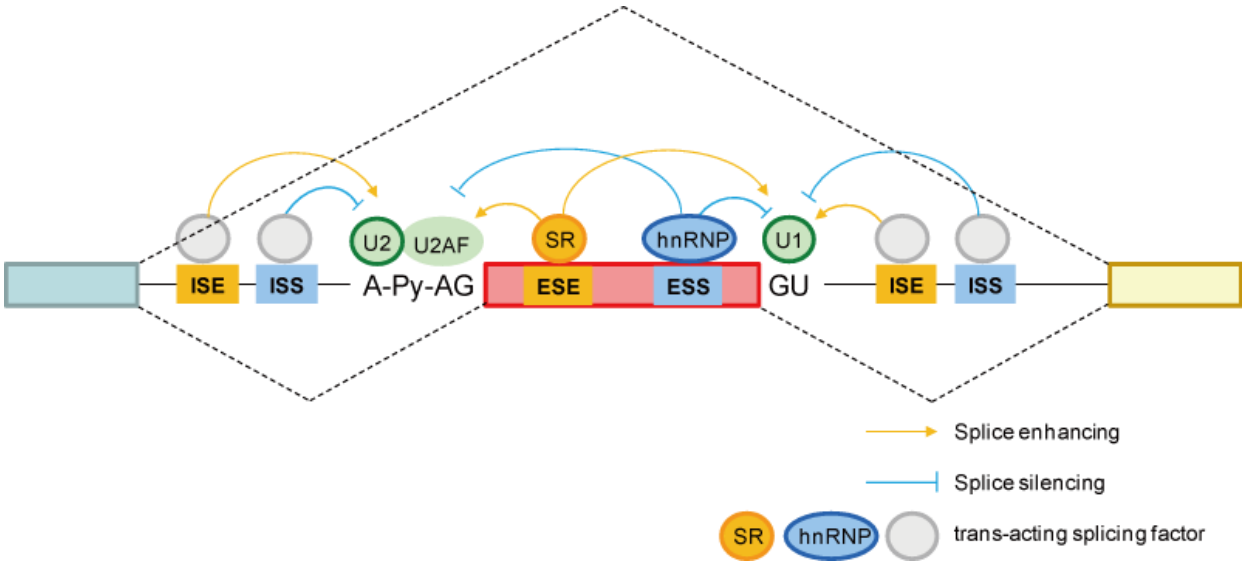

Figure 9: Splicing protein interactions. The protein-protein interactions of proteins bound to an ISS (intronic splicing silencer), ESS (exonic splicing silencer), ISE (intronic splicing enhancer), and ESE (exonic splicing enhancer) and the effect it has on splicing enhancing or silencing. Adapted from http://www.h-invitational.jp/h-dbas/index.jsp

SR proteins, shown in **figure 10**, are phospho-proteins which, by definition, harbour "one or two N-terminal RNA recognition motifs (RRMs), [also called RNA binding domains (RBD)], followed by a downstream RS domain of at least 50 amino acids (aa) with >40% RS content characterized by consecutive RS or SR repeats."[30] The RS domain mediates protein-protein interactions.[23] The SR proteins participate in constitutive splicing by stabilizing interactions

between components of the splicing machinery and thereby influence the choice of splicing sites in alternative splicing (**figure 8a**).[31,32] RRMs control the recognition of ESEs whereas the RS domain binds directly with the pre-mRNA while spliceosome assembly is occurring.[33]

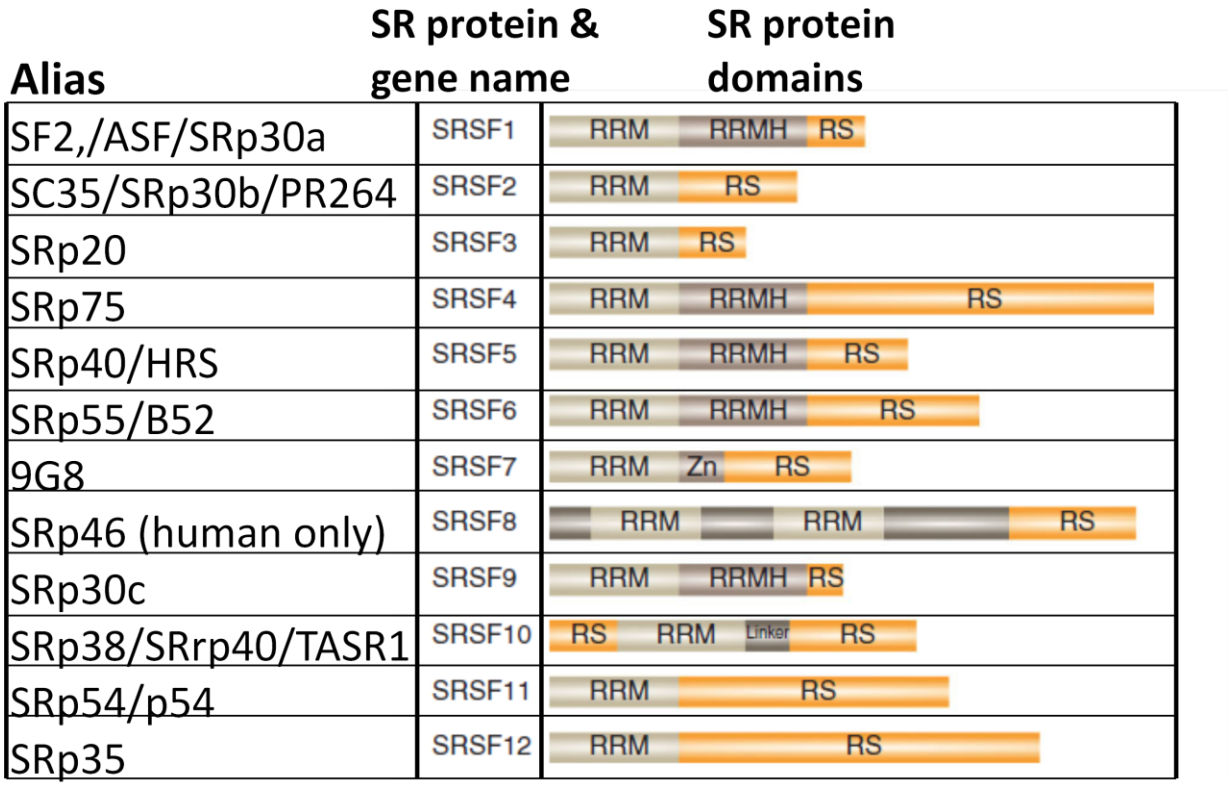

Figure 10: Domains of SR proteins, SRSF 1-12 and their aliases. This material is reproduced with permission of John Wiley & Sons, Inc. Busch, A., and Hertel, K.J. Evolution of SR protein and hnRNP splicing regulatory factors. WIREs RNA. 3:1, p. 2, Copyright 2011 John Wiley & Sons, Ltd. Information also adapted, with permission from: Manley JL, Krainer AR. "A rational nomenclature for serine/arginine-rich protein splicing factors (SR proteins)." Genes. Dev. 24, p. 1074, 2010.

SR proteins are present in all metazoan species and in some lower eukaryotes.[34,35] The presence of SR proteins is species specific and is correlated to the existence of RS domains in other components of the splicing machinery. In humans, there are twelve SR proteins, encoded by twelve genes designated as Ser (S) and Arg (R) rich splicing factor (SRSF) 1-12.[36] **Figure 10** outlines the previous SR protein aliases and their current protein and gene distinctions.[37,38] As mentioned previously, all proteins have the characteristic RS domain, which is variable in length, and contains at least one RBD (**figure 10**). Of those proteins possessing two RBDs, the second is a poor fit to the consensus sequence of the first RRM, known as the RRM homolog (RRMH). The exception to this is SRSF7 which has a RRM and a zinc-knuckle domain which is capable of binding RNA.[39]

The RS domains act as a nuclear localization signal and mediate interaction with the transporter protein transportin-SR.[40] Many of the SR proteins are located in nuclear compartments called speckles throughout the nucleus and are the primary component in these speckles.[41,42] There are two different speckle structural types.[43] The interchromatin granule clusters (IGC) are 20-25nanometres (nm) in diameter and act as sites for pre-mRNA splicing factors. The perichromatin fibrils are 5nm in diameter and are sites of actively transcribing genes and co-transcriptional splicing. The RS domain is responsible for targeting SR proteins to the IGC speckles; however, during splicing, the proteins are recruited from IGC storages to the perichromatin fibrils at the site of splicing. This recruitment step requires both the RBD and RS domain and phosphorylation of the RS domain.[44,45,46,47]

In splicing, at least one, usually multiple, SR proteins recognize the ESE and subsequently recruit the spicing machinery to the adjacent intron.[37,48] An SR protein must be phosphorylated to allow for efficient splice site recognition and dephosphorylated in splicing catalysis.[49,50] The phosphorylation of SR proteins is achieved at the RS domain by five kinases: SR protein kinase 1 and 2 (SRPK1/2), Clk/Sty kinase, cdc2p34 and topoisomerase (topo).[51,52,53,54] As depicted in **figure 11**, there are four proposed mechanisms regarding how SR proteins influence splicing. The first, **figure 11a**, suggests the RS domain of an ESE-bound SR protein interacts directly with the RS domain U2AF35 which recruits U2AF65 to the mRNA. This interaction recruits the spliceosomal components required for the initiation step in splicing.[37] The second mechanism, **figure 11b**, is called the co-activator model where the SR protein is bound to the ESE and interacts with the splicing machinery indirectly through SRm160/300 (discussed previously in this section). The third, or inhibitor model, **figure 11c**, occurs when no SR protein is bound. In this model an inhibitor binds downstream to prevent splicing upstream. The final mechanism, **figure 11d**, proposes that the RS domain contacts the pre-mRNA directly and interacts with U170K which recruits U1snRNP to the 5'ss.[55,56] The magnitude of splicing promotion is dependent on several factors: the number of SR proteins on an ESE, the distance between the ESE and the intron, and the number of Ser-Arg repeats within the RS domain of the bound SR protein.[57]

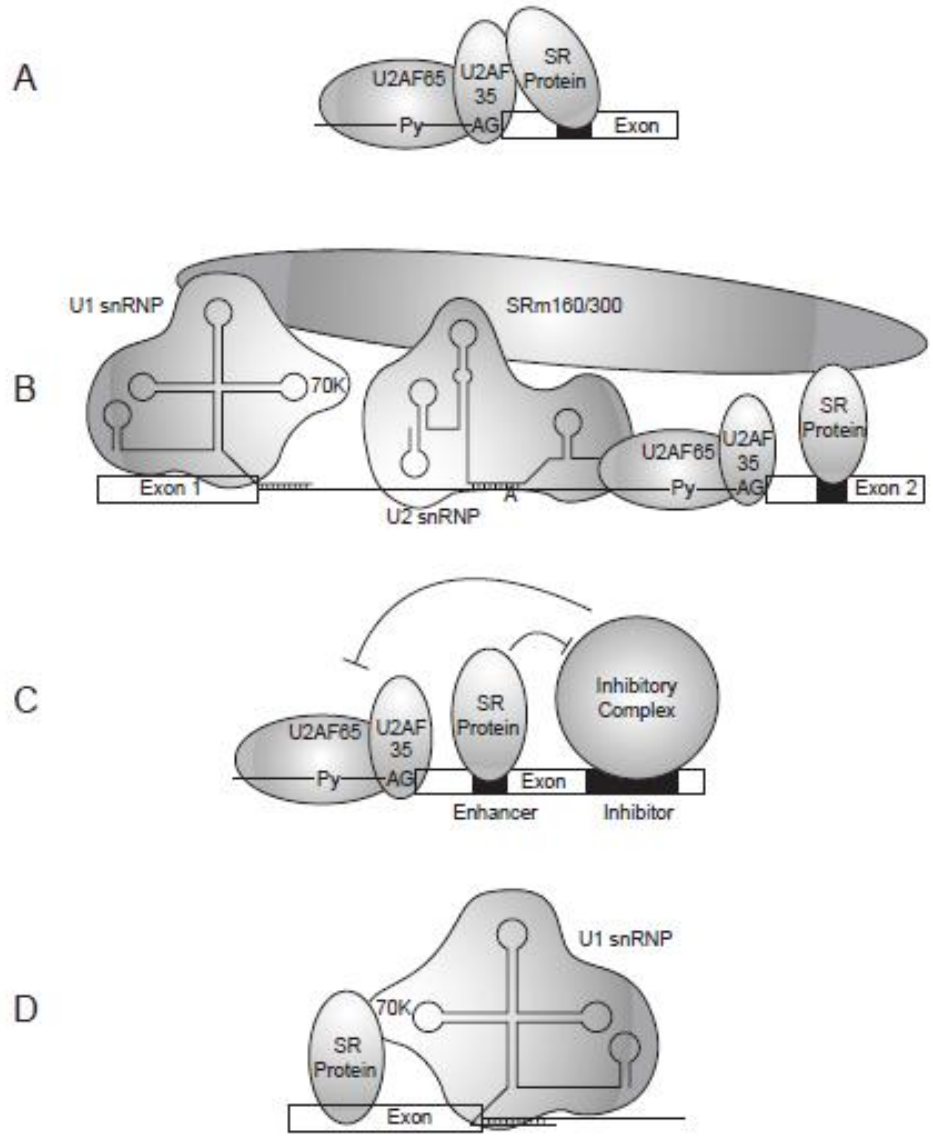

Figure 11: "The regulated exon-dependent functions of SR proteins. A: U2AF recruitment model. An enhancer-bound SR protein interacts with the RS domain of U2AF35, thereby recruiting U2AF65 to the pre-mRNA. B: Coactivator model. In this model, the splicing enhancer functions through interactions with the splicing coactivator SRm160/300, which also interacts with U1 snRNP and U2 snRNP. Some of these interactions may be indirect. C: Inhibitor model. In the absence of the enhancer-bound SR protein, a downstream splicing inhibitor functions to prevent the splicing of the upstream intron. The function of the splicing enhancer is to counteract the splicing inhibitor. D: Recruitment of U1 snRNP to a 5' splice site. An SR protein bound to the upstream exon interacts with U1-70K and recruits U1 snRNP to the 5' splice site." Taken from Graveley, B.R. "Sorting out the complexity of SR protein functions." RNA. 6, 1197-1211, 2000.

In select cases, SR proteins can also act as splicing repressors. To repress splicing the protein will bind to the intron. An example of this occurs in adenovirus infection; SRSF1 binds an intronic repressor element upstream of the 3'ss BPS. This prevents the recruitment of snRNP U2 to the BPS effectively inactivating the 3'ss.[58]

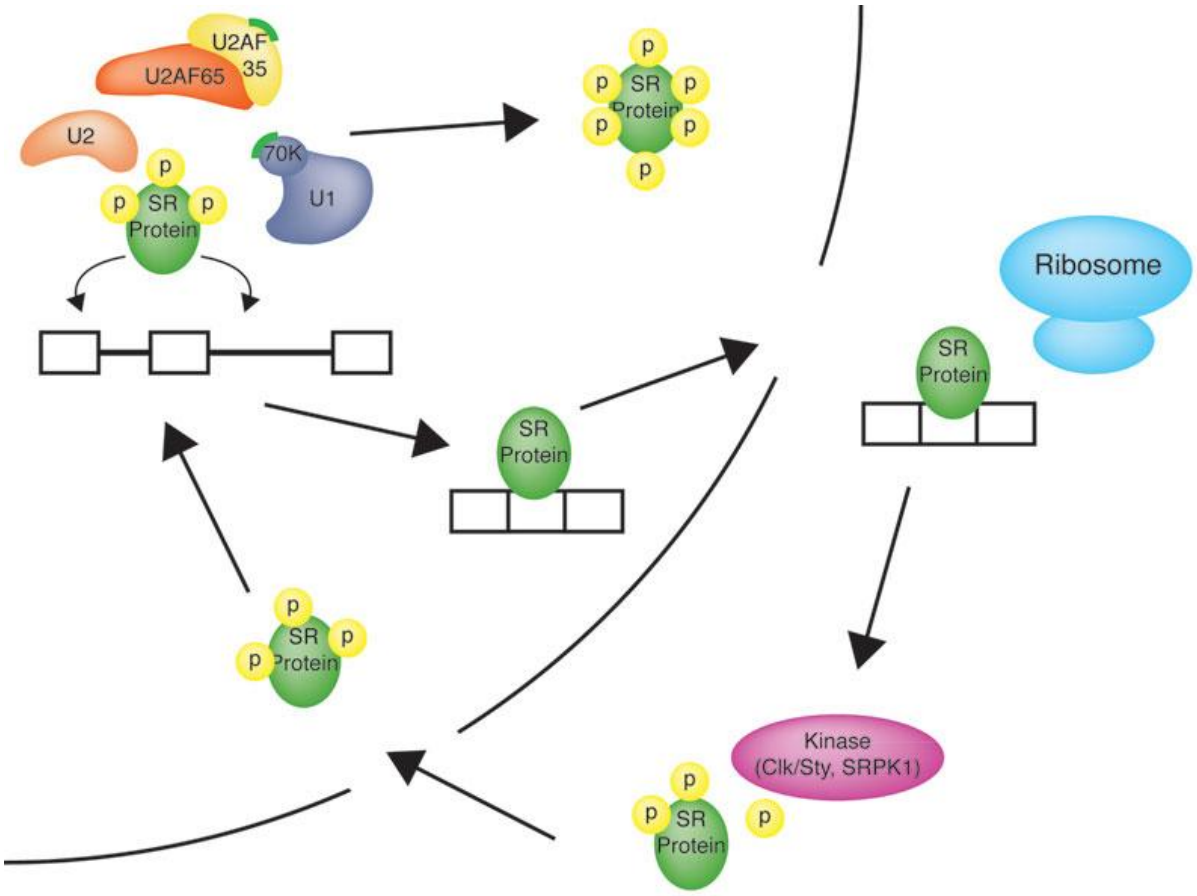

Figure 12: SR protein movement between cytoplasm and nucleus. Export and import is determined by the phosphorylation status of the SR protein and its ability to bind mRNA. Reproduced with permission from: Mueller WF, Hertel KJ. "The role of SR and SR-related proteins in pre-mRNA splicing". And in: Zdravko L, ed. RNA Binding Proteins. Austin/New York: Landes Bioscience/Springer Science+Business Media, 2012: (Fig. 5); epub ahead of print http://www.landesbioscience.com/curie/chapter/5032/.

SR proteins are predominantly found in the nucleus; however, three proteins shuttle between the cytoplasm and the nucleus: SRSF1, SRSF3 (SRp20), and SRSF7 (9G8). Nuclear import and export requires cellular factors and complex, highly regulated pathways, depending on the specific SR protein. Regardless of which SR protein is involved, it must be phosphorylated before being imported or exported.[59] SRSF7 (9G8) and SRSF3 (SRp20) promote nuclear export of intronless histone H2A mRNA by binding to a 22nt sequence within the mRNA. Additionally, SR proteins are known to remain associated with spliced mRNA after intron removal.[60,61] Because of this, and their ability to shuttle between the nucleus and cytoplasm, it is believed that SR proteins play a role in the export of spliced mRNA (**figure 12**).[59] Nuclear import is mediated by the protein transportin-SR. For SR proteins to be transported into the nucleus, they must first be phosphorylated, followed by contact with the

transportin-SR at the RS domain to move the protein through a nuclear pore.[62,63] Characteristically, SRSF1 shuttles between the cytoplasm and the nucleus at a high rate.

Translation is another process that SR proteins influence both directly and indirectly. SRSF1 activity influences the pre-mRNA alternative splicing of a kinase that regulates translational initiation, MNK2 (MAP kinase-interacting serine/threonine-protein kinase 2). High levels of SRSF1 increase the production of a MNK2 isoform which enhances cap-dependent translation.[64] SRSF1 is also involved directly in the regulation of translation by causing the release of a cap-dependent translation inhibitor. It achieves this through its ability to associate with polyribosome fractions isolated from cytoplasmic extracts.[65,66] This association increases the "translational efficiency of an ESE-containing luciferase reporter through mediating the recruitment of components of the mammalian target of rapamycin (mTOR) signalling pathway."[36] SRSF3 (SRp20) promotes translation of a viral RNA initiated at an internal ribosome entry site.[67] Finally, SRSF7 (9G8) has been shown to increase the translational efficiency of unspliced mRNA containing a constitutive transport element.[68]

1.2.3 SR protein SRSF1: SRSF1 is a general splicing activator. Structurally it is a 33 kDa protein factor containing 248 amino acid residues, including an 80 aa residue RBD at the N-terminus and a 50 aa residue C-terminal RS domain.[69,70] The RBD shows high homology to previously characterized RBDs in many RNA binding proteins; specifically the mammalian U1 snRNP indicating that an interaction occurs between SRSF1 and U1 snRNP.[69,71] SRSF1 is believed to be essential early on in spliceosome assembly.[72,73]

SRSF1 has the characteristic RS domain and two RRMs (described in section 1.2.2). The RRMs are connected by a glycine- and arginine-rich linker. They independently bind RNA but for optimal RNA interaction, they act synergistically.[74,75] Both of the motifs contribute to the protein's RNA-binding specificity.[76] Interestingly, the two RRMs are not identical as RRM2 is missing critical residues in the ribonucleoprotein (RNP) RNP-1 and RNP-2 motifs. These residues are associated with RNA binding, thus, the way RRM2 binds to RNA is likely different from RRM1 and therefore its exact mode of binding is still unclear.[77] (Further structural information in **appendix A**)

Another important characteristic of SRSF1 is the necessity for it to be phosphorylated as a regulating aspect of its function. The RS domain is phosphorylated by SRPK1 at approximately 12 serines through a directional (C- to N-terminal) and processive mechanism. This directs the

SR protein to the nucleus and influences its protein-protein interactions associated with splicing (**figure 12**).[78] At this point the SR protein is only partially phosphorylated or hypo-phosphorylated (p-SRSF1).[79,80] Once inside the nucleus it is phosphorylated further by Clk/Sty (Cdc 2-like kinase/serine threonine tyrosine). The protein is now fully phosphorylated or hyper-phosphorylated (pp-SRSF1).[81] Hyper-phosphorylation facilitates the recruitment of the SR protein to the site of active transcription and the active splice sites.[47]

Contrary to the initially proposed mechanism for U1 snRNP recruitment to the 5'ss, it is the RRM of the SR protein and not the RS domain that mediates this process.[82] The phosphorylation status of SRSF1 determines the types of protein-protein interactions it will participate in with regards to U1 snRNP recruitment. At the active splice site pp-SRSF1 simultaneously recognizes an ESE and U1-70k (a specific component of U1 snRNP). This permits the formation of a ternary complex consisting of the ESE, the SR protein and U1 snRNP. U1 snRNP is recruited to the 5'ss by U1-70k through an interaction mediated by the RRM domain of pp-SRSF1 and U1-70k (**figure 13b**). As p-SRSF1, the RS domain interacts with its own RRM in an intra-protein interaction preventing U1-70k from interacting with the SR protein (**figure 13a**). In summary, the phosphorylation status of the RS domain on SRSF1 determines the type of protein-protein interaction it takes part in (intra- or inter-interaction).[83]

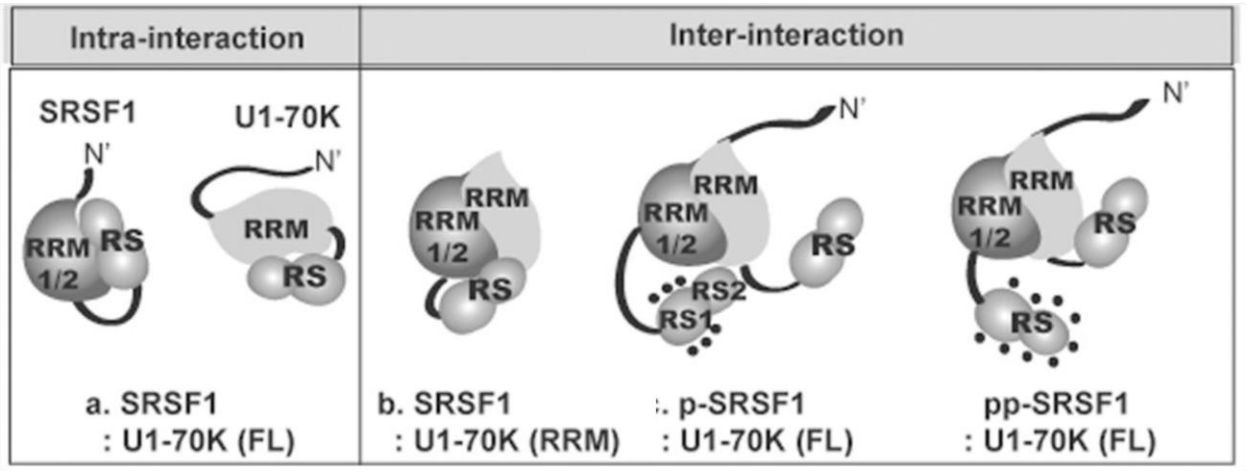

Figure 13: Binding modes. Models depicting (a) intra and (b) intermolecular binding modes within and between SRSF1 and U1-70K. Adapted with permission from: Choa, S., Hoanga, A., Sinhab, R., Zhongc, X., Fuc, X, et al. "Interaction between the RNA binding domains of Ser-Arg splicing factor 1 and U1-70K snRNP protein determines early spliceosome assembly." PNAS. 108, pg. 8235. Copyright 2011 National Academy of Sciences, U.S.A.

Nuclear export of SRSF1 requires the RS domain and binding to RNA (**figure 12**). It is postulated that the RS domain acts as a nuclear export signal. Upon replacement of the RS domain with one of a nonshuttling protein, SRSF1 is confined to the nucleus. However, when the RS domain was attached to the nucleoplasmin reporter NPc, nuclear export could not be activated.[59] This indicates that the RS domain is not the only factor influencing nuclear export. Through immunoprecipitation assays of labelled RNA, it was displayed that SRSF1 remains bound to mRNA in the cytoplasm.[84] This suggests that SRSF1 is exported while bound to the mRNA exon and then dissociates in the cytoplasm. Further studies indicate that SR proteins interact with TAP/NFX1 (Tip-associated protein/nuclear transcription factor X I), a primary receptor for general mRNA nuclear export.[85] This interaction is complex and influenced by sequence determinants and post-translational modifications. However, it has been shown that TAP binding to SRSF1 involves R90, 93, 117, 118 within the linker region connecting RRM1 and RRM2 of SRSF1, shown in **figure 14**.[77] Overall, the nuclear export of SR proteins, like SRSF1, is strongly coupled to TAP-mediated mRNA export.

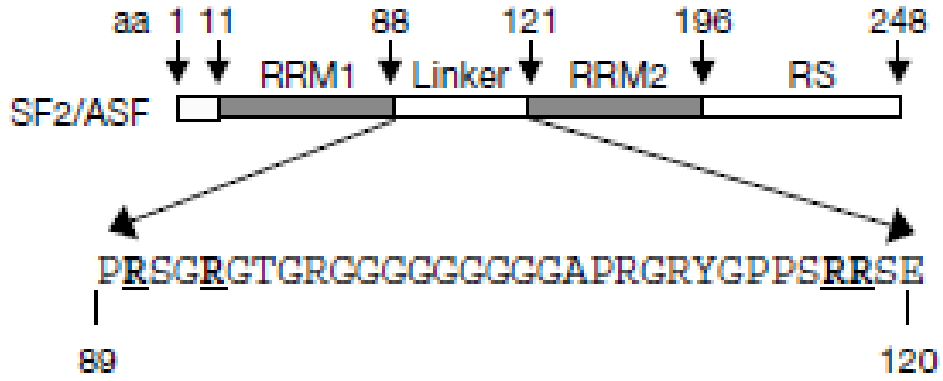

Figure 14: Schematic of SRSF1 RRM1 and 2 and the linker region. The linker region is important in the binding of SRSF1 to TAP, specifically R90, 93, 117, 118. A = alanine, C = cysteine, E = glutamic acid, G = glycine, P = proline, R = arginine, S = serine, T = threonine, Y = tyrosine. Reprinted by permission from Macmillan Publishers Ltd: EMBO J. "Structural and functional analysis of RNA and TAP binding to SF2/ASF." Tintaru, A. M., et al. 8, p. 761, copyright 2007.

SRSF1 is widely expressed throughout the body and is involved in a number of vital cellular processes. It is known to be vital in cell viability, embryonic development and pleiotropic activities due to its crucial role in the splicing and alternative splicing of proteins.[86] In conjunction with topo I, SRSF1 promotes genomic stability by preventing the formation of R-loops. R-loops are DNA-RNA hybrids that form during transcription. They slow the progression

of the replication fork and are associated with genomic instability because they increase the likelihood for DNA double-strand breaks and DNA rearrangements.[87,88] Abnormalities in SRSF1 activity in developing cells can have serious physiological significance. It is important to note that the following findings concern developing cells (embryos) and should not be extrapolated to fully developed cells. In mice, cardiac postnatal splicing transitions are largely dependent on SRSF1 activity. When SRSF1 is knocked out in a mouse model, it results in severe cardiomyopathy and disruption of alternative splicing events. Without the protein present, the heart displays a hypercontraction phenotype because of a defect in the postnatal splicing switch of Ca^{2+}/calmodulin-dependent kinase (CaMKIIδ) transcript. In the absence of SRSF1, the kinase mistargets and is located in the sarcolemmal membrane, causing severe excitation.[89,90]

SRSF1 is also a known oncoprotein. Elevated levels of the SR protein are found in various cancer and tumour cells: ovarian, gastric carcinoma, colon, thyroid, small intestine, kidney and lung.[64,91,92] Within cancer cells, the up regulation of SRSF1 results in aberrant splicing which promotes metastasis, cell motility, invasiveness, immortality and other characteristics associated with tumours. Additionally, the over expression of SRSF1 deregulates downstream components of Ras-MAPK and PI3K-mTOR pathways. These pathways are responsible for establishing and maintaining the cancer transformed phenotype. Over expression also inactivates putative tumour suppressors like BIN1, further contributing to the survival of the cancer cells.[64] These results suggest inhibition of SRSF1 may also be used as an anticancer strategy.

In the literature, there are conflicting views with regards to whether SRSF1 plays a redundant role in human splicing.[93] Using a newborn/embryonic mouse SRSF1 knockout model, it was shown that the SR protein is not redundant in developing cells.[94] Furthermore, SRSF1 was shown to be an essential factor for cell survival in chicken Dt40 cells. Depletion of the protein led to cell death. Further, its depletion effects could not be rescued by expression of SRSF2 (SC35) or SRSF10 (SRp40). With respect to these findings, SRSF1 may not function as a redundant SR protein.[95,96] However, when SRSF1 was inhibited in HIV-1 infected cells (i.e. mature cells) by IDC16, it was found to have no effects on cell viability.[97] Overall, there is literature evidence to reach a general conclusion that at the proper concentration and in non-embryonic cells, inhibiting SRSF1 will have no serious global consequences.

1.2.4 Splicing defects and disease: It is evident that SR proteins play a vital role in the control and regulation of splicing and alternative splicing. Thus, mutations or aberrant splicing due to disease (genetic, viral or bacterial) would result in serious effects. Splicing mutations can be separated into four categories: *cis* acting mutations that disrupt the use of constitutive splice sites; *cis* acting mutations affecting the use of alternative splice sites; *trans* acting mutations affecting the basal splicing machinery and; *trans* acting mutations affecting the regulators of alternative splicing.[98]

Cis mutations can result in exon skipping, use of pseudo 3' or 5'ss or the retention of the mutated intron. Point mutations like these usually introduce premature termination codons (PTC) in a transcribed mRNA, which will produce a non-functional protein. PTCs usually lead to nonsense-mediated decay (NMD), or degredation, of the mRNA before it is translated into a protein. PTCs cause a They can also cause a shift in the ratio of natural protein isoforms within the cell; this is the case in familial isolated growth hormone deficiency type II (IGHD II), frontotemporal dementia and Parkinsonism, and atypical cystic fibrosis.[98,99,100]

Trans mutations can affect the regulation of and possibly the entire splicing process. Mutations of the splicing machinery arise in retinitis pigmentosa and spinal muscular atrophy; whereas mutations affecting splicing regulators can lead to myotonic dystrophy (DM), neoplasia and malignancy.[98]

There are multiple viral infections that are able to alter normal cellular splicing patterns once they infect a cell. This, in part, allows the virus to propagate and maintain its pathogenesis and in some cases, allows the virus to transform normal cells into cancerous cells. Human papilloma virus (HPV), Murine leukemia virus (MLV) and adenovirus are three examples of viruses whose symptoms can be partially attributed to abnormal cellular splicing.[101,102,103]

1.2.5 Identification of splicing inhibitors: Modern drug discovery can be approached from various avenues. With extensive research in mapping the structure of various drug targets, proteins and genes, designing a compound to target these structures can be directed and methodical (structure-based and rational drug design). Further, building models of the target of interest based on similar known structures, through homology modelling, allows for some direction in drug discovery. However, when a large multi-component complex, such as the spliceosome, is the therapeutic target, i.e. no structural data is available, the only option to

identify active compounds is through compound library screening. This strategy is routinely applied in industry with great success.

For instance, to identify molecules that block the progression and ease the symptoms of spinal muscular atrophy (SMA), compound library screening has been used extensively. "SMA is an inherited neuromuscular disorder caused by homozygous loss of function of survival motor neuron (*SMN1*) gene"[104] which encodes survival motor neuron (SMN) protein. The second centromeric copy of the SMN gene (*SMN2*) is located in the same region as *SMN1* but only expresses a limited amount of functional full-length SMN protein.[105,106] A single nucleotide change in exon 7 of *SMN2* results in the removal of exon 7 from SMN2 mRNA; this is associated with a defective SMN protein.[107,108] The amount of full-length SMN protein, containing exon 7 is inversely related to disease severity in SMA patients and mice. Compound library screening led to the identification of the following compounds, shown in **figure 15**: histone deacetylase inhibitors (sodium butyrate[109], and SAHA[110]), an anthracycline (aclarubicin[111]), a phosphatase inhibitor (sodium vanadate[112]), a nonsteroidal anti-inflammatory drug and cyclooxygenase inhibitor (indoprofen[113]), aminoglycosides (amikacin[114]), and a Na^+/H^+ exchanger inhibitor (EIPA). These compounds all increase or positively influence the inclusion of exon 7 in SMN2 mRNA to ease the clinical symptoms of SMA. The mechanisms of action of these compounds are different but the common link between them is a mutual ability to increase the amount of normal SMN protein through their influence on alternative splicing.[104]

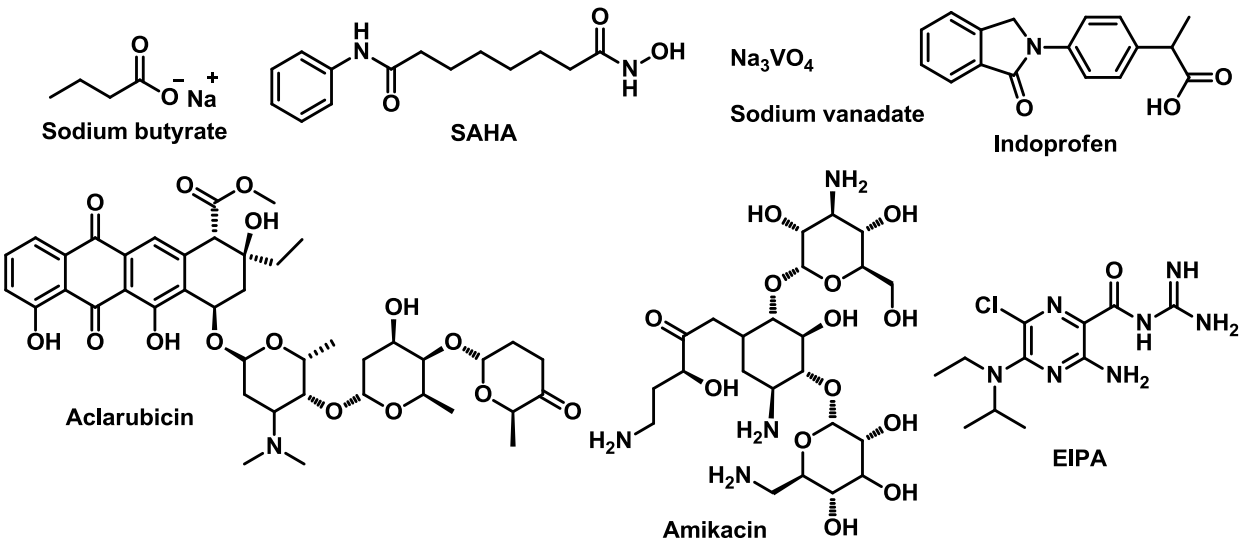

Figure 15: SMA splicing inhibitors. Inhibitors identified through compound library screening.

A further illustration of this point is shown in the discovery of Camptothecin's ability to affect splicing. Using human leukemia cell lines, Camptothecin, a known topoisomerase inhibitor and chemotherapeutic agent, was also identified in a screen of several cytotoxic agents to have an effect on caspase-2 pre-mRNA splicing. Its mechanism of action involves induction of exon 9 inclusion in caspase-2 pre-mRNA which effectively inhibits topo I.[115] Its derivatives are also potent chemotherapeutic agents.

Several other compounds have been discovered through random screening, or through other methods, as splicing inhibitors; PTC 124, SFV785, TG003, SRPIN340 (**figure 16**). PTC 124 is a molecule that selectively promotes the ribosome to read through premature stop codons but not through normal termination codons. It was discovered following two high-throughput screens of approximately 800,000 molecules in an attempt to find molecules that promote UGA nonsense suppression. Of the scaffolds that were identified and optimized, PTC 124 emerged as a molecule with an o-fluorophenyl motif linked to benzoic acid by a 1,2,4-oxadiazole, which was also orally bioavailable in aqueous suspension. It is currently in phase 3 clinical trials.[116]

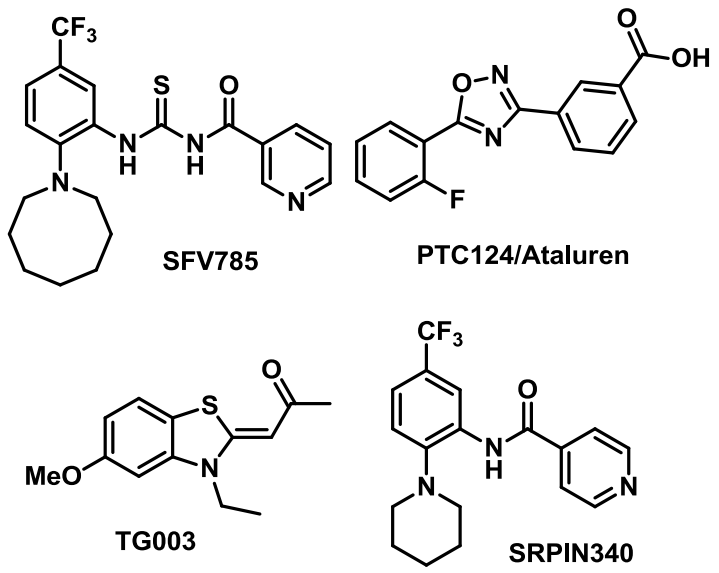

Figure 16: Splicing inhibitors: SFV785, PTC124, TG003 and SRPIN340.

SFV785 is a SRPK1 inhibitor also found to have anti-viral activity against the dengue virus (DENV) through inhibiting its propagation. The mechanism of action is complicated but in short, the compound alters the distribution of the structural envelope protein, which in turn alters

the protein's co-localization with the DENV replication complex. SFV785 affects viral assembly and not viral synthesis or translation, which results in a decrease in infectious virus titers.[117]

TG003 was identified in a screening of 100,000 molecules to be a Clk1/Sty inhibitor. Clk1/Sty is a protein kinase in the Clk family and is known to phosphorylate SR proteins. Preventing their phosphorylation has serious effects on cellular splicing. Specifically, Clk1/Sty has a role in SF2-dependent splicing of β-globin pre-mRNA in vitro and inhibiting it suppresses Clk-mediated phosphorylation.[118] This compound has the potential to influence abnormal splicing resulting from Clk-mediated phosphorylation and associated diseases.

SRPIN340 is a selective inhibitor of SRPK1 and SRPK2. This molecule inhibits the kinases' ability to phosphorylate SR proteins, a necessary step in splicing and alternative splicing. SRPIN340 was tested in an HIV-1 cell line and failed to inhibit replication; however, it was found to strongly inhibit replication of the RNA virus Sindbis.[119]

1.3 HIV-1 splicing: HIV-1 alternative splicing is vital for the production of viral proteins and future virus particles. In HIV-1 replication the transcription of the integrated proviral DNA by RNA polymerase II generates a polycistronic pre-mRNA that contains at least four 5'ss D1-4 and eight 3'ss A1, 2, 3, 4a, 4b, 4c, 5, and 7 that enable alternative splicing of more than 40 different mRNAs (**figure 17**).[120] The HIV-1 DNA genome expresses a primary transcript of 9 kilobases (kb) that not only serves as genomic RNA for progeny virus but also as the mRNA that encodes the viral *gag* and *gag-pol* proteins. Successful infection and production of new infectious viruses requires the balanced expression of seven additional viral proteins, *env*, *tat*, *rev*, *nef*, *vif*, *vpr*, and *vpu*.[121] To achieve this proteomic diversity the primary transcript is alternatively and incompletely spliced and nuclear export of the unspliced transcript is regulated. This process is highly orchestrated.[122,123,124] More simply, the SR proteins SRSF1, SRSF2 (SC35), SRSF5 (SRp40) and SRSF7 (9G8) play specific roles in HIV-1 splicing by stabilizing spliceosomal components through protein-protein interactions mediated by their RS domains (**figure 8a**).

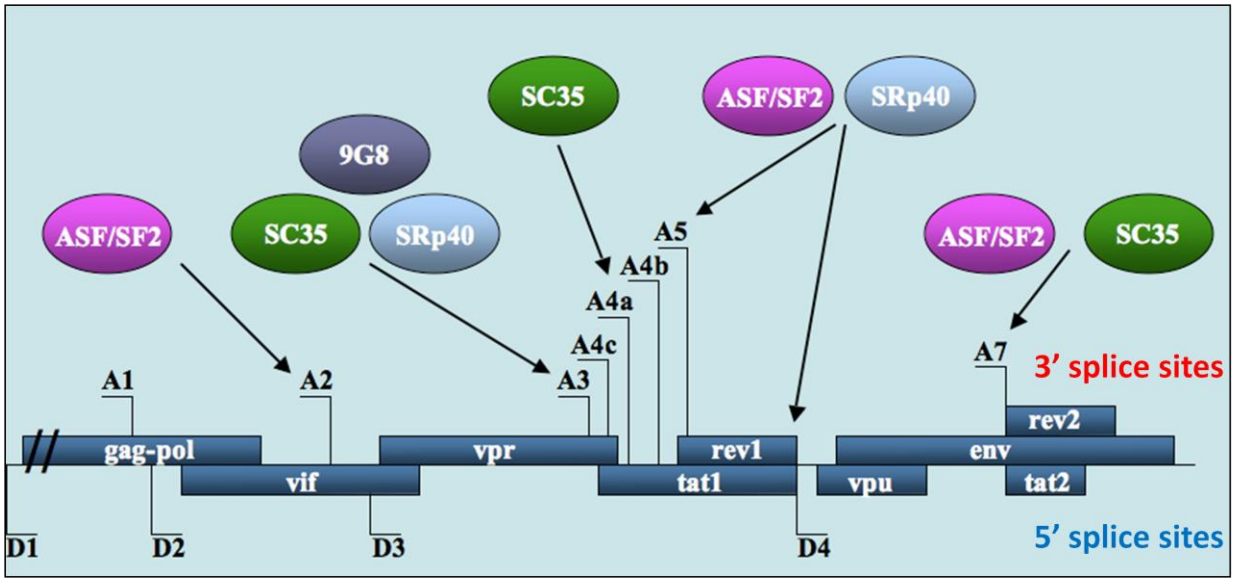

Figure 17: HIV-1 splice sites. 3' splice sites, A1, A2, A3, A4a-c, A5 and A7. 5' splice sites D1-4. SR proteins required for alternative splicing of HIV pre-mRNA and the specific proteins they generate. Adapted with permission from: Soret, J., Bakkour, N., Maire, S., Durand, S., Zekri, L., et al. Selective modification of alternative splicing by indole derivatives that target serine-arginine-rich protein splicing factors." PNAS. 102, p. 8768, Copyright 2005 National Academy of Sciences, U.S.A.

Regulation of HIV-1 splicing and alternative splicing is a complex process, with changes in the splicing patterns of HIV-1 shifting towards the production of mRNA isoforms with increasing levels of intron content, depending on the stage in viral replication. In the early phase, the virus transcribes mRNAs encoding the regulatory tat, and rev, and accessory nef proteins (1.8kb). In the intermediate phase, the interaction of Rev with the RRE produces the Env glycoprotein (4kb). In the late phase, Gag and Gag-Pol mRNAs are produced from unspliced transcripts (9kb) (**figure 18**).[125,126,127]

Cis-acting sequences are able to alter the strength of splice sites. In HIV-1, the different cis-regulatory sequences have been extensively studied and their consensus sequences identified. There are four ESSs, termed ESSV, ESS2, ESS3 and ESS2p. The three ESEs are named based on their regulatory sequences, $(GAA)_3$, ESE2 and GAR where the regulatory sequence for ESE2 is AGUAGAUC. There is only one ISS identified referred to as ISS.[128]

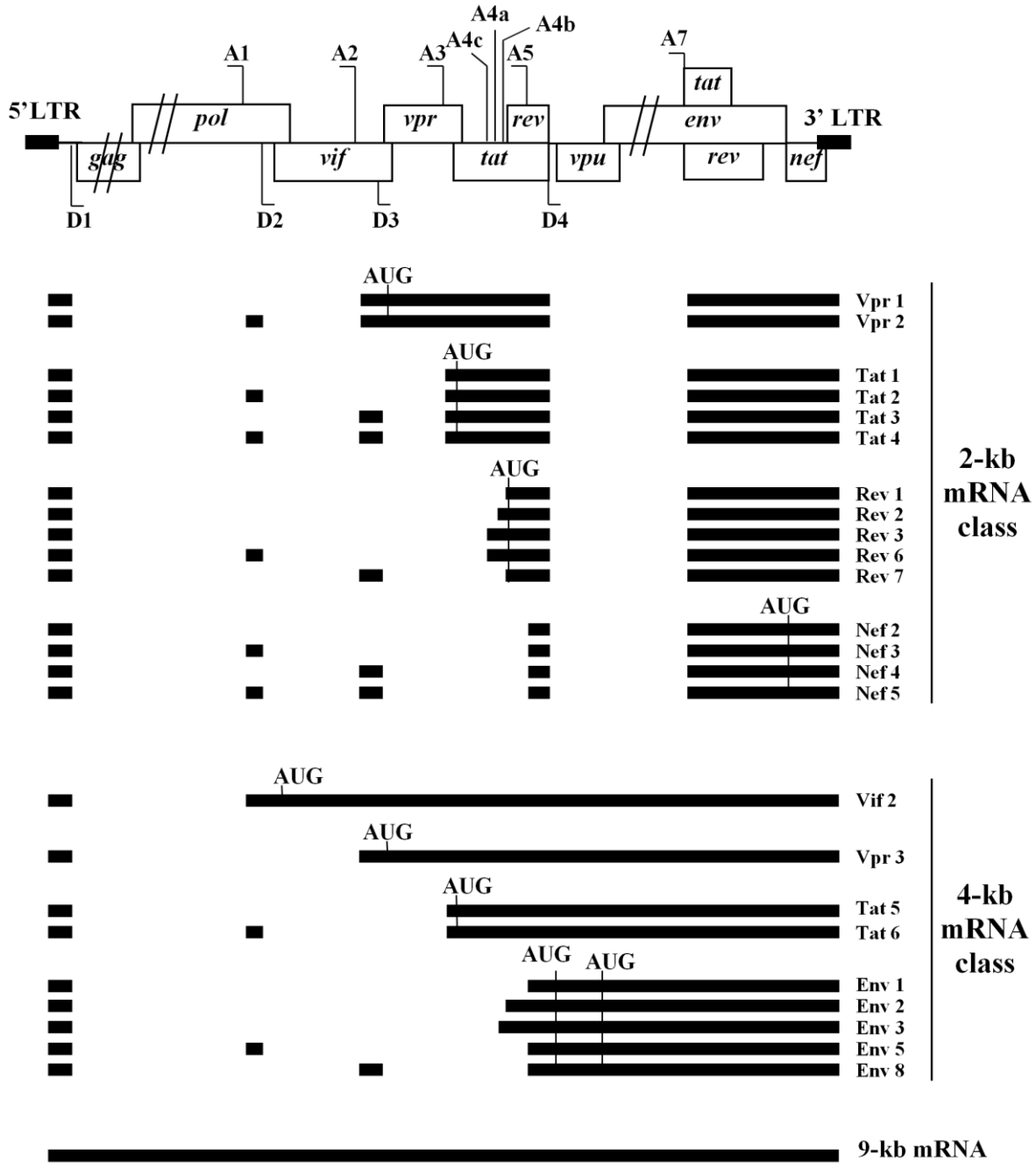

Figure 18: HIV-1 splicing pattern. "Schematic representation of HIV-1 proviral DNA. Open boxes represent the open reading frames encoding the viral proteins. Black boxes represent exons generated by combination of donor sites (D1 to D4) and acceptor sites (A1 to A7). The viral translation initiator codons are indicated by AUG." Taken with permission from: Jacquenet, S., Decimo, D., Muriaux, D., Darlix, J. "Dual effect of the SR proteins ASF/SF2, SC35 and 9G8 on HIV-1 RNA splicing and virion production." Retrovirology. 2:33, p. 2, 2005.

Down regulation of splicing has been shown to occur through the binding of hnRNPs at the 3' splice sites A2, A3, A7, and A6 (not in **figure 17**).[129,130,131,132,133,134] This inhibits splicing

by interfering with spliceosome assembly by counteracting the SR protein-mediated stabilizing interactions.[135] Furthermore, studies have shown splicing enhancer sequences as binding sites for SR proteins when they are located downstream of splice acceptor sites.[130,136,140] Downstream binding of SR proteins can increase the efficiency of U2AF binding to the PPT. This is accomplished either by displacing the hnRNP A1 protein which blocks 3'ss access to spliceosomal components or by the U2AF RS domain directly interacting with the SR protein's RS domain.[137] The RS domains of SR proteins, when bound to ESEs can also stabilize the binding of U1 snRNP to the 9 nucelotide sequence upstream and downstream of the 5'ss. Stabilization, facilitated by RS domain interactions, also occurs in the binding of U2 snRNP to the BPS.[55,56]

1.3.1 Role of SRSF1 in HIV-1 splicing: SRSF1 functions as an essential protein in splicing regulation. Varying the concentration of SR proteins experimentally resulted in changes in splicing activity, suggesting that SRSF1 modulates alternative splice site selection in a concentration dependent manner.[138] With respect to HIV-1 infected cells, over expression of SRSF1 results in a large reduction of genomic RNA. More specifically, it causes an increase in vpr RNA and together with the over expression of SRSF2 (SC35) and SRSF7 (9G8), a large reduction in total gag; altogether, this over expression leads to the down-regulation of the late steps in HIV-1 replication.[139] Thus HIV-1 must control the regulation of SR proteins levels in the cell to ensure proper replication.

SRSF1 is capable of specifically recognizing pre-mRNA 5'ss, likely through interactions with U1 snRNP. In addition to interacting with U1 snRNP, SRSF1 stimulates splice sites A2, A5, and A7 (**Figure 17**); however, binding is not strictly dependent on the RS domain which further supports the protein's interaction with hnRNPs.[134,140,141]

The 3'ss at A2 is recognized as being under negative control by the hnRNP A1 family. A2 is controlled by an ESS, termed ESSV, located downstream in exon 3, within the *vif* coding region.[142] It is characterized by its UAG sequences, mostly in the motif PyUAG.[143] ESSV suppresses splicing at A2 when hnRNPs bind. SRSF1 is believed to activate site A2 by binding in competition with hnRNP A and hnRNPB binding.[131,141] The SR protein activates A2 splicing independent of the presence of its RS domain; therefore, it is probable that SRSF1 competes with binding preventing splicing suppression instead of directly facilitating spliceosomal assembly.

Both over expression of SRSF1 or deletion of ESSV experimentally resulted in an accumulation of *vpr* mRNA and an increase in the inclusion of exon 3 in 4kb and 1.8kb mRNAs.[129,141,142]

Splice site A5 produces the singly spliced *env* mRNA and is followed by an SRSF1 protein-dependent ESE.[144] The ESE is located in the 5' proximal region of exon 5 and just downstream of A5. It is a GAR element which is dependent on SRSF1 and SRSF5 (SRp40). The GAR element acts bidirectionally, enhancing both 3'ss A5 splicing and U1 snRNP recruitment to 5'ss D4.[144]

The HIV-1 3'ss A7 is negatively regulated by ISS, ESS3 and ESE3 and all three elements bind hnRNP A1 synergistically.[134] This binding regulates splicing of the *tat* intron. ESE3 contains a $(GAA)_3$ sequence which has negative effects on splicing at A7 when it is deleted.[145] This sequence overlaps with the hnRNP binding site (AUAGAA) and is therefore identified as a Janus element, meaning it can bind more than one regulatory protein. It has the ability to bind both hnRNP and SRSF1 proteins resulting in either negative or positive activity. The nature of activity is determined by the relative amounts of the two proteins in the nucleus.[136] SRSF1 is again in competition with hnRNP for binding at a 3'ss.

1.4 Identification of IDC16 and SR protein target: In a collaborative research program between the medicinal chemistry group at Institut Curie, led by Dr. Grierson, and an RNA biologist Pr. Jamal Tazi (University of Montpellier II), the compound library screening approach was used to identify compounds able to inhibit ESE-dependent splicing. A library of several thousand structurally diverse molecules was screened to identify molecules able to inhibit the phosphorylation of SRSF1 by kinase topoisomerase I (topo I). Twenty-eight compounds were found to be active. Further testing indicated that the active drugs inhibited an early step in the spliceosome assembly pathway as opposed to topo I. Based on this second assay, a total of 25 related heterocyclic compounds were identified as active, belonging to the pyrido-carbazoles, benzopyrido-indoles, or pyrido pyrrolo isoquinoline families.[120]

All 25 heterocyclic compounds are known to be DNA-intercalating agents i.e., they insert themselves between base pairs of DNA, thereby interfering with DNA processing reactions such as transcription.[146] Through further testing, it was found that the active drugs can inhibit the kinase reactions without an apparent requirement for DNA. This suggested that "[SRSF1] and/or topo I are targets for these compounds."[120] From subsequent binding affinity measurements using the intrinsic fluorescence of the polycyclic compounds, it was determined that the drugs

bind to SRSF1 and not to topo I. Three separate experiments were done to measure binding after different parts of the protein were deleted and once again after they were recovered. The three experiments investigated the consequences of deletions in part of the RS domain, the complete RS domain, and the RRM. The conclusion of this study was that the RS domain was the major drug-binding element; however, the RRM domain played a role in the overall binding structure.

With this knowledge, the active compounds were screened for selective inhibition of ESE-dependent splicing events. One compound, IDC16 emerged as having a "strong inhibitory effect on different substrates harbouring [SRSF1] high-affinity binding site."[97] This experiment provided proof that IDC16 is an alternative splicing inhibitor (IC_{50} within the micromolar range), acting through binding to the SR protein SRSF1.

1.4.1 HIV application: HIV-1 is known to rely heavily on alternative splicing to produce its key viral proteins. Alternative splicing is controlled, in part, by SR proteins. As IDC16 inhibits the SR protein SRSF1 by interfering with the protein's the ESE activity, the subsequent production of proteins in the cell is altered. Following this discovery, the ability for IDC16 to block HIV-1 replication was studied. It was shown that the compound is active and that it "strongly impedes the production of spliced products."[120] This compromises the further synthesis of HIV-1 pre-mRNA and the assembly of infectious particles.[93] Therefore, it can be concluded that IDC16 is acting as an inhibitor of HIV-1 replication.

1.4.2 IDC16 and inhibition of HIV-1 replication: To establish that IDC16 inhibits HIV-1 replication through a mechanism different than the drugs used in HAART, peripheral blood mononuclear cells (PBMC) were infected with one of two HIV-1 strains (GAR and CLO) then treated with IDC16. These strains are known to be resistant to different HIV/AIDS therapeutic agents used in HAART, therefore if a compound targets the viral enzymes, RT, integrase or protease, it should be ineffective at inhibiting HIV-1 replication in the resistant strains. The replication of HIV-1 was inhibited, indicating that IDC16 is, in fact, acting through a splicing-based mechanism (**figure 19**).[97,120]

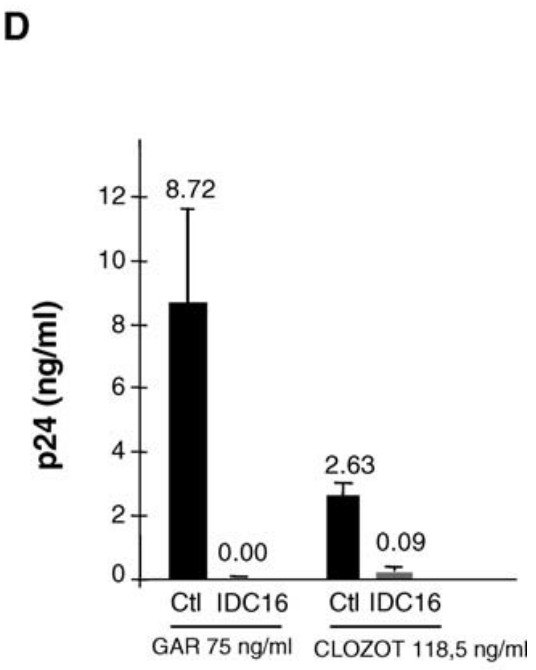

Figure 19: IDC16 inhibition against HAART resistant viral strains. "Activated PBMCs from healthy donors were infected with two HIV-1 clinical isolates (GAR and CLO) in the absence (Ctl) or presence of 1 μM of IDC16 (1DC16). Supernatants were harvested after 14 d of infection days, and viral capsid protein p24 antigen was quantitated using standard ELISA protocol." Taken with permission from Bakkour, N., Lin, Y. L., Maire, S., et al. "Small-Molecule Inhibition of HIV pre-m-RNA Splicing as a Novel Antiretroviral Therapy to overcome Drug Resistance." Plos Pathogens. 3, 1530-1539, 2007.

Further testing revealed that in the presence of IDC16, HIV infected macrophage cells' survival was increased. This suggested that IDC16 may protect these cells from the usual viral destructive processes. Additional tests analyzed a small fraction of selected genes to compare the general impact on alternative splicing of IDC16 and AZT, the first nucleoside reverse transcriptase inhibitor approved for HIV-1 therapy. It was found that AZT altered host cell gene expression while IDC16 did not; this indicates that SRSF1 function may be redundant in normal human cells as its inhibition did not affect gene expression.[97] The relative antiretroviral effects were also compared between the two compounds. MT2 cells were infected with an HIV-1 strain in the absence or presence of AZT or IDC16. The viral infectivity was completely abolished when five times less IDC16 (1μM) was used in comparison to AZT (5μM) (**figure 20**).[97]

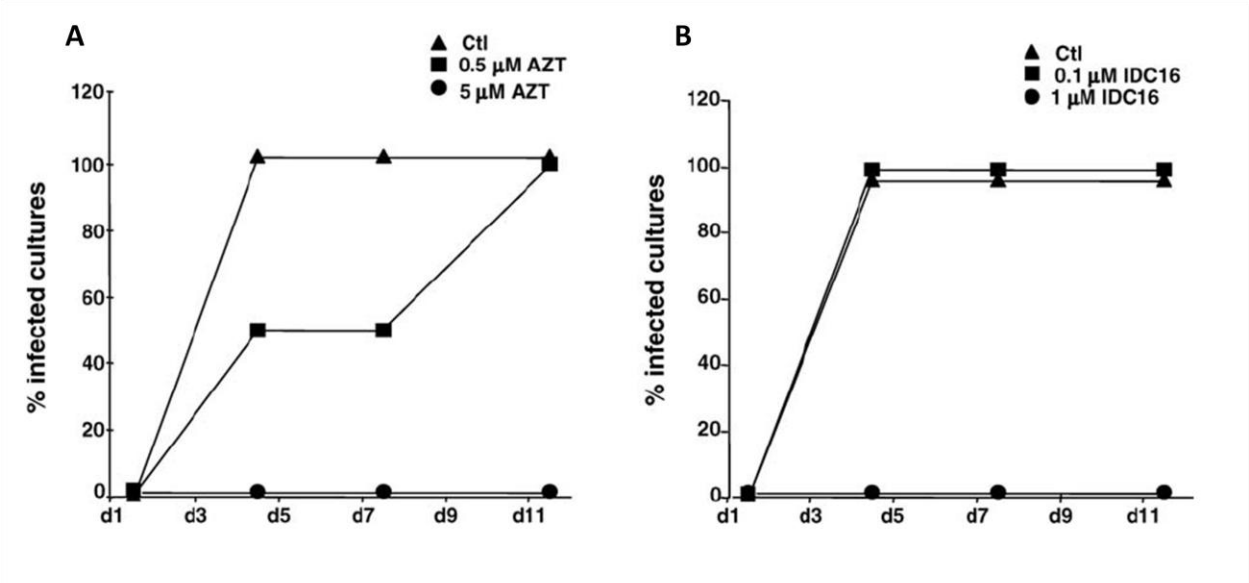

Figure 20: "Comparison of HIV-1 inhibition in [cells] treated with AZT or IDC16. (A and B) MT2 cells cultured in a 96-well plate were infected with pNL4.3 at 100 TCID50 in the absence or presence of IDC16 (A) or AZT (B) for 18 h. Cells were then washed and changed to fresh medium with/without IDC16 or AZT. Half of the culture medium was refreshed each 2 or 4 d in the presence of drugs. The formation of syncytia was scored at the indicated time points." Taken with permission from Bakkour, N., Lin, Y. L., Maire, S., et al. "Small-Molecule Inhibition of HIV pre-m-RNA Splicing as a Novel Antiretroviral Therapy to overcome Drug Resistance." Plos Pathogens. 3, 1530-1539, 2007.

1.5 Interest in targeting SRSF1 as an anti-HIV/AIDS strategy: SR proteins are believed to play a redundant role in human cellular splicing. However, as shown in figures 17 and 18, the alternative splicing of HIV-1 mRNA is, for each event, dependent on a specific SR protein HIV-1 uses human SR proteins to ensure the production of crucial viral proteins.[93] These proteins are essential for commandeering and up-regulating the host cell machinery to produce new viral proteins through the process of alternative splicing.[124]

Selective inhibition of SRSF1 introduces a new approach to HIV/AIDS treatment wherein a human factor is targeted instead of a viral protein (RT, integrase or protease). A potentially important advantage to this approach is that as SR proteins are not susceptible to mutation in human cells, the question of drug resistance during HIV treatment may, thus, be eliminated.[31]

1.6 IDC-16, a platform for a research project: IDC16 is a planar (2D) hydrophobic tetracyclic indole compound that has the ability to intercalate DNA.[147,148,149,150] It displays "weak" cytotoxicity *in vivo*, and for this reason it has no potential as a drug for the treatment of HIV as a chronic infection.[97] To develop a safe anti-HIV/AIDS drug based on the mechanism of

action of IDC16 it will be necessary to design molecules that lose their affinity for DNA while maintaining potency and selectivity toward the alternative splicing factor SRSF1.

1.7 Research hypothesis: Based upon this reasoning, our hypothesis is:

The synthesis of appropriately functionalized and conformationally mobile ring opened mimics of IDC16 will lead to the identification of new HIV replication inhibitors that:

- **target the same protein as IDC16 and act through the same mechanism of action**
- **do not intercalate DNA**
- **retain similar or superior anti-HIV activity when compared to IDC16**
- **are not cytotoxic**

1.8 Design strategy and research objectives: Analysis of the structure of IDC16 suggests two elements that are deemed to be important for activity (**figure 21-I**):

- The N-methylpyridinone-imine, or A-ring, and indole(pyrrole) nitrogen, on the left side of the molecule.
- The 2-chloro substituted pyridine, or D-ring, on the opposite extremity.

And there are two elements deemed unimportant (**figure 21-I**):

- The pyrrole and phenyl rings, or B- and C-rings, respectively, whose only purpose is to provide hydrophobic contacts; these rings contribute to the undesirable flat polycyclic structure of IDC16.

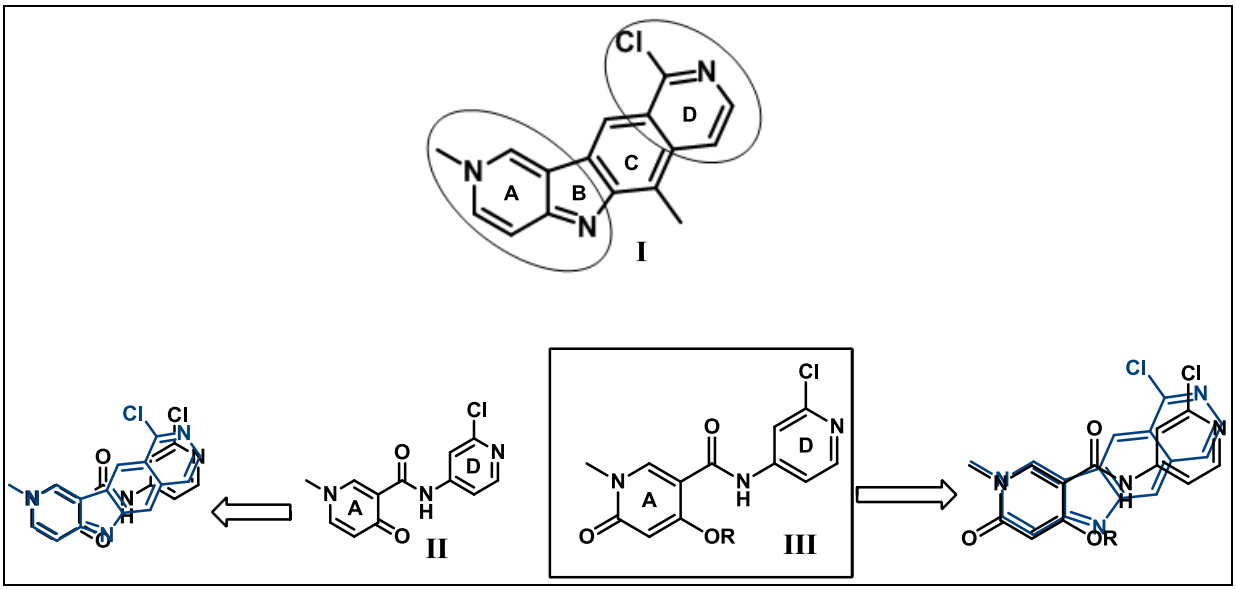

Figure 21. Design strategy. I. IDC16 with important elements, A and D rings, circled and unimportant B and C rings labelled. II. 4-pyridinone and its superposition on IDC16. III. 2-pyridinone and its superposition on IDC16.

Our design strategy is two-fold:

I) To identify suitable alternatives for the central portion of the molecule (rings B and C) that confer conformational mobility. In this context, it is probable that the flat structure of IDC16 does not permit optimal binding interaction with the SR protein target.

II) To modify the substituents on the A- and D-rings such that the derived molecules display greater potency relative to IDC16. We suspected that greater affinity or binding for the proposed target protein SRSF1 will be the consequence of improved and/or supplementary H-bonding opportunities and hydrophobic-type interactions.

In the absence of any structural biology data as to how IDC16 interacts with SRSF1, the project initially focused on the synthesis of "libraries" of conformationally mobile IDC16 mimics having a similar overall shape to IDC16 when projected in 2D. In other terms, these molecules can populate different low energy conformational spaces, including the planar conformational state.

In this context, we initially envisioned connecting rings A and D via a simple amide bond to create a di(hetero)aryl amide (DHA) structure, **II** (**figure 21**). Because the 2D representation of this type of compound places the A and D-rings in virtually the same space as in IDC16, this allows for the same types of contacts to be made with the target protein as are involved in IDC16 binding. In this way, mimicking the 2D structure of IDC16 should allow us to translate the information contained in its structure, which is essential to its anti-HIV activity, into a new type of compound that is active. The essential difference between IDC16 and the DHA compounds **II**, is the possibility for the heteroaromatic rings at each end of their structure to twist out of plane, i.e. rotation can occur around the bond attaching the amide C=O to the A-ring and around the bond from the amide nitrogen to the D-ring. Note that in structure **II** the nitrogen in the reactive imine motif has been replaced by an oxygen atom so as to provide a stable 4-pyridinone system. This substitution maintains the H-bonding potential of the indole nitrogen of IDC16. The 4-pyridinone scaffold was worked on separately in the laboratory by Dr. David Horhant, who used it to synthesize a library of DHA derivatives.

Built on this analysis, my research project has focused on the use of the alternative N-methyl-2-pyridinone system as the common "left side," or A-ring component in the synthesis of IDC16 mimics **III** (**figure 21**). By comparison to compound **II**, which very closely resembles IDC16, this project incorporates two intrinsic innovations:

- The presence of the carbonyl (C=O) functionality at the 2-position in ring A (i.e. adjacent to the nitrogen atom) in ring A.
- The presence of an oxygen atom at C-4 which can be functionalized in different ways in order to seek out supplementary binding interactions and/or to enhance solubility properties

The superposition of the 2-pyridinone **III** on IDC16 shows the similarities in 2D structure between the two molecules. However, in comparison to the 4-pyridinone **II**, the 2-pyridinone superposition does vary more from IDC16; therefore the synthesis of a library of IDC16 mimics built around the 2-pyridinone scaffold will allow for us to investigate the binding space beyond that which IDC16 occupies while bound to the SR protein target. This diverse library will contain molecules which have alternative H-bonding opportunities on the A and D rings that have the potential to strengthen the interaction with the target protein. Based on the five objectives below, that have been defined for this project, all of the molecules in the library can be categorized as amide-type mimics and C-4 substituted IDC16 mimics.

1.8.1 Objective-1: The initial experimental objective, expressed in **figures 21** and **22a**, was to develop a methodology to link the A and D rings via an amide bond to give benzanilide-type (diheteroarylamide; DHA) compounds in which the C-4 substituent corresponds to an OMe group. The D ring would be substituted with various (hetero)aromatic motifs. As illustrated in **figure 21** and **22b**, the 2D superposition of the amide analogue on IDC16 shows the two compounds are very similar. The carbonyl on C-2 and the substituents on the (hetero)aromatic ring project outside the space occupied by IDC16, allowing for the investigation of supplemental and optimal binding interactions.

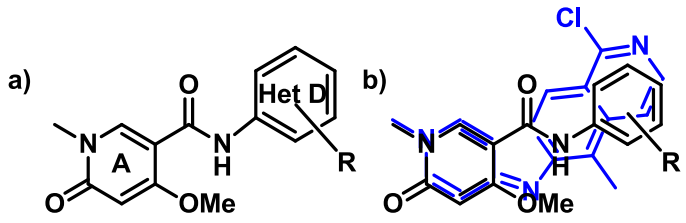

Figure 22: Objective-1. a) IDC16 amide analogue with the A and D rings labelled. b) The 2D superposition of the amide analogue and IDC16.

1.8.2 Objective-2: The synthesis of compounds in which the central amide bond is replaced by a 1,2,4-oxadiazole motif, a known amide bond bioisostere[151], **figure 23a**. The fundamental reasons that motivate this choice are:

- Oxadiazoles possess different physiochemical properties than their amide counterparts. They are often used to replace esters or amides because they have a greater hydrolytic and metabolic stability.[152] This superior stability often results in improved pharmacokinetics and *in vivo* performance.
- The synthesis of the oxadiazole ring system is, in certain cases, proven to be operationally easier and higher yielding relative to amide bond formation. This is likely to also be one reason why oxadiazoles are present in a number of biologically active molecules and drugs.[153]
- The substituted oxadiazole ring and amide bond have a different geometry. The "2D" structure, shown in **figure 23b** differs from IDC16, in terms of the spatial orientation of the "D-ring". This makes it a good candidate to explore the binding space into which IDC16 fits by attaching various aromatics and heteroaromatics to the ring.

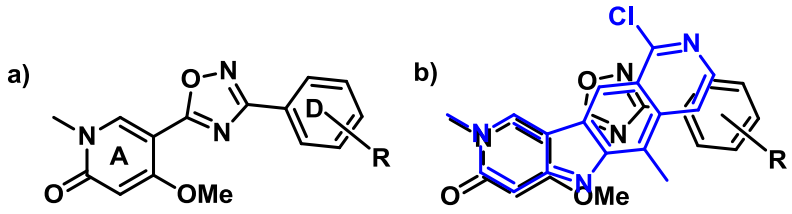

Figure 23: Objective-2. a) 1,2,4-oxadiazole analogue with A and D rings labelled. b) oxadiazole superimposed on top of IDC16 (in blue).

1.8.3 Objective-3: To synthesize IDC16 analogues in which the amide linkage in **figure 22** is embodied in an isoxazolidin-6-one that is fused to the 2-pyridinone scaffold (**figure 24**). This provides more highly constrained IDC16 mimics in which the D-ring occupies a defined position in the IDC16 binding space. Note that for this objective particular attention will be given to exploring the influence that attaching bicyclic D-ring motifs onto the N-5 nitrogen has on anti-HIV activity. **Figure 24a** shows that a bicyclic ring system best mimics the right side or D-ring of ICD16 (i.e. one of the rings superimposes on the D-ring of IDC16). Importantly, attaching a simple monocycle on N-5 as in **figure 24b** provides a structure that is significantly different from IDC16. This allows for the further investigation of the binding space occupied by IDC16. It

is interesting to note that although the 2D projection closely resembles IDC16, it is probable that the two ring systems in these molecules are significantly skewed (i.e. out of plane). ChemBioDraw was used to predict the 3D shape of these molecules and the D-ring was perpendicular to the A-ring. This should influence strongly the capacity for such molecules to intercalate DNA.

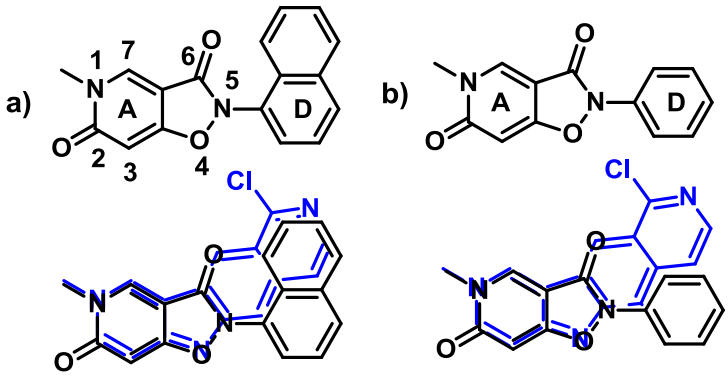

Figure 24: Objective-3. a) Isoxazolidin-6-one analogue with A and D rings labelled and the ring structure numbered. Bicyclic-system, superimposed on IDC16 shows it is very close in 2D structure. b) Monocyclic-system, superimposed on IDC16 shows its 2D structure is different than IDC16 with respect to the D-ring.

1.8.4 Objective-4: Looking further at the positioning of the D-ring component in the DHA analogues, the goal was to synthesize compounds where a 4-arylpyrazolidinone structure is fused to the 2-pyridinone scaffold (**figure 25a**). In these analogues, various (hetero)aromatics will be attached at the position 4 nitrogen. In comparison to the isoxazolidinone structures in objective 3, the D-ring is projected downward with respect to the 2-pyridinone A-ring. **Figure 25b**, displays the difference in the 2D structure between these mimics and IDC16; the A-ring remains the same but the D-ring is now occupying a space previously unoccupied by IDC16. This alteration has the potential to capture alternate binding interactions with the SR protein target.

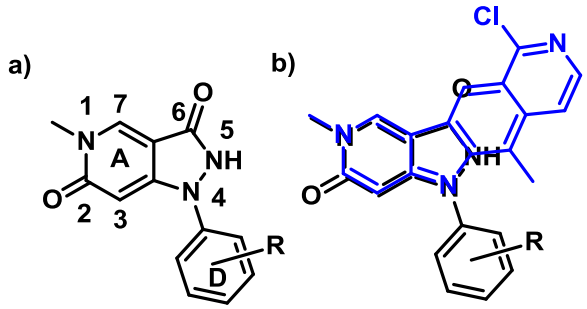

Figure 25: Objective-4. a) Arylpyrazolidinone analogue with A and D rings labelled and the ring atoms numbered, where R is different substituents attached at different positions on the D-ring. b) Arylpyrazolidinone analogue superimposed on IDC16. The D-ring is projected into space not occupied by IDC16.

1.8.5 Objective-5: Expanding on objective 4, the idea is to synthesize a compound library where amines and alcohols are attached at the C-4 position of the 2-pyridinone (**figure 26a**). The diarylether or diarylamine bond allows for further investigation of binding to the proposed protein target SRSF1; as seen in **figure 26b**, the 2D structure of the D-ring is very different from IDC16. In fact, these compounds are less constrained forms of the ring systems in objective 4, **figure 25a**. Furthermore these structures will introduce 3D character into the collection of compounds synthesized because the aromatic rings can rotate out of plane around the ether or amine bond.

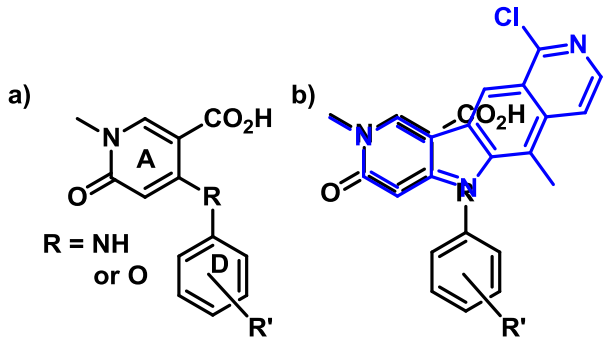

Figure 26: Objective-5. a) Biarylamine/ether analogue with A and D rings labelled. b) The superposition of the analogue on IDC16, the right hand side of 2D structure differs greatly from IDC16.

1.9 Project summary: Compared to IDC16, the 2-pyridinone scaffold has more sites for substitution, and the derived IDC16 mimics defined in objectives 1 to 5 are easier to synthesize. The ring opened nature of the mimics allows for the introduction of 3D character and different spatial orientation when compared to IDC16. As the hypothesis states, these changes will be explored in an effort to increase potency and selectivity with regards to anti-HIV activity

and reduced cytotoxicity. Through these five objectives, the project has made the following conservations of and adjustments to IDC16:

- The polar nature of the A and D rings has been conserved.
- The B and C rings have been replaced.
- Different shapes and 2D structures with respect to IDC16 have been explored.
- An option for mobility has been introduced allowing the molecules to twist out of plane.

2. Chemistry: Results and Discussion

2.1 2-Pyridinone synthesis: To synthesize all molecules defined within the 5 objectives, it was first necessary to access the starting 2-pyridinone scaffold **4**. This compound was readily prepared in two steps according to the literature and is illustrated in **scheme 1**.[154] This involved the reaction of diethyl 1,3-acetonedicarboxylate with triethyl orthoformate ($(EtO)_3CH$) to give intermediate **1**. This intermediate was in turn reacted with methylamine to produce the pyridinone **2**. In this multistep, one-pot process, the cyclization of **1** to **2** occurs by a 1,4-addition of the amine followed by retro-Michael elimination of the anion ^-OEt to give **I**. Subsequently, the lone pair on the nitrogen in **II** engages in a nucleophilic attack on the ester C-6 carbonyl carbon resulting in amide formation giving **III** and the loss of another molecule of ^-OEt. Note that ammonium hydroxide or different alkylamines can be used instead of methylamine to synthesize different N-substituted pyridinones.[155] Ethyl 4-hydroxy-N-methyl-2-pyridinone-5-carboxylate **2** was then elaborated to N-methyl-4-methoxy-2-pyridinone-5-carboxylate **3** by O-methylation using cesium carbonate (Cs_2CO_3) and dimethyl sulphate and subsequent ester hydrolysis using lithium hydroxide (LiOH) in THF:MeOH:H_2O (2:2:1) (tetrahydrofuran:methanol:water) at room temperature provided the target compound 4-methoxy-N-methyl-2-pyridinone-5-carboxylic acid **4** in an overall yield of 85%.

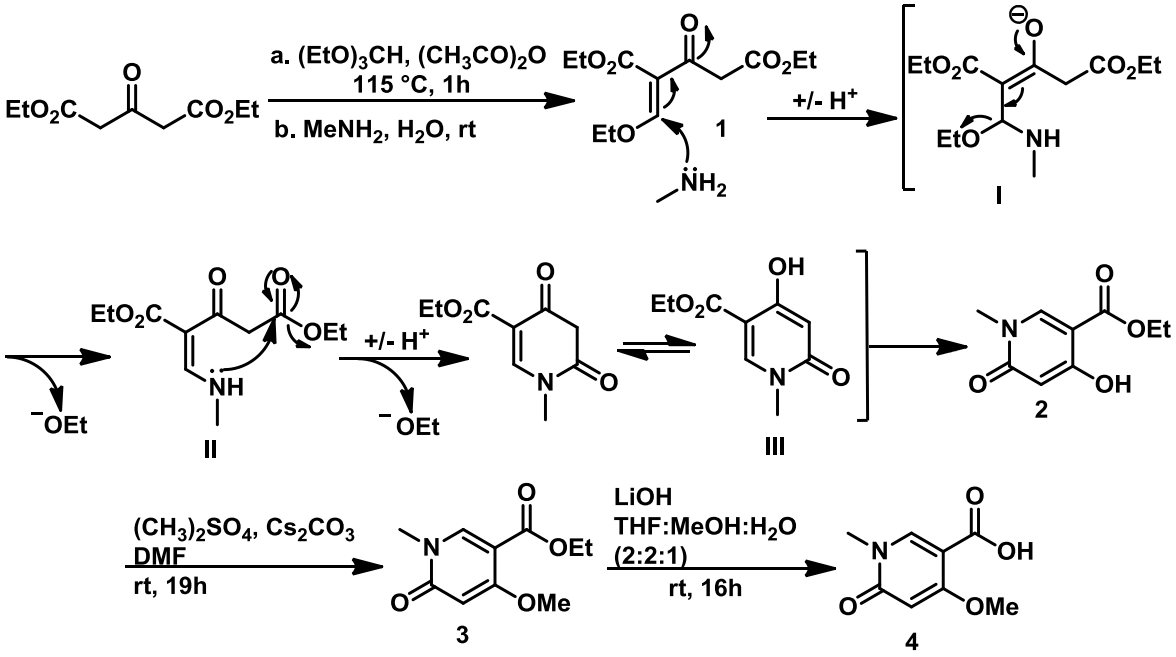

Scheme 1: 2-Pyridinone synthesis. Compound 4 was obtained in a 3-step synthesis, starting from diethyl 1,3-acetonedicarboxylate and triethyl orthoformate with methyl amine to give compound 2. O-Methylation at C-4 gave compound 3 which was reduced to the carboxylic acid 4.

An alternative synthesis of **3** would require the C-4 OH group to be replaced by a chlorine atom (Cl) through the reaction of **2** with phosphorous oxychloride ($POCl_3$), to give **7**, followed by displacement of Cl by methoxide anion to give **3**. However, under these conditions preferential transesterification occurred to produce a mixture of the methyl and ethyl ester products in which complete Cl to OMe displacement was not achieved. The dimethyl sulphate O-methylation procedure thus proved to be the most effective.

The structures of compounds **2-4** were verified by NMR (nuclear magnetic resonance) and mass spectroscopy. For compound **2** the NMR data corresponds to the values reported in the literature.[154] For all three compounds there are two characteristic peaks; the proton at position 3 was found at 5.71 ppm and the C-6 H was found at 7.90 ppm (in DMSO-d6). **Figure 27** shows the NMR spectrum of the starting 2-pyridinone-5-carboxylic acid **4**, the peaks corresponding to positions 3 and 6 are highlighted. The chemical shifts of the H-3 and H-6 differ because they are in different chemical environments. As seen in **figure 28a**, C-6 is the β-carbon to the exocyclic carboxylic acid. The β-carbon is electron poor, with a partial positive (δ^+) charge and therefore the proton is deshielded and more downfield. The proton attached to C-3 is the β-proton to an electron donating methoxy group, **figure 28b**. This makes the carbon inherently δ^- and since the

proton is in an electron rich environment it is shielded and therefore more upfield than the proton at C-6.

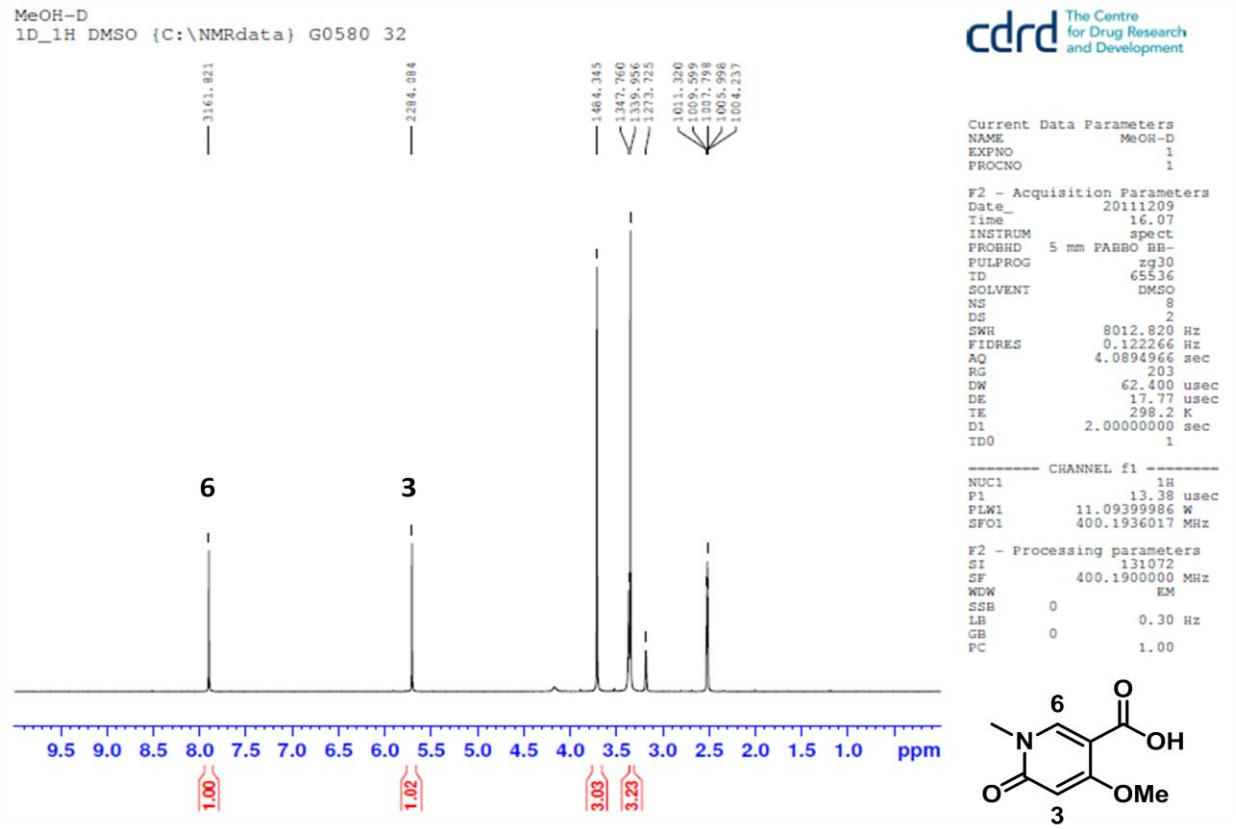

Figure 27: NMR spectra of 2-pyridinone starting material (4). The peaks corresponding to the protons on C-3 and C-6 are labelled.

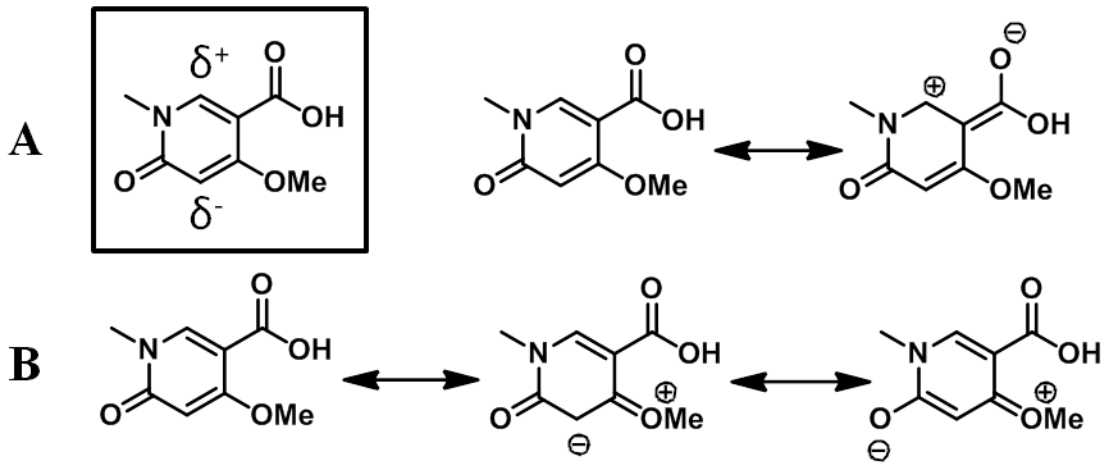

Figure 28: Electronic environment of H-3 and H-6 in the 2-pyridinone (3). A. The proton at C-6 is in a δ^+ environment because it is attached to the β-carbon of a carboxylic acid. B. The proton at C-3 is attached to the β-carbon of an electron donating methoxy group and therefore in a δ^- environment.

According to the literature, the difference observed between the chemical shifts of the protons at C-6 and C-3 in the 2-pyridinone is characteristic of protons in similar environments. As seen in **figure 29a**, the *cis*-proton to the methyl ether is in an electron rich environment and has a chemical shift of 5.36 ppm, comparable to the C-3 proton on the 2-pyridinone.[156] A similar trend is observed with crotonic acid, **figure 29b**. The α-proton and β-proton to the carboxylic acid have chemical shifts of approximately 5.8 ppm and 7.1 ppm, respectively.[157] In both of these examples, the δ^- carbon has a more upfield chemical shift and the δ^+ carbon has a more downfield chemical shift; this is the same trend observed with the 2-pyridinone.

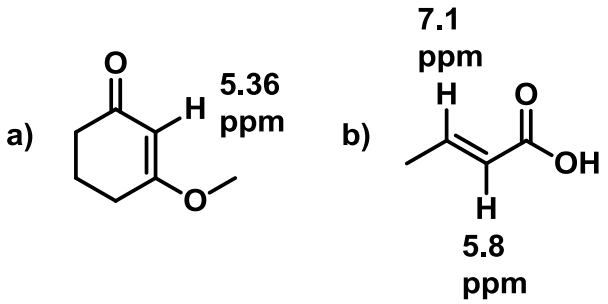

Figure 29: Literature examples of chemical shifts of H-3 and H-6. a) The chemical shift of the α (5.36 ppm) proton in 3-methoxycyclohex-2-enone. b) The chemical shifts of the α (5.8 ppm) and β (7.1 ppm) protons in crotonic acid.

2.2 Amide library: A library of 16 amide analogues **5a-q** was synthesized by reacting pyridinone carboxylic acid **4** with different aromatic and heteroaromatic amines that were selected based on their structure, functionality or biological significance. Please note that the amines used to synthesize compounds **6b**, **e**, **f** and **10d** were synthesized by Dr. Mitra Matloobi. Initially, the peptide-type coupling was attempted using oxalyl chloride ($(COCl)_2$) in dichloromethane (DCM) with DMF (dimethylformamide) as a catalyst. A strong motivation for selecting this procedure was that, due to the mild conditions of this reaction and the absence of formation of contaminating by-products, the formation of the different amides could be carried out in parallel using a synthesis robot. This would have allowed for 10-20 reactions to be performed at the same time, speeding up the synthetic process. Unfortunately, this procedure proved to be ineffective as starting material 2-pyridinone-5-carboxylic acid **4** was not soluble in DCM. As a result, the conversion to product was typically low, 0-15%. For this reason we turned to the use of thionyl chloride ($SOCl_2$). Using $SOCl_2$ as both the reagent and the solvent, the conversion of 2-pyridinone-5-carboxylic acid **4** to its corresponding acid chloride derivative was

complete when carried out at reflux for one hour. Unfortunately, due to the corrosive nature of this reagent it was not possible to adapt this procedure to the synthesis robot. Further, as the intermediate acid chloride **4a**, a white solid (not purified), is moisture sensitive, prior preparation of this compound on a large scale and its use as a reagent in the amide coupling on the robot was similarly precluded.

In separate and sequential experiments the acid chloride **4a** was generated, the excess $SOCl_2$ was removed under vacuum and the derived acid chloride was reacted with a series of different amines, at room temperature, using pyridine as both the base and solvent, to give the amides **5a-q** (**Scheme 2**).

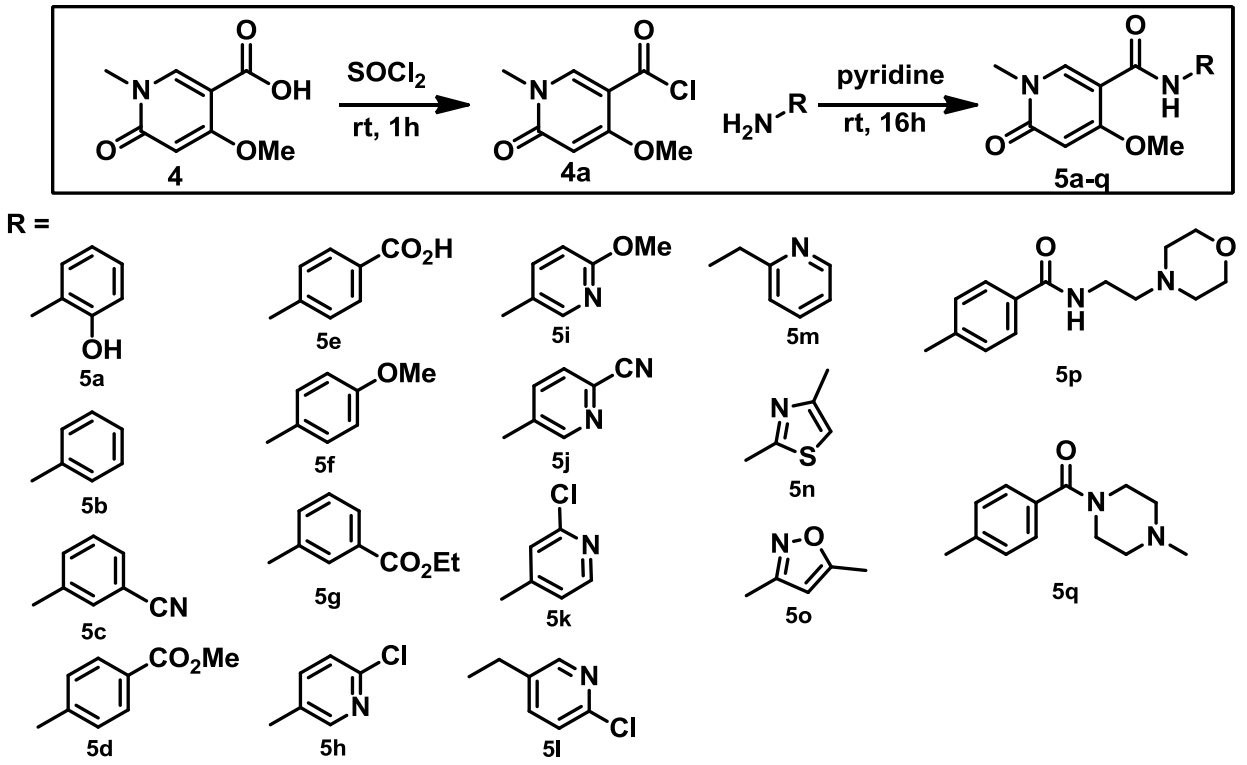

Scheme 2: Amide bond formation using $SOCl_2$ and pyridine. The synthesis was used to make amides 5a-q.

Several difficulties were encountered during the synthesis of the amide library **5a-q**, under these conditions. Using pyridine as a base (to absorb HCl) and as the solvent was effective with the simple amines but less effective with more non-nucleophilic ones. Using an unreactive, poorly nucleophilic amine and a highly reactive acid chloride can result in alternate quenching of the acid chloride through reaction with impurities in the commercial amine reagent, through

reaction with pyridine solvent, or in the decomposition of the acid chloride itself via a ketene-"like" intermediate whereby the pyridinone nitrogen promotes the loss of a chlorine anion (**figure 30**). One or more of the alternative reactions described was probably occurring in some of the amide couplings as two main observations were noted. There were multiple spots visible on TLC (thin layer chromatography) corresponding to compounds other than the desired product, resulting from the possible side reactions previously discussed. Alternatively, the TLC displayed mostly starting material, the 2-pyridinone-5-carboxylic acid **4** and the amine. This means the amine was non-nucleophilic and nonreactive towards the acid chloride **4a** and therefore no amide bond was formed and since the acid chloride is not stable on TLC it was quenched to reform the carboxylic acid. Further, as it was difficult to entirely remove pyridine under vacuum, purification using silica gel flash column chromatography was challenging because pyridine altered the polarity of the eluent. This caused the desired amide to move through the column too quickly, not allowing it to be separated properly from the reaction impurities.

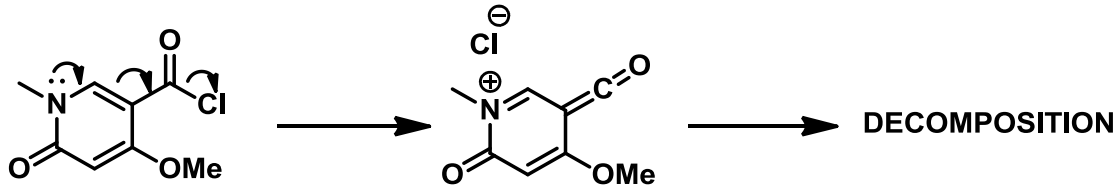

Figure 30: Acid chloride decomposition. The lone pair on the 2-pyridinone nitrogen promotes the loss of the chlorine atom. This results in a ketene-like intermediate which is highly unstable and very reactive. There are multiple locations which can react and will result in the decomposition of the 2-pyridinone

To overcome the problems experienced with this procedure, peptide coupling using BOP-Cl (bis(2-oxo-3-oxazolidinyl)phosphonic chloride) was studied. Amides **5p** and **5q** were prepared using BOP-Cl in the presence of triethylamine (Et_3N) and N,N-dimethylethylenediamine in DMF at room temperature.[158] However, this procedure was quickly abandoned, as isolation and purification were more challenging than the acid chloride and pyridine procedure because there were more side reactions that occurred, according to TLC.

To overcome the problems with the use of pyridine in the acid chloride procedure, it was replaced with Et_3N as the base and THF as the solvent. For nine amides (**6a-i**) the acid chloride **4a** was synthesized in the same manner, using $SOCl_2$, and was reacted with the requisite amines in dry THF, with Et_3N (**scheme 3**).[159] In the experiment, the acid chloride was soluble in THF and most of the amines were at least slightly soluble. This procedure was more effective for the peptide-type couplings and resulted in higher yields (average of 64% versus an average of 41%)

and, in some cases, easier isolation of the target compound. As the THF was easily removed and less polar than pyridine, it did not interfere with purification using silica gel flash column chromatography.

Note also, that an alternate purification procedure whereby the crude mixture was simply washed with acetone could be used to obtain compounds **5c-e** pure. As these polar amide products were not soluble in acetone, this method could be used to wash out the non-polar impurities. In the remaining instances, washing with acetone was used as a pre-purification measure to make silica gel column chromatography easier.

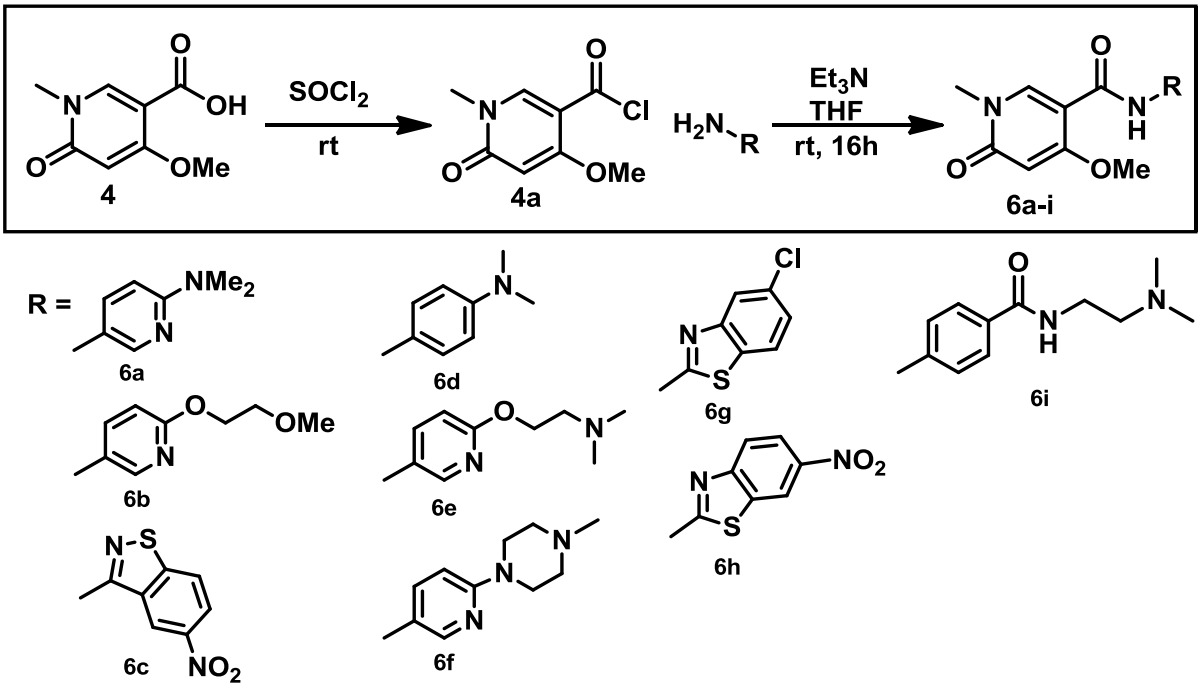

Scheme 3: Amide synthesis using $SOCl_2$ and Et_3N. This procedure was used to synthesize amides 6a-i.

The procedure, using Et_3N, had one major drawback; triethylammonium chloride ($Et_3NH^+Cl^-$) and other unidentified contaminants were present in many of the products. Treating the crude product mixtures with aqueous potassium bicarbonate ($KHCO_{3(aq)}$) worked for some compounds but not all. This problem was overcome by changing the base to potassium carbonate (K_2CO_3). Under these conditions a cleaner reaction occurred as the KCl produced was easily removed by adding water to the crude mixture and filtering. Subsequent amide couplings to give **24a-h** and any repeated amide formations from **scheme 2** to **4**, were performed using this procedure. Reaction work-up, isolation, purification and yields all improved. Furthermore,

carrying out the reaction such that the amine was added to the acid chloride at 0°C and under a nitrogen atmosphere contributed to the higher yields observed using this procedure.

Another challenge encountered was that the target compounds (**5a-q** and **6a-i**) had poor solubility in organic solvents, making their purification more challenging. In order to increase the solubility of the product molecules a methoxyethanol chain was introduced at C-4 on the 2-pyridinone scaffold in place of the methoxy group as in **3**. This substitution successfully increased the solubility of the amides and circumvented these difficulties. The longer chain also had the potential to provide supplementary binding interactions with the target protein. It is logical to think this chain will slightly decrease the compounds' water solubility and this is confirmed by mathematically determining the partition coefficient using ChemBioDraw. The partition coefficient (log p) for 4-methoxy-2-pyridinone-5-carboxylic acid **4** is -1.55 and for 4-(2-methoxyethoxy)-2-pyridinone-5-carboxylic acid **9** the log p is -1.7. A larger log p value indicates the compound is more soluble in octanol than water. However, because the difference between the two values is very small, the change in water solubility should be minimal and not detrimental.

To obtain compound **9** (**scheme 4**) ethyl N-methyl-4-hydroxy-2-pyridinone-5-carboxylate **2**, was reacted with $POCl_3$ in the presence of Et_3N to substitute the 4-position OH with chlorine, **7**. This was followed by hydrolysis of the ethyl ester using aqueous LiOH to give N-methyl-4-chloro-2-pyridinone-5-carboxylic acid, **8**. The methoxyethanol chain was introduced by reacting **8** with a solution of Na in methoxyethanol to give compound **9**. As mentioned, transesterification was a problem previously (see section 2.1) but in this instance it did not occur as the anion of carboxylic acid **8** does not engage in ester formation. The preparation of amides **10a-f** from acid **9** was achieved via the acid chloride route ($SOCl_2$, followed by the addition of the amine and Et_3N in THF). Note that isolation of some of the product molecules, **10a, d-f** was also hindered by contamination by Et_3N salts. However, the alternative procedure using K_2CO_3 should enable us to circumvent this problem in future work.

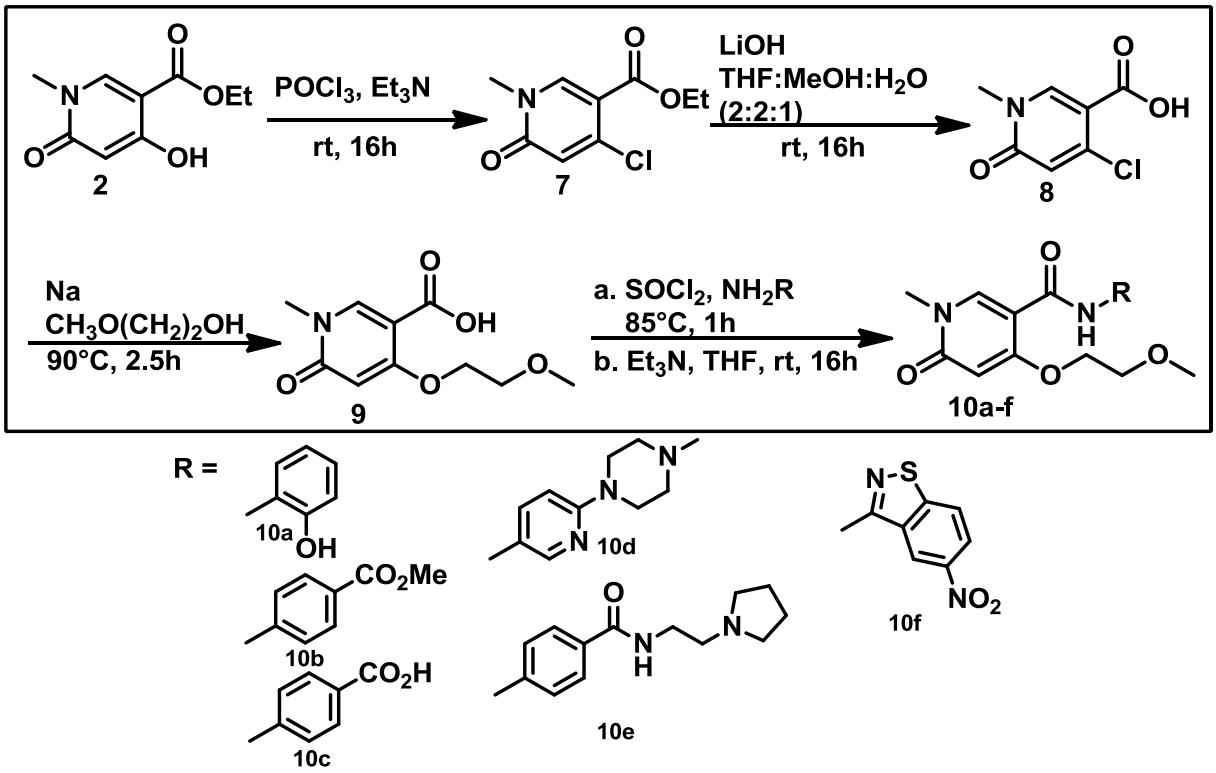

Scheme 4: C-4 methoxyethanol amide synthesis. This procedure introduced a methoxyethanol substituent at C-4 in the 2-pyridinone to give compound 9. Compound 9 was then used to synthesize amides 10a-f.

The structures for the DHA compounds were confirmed by NMR and mass spectroscopy. As in the spectra for compounds **2-4**, the peaks corresponding to H-3 and H-6 in the proton spectrum were observed at 5.9 ppm-6.0 ppm and 8.2 ppm-8.5 ppm, respectively. The NMR spectra indicated the presence of the amine component in the product and the mass spectra confirmed product formation. As expected, the chemical shift of the protons at positions 3 and 6 of the 2-pyridinone did not vary much between the amide products. The small variation in the proton at position 6 can be attributed to the difference in polarity of the aromatic and heteroaromatic rings attached at position 5 by an amide bond. A more polar substituent slightly decreases the electron density at C-6 resulting in a deshielded proton and a downfield shift. **Figure 31** shows the NMR of compound **5h**, where each proton and its corresponding location on the molecule is also labelled.

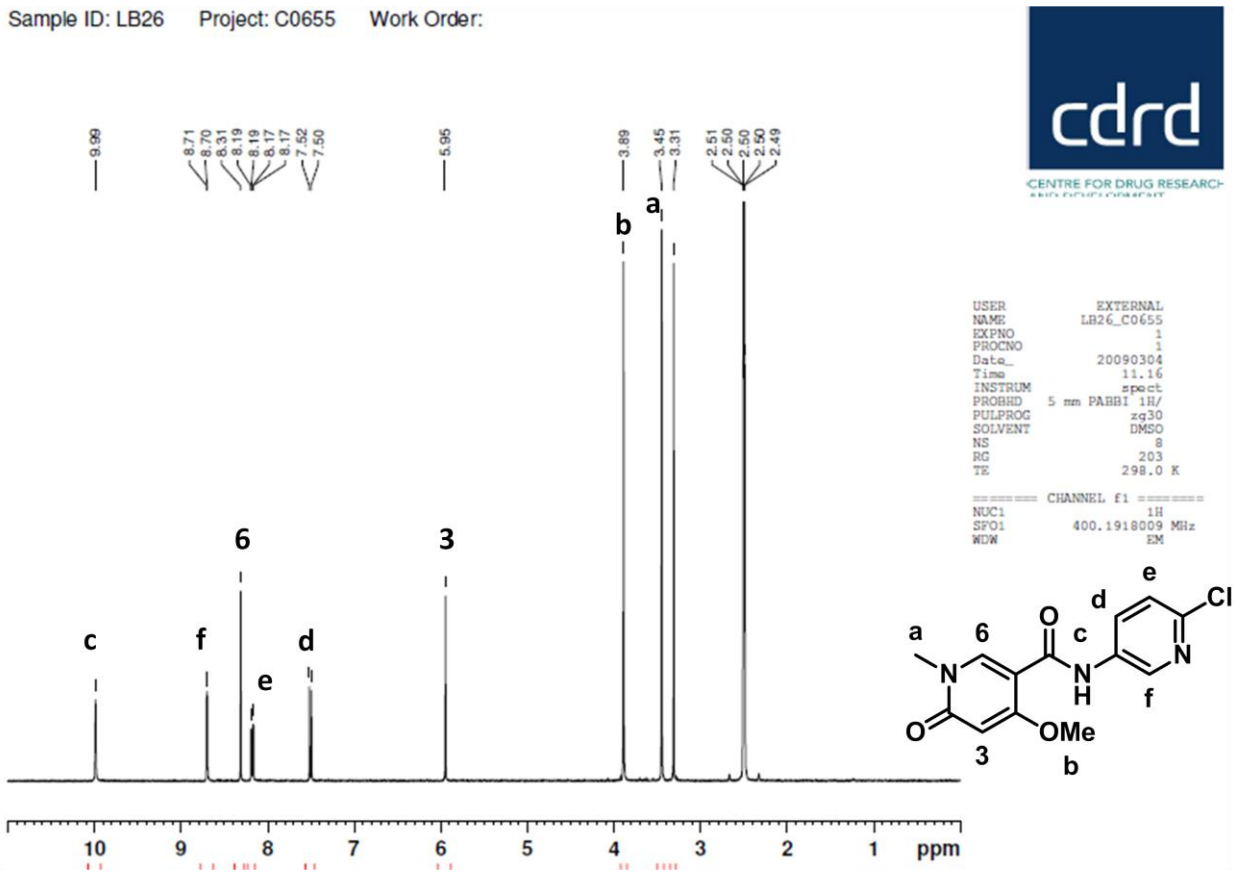

Figure 31: NMR characteristic of an amide (5h). The peaks corresponding to the protons at position C-3 and C-6 are labelled with numbers and the remaining protons are labelled with letters.

Overall, the average yield for the procedure using pyridine was about 41% (exact yields ranging from 14-77%), and approximately 64% (ranging from 9-113%) for the Et_3N and THF procedure on both the C-4 methoxy and C-4 methoxyethoxy substituted 2-pyridinones. Note, that the yields for the Et_3N and THF procedure are inflated, and occasionally greater than 100%, due to the presence of the triethylammonium salt in the final compound thereby adding mass to the measured yield. In general, the amide coupling procedures were unpredictable; some amines worked well, others did not, making purification and isolation challenging regardless of the method used. This is likely because the acid chloride is highly reactive and was partially quenched or decomposed before reacting with the amine. The reactivity of the acid chloride in the amide coupling reactions can be controlled by decreasing the temperature to 0°C and maintaining a nitrogen atmosphere environment. This was consistently done with the K_2CO_3 procedure and, referring to section 4, the average yield for this procedure was 50% (ranging from 9-99%). Moreover, the distinct advantage to using these conditions was that there was no salt

present so final yields were more accurate and purification was much easier. However, the reactivity of the non-nucleophilic amines was not addressed with these changes.

2.2.1 Copper coupling: As the acid chloride procedure was not easily generalizable to the wide range of aromatic and heteroaromatic amines that were used to construct the library of DHA compounds, alternative strategies were investigated to incorporate the D-ring component into these molecules. Copper (Cu) chemistry, i.e. Cu catalyzed amide Ar-Br coupling, is a potentially more efficient strategy as it circumvents the problems experienced (and outlined above in section 2.2) using unreactive amines. This technique has been effectively used to couple a wide range of heteroaromatic primary amides with arylhalides. [160]

Initially, we attempted copper coupling on the primary amide derivative **11a**, prepared by reacting ethyl N-methyl-4-methoxy-2-pyridinone-5-carboxylate **3** with a solution of ammonia in methanol (**scheme 5**).[161] Remarkably, reaction of this intermediate with copper iodide (CuI), N,N′-dimethylethylenediamine, K_2CO_3 and iodobenzene in DMF at 110°C for 24 hours resulted in preferential addition of the phenyl group to C-3 of the 2-pyridinone to give compound **12a** in 10% yield after purification by column chromatography.[160] In light of this result, the corresponding reaction was carried out on N-methyl-4-phenoxy-2-pyridinone-5-carboxamide **11b**, substituted by a more bulky phenoxy group at C-4 (see section 2.5 for the synthesis of this 4-phenoxy-2-pyridinone). In this instance, the desired coupling reaction with iodobenzene worked well, giving compound **12b** in 70% yield (**scheme 5**). Taken together, these results indicate that when there is a bulky substituent on C-4, the Cu coupling of the primary amide function occurs as planned. Thus, if the copper coupling approach is to be utilized in the future, it will be necessary to ensure that an appropriate bulky group is present at C-4.

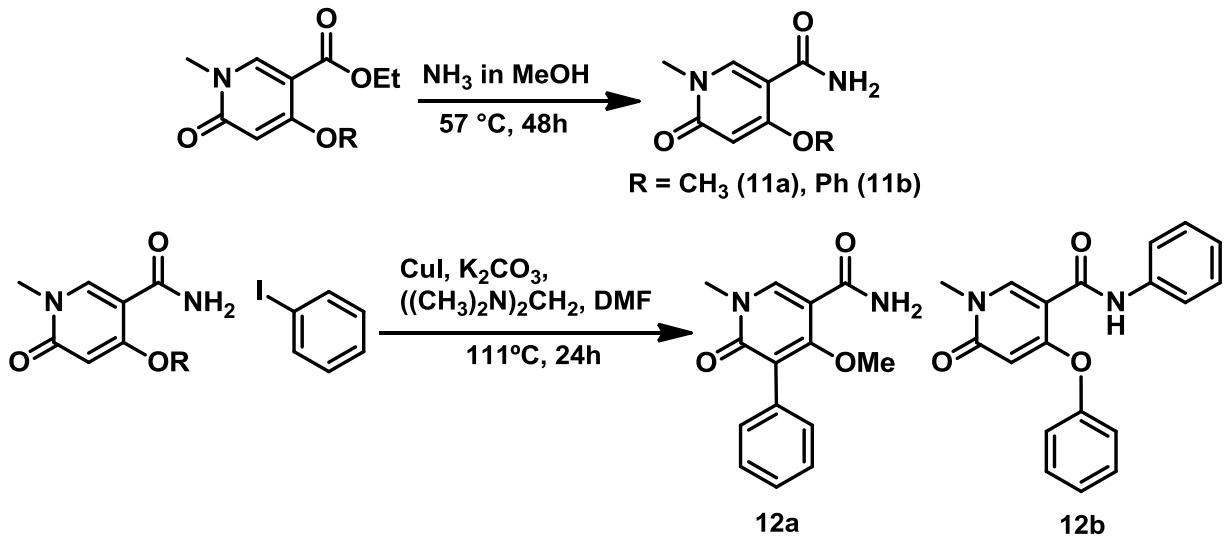

Scheme 5: Copper chemistry. The primary amides of C-4 methoxy and phenoxy substituted 2-pyrdinones were synthesized using ammonia. Copper coupling between the primary amides and iodobenzene followed in the presence of copper iodide (CuI) and potassium carbonate. Coupling proceeded as expected for compound 12b with a phenoxy at C-4. However, coupling occurred at C-3 when a methoxy was present at C-4.

Addition at the C-3 position of a pyridinone has been reported in the literature. For instance, the iodo group in 3-iodo-4-phenoxypyridinone (IOPY) was displaced by various heteroaromatics and alkyl chains. According to **scheme 6a**, iodine was substituted at C-3, using various methods, including the use of copper iodide and, separately, copper cyanide.[162] The proton at position 3 in the 2-pyridinone **11a** is in a malonate-type environment. Metal (Pd or Cu) coupling of an enolate like **11a** with an aryl halide is demonstrated in the literature. For example, coupling of 3,6-bromo-2,4-methoxybenzoquinone with an indole boronate using palladium is shown in **scheme 6b**.

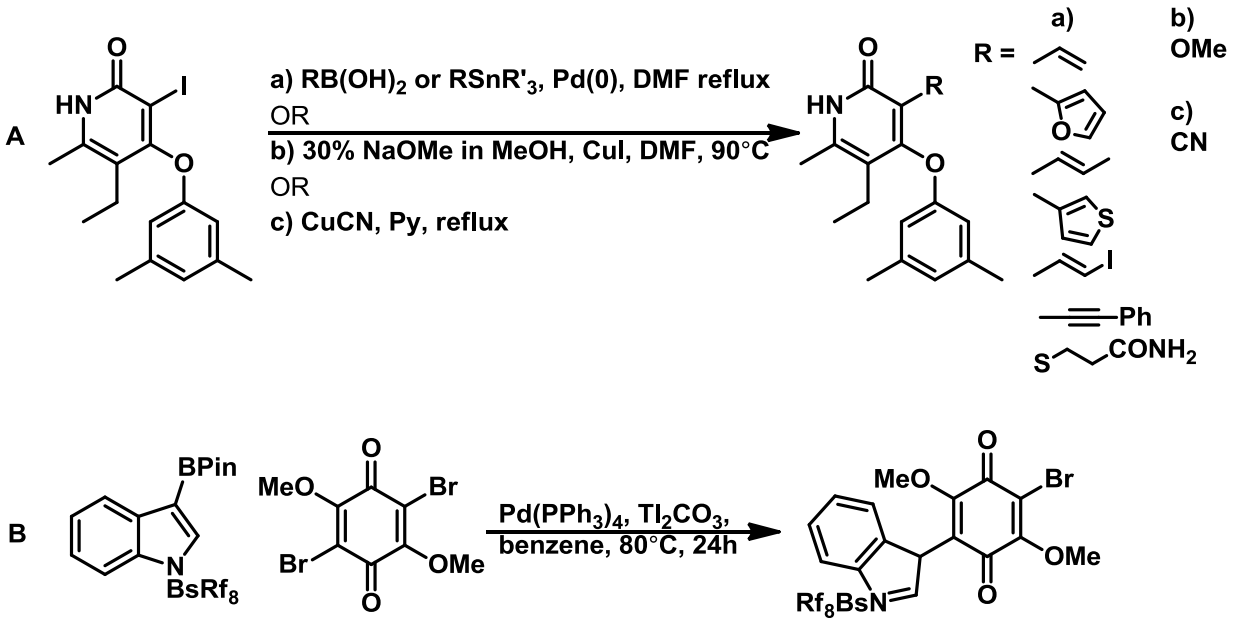

Scheme 6: Copper coupling examples from the literature. A. Coupling of IOPY with various R groups using procedure a, b or c. B. Palladium coupling of 3,6-bromo-2,4-methoxybenzoquinone with an indole boronate.

The mechanism for the copper coupling reaction shown in **scheme 5**, begins with copper (I) iodide reduced to copper (0) by binding of the ligand (N,N′-dimethylethylenediamine). This is followed by an oxidative addition of iodobenzene, resulting in copper (II). A transmetallation occurs where the amide adds to copper and iodine is picked up by the base. Finally, there is a reductive elimination where the two components in the complex come together to form the product and the catalyst (copper (0)) is regenerated. In the case where there is a methoxy substituent at C-4, C-3 of the 2-pyridinone will be deprotonated and the transmetallation will occur at that location.

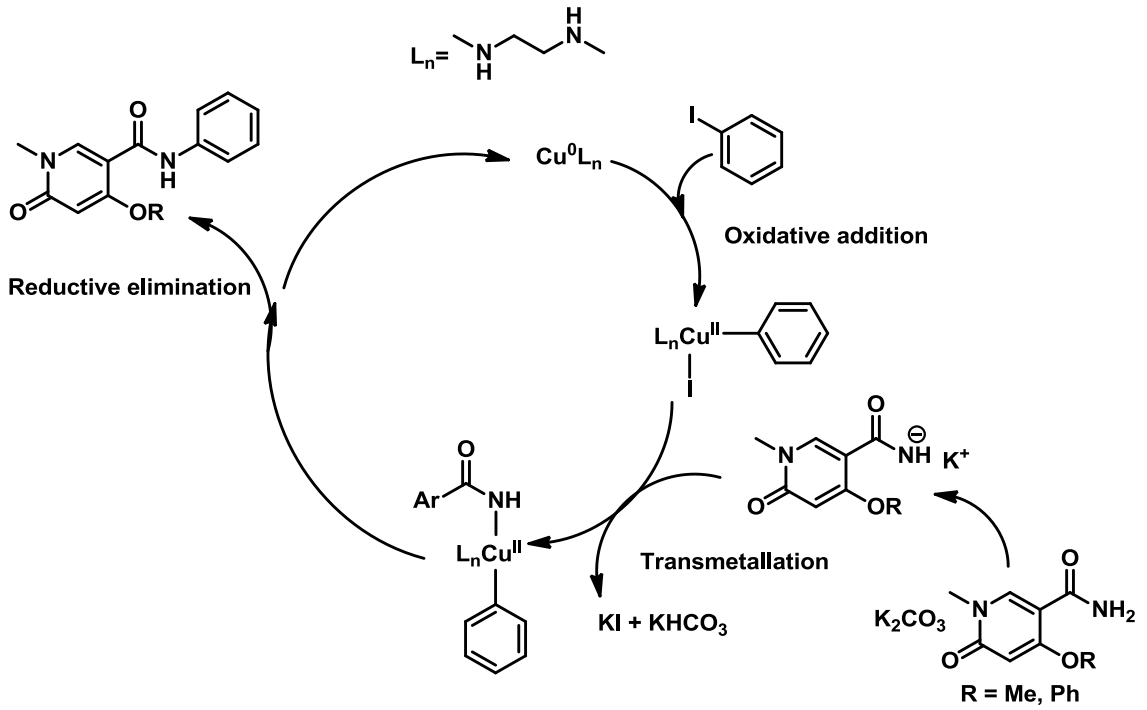

Scheme 7: Copper coupling mechanism. It begins with an oxidative addition of iodobenzene. Then there is a transmetallation whereby the amide adds to the catalyst. This is followed by a reductive elimination of the desired coupling product and regeneration of the catalyst.

2.3 1,2,4-Oxadiazole library: The second objective was to synthesize a library of 1,2,4-oxadiazole compounds. The synthesis of oxadiazoles **13a-m** (**Scheme 8**) was achieved by reaction of the acid chloride **4a**, obtained by refluxing **4** in $SOCl_2$, with the requisite amidoxime **13a-m** in the presence of K_2CO_3 and under a nitrogen atmosphere. The amidoximes precursors were synthesized by a "Directed Studies" student, Anthony Gador. This involved reaction of a (hetero)aromatic nitrile with hydroxylamine hydrochloride in the presence of sodium bicarbonate ($NHCO_3$) in an ethanol/water mixture (4:1).[163] Each amidoxime product was purified by recrystallization and used as provided, to synthesize the 1,2,4-oxadiazoles.

The construction of the oxadiazole ring involved, in the first step, the formation of the intermediate O-pyridoylamidoxime, **IV**, via attack of the amidoxime oxygen anion on the acid chloride carbonyl carbon centre. The HCl liberated in this reaction was absorbed by K_2CO_3. The isolated (not purified) intermediate **IV** was, in turn, heated in DMF to effect ring closure by intramolecular nucleophilic attack of the amine on the carbonyl carbon to give **V**, which spontaneously aromatized through the loss of a molecule of water. Compounds **13a-m** were synthesized in yields ranging from 11-63%, with an average yield of 32% after purification by

column chromatography. K_2CO_3 was used instead of Et_3N in an attempt to eliminate the problems experienced in objective 1 with the $Et_3NH^+Cl^-$ salt.

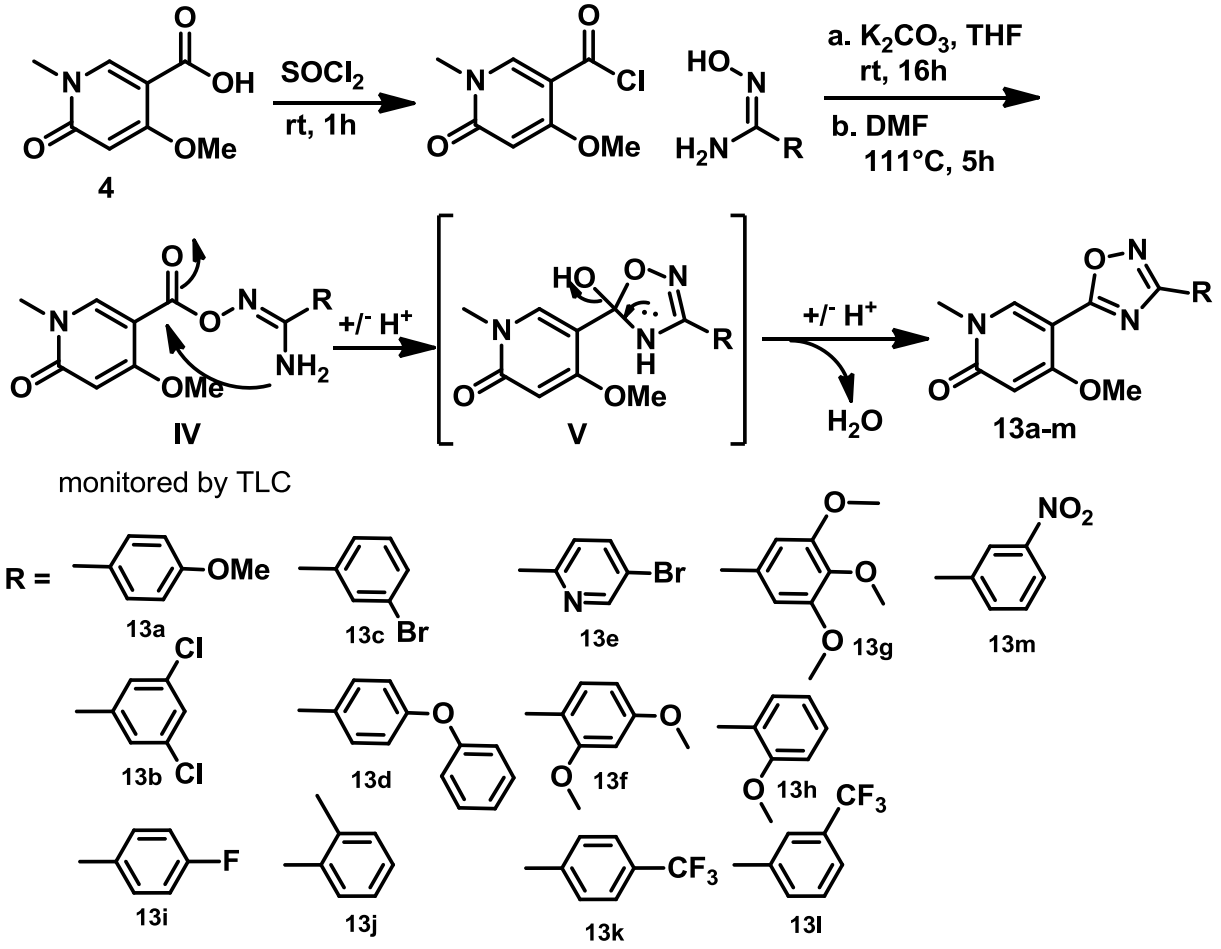

Scheme 8: 1,2,4-Oxadiazole synthesis. This procedure was used to synthesize the oxadiazoles 13a-m.

The NMR spectrum for compound **13i**, **figure 32**, serves to illustrate that typically in the product molecules **13a-m** there is very little change in the chemical shift of the proton at C-6 relative to the same hydrogen in the starting 2-pyridinone-5-carboxylic acid **4**. As the polarity of the (hetero)aromatic substituent on the oxadiazole component changes, a relatively small shift in the H6 proton occurs (8.35 ppm-8.83 ppm). This occurs because the C-6 proton experiences an environment primarily influenced by the oxadiazole. A change in polarity of the (hetero)aromatic ring has less of an influence because it is not in close proximity to the C-6 proton. As expected, the chemical shift of the proton at C-3 did not change between compounds **13a-m** (6.03 ppm-6.06 ppm) because its environment did not change. Replacing the substituent on C-4 would alter

the H3 proton's environment however this did not happen because a methoxy group was present at C-4 on all molecules.

Globally, the oxadiazole compounds were more soluble in organic solvents than the corresponding amides prepared in objective 1. Thus, purification and isolation of the desired product was easier. Isolated product yields ranged from 11-63%. Changing the base from Et_3N, used in the amide coupling reactions, to K_2CO_3 was motivated by the problems experienced with removing the triethylammonium chloride salt.

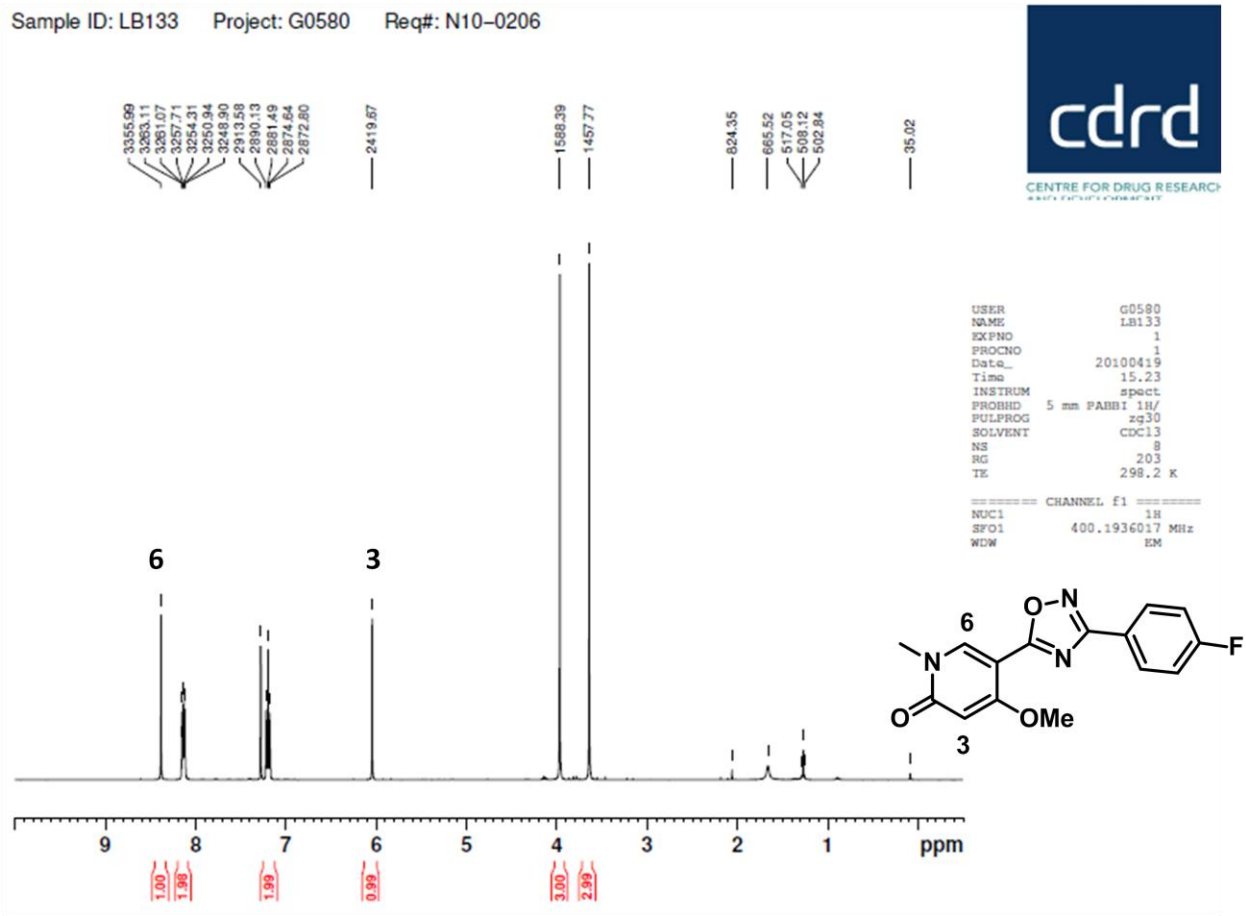

Figure 32: NMR spectra of one of the oxadiazole compounds (13i). The peaks corresponding to the protons on C-3 and C-6 are labelled.

Although the preparation of the oxadiazole ring worked reasonably well in most instances, the observed variation in yields from 11-63% was found to roughly parallel the degree of solubility of the amidoxime precursors in THF. This could influence their contact and reaction with acid chloride **4a**. In this scenario, the acid chloride could be quenched or decompose as

described earlier. Therefore, this synthetic procedure still needs to be optimized and adapted to ensure all oxadiazole yields are consistently high. For the needs of this project, optimization was not necessary as the procedure produced enough of each compound in order for them to be tested.

2.4 Isoxazolidin-6-one library: The third objective was to synthesize a library of N-aryl substituted isoxazolidinones **VIII** using copper coupling of **VII** with diverse aromatic and heteroaromatic halides. Our synthetic strategy, **scheme 9**, was dependent upon having in hand an efficient preparation of the hydroxamic acid intermediate **VI** and a means for its efficient conversion to the isoxazolidinone **VII**. To synthesize the hydroxamic acid, the acid chloride **8a** is readily obtained from the 4-chloro-2-pyridinone-5-carboxylic acid **8** using $SOCl_2$. The acid chloride can then in turn be reacted with hydroxylamine hydrochloride ($NH_2OH{\cdot}HCl$) in the presence of a base to give the hydroxamic acid **VI**. Through the application of heat, the isoxazolidin-6-one **VII** can then be formed through a cyclization reaction in the presence of a base. However, all attempts to synthesize this key hydroxamic acid precursor **VI** were unsuccessful.

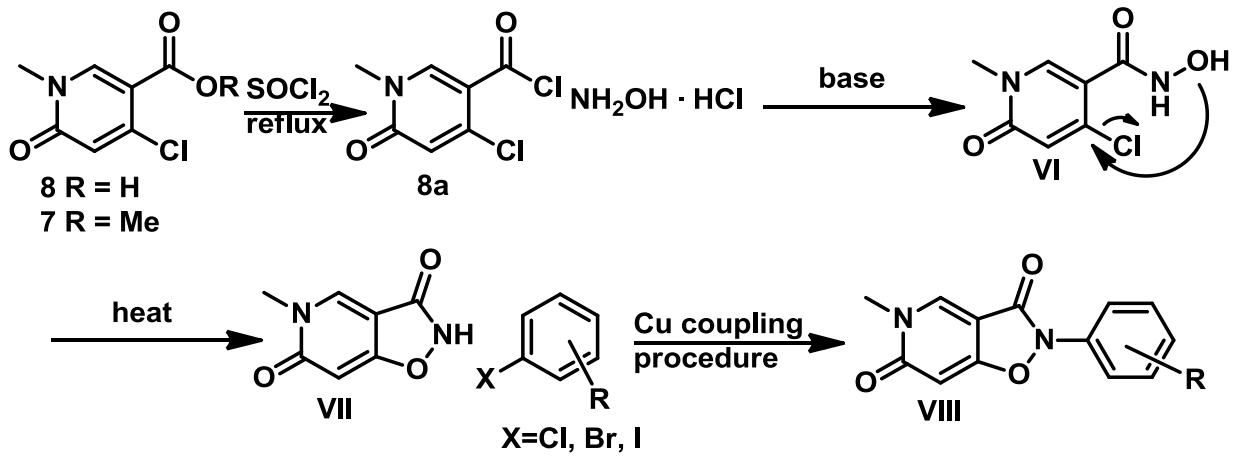

Scheme 9: Isoxazolidinone synthesis. This procedure was attempted numerous times however compound VI was never synthesized therefore the isoxasolidinone VII synthesis could not proceed.

In practice, the synthesis of the hydroxamic acid **VI** should proceed in a similar manner as the amide coupling reactions in objective 1. Instead, the reaction of the acid chloride **8a** with NH_2OH resulted in the formation of multiple products, according to TLC, from which the desired product could not be isolated. Numerous other procedures were explored starting from

both ethyl 4-chloro-2-pyridinone-5-carboxylate **7** and 4-chloro-2-pyridinone-5-carboxylic acid **8**. Compound **7** was added to a solution of aqueous sodium hydroxide ($NaOH_{(aq)}$) and hydroxylamine hydrochloride in methanol at room temperature.[164] Alternatively, potassium hydroxide (KOH) was used to neutralize the hydroxylamine hydrochloride *in situ* followed by the addition of **7** to make the hydroxylamate potassium salt. This was followed by neutralization of the salt with acetic acid.[165] Another procedure required the use of aqueous NH_2OH with **7** in a 1:1 solvent mixture of THF:MeOH, followed by the addition of potassium cyanide (KCN) to act as a catalyst.[166] None of these procedures worked.

Starting from **8**, the acid chloride **8a** was combined with $NH_2OH{\cdot}HCl$ in the presence of various bases in THF at room temperature.[167] Five different bases were tried using this procedure: KOH, Cs_2CO_3, NaOH, Et_3N and K_2CO_3. An alternative to the acid chloride approach is to use the corresponding acid fluoride. Exchanging the chlorine atom with fluorine has important consequences in terms of stability, purification and characterization of the derived acyl halide.[168] An acid fluoride is more stable than an acid chloride therefore it can be purified using silica gel column chromatography, isolated and its structure confirmed by mass spectroscopy. Consequently, it can be anticipated the reactivity of the acyl fluoride will be more controlled and the reaction will be cleaner. The acid fluoride **8b** was synthesized from **8** using cyanuric fluoride in 80% yield, according to **scheme 10**. The pure acyl fluoride **8b** was dissolved in DCM in the presence of Et_3N, followed by the addition of $NH_2OH{\cdot}HCl$, at room temperature.[169] Similarly, this reaction did not produce the desired hydroxamic acid **VI** in a significant and isolable yield.

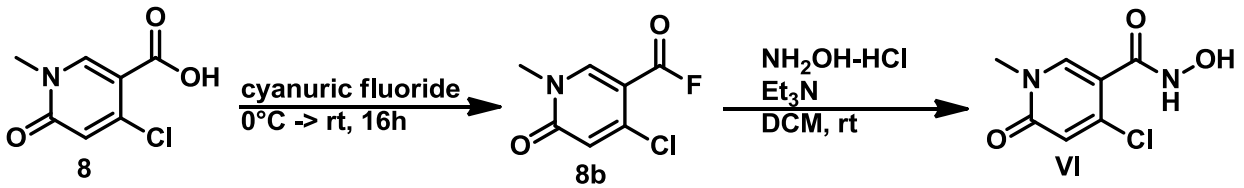

Scheme 10: Acid fluoride synthesis using cyanuric fluoride. The acid fluoride was synthesized by reacting compound 8 with cyanuric fluoride to obtain compound 8b. Reacting 8b with hydroxylamine hydrochloride in the presence of triethylamine did not result in the synthesis of hydroxamic acid VI.

The reaction of NH_2OH with the chlorine atom at C-4 on compounds **7** and **8** was observed in many of the reactions (compound **IX**, **scheme 11**); however, the isolated yield was very low, <10mg (<10%). This C-4 substituted compound was confirmed by mass spectroscopy through the detection of both the appropriate mass, m/z = 185, and the absence of the chlorine

isotope peak, which is detectable in the starting materials **7** and **8**. Logically, the acid chloride should be more reactive than the chlorine atom at C-4 so the reaction with hydroxylamine should occur preferentially with the acid chloride. A possible explanation for this observed side reaction is that if the acid chloride was not formed completely, the only other reaction that could occur was displacement of the chlorine at C-4 by NH_2OH. Impurities in the reaction mixture from hydroxylamine, the base or solvent, such as water, may have quenched the acid chloride before it had a chance to react with NH_2OH.

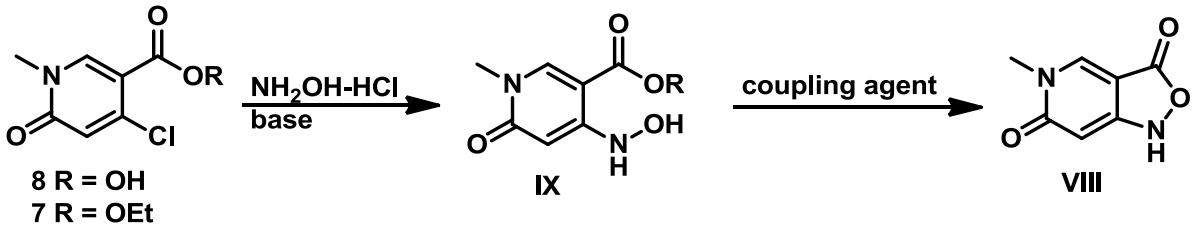

Scheme 11: Isoxazolone synthesis. C-4 substitution with NH_2OH-HCl (IX) and subsequent isoxazolone formation (VIII).

In light of the difficulties encountered with the formation hydroxamic acid **VI** (in detectable quantity), this reaction and library were abandoned. However, the procedure outlined in **scheme 11** introduces the idea of approaching this reaction from a different perspective, whereby the desired 5-membered ring is synthesized first by a S_NAr reaction at the C-4 position on the 2-pyridinone followed by the cyclization. For future attempts at this synthetic objective approaches like this will need to be investigated to ensure success.

One alternative to these reactions is to use O-benzylhydroxylamine and a Lewis acid (**scheme 12**). In the literature, this procedure was used to synthesize O-benzylhydroxamides (**XI**) from *N*-benzoyl-4-benzyl-2-oxazolidinone (**X**) in 50-90% yield.[170] The Lewis acid coordinates to the two carbonyl groups in compound **X**, similar to the coordination observed in an aldol reaction. This coordination activates the benzoyl carbonyl and makes the oxazolidinone a better leaving group. For our purposes, using the 2-pyridinone scaffold, the Lewis acid may be unnecessary however this procedure is worth investigating further.

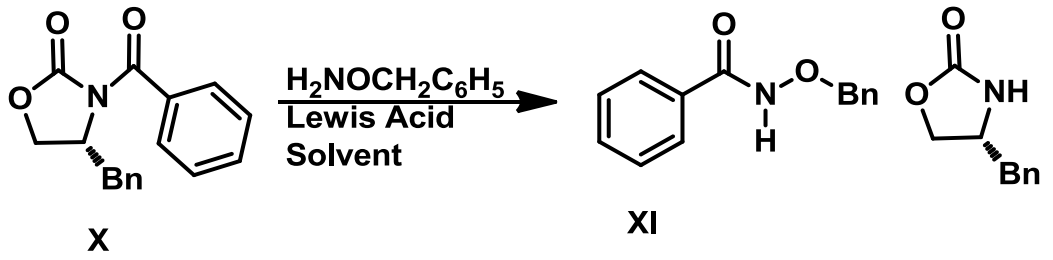

Scheme 12: O-benzyl hydroxamic acid synthesis. Use of O-benzylhydroxylamine to synthesize a hydroxamic acid (XI).

Another alternative option for the preparation of the target compound **VIII** would be to displace the C-4 Cl in 4-chloropyridinone-5-carboxylic acid **8** by an N-protected hydroxylamine-based reagent, **scheme 13**, such as oxime **19**, followed by N-deprotection and intramolecular amide formation. In fact this approach was used to prepare the 3-amino substituted benzisoxazole derivatives **22a-b** and it is described in more detail in section 4 (see **scheme 21**).

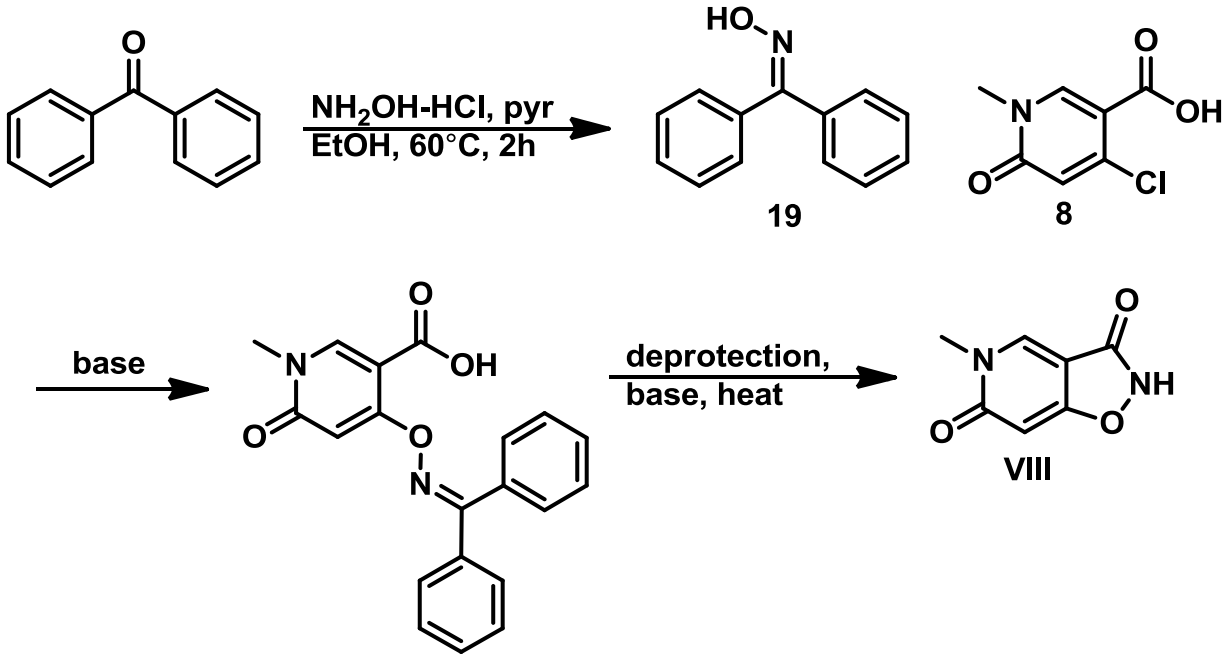

Scheme 13: Isoxazolidin-6-one alternative synthesis. Synthesis of isoxazolidin-6-one (VIII) using N- protected hydroxylamine.

A further option we intend to explore in future studies is to direct attention toward the preparation of the corresponding arylpyrazolidinones **XVII**, **scheme 14** (i.e. molecules where O is replaced by NH). The idea here is to use the chemistry developed in objective 1 to prepare the 4-chloro substituted amide derivatives **XII** and to subsequently introduce the requisite nitrogen

atom at C-4 followed by ring closure through the formation of an N-N bond. Note that in the amides **XII** the N-aryl substituent found in the target molecules **XVII** is already present. The procedure for this alternative is outlined in **scheme 14** whereby the C-4 chlorine of amide **XII** is displaced by azide anion from an azide source such as sodium azide (NaN_3) to give phenyl 4-azido-2-pyridinone-5-carboxamide, **XIII**. Subsequently the arylpyrazolidinone **XVII** is formed by treatment of **XIII** with a base, such as K_2CO_3 or NaH (sodium hydride), and the release of nitrogen gas (N_2).[171] The mechanism for the ring formation involves deprotonation of the amide nitrogen to give the intermediate anion **XIV** which then attacks the nitrogen directly attached to C-4 of the 2-pyridinone forming a N-N bond, **XV**. There is as subsequent rearrangement whereby N_2 is released followed by neutralization of **XVI** to give the N-aryl amide substituted pyrazolidinone **XVII**.

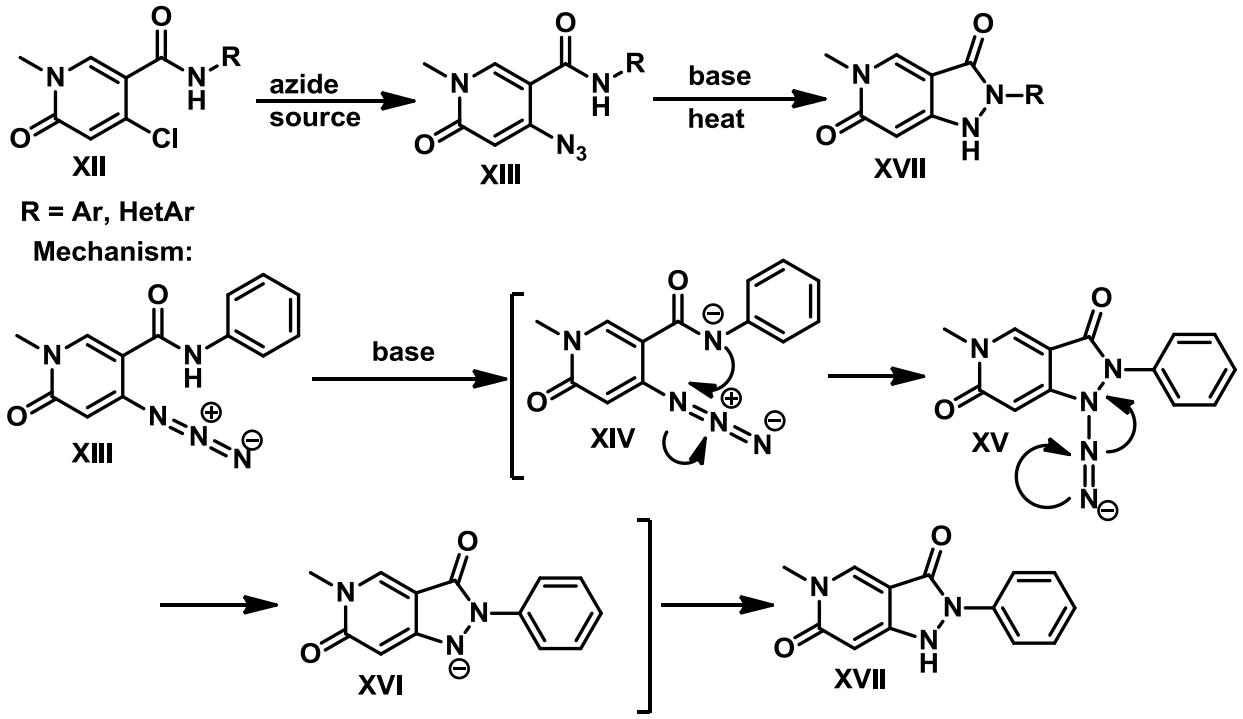

Scheme 14: Amide-substituted arylpyrazolidinone synthesis. The synthesis and the mechanism are outlined.

Substituting the isoxazolidinone ring with a pyrazolidinone results in similar spatial orientation of the final product but different H-bonding properties; in the isoxazolidinone there is a hydrogen bond acceptor (oxygen) and in the pyrazolidinone there is a hydrogen bond donor

(NH). Therefore, it would be advantageous to have both types of molecules to determine if the substitution of oxygen with NH changes the binding properties.

2.5 4-Arylpyrazolidinone library: The fourth objective of the project was to attach (hetero)aromatic substituents to the 2-pyridinone such that, when projected in 2D, the aromatic ring is oriented into space previously unoccupied by IDC16. Two strategies were investigated in an attempt to develop a synthetic scheme that could be used in the preparation of a wide variety of N-4 aryl/heteroaryl substituted pyrazolopyridine-2,6-diones. In the first approach, shown in **scheme 15**, compounds **15a-b** were prepared in two steps: i) reaction of the acid chloride **8a** with the desired hydrazine in the presence of K_2CO_3, in THF at room temperature for 16 hours and ii) subsequent cyclization of the derived intermediate hydrazide **14a** and **b** in the presence of K_2CO_3 in DMF using microwave irradiation at 200°C. Compound **15c** was prepared in one step following reaction of the acid chloride **8a** with the arylhydrazine. Microwave irradiation was not required for cyclization. This approach was only applied to 3 hydrazines and resulted in incomplete conversions (yields 65%, 48% and 57% respectively) after microwave reaction times of 1 hour; note that microwave reaction times are generally less than 30 minutes. Further there are not many commercially available hydrazines. Therefore, for the purposes of this project the procedure was not useful and was not pursued further.

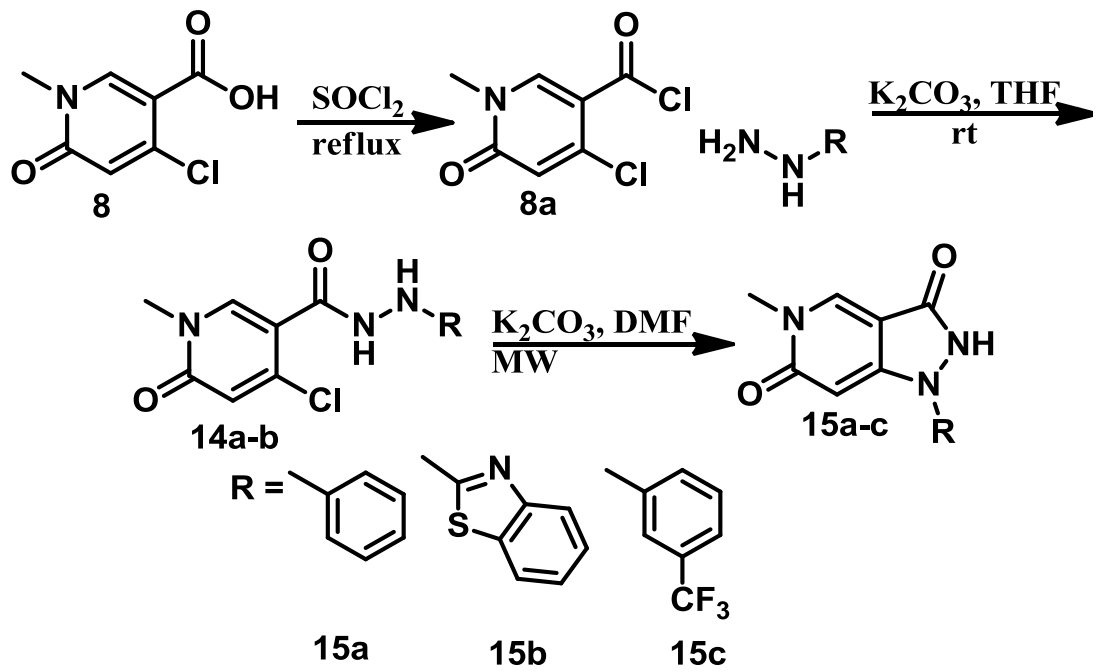

Scheme 15. 4-Arylpyrazolidinone synthesis. This procedure was used to first synthesize the hydrazides 14a-b followed by cyclization to the arylpyrazolidinones 15a-c.

The NMR spectra for compounds **15b** and **c**, **15b** shown in **figure 33**, were characterized by a downfield shift of the C-3 proton when compared to the 2-pyridinone-5-carboxylic acid **8**, 6.71 ppm and 7.41 ppm respectively. This can be attributed to the deshielding effect of the polar substituents attached at C-4 pulling electron density away from C-3. It is interesting to note that this observation was not characteristic of **15a**; the C-3 proton was more upfield at 6.3 ppm when compared to **8** at 6.64 ppm. This is because the substituent at C-4 is an N-phenyl instead of a chlorine atom and is less electronegative, resulting in less electron density being pulled away from C-3 and a more upfield chemical shift.

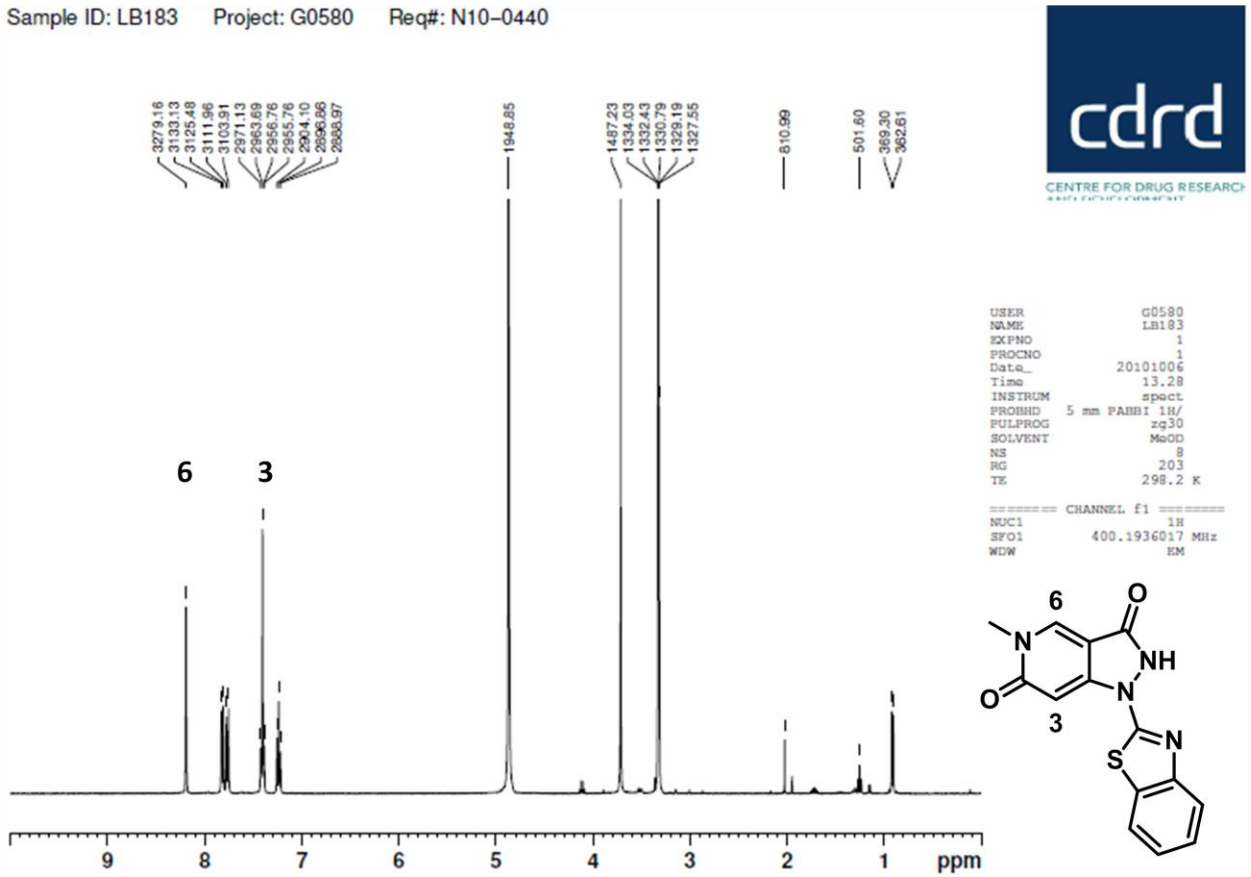

Figure 33: Arylpyrazolidinone NMR spectra (15b). The protons on C-3 and C-6 are labelled.

In the second method that was envisioned for the preparation of the target pyrazolopyridiones, the idea was to use different C-4 N-(hetero)aryl substituted pyridinones **16a-d** as key intermediates (the preparation of these compounds is described under objective 5, section 2.6; **scheme 17**). Construction of the pyrazolone ring from these intermediates **16a-d** would involve converting them to the primary amides **XVIII** using ammonia in MeOH according to the procedure outlined in section 2.2.1, **scheme 5**. Subsequently, formation of an N-N bond between the two nitrogen atoms would occur using PIFA (phenyliodine(III)bis-(trifluoroacetate)) with trifluoroacetic acid (TFA), **XX**, according to **scheme 16**. The proposed mechanism, **scheme 16**, for the N-N bond formation proceeds starting with the amide carbonyl oxygen attacking the iodine, assisted by the lone pair on the amide nitrogen, **XVIII**. This intermediate **XIX** reacts intramolecularly with the nucleophilic amine moiety, causing the iodo moiety to leave giving rise to the desired arylpyrazolidinone **XX**, and an iodocomplex with a negative charge.[172]

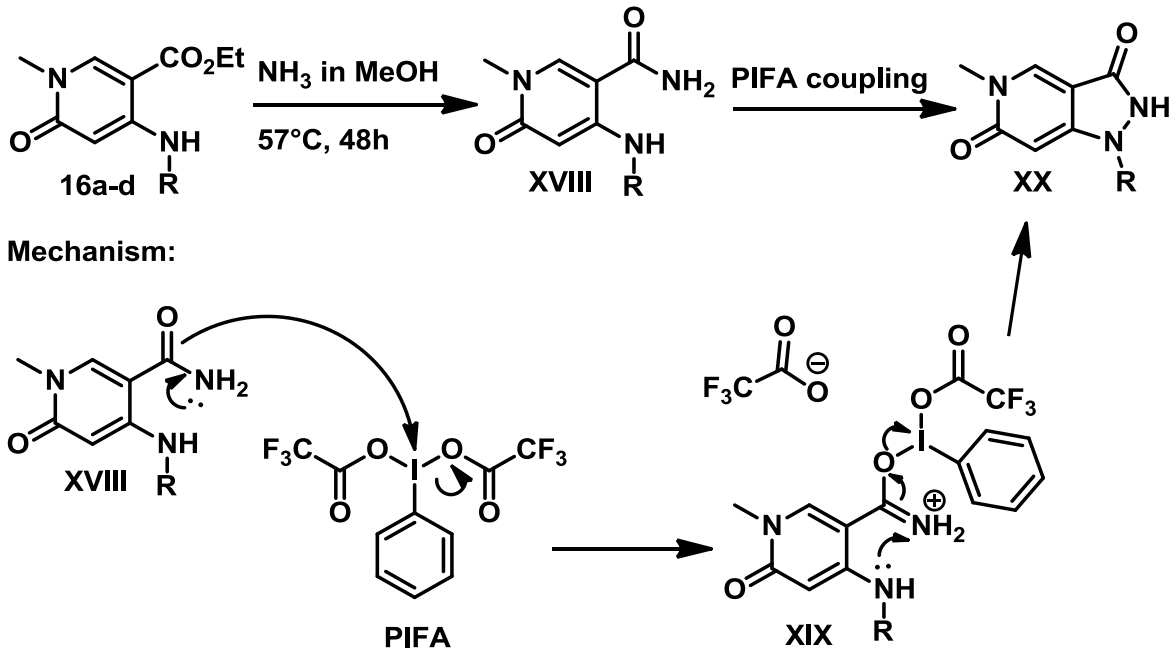

Scheme 16: Arylpyrazolidinone synthesis using PIFA. The mechanism proceeds by attack on PIFA by oxygen, assisted by the lone pair on the amide nitrogen to give intermediate XIX. The nucleophilic amine then attacks the amide nitrogen in an intramolecular reaction to create XX. PIFA is regenerated and the desired arylpyrazolidinone is formed, XXI.

This procedure has the potential to be successful, however, the microwave procedure to produce the C-4 substituted amines **16a-d** involved very harsh conditions (>6 hours in the microwave at 175°C) and was low yielding (average yield was 28%); therefore, it is not conducive for library synthesis and the scheme was abandoned without investigating the 5-membered ring formation step. As is proposed in section 2.6, the biarylamines could be synthesized via a S_NAr reaction of the amine anion with Cl at C-4 in 4-chloro-2-pyridinone-5-carboxylic acid **8**. If this procedure is optimized, the products could be used in the PIFA reaction to create a library of arylpyrazolidinones.

2.6 Position 4 functionalization: In this section, the objective was to construct a series of 4-(hetero)arylamine/ether substituted pyridinones with an ester or acid function at C-5 through a S_NAr reaction. These molecules differ from the DHA compounds described in objective 1 in that the (hetero)arylamine component does not form part of the amide system. In these new IDC16 mimics, the opportunity exists to explore the influence of projecting this D-ring (heteroaromatic ring) component into a different space in the supposed IDC16 binding pocket in SRSF1.

In the pursuit to synthesize C-4 substituted compounds, a small collection of biarylamines were prepared according to **scheme 17**. The synthesis of compounds **16a-d** was accomplished by heating ethyl 4-chloro-2-pyridinone-5-carboxylate **7** in the microwave with the desired aromatic amine at 175°C. The compounds **16a-d** were obtained in 4%, 89%, 16% and 4% respectively following purification by column chromatography. The microwave was used because, according to the literature, this reaction required heating the reagents at a high temperature for multiple hours. We thought microwave irradiation would allow us to achieve the same result in a shorter period of time. This, however, was not the case.

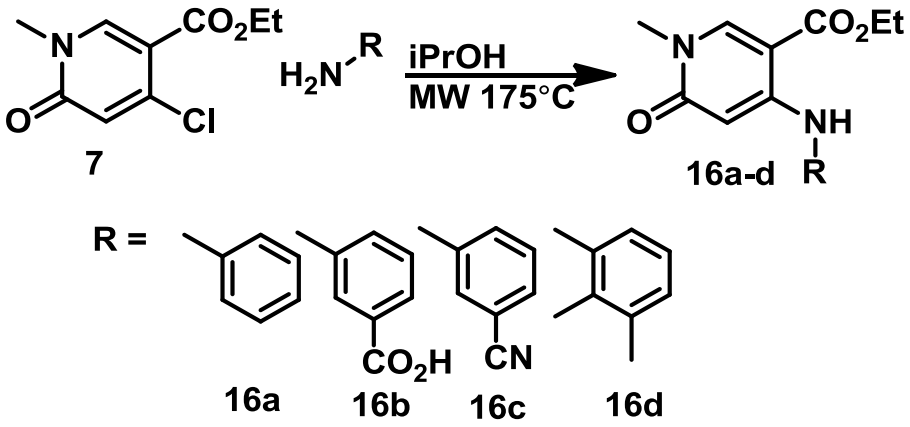

Scheme 17: C-4 substitution using microwave conditions. Compound 7 was reacted with four amines at high temperatures in the microwave to give compounds 16a-d.

Analysis of the NMR spectra of compounds **16a-d** through comparison to the starting ethyl 4-chloro-2-pyridinone-5-carboxylate **7**, shows that there is an upfield shift in the proton at C-3, (5.86 ppm versus 6.66 ppm) as is shown in the NMR of **16a** in **figure 34**. This proton is shifted upfield because a less electronegative nitrogen is present at C-4 resulting in a more shielded δ^- proton, which causes the chemical shift to move upfield. The proton on C-6 does not change significantly because its environment remains the same. Additionally, the chemical shift of the C-3 proton changes according to the polarity of the amine (5.91 ppm (**16c**) > 5.86 ppm (**16a,16b**) > 5.28 ppm (**16d**)).

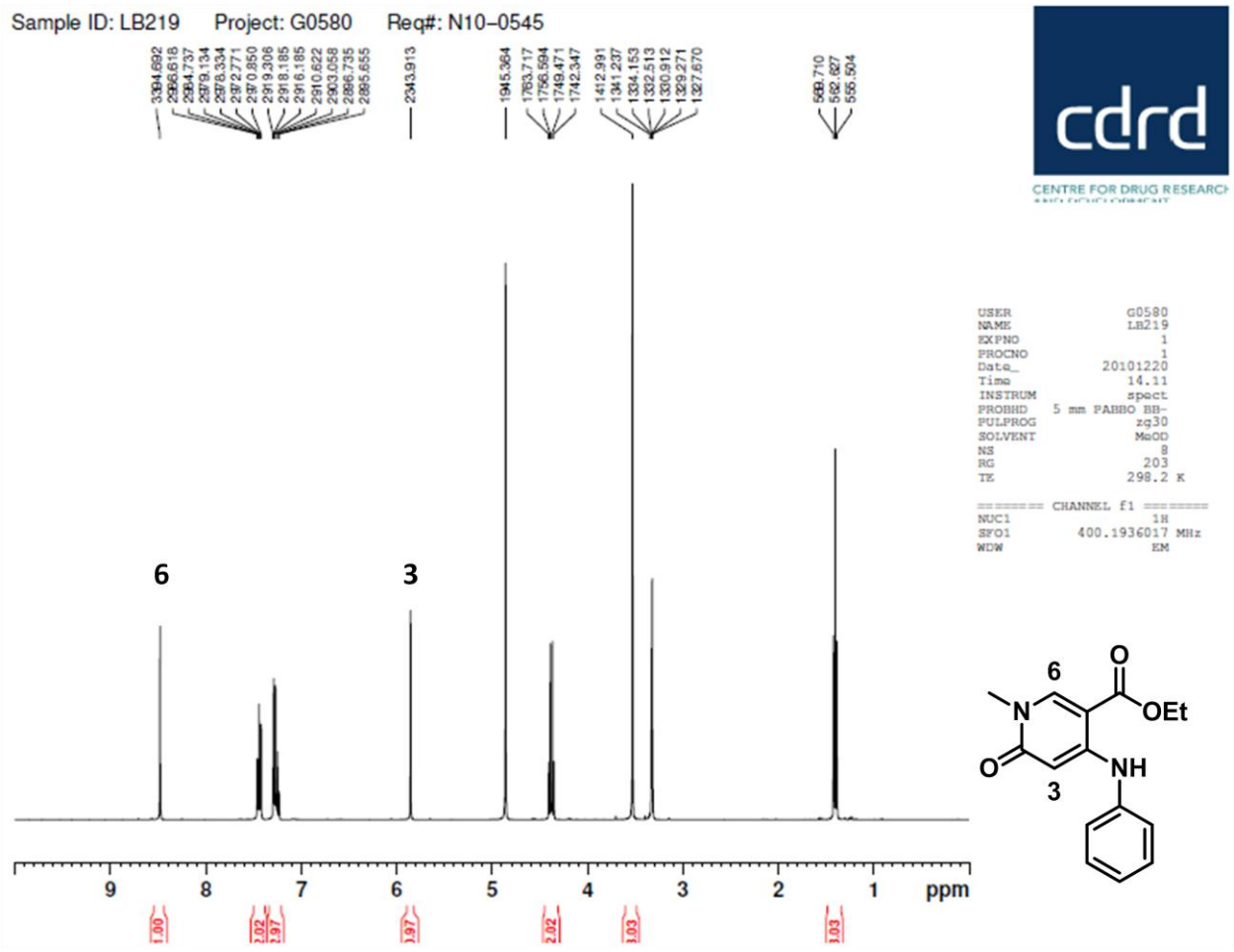

Figure 34: NMR spectra of a C-4 amine substituted 2-pyridinone (16a). The protons on C-3 and C-6 are labelled.

Unfortunately, as mentioned in section 2.5, the microwave procedure to produce the C-4 substituted amines **16a-d** was low yielding (4-16% for **16a** and **c-d)**, not applicable to a variety of substrates and required reaction times of 7-14 hours. The only exception was an 89% yield observed with 3-aminobenzoic acid **16b**. The reason for this is not clearly evident because the carboxylic acid is a weak electron withdrawing group which should slightly decrease reactivity instead of increasing it. Overall, this procedure needs to be optimized to decrease reaction times and increase yields.

In an extension of **scheme 17**, we thought it would be interesting to introduce 3-amino-5-nitrobenzisothiazole at C-4 on the 4-chloro-2-pyridinone-4-carboxylic acid **8**, in an attempt to investigate the binding space of the SR protein target. To accomplish this, the anion of the aminoisothiazole was created using lithium diisopropylamide (LDA) at -78°C (**scheme 18**) and

was reacted with **8**, according to the literature.[154] Compound **16e** was isolated in 4% yield and tested.

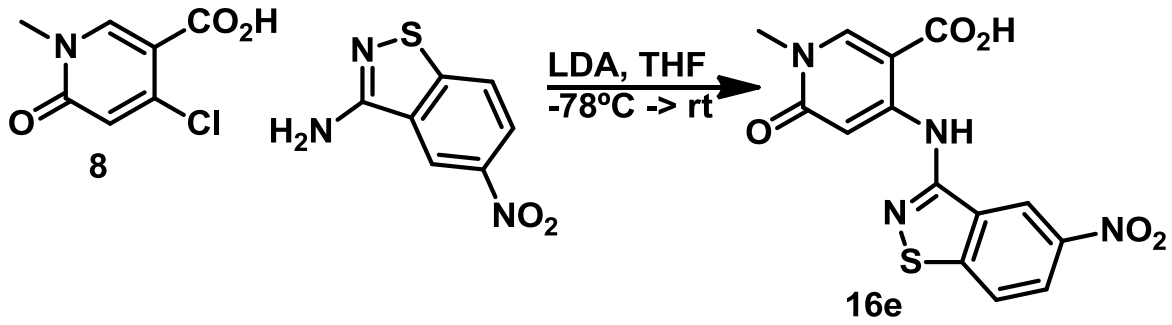

Scheme 18: C-4 functionalization with 5-nitrobenzoisothiazol-3-amine. The amine anion was reacted with compound 8 at low temperature to give compound 16e.

In the initial HIV tests carried out in the laboratory of Pr. Tazi, this compound was found to display activity comparable to IDC16 (precise values not communicated). The discovery of compound **16e** strongly justified and supported the project objectives 4 and 5, to investigate compounds where aromatic and heteroaromatic compounds are attached at C-4. Unfortunately, the procedure to produce compound **16e** remains low yielding (4%). Note also, it was not fully characterized, as the mass spectra only displays a small parent peak at m/z = 351 for the desired compound. Since full characterization was not done, it is doubtful the correct compound was obtained. This notion is reinforced by previous work in the lab, done by Dr. Mitra Matloobi, indicating that in the presence of sodium hydride (NaH), 3-amino-5-nitrobenzisothiazole likely undergoes an intramolecular reaction. Through examination of NMR and mass spectra data it appeared that the compound had likely decomposed, but a definite conclusion was never reached. This helps partially explain why the formation of **16e**, if it was in fact prepared, is very low yielding and not readily reproducible.

Turning to the literature for a further explanation, it is shown that LDA can act as both a strong base and occasionally as a hydride source.[173] It is LDA's ability to act as a hydride source or H^- nucleophile that is important with regards to the synthesis in **scheme 18** where a strong base is used to deprotonate 3-amino-5-nitrobenzisothiazole. This provides further evidence that this synthetic methodology is not the optimal way to synthesize compound **16e** as a similar reaction is probably occurring with 3-amino-5-nitrobenzisothiazole as is seen in **scheme 19**. Because the N-S bond is weak, the nucluophile H^- can add to the sulphur breaking the N-S bond.

The molecule decomposes further forming 2-mercapto-5-nitrobenzonitrile and an imine functionality which equilibrates to N-methyl-3-amino-2-pyrdinone. This is because the 2-pyridinone can be considered a leaving group since the negative charge can be stabilized by the aromatic character in the 2-pyridinone.

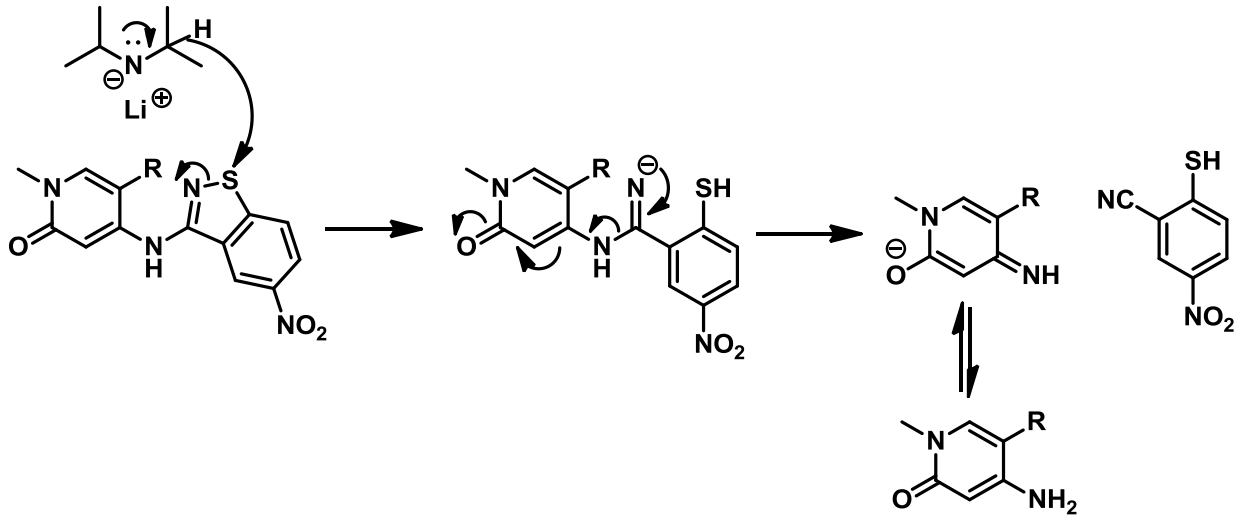

Scheme 19: Lithium diisopropylamide (LDA) as a hydride source. LDA can act as a hydride source in reactions with the 3-amino-5-nitrobenzisothiazole 2-pyridione amine. In this case the amino bond forms but subsequently decomposes because H- attacks the sulphur atom resulting in an imine, where the negative charge is stabilized by the 2-pyridinone and in equilibrium favouring the 4-amino-2-pyridinone, and 2-mercapto-5-nitrobenzonitrile.

According to the literature, the aromatic substitution of a chlorine with a nucleophile, is somewhat challenging. Overall, there are three main approaches used in the literature. The first option is to use a S_NAr reaction with a neutral aromatic amine (as was done in **scheme 17**) and give it energy to react by heating at high temperatures or by using an acid catalyst (usually HCl).[174] Secondly, palladium coupling is used in the Buchwald-Hartwig amination of 4-chloro-2-pyridinone; however the yields are low to moderate for these reactions (15-87%).[175] Finally, a S_NAr reaction using an amine anion to displace the chlorine is possible (as was done in **scheme 18**). Using the amine anion appears to be the best avenue for the scope of biarylamine synthesis that we are interested in. According to the literature, this procedure gives yields of at least 85%.[174] However, this reaction will need to be optimized as initial attempts using aniline resulted in a yield of only 4%. This poor result motivated our choice to pursue alternative methodologies to generate an amine anion.

To obtain an amine anion without using a strong base like NaH, the plan was to utilize the strong attractive property between silicon and fluorine to create an amine anion. This amine anion would be very reactive and it was hypothesized that it would easily and quickly displace the chlorine atom at the C-4 position on ethyl 4-chloro-2-pyridinone-5-carbxylate **7**. Efforts to synthesize the silylated amine using trimethylsilyltriflate (TMSOTf), trimethylsilylchloride (TMSCl), and hexamethyldisilane (HMDS) followed by subsequent treatment with cesium fluoride (CsF) and **7** were all unsuccessful. Aniline was used in all the procedures and the treatment with CsF and **7** followed all the silylation attempts. To silylate the amine, in the first procedure attempted, aniline was dissolved in dry DCM and diisopropylethylamine (DIPEA) was added at 0°C followed by the addition of TMSOTf dropwise.[176] The second attempt involved the lithiation of aniline using butyllithium (^{n}BuLi) followed by the addition of TMSCl; this procedure was attempted multiple times.[177] The final procedure that was tried required aniline to be dissolved in HMDS and refluxed for 16 hours.[178]

It is unclear whether the problem with these reactions was rooted in the silylation step or the reaction of the silylated amine with CsF and subsequently **7**. The silylation step was challenging because the reagents and product are moisture and air sensitive.[179] Careful precautions were taken to try to ensure the exclusion of air and moisture but it may have been introduced through errors in technique or improper equipment and experimental set up. According to the literature, cesium fluoride must be activated in order to be an effective fluorine source. To activate CsF it was dissolved in water, then the water was removed in vacuo and the solid was dried on the high vacuum at 200°C for 48 hours.[180] If this activation step was unsuccessful the reaction would not proceed because there would be no free fluoride ion to react with the silyl group. Eventually, this approach for synthesizing arylpyrazolidinones was abandoned in order to advance the project.

Because biarylamine bond formation was proving to be a challenging task, we wanted to investigate if biarylether bond formation would be easier. A phenoxy substituent (**17**), and a 2- and 4-hydroxypyridine (**18a** and **18b**) motif were successfully introduced at C-4 (**scheme 20)**. Compounds **17**, **18a** and **18b** were obtained through a S_NAr reaction of deprotonated phenol (**17**), 4-hydroxypyridine (**18a**) or 2-hydroxypyridine (**18b**) with ethyl 4-chloro-2-pyridinone-5-carbxylate **7**, achieved in the presence of Cs_2CO_3 to give the desired compounds in 77%, 78% and 10% yields respectively after purification by column chromatography.[181, 182]

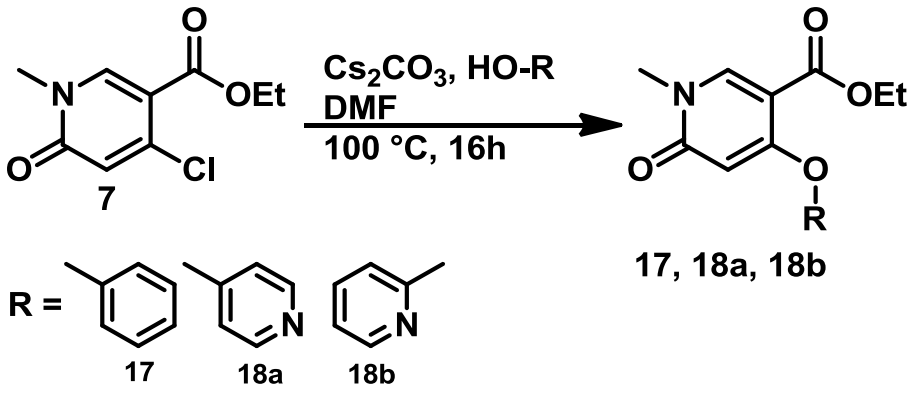

Scheme 20: C-4 alcohol functionalization. Compound 7 was reacted with 3 different alcohols in the presence of cesium carbonate (Cs2CO3) at high temperature to synthesize compounds 17, 18a and 18b.

Compounds **17**, **18a** and **18b** were selected because they are simple substrates on which to test the reaction conditions. This reaction was not applied to other substrates because we were interested in other, less simple aromatic and heteroaromatic compounds, where this procedure would be unsuccessful.

The chemical shift of the C-3 proton in the NMR of these compounds (**17**, **18a** and **18b**) differed notably. The more polar pyridine ring deshielded the C-3 position and resulted in the downfield shift observed in **18a** and **18b** compared to **17** (6.51 ppm and 6.24 ppm versus 5.68 ppm). Between the two pyridines, the 4-hydroxypyridine substituted 2-pyridinone is characterized by its C-3 proton having a more downfield chemical shift.

3 Biology

The DHA molecules were tested by Dr. Peter Cheung at the BC Centre for Excellence in HIV/AIDS at St. Paul's hospital. Initially, the compounds were screened for their ability to inhibit HIV-1 replication. This test identified four active molecules, which were further tested for their dose-response. Subsequently, the active compounds were screened for their ability to inhibit HIV-1 replication in HIV-1 strains resistant to HAART. Evaluation of the potential cytotoxicity of the compounds prepared in this thesis using an appropriate assay remains. For this purpose the Guava® Nexin Assay (cat #. 4500-0450, Millipore) described in section 3.2 will be used.

3.1 HIV-1 test: Of the 240 compounds tested, 50 correspond to molecules described in this thesis, the others were synthesized by other members of our research group. AZT was synthesized by Sigma-Aldrich (St. Louis, MO). Indicator cell line GXR-5 was generously provided by Dr. Mark Brockman (Harvard Medical School). HIV-1 CXCR4-tropic laboratory adapted strain NL4-3 was obtained through the NIH AIDS Research and Reference reagent program (Division of AIDS, NIAID, NIH).

To screen for anti-HIV activity we used a human T-cell-based reporter cell line (GXR-5) that expresses the HIV-1 receptor CD4, both the CXCR4 and CCR5 co-receptors, and green fluorescent protein (GFP) as a direct and quantitative marker.[183] GXR-5 cells express GFP due to the activation of the tat-dependent promoter upon HIV infection, and the level of infection can be monitored using Flow cytometric analysis (guavaSoft 2.2 software, Guava HT8, Millipore).

For the initial screen, 240 DHA analogues were screened for anti-HIV activity by co-culture of $1x10^6$ non-infected GXR-5 cells and 1% HIV-1NL4-3 infected cells. Infection was performed in a T25 flask containing 5ml RPMI 1640 supplemented with 10% FBS. Each molecule was then added to the culture at a final concentration of 2μM from a 5mM stock, in DMSO. At four days post-infection, the level of infection was determined by flow cytometry using GFP expression as the readout. Due to the fact that the above assay used infected cells and cell-free viruses for inoculation, this assay measured the HIV-1 infection in both virus to cell spread and cell to cell spread.[184]

Four graphs summarizing the results of all compounds tested (including those synthesized by other lab members) are located in **figure 35a-c**. The active molecules are identified by an arrow under the bar corresponding to the percentage of HIV-1 infected cells in the presence of the active molecule. It can be seen that 2μM AZT showed a 93%, 97% and 91%

inhibition on day 4 post-infection on plate 1, 2 and 3 (data for control on plate 3 not shown), respectively; while 2μM of C8, E5, C2, and D3 showed a 84%, 82%, 90%, and 89% inhibition, respectively. These results show that the activity of the four DHA molecules was comparable to that of AZT as a control: C8 and E5 were approximately 90% as effective, C2 was approximately 99% as effective and D3 was approximately 94% as effective as AZT. The compounds shown to the right of the graphs are inactive compounds with a similar structure to the active molecules. **Figure 35a** highlights compound LB45 (E5), the molecule synthesized within this thesis. The initial screen to identify active molecules, shown in figure 35, was performed once. However the active molecules were retested once (for a total of two screens) and the average percentage inhibition was calculated along with the standard deviation. The results for the repeated experiments on compounds C8 and E5 can be found in Appendix B. Additionally, the effect of DMSO was measured at volumes of 50μl to 3μl and found to be negligible. Note, that as only 2μl of DMSO was used in the screen, according to the data and graph in Appendix C, it has no effect on HIV-1 inhibition.

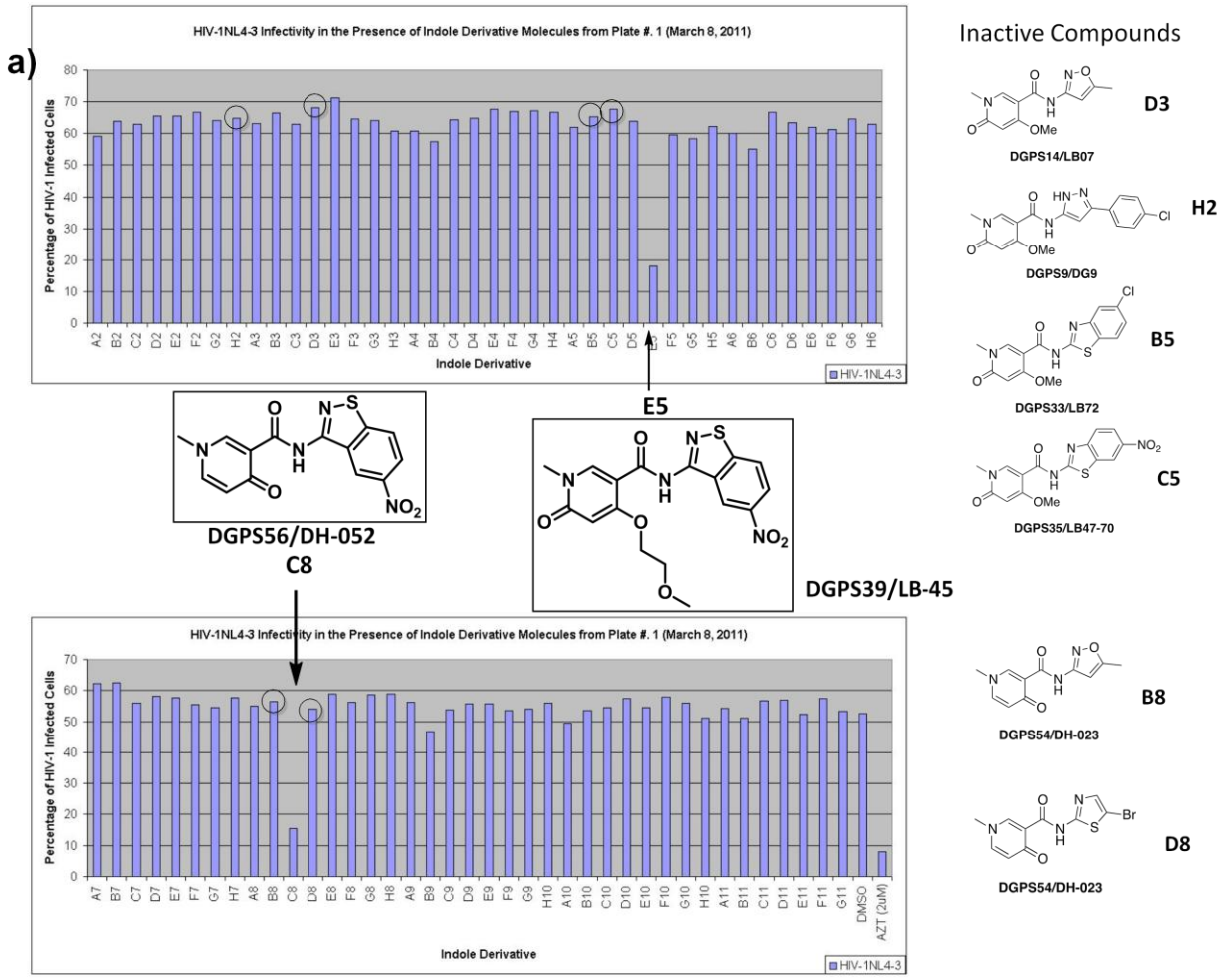

Figure 35a: Summary of biological results. The percentage of HIV-1 infected cells is shown in the graphs after being treated with 2µl of the indole derivative labelled on the x-axis. The active compounds C8 and E5 are highlighted. The compounds on the right are inactive compounds with structures related or similar to C8 and E5. The inactive compounds' corresponding bars on the graph are circled.

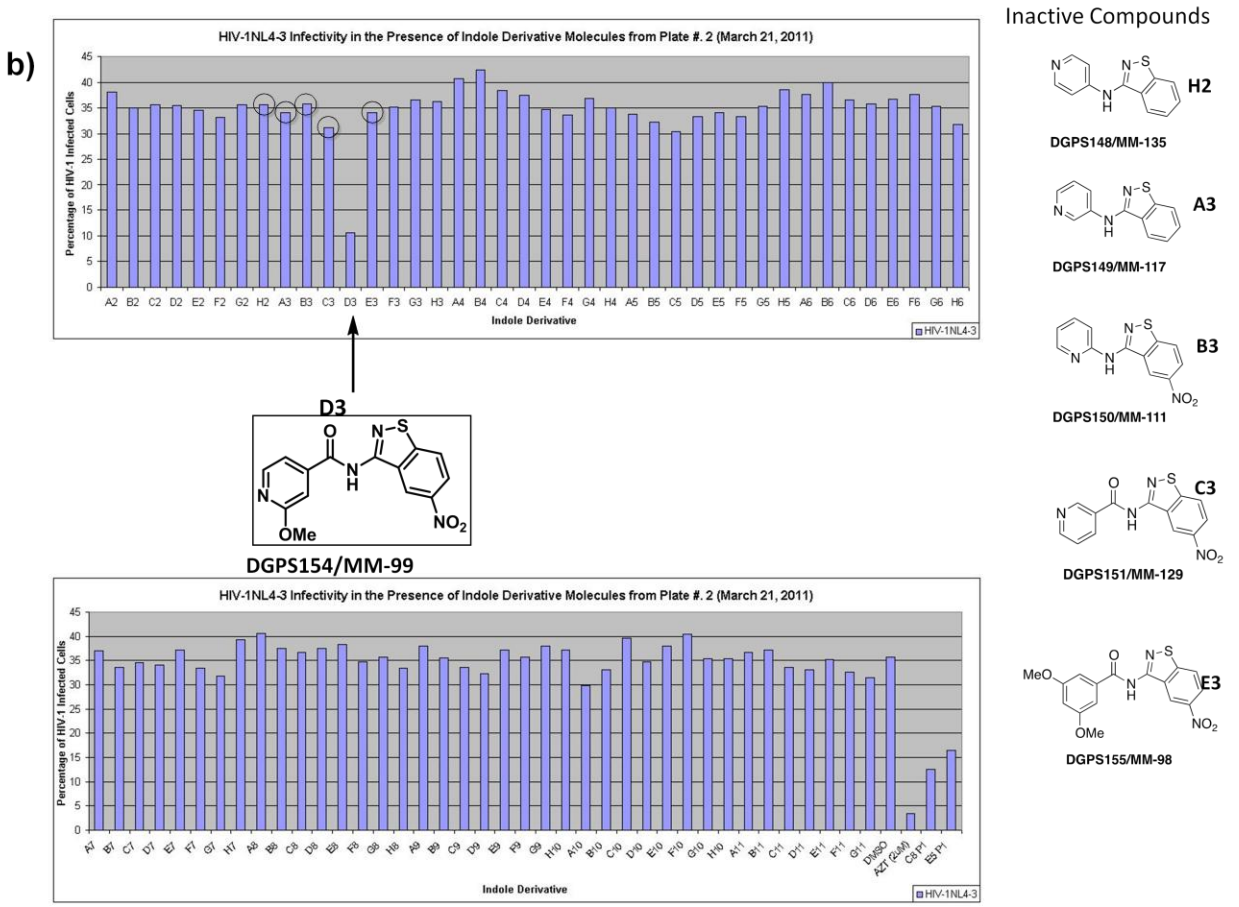

Figure 35b: Summary of biological results. The percentage of HIV-1 infected cells is shown in the graphs after being treated with 2µl of the indole derivative labelled on the x-axis. The active compound D3 is identified in the graph measuring percentage of HIV-1 infected cells. The inactive compounds' corresponding bars on the graph are circled.

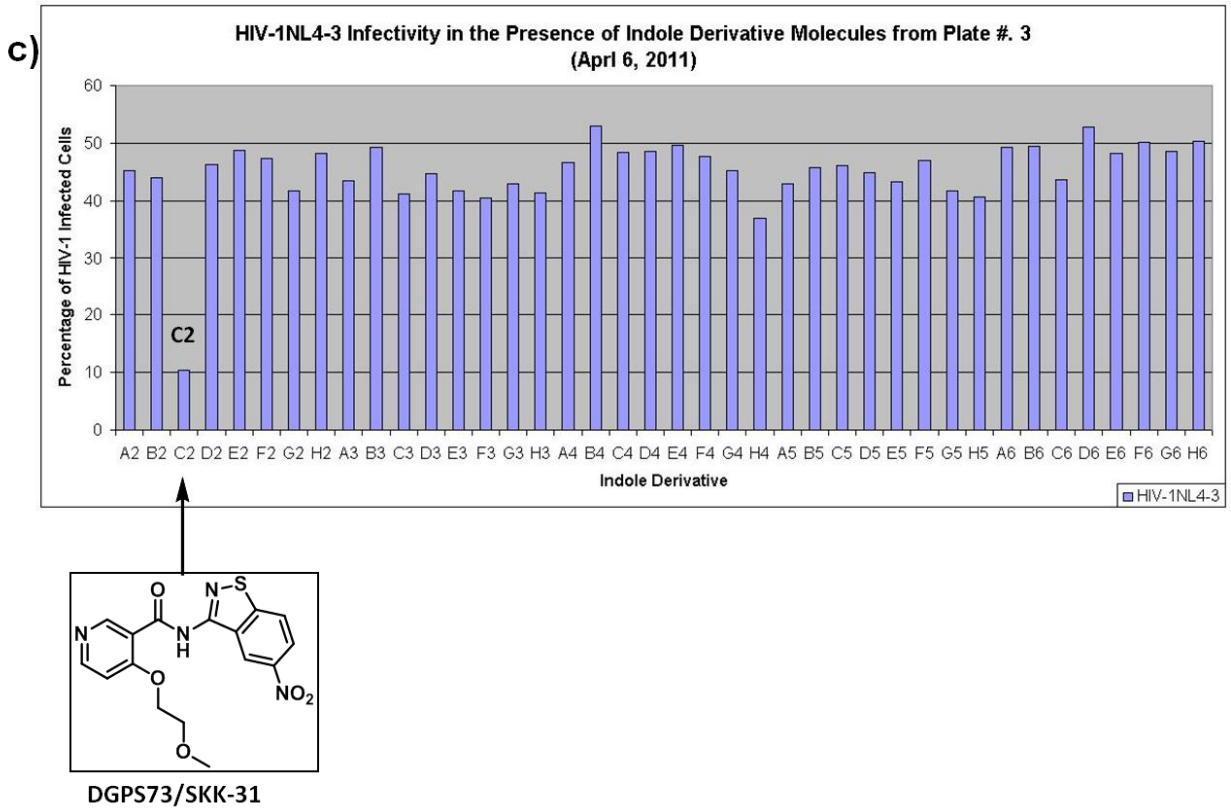

Figure 35c: Summary of biological results. The percentage of HIV-1 infected cells is shown in the graphs after being treated with 2µl of the indole derivative labelled on the x-axis. The active compound C2 is identified in the graph measuring percentage of HIV-1 infected cells.

3.1.1 Dose-response experiments: The active molecules were tested in a dose-response experiment, DGPS56/DH-052 (C8), DGPS39/LB-45 (E5), DGPS154/MM-99 (D3), DGPS73/SKK-31 (C2), at concentrations of 1µM, 2µM and 4µM, with Nelfinavir 1µM (a protease inhibitor more potent than AZT) as a positive control. **Figure 36** summarizes the results of this experiment. The ability of DGPS56/DH-052 and DGPS154/MM-99 to inhibit the virus increased as their concentration increased. For compounds DGPS39/LB-45 and DGPS73/SKK-31 the change in concentration had no significant effect on the inhibition of HIV-1 replication. This could be due to the fact that the difference between concentrations was not large enough to observe a significant difference. DGPS56/DH-052 appeared to be the most potent.

Dose-Response Study

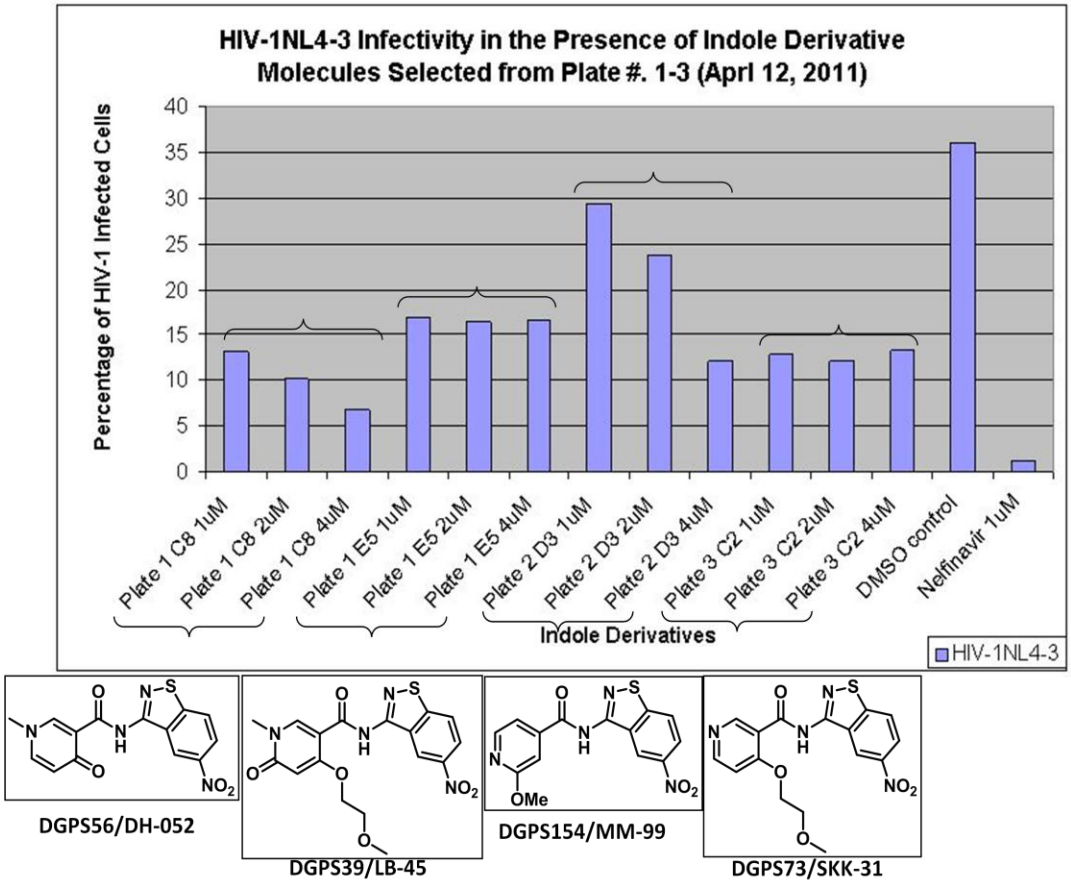

Figure 36: Summary of dose response experiment. The concentration of the active compounds was varied in the same HIV-1 transmission assay. The concentrations were 1, 2 and 4µM and HIV-1 infection appeared to decrease as the concentration of the compounds increased, with the exception of DGPS39/LB-45 which stayed about the same. The compounds were compared to AZT at 1µM concentration.

3.2 Cytotoxicity test: The cytotoxicity tests have not been performed yet. It is important to note that during the original HIV test there were no adverse effects observed on cell growth at 2µM. In addition, the rate of cell growth was similar between the treated cells and both the positive and negative controls.

The test that will be used to assess cytotoxicity is the Guava® Nexin Assay (cat #. 4500-0450, Millipore).[185] During programmed cell death, phosphatidylserine (PS), a phospholipid, is externalized to the cell surface, whereas it is normally localized on the internal surface of the cell membrane.[186] Annexin V is a calcium-dependent phospholipid binding protein with a high affinity for PS.[187] Early in the apoptotic process, when PS moves to the cell surface, annexin V can bind to it. This assay uses Annexin V conjugated to phycoerythrin (Annexin V-PE) to detect PS on the cell membrane surface of apoptotic cells.[188,189,190] Additionally, 7-AAD (7-

Aminoactinomycin D) is used to measure cell membrane structural integrity because this impermeant dye is excluded from live, healthy cells and early apoptotic cells.[191] Overall, this assay can distinguish between three types of cells:

1. Non-apoptotic cells: Annexin V(-) and 7-AAD(-)
2. Early apoptotic cells: Annexin V(+) and 7-AAD(-)
3. Late stage apoptotic and dead cells: Annexin V(+) and 7-AAD(+)

3.3 Preliminary investigation into compound mechanism of action: It was necessary to confirm that the active molecules targeted splicing and not those proteins targeted by the traditional HIV-1 therapy, HAART. The active molecules (identified in **figure 35a-c**) were tested for their ability to inhibit HIV-1 replication of HAART RTI-resistant strains. The resistant strains used were the highly resistant E00443_v, the moderately resistant E00435_4 and the slightly resistant E 00476_v. The full resistance profile can be found in **Appendix D.**

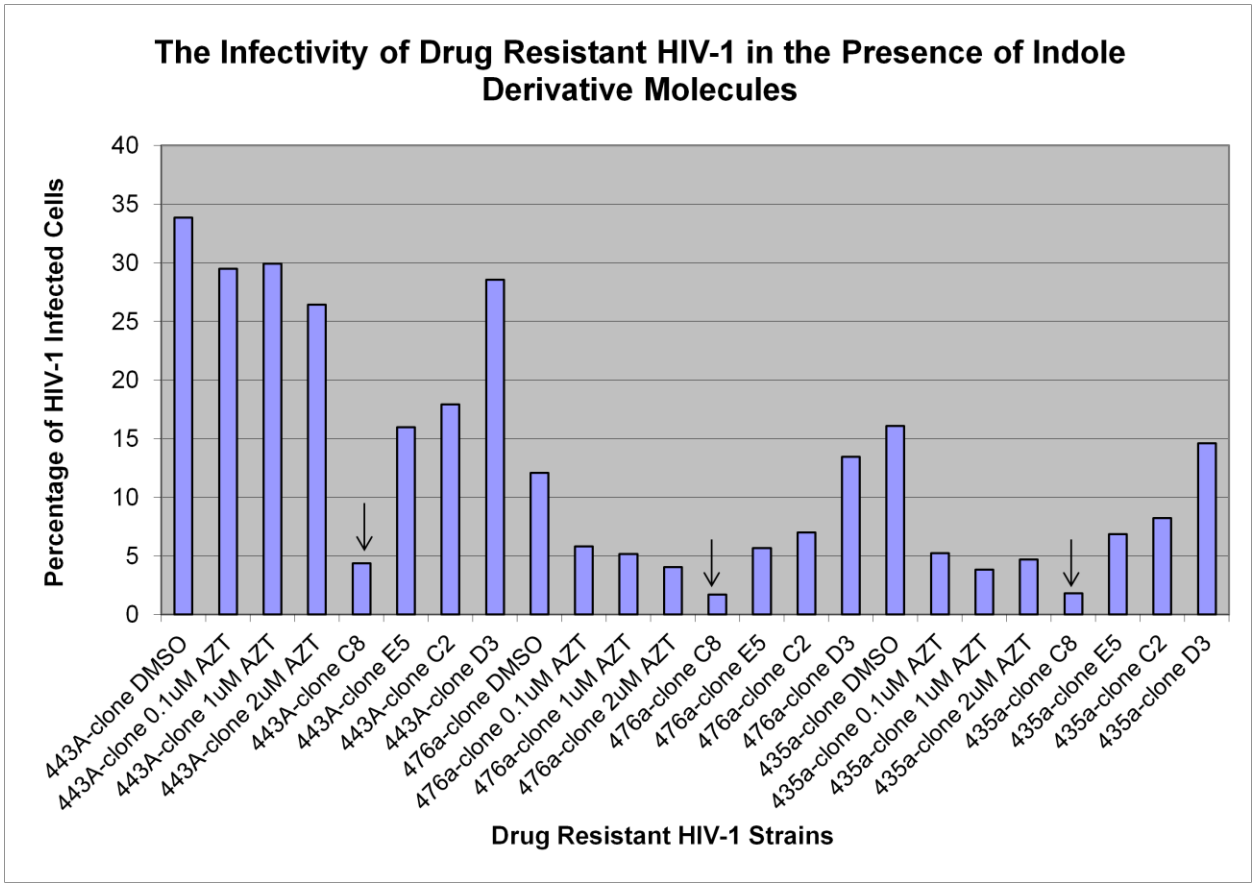

Figure 37: Summary of initial mechanism of action investigation. C8 is the only compound whose results are accurate. The bars corresponding to HIV-1 inhibition by C8 are pointed to by an arrow.

The same procedure in the initial screen was used (see section 3.1), replacing the HIV-1 strain NL4-3 with the resistant ones. **Figure 37** outlines the results of this test. It is evident that compound C8 is still active against the HAART resistant strains; therefore, at this time, we consider it probable that C8 is not an RT inhibitor. The exact experimental values can be found in **appendix E**, **table 2**.

3.4 Interpretation of biological results: The four active molecules have a common motif, a 5-nitro-3-aminobenzisothiazole linked through an amide bond to the A-ring. The A-ring varies but has N in the same spot (except for compound D3, which is the least active) and a C-4 oxygen atom which is part of a carbonyl or part of a polar side chain (**Figure 38**).

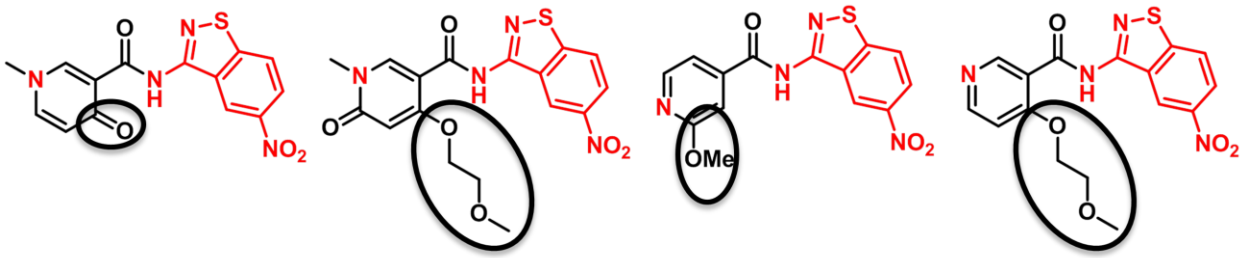

Figure 38: Common moieties in the four active compounds. The red colour highlights the identical 5-nitrobenzothiazole on the right and a N-containing ring on the left. The circles indicate the important chain or functionality present on C-4 or C-2 in each molecule.

An interesting feature is that the corresponding compounds with the isomeric benzothiazoles as the D-ring component were inactive. When the two systems (active and inactive) are superimposed on IDC16 in **figure 39**, it is evident that if the heteroaromatic ring is projecting straight out to the right (as in DGPS33/LB-72 and DGPS35/LB-70) with a similar 2D structure to IDC16, the compound is inactive, **figure 39a**. Alternatively, when the aromatic ring is projected downward or perpendicular to IDC16, **figure 37b**, it produces an active molecule. This suggests that, while in this orientation, there are supplementary binding interactions accessed by the 5-nitrobenzisothiazoles in which the inactive amides cannot participate. Secondly, the oxygen containing functionality is specific to each scaffold's activity; when it is absent or changed, the molecule is no longer active.

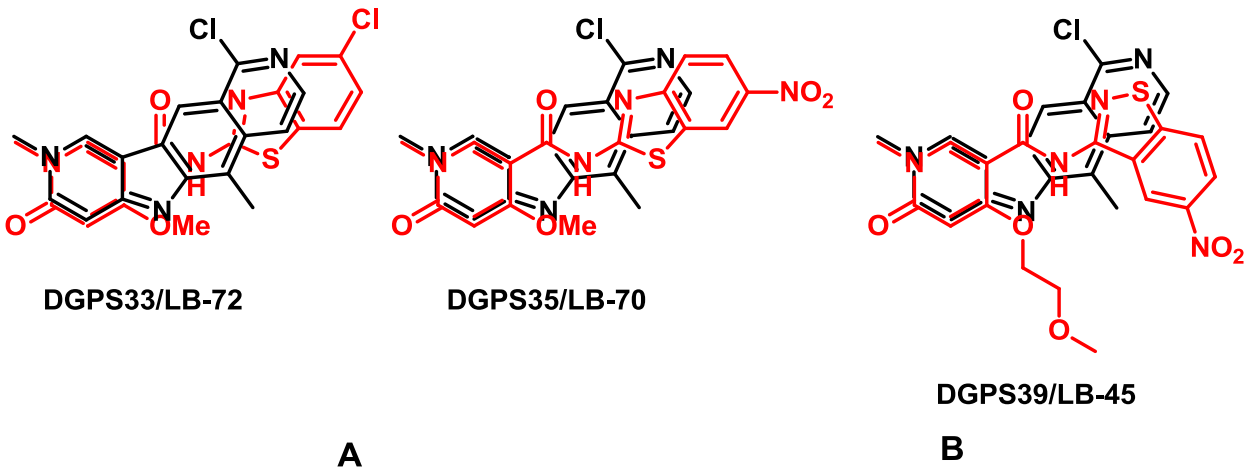

Figure 39: Active and inactive compound 2D superposition. A) Superposition of IDC16 and inactive benzothiazole amide analogues. B) Superposition of IDC16 and active benzisothiazole analogue.

4 Active Molecule Optimization

4.1 Structure activity relationship (SAR): Following the analysis of the biological results (see chapter 3), a structure activity relationship (SAR) was initiated for the active molecule DGSP39/LB-45 (**figure 35a**). Through examination of the benzisothiazole ring on the right hand side, it is possible to identify sites for modification: for example, changing the sulphur and/or nitrogen in the isothiazole, and removing or reducing the nitro group and substituting the nitro group. The two alterations that were addressed in this project were the sulphur atom and the nitro functionality.

Sulphur containing compounds, especially those in an isothiazole, are present throughout commercially used products and drugs. They are present in fungicides, cosmetics, dyes, photography agents, bactericides and have antimicrobial properties.[192] Even though this heteroaromatic ring has been more widely incorporated in pharmacologically active molecules, there are still some drawbacks to its usage. Sulphur can be reactive and is possibly more bioactive in a benzisothiazole, versus a benzthiazole, because of the weak N-S bond.

The presence of a nitro group in a bioactive compound is generally undesirable, especially when it is attached to a (hetero)aromatic ring. Nitro groups are strongly electron withdrawing and create an area of electron deficiency in a molecule. This localized area is reactive towards other molecules in the body like proteins, enzymes, nucleic acids, etc. and has the ability to undergo nucleophilic addition. Nitro groups can also undergo redox chemistry which involves a "six electron reduction of the nitro group to the corresponding amine, catalyzed by the CYP450 enzymes, xanthine oxidase, aldehyde oxidase and quinone reductase."[1] The reduction of a nitro group leads to the formation of reactive intermediates which are capable of inflicting DNA damage. The toxicity resulting from the reactive nitro group is usually contained to a local site, thus nitro groups are useful in drugs, such as antibiotics and fungicides.[193]

In a preliminary SAR study, our goal was to identify if the sulphur and the nitro functionality in the benzisothiazole ring were essential for anti-HIV activity. In this context, we have prepared analogues of DGSP39/LB-45 in which the sulphur atom has been replaced by an oxygen and nitrogen (NH) atom, and the nitro group was simultaneously replaced by a hydrogen atom as in the aminoisoxazoles and aminoindazoles, compounds **24b, d, f,** and **h**, with and without the nitro group.

4.2 Chemistry: The requisite 3-aminoisoxazoles, **22a** and **b**, served as the right side components in the target analogues **24a-h** and were prepared according to **schemes 22** and **23**. In the synthesis of both compounds a benzophenone oxime **19**, obtained in 85% yield by reaction of benzophenone with hydroxylamine hydrochloride in ethanol with pyridine as a base at 60°C for 2 hours, was used as the hydroxylamine source (**scheme 21**).[194] Benzophenone was selected because the synthesis of the aminoisoxazoles required an N-protected form of hydroxylamine; benzophenone protection can be removed easily following the isoxazole synthesis by the addition of water. Furthermore, benzophenone is very non polar and can easily be removed from the crude mixture. For use in the synthesis of the aminobenzisoxazoles **22a-b**, the potassium salt of the benzophenone oxime **19** had to first be formed *in situ* using potassium tert-butoxide (K^tOBu) in THF, at room temperature for 30 minutes. This intermediate benzophenone anion had to be used immediately without purification or isolation.

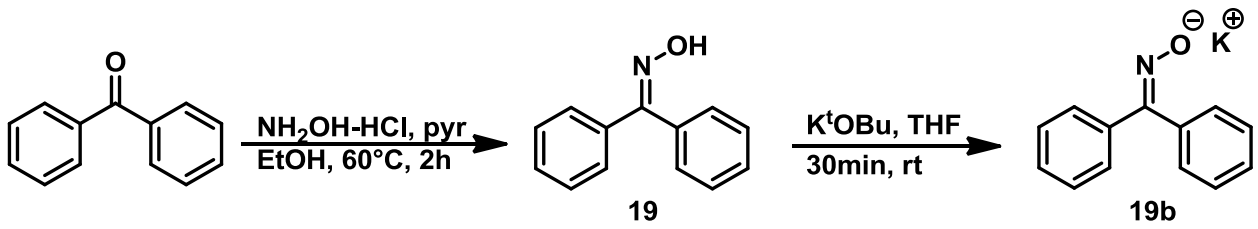

Scheme 21: Synthesis of benzophenone oxime 19 and the potassium salt 19b.

The synthesis of 5-nitro-3-aminobenzoisoxazole **22a** was achieved in three steps according to **scheme 22**. First 2-chlorobenzonitrile was prepared from 2-chloronitrile according to the literature, by reacting the nitrile with nitric acid in the presence of sulfuric acid at room temperature for 1 hour.[195] Nitration occurred at the *meta* position (C-5) to the nitrile which is at position C-1 of the ring. The nitrile is an electron withdrawing substituent and strongly deactivating which directed the nitro group to the *meta*, or C-5 position. The desired compound **20** was isolated following vacuum filtration and cold water wash, in 90% yield. The second step of the synthesis involved a S_NAr reaction between benzophenone oxime anion **19b** and 2-chloro-5-nitrobenzonitrile **20**. Following the addition of **20** to the THF suspension of **19b**, the two compounds were allowed to react at 55°C for 24 hours to give the intermediate benzophenone O-(5-chloro-2-benzonitrile) oxime **21a** in 76% yield after purification by column chromatography. The intermediate benzophenone O-(2-benzonitrile) oxime was then cyclized to the corresponding

5-nitro-3-aminobenzisoxazole **22a** through an intramolecular reaction in an acidic environment of TFA:HCl (4:1) at 55°C for 2 hours.[196] The target compound **22a** was isolated in 84% yield following purification by a wash with hexane.

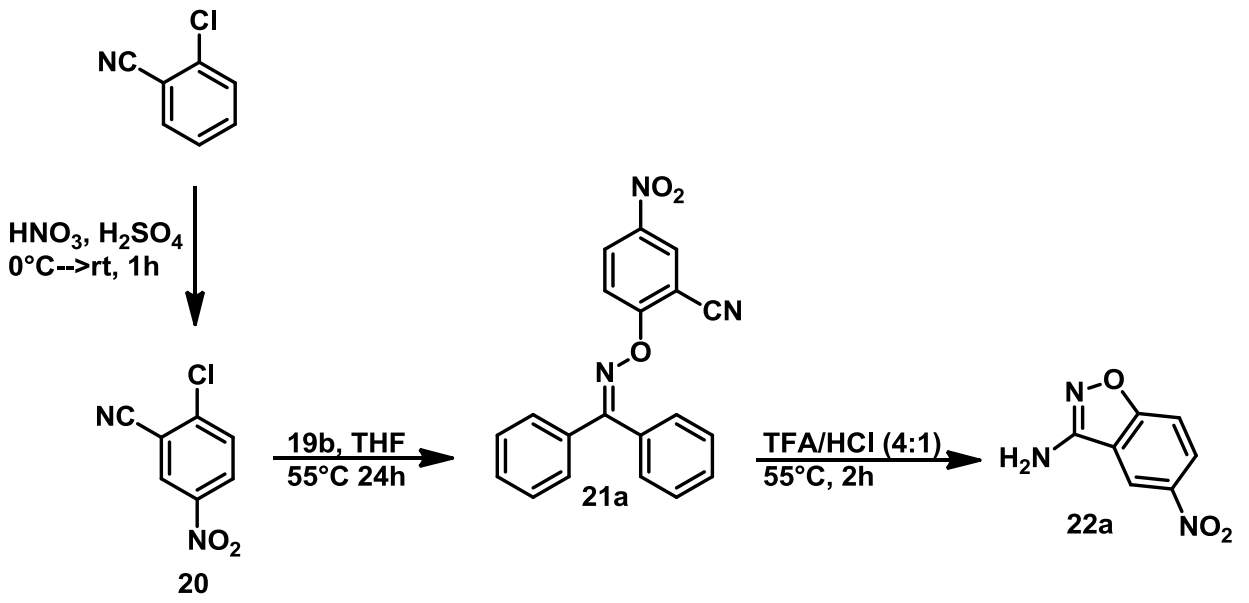

Scheme 22: Two step synthesis of 5-nitro-3-aminobenzisoxazole. Synthesis of 2-chloro-5-nitrobenzonitrile 20, oxime potassium salt 19b, intermediate O-(5-nitro-2-benzonitrile) oxime 21 and 5-nitro-3-aminobenzisoxazole 22a.

Similarly, in the preparation of 3-aminobenzisoxazole **22b**, benzophenone oxime anion **19b** was reacted with 2-fluorobenzonitrile at 55°C for 48 hours to give the intermediate benzophenone O-(2-benzonitrile) oxime **21b** in 96% yield following purification by column chromatography (**scheme 23a**). The cyclization of **21b** also occurred in an acidic environment of TFA:HCl (4:1) at 55°C for 2 hours to give the desired 3-aminobenzisoxazole **22b** in 93% yield after purification by column chromatography.

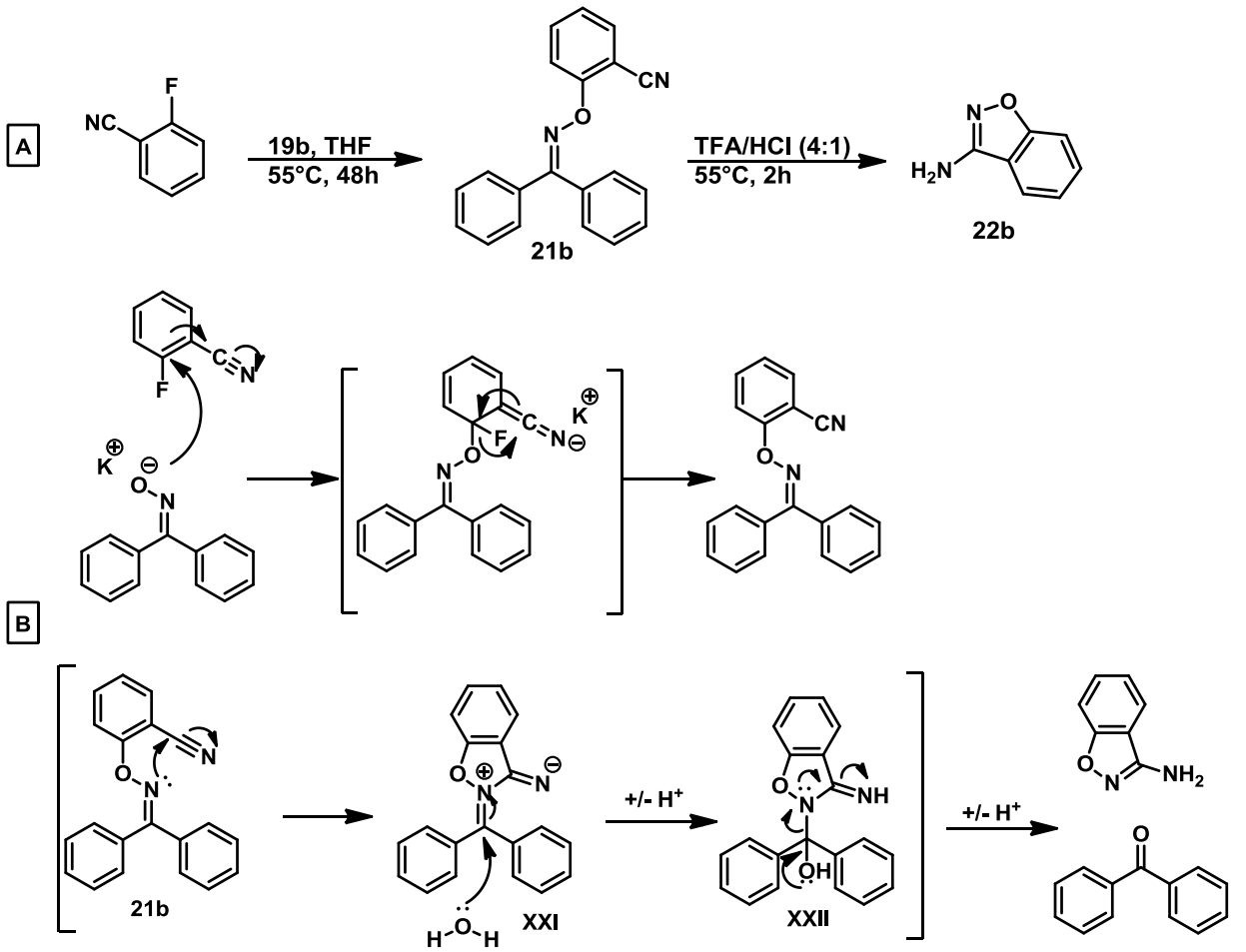

Scheme 23: Synthesis and mechanism of 3-aminoisoxazole. A. Synthesis of 3-aminoisoxazole 22b from intermediate 21b. B. The mechanism of isoxazole formation.

The mechanism of this reaction is shown in **scheme 23b** and begins with a nucleophilic attack of the oxygen anion of the benzophenone oxime **19b** on the halogen-substituted carbon of the benzonitrile. The halogen is eliminated as potassium halide (either potassium fluoride or chloride). This reaction occurred cleanly with both substrates but occurred more quickly with 2-chloro-5-nitrobezonitrile (24 hours) than 2-fluorobenzonitrile (48 hours) because the nitro functionality is an electron withdrawing, ring deactivating substituent. This, combined with the electronegative chlorine, makes the C-2 carbon very electron poor and susceptible to nucleophilic attack. Conversely, 2-fluorobenzonitrile does not have an electron withdrawing nitro functionality, but fluorine is a better leaving group than chlorine in S_NAr reactions. However, despite the difference in halide leaving groups, the presence of the nitro group is sufficient to make the C-2 position on the 2-chloro-5-nitrobenzonitrile more electron deficient and more reactive than the C-2 position on the 2-fluorobenzonitrile.

Subsequently, the intramolecular reaction of the intermediate benzophenone O-(2-benzonitrile) oxime **19a** begins with an attack on the nitrile carbon by the nitrogen lone pair of electrons of the benzophenone oxime to produce an isoxazolidine 5-membered ring **XXI**. Water then adds to the iminium ion-type intermediate to give **XXII** and aromatization of the benzisoxazole ring is achieved through the lone pair of electrons of the isoxazolidine ring nitrogen **XXII,** aromatizing the ring and forming a more stable exocyclic amine.

The final step of this reaction involves treatment with TFA and HCl to form the 3-aminobenzisoxazole. This step was very clean and the only impurity was benzophenone which, because it is very non polar, was easily removed by silica gel flash column chromatography or by washing with hexane. Yields were greater than 80%, as a small amount of the target compound was lost during the purification process. A sample NMR of **22b** is shown in **figure 40**. The aromatic and amine peaks are labelled and correspond to those in the literature.[196]

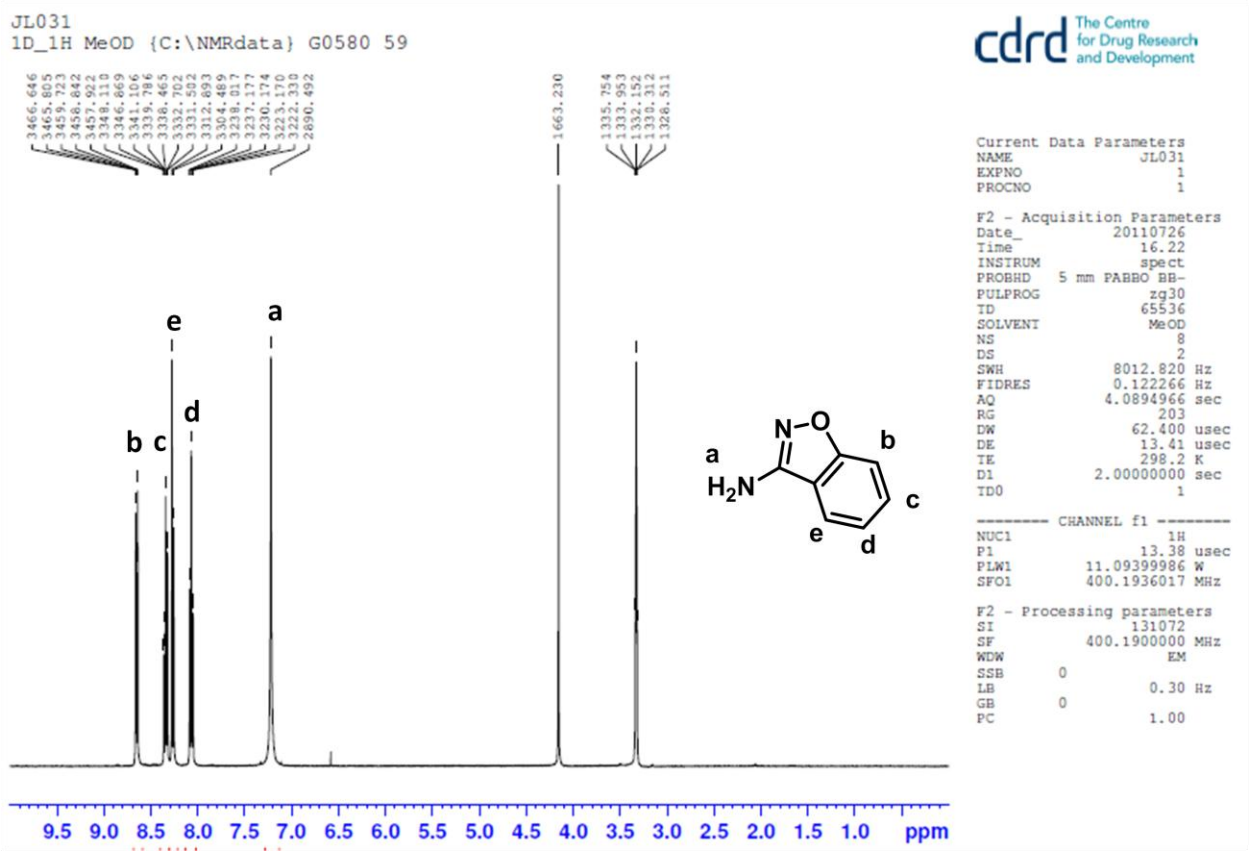

Figure 40: NMR spectra of 3-aminobenzisoxazole (22b). The peaks a-e corresponding to the protons on the compound 22b are labelled.

The corresponding 3-aminoindazoles (**23a** & **23b**) were synthesized, according to **scheme 24a**, by reacting the same two benzonitriles, from **scheme 22** and **23** with hydrazine in butanol at reflux.[197] Again, a S_NAr substitution reaction is involved. The target aminoindazoles, **23a** and **23b**, were isolated in 81% and 97% yield respectively after purification by separate water and ethyl acetate washes followed by vacuum filtration or column chromatography. Compounds **19**, **20**, **21a-b**, **22a-b**, and **23a-b** were synthesized with the help of a summer student, June Lee, whose research I oversaw and directed.

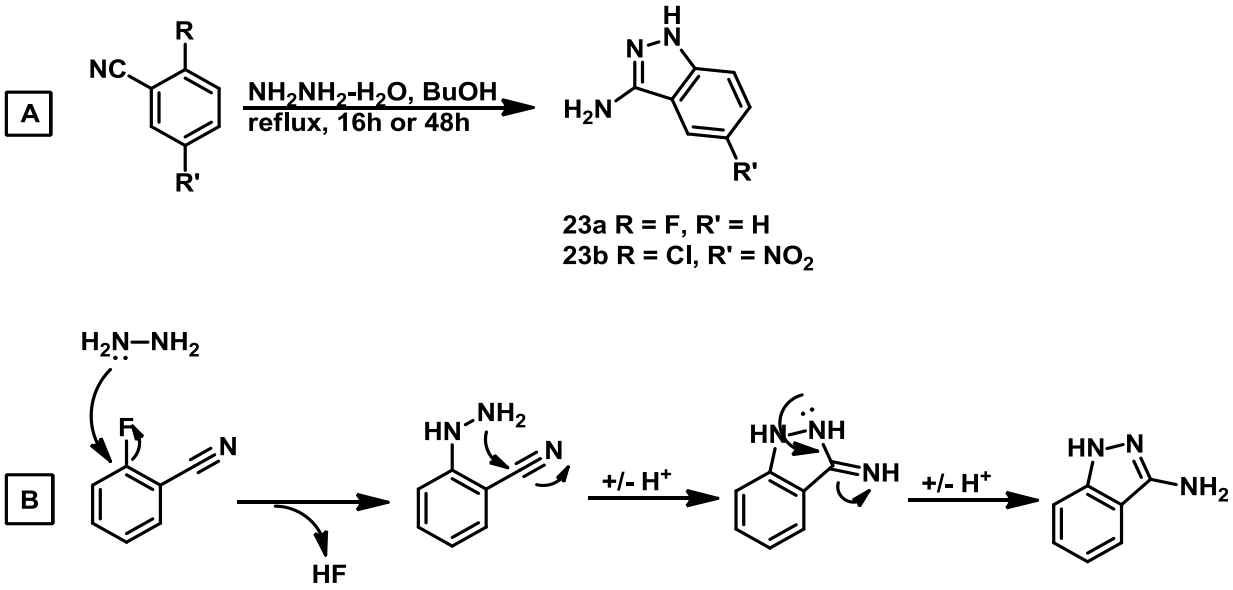

Scheme 24: Synthesis and mechanism of 3-aminoindazoles. A. Synthesis of aminoindazoles (24a & b) using hydrazine hydrate. B. Mechanism of aminoindazole formation.

The synthesis of the 3-aminoindazoles (**23a** & **b**) was slightly more challenging when using 2-chloro-5-nitrobenzonitrile **20** rather than 2-fluorobenzonitrile. This is because there were more side reactions using **20** (according to TLC), likely due to the fact that the nitro-substituent and hydrazine are both very reactive. Purification for both aminoindazoles was challenging. The synthesis of 3-aminoindazole was clean however the R_f (retention factor) values for the product and starting material, 2-fluorobenzonitrile, were similar. It was difficult to separate them using column chromatography; therefore the isolated yield was lower for the 3-aminoindazole than the 3-amino-5-nitroindazole. Impurities in the synthesis of 3-amino-5-nitroindazole made the purification slightly more difficult and yields, overall, were slightly lower than 100%. **Figure 41** shows an NMR of **23b**; the aromatic, and amine peaks correspond to literature values.[197]

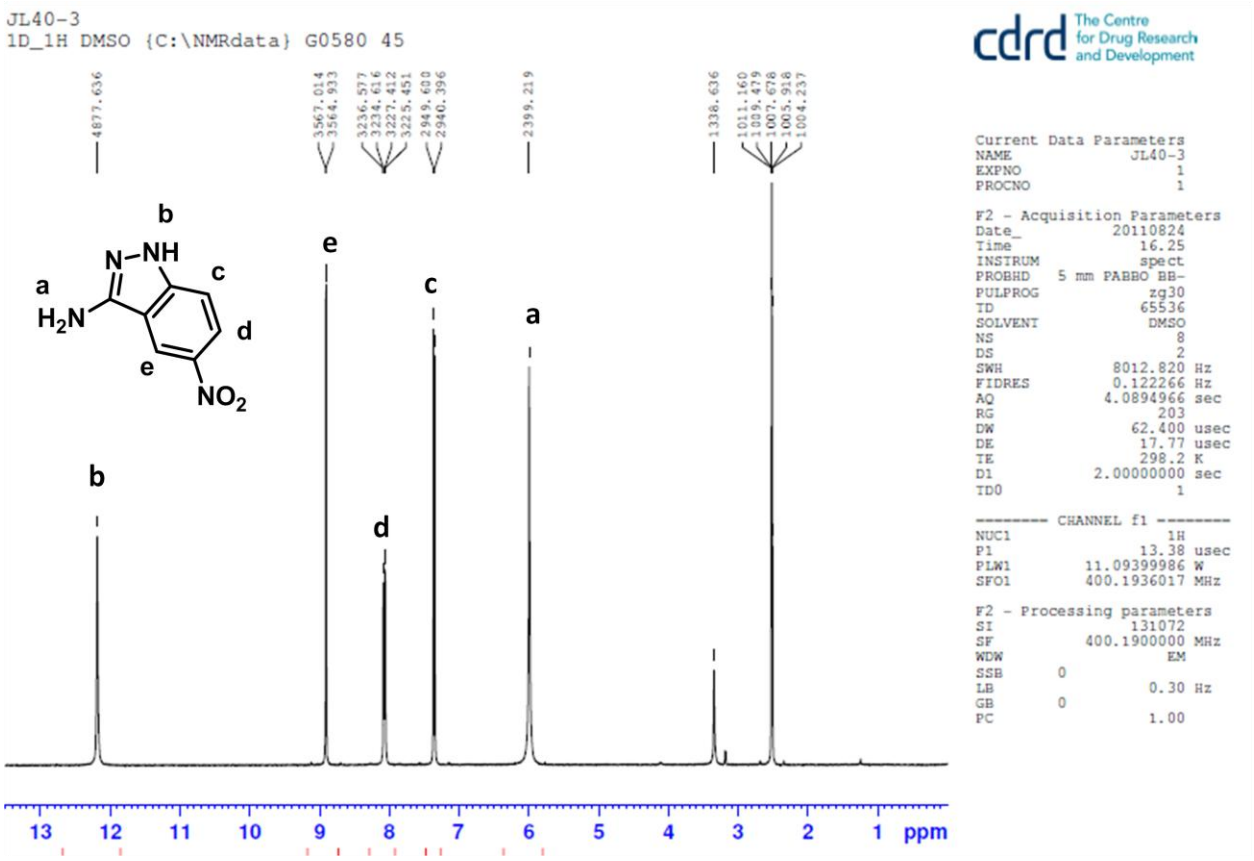

Figure 41: NMR spectra of 5-nitroindazol-3-amine (23b). The peaks a-e corresponding to the protons on the compound 23b are labelled.

Compounds **22a**, **22b**, **23a**, and **23b** were then coupled with 4-methoxy-2-pyridinone-5-carboxylic acid **4** and 4-methoxyethoxy-2-pyridinone-5-carboxylic acid **9**. According to **scheme 25**, the 3-aminobenzisozazoles (**22a-b**) and 3-aminoindazoles (**23a-b**) were reacted with the corresponding acid chlorides **4a** and **9a**, synthesized using $SOCl_2$ at reflux, in the presence of K_2CO_3 and THF, under nitrogen and at 0°C, to give the desired amides **24a-h** in 99%, 63%, 8.5%, 19%, 38%, 47%, 62% and 69% yields, respectively, following purification by either a water and ethyl acetate wash followed by vacuum filtration or by column chromatography.

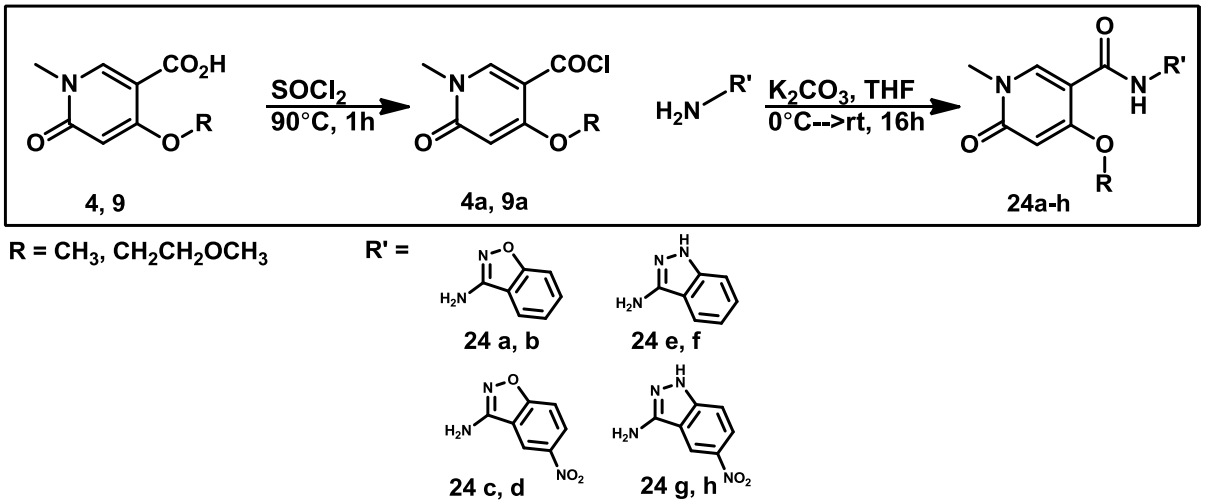

Scheme 25: SAR amide synthesis. Amide synthesis using aminobenzisoxazoles and aminoindazoles with two different 4-substituted 2-pyridinone scaffolds to make compounds 24a-h.

This procedure, adapted from the 1,2,4-oxadiazole synthesis, was the most effective at producing the desired amide. There were no problems with a triethylammonium salt or pyridine. The yields were, overall, moderate to excellent (38% to 99%) however, there were two compounds **24 c** and **d** with poor yields (9% and 19%). The reason for this is not clearly evident but the problem is likely rooted in the 3-amino-5-nitrobenzisoxazole because both compounds contain this amine. At the present time no conclusions can be made with regards to why these amines were the only ones to produce poor yields; the reactions will need to be repeated in order to further elucidate the problem. The variable yields observed between the other final products (**24 a-b** and **e-h**) were likely caused by factors similar to those observed with the oxadiazoles and amide coupling reactions. Additionally, the isolation and purification process was difficult at times as some impurities, especially with the nitro-substituted amines, had R_f values very similar to the product making it difficult to separate them, resulting in lower yields.

A representative NMR of **24h** is shown in **figure 42**. Again the C-3 and C-6 protons are the ones of particular interest. The peak for the C-3 proton did not differ between all the compounds (5.99 ppm-6.05 ppm) as there was either a methoxy or a methoxy ethanol substituent present. The chemical shift of the proton on C-6 followed a general pattern whereby the nitro containing molecules had a slight downfield shift compared to the same molecule without the nitro group, i.e. 8.43 ppm versus 8.66 ppm.

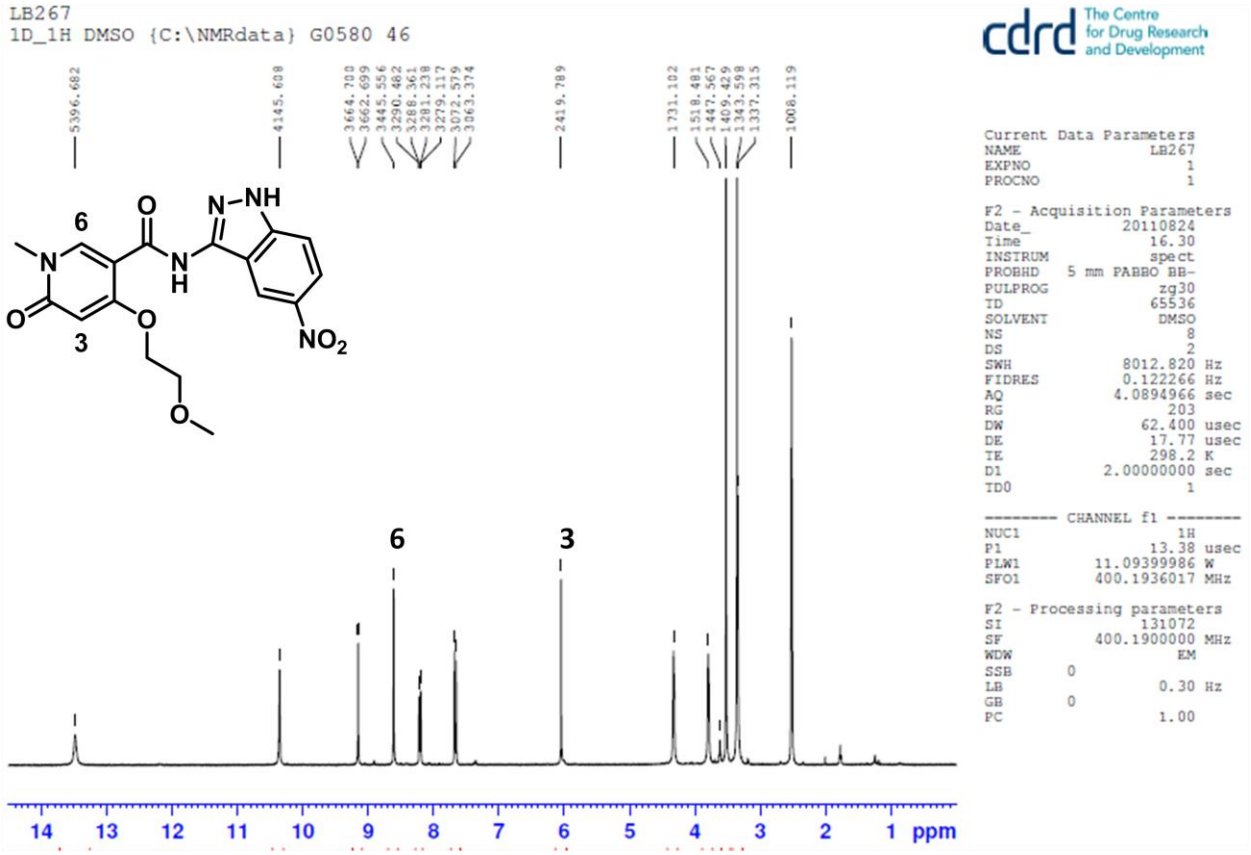

Figure 42: Representative NMR spectra of SAR compounds (24h). The protons on C-3 and C-6 are labelled.

5 Conclusion

In the absence of structural data for a specific protein target, compound library screening is the only approach one can adopt to identify an active inhibitor. Splicing and alternative splicing is a vital cellular process whereby a pre-mRNA is modified, through the removal of introns and rejoining of exons, to produce a mature mRNA which is translated into a distinct protein. The spliceosome is a massive, multicomponent entity responsible for the regulation and proper activity of splicing and alternative splicing. Abnormalities in the splicing processes and splicing machinery have the potential to result in human disease. Being able to control or modify aberrant splicing through the use of small molecules would be a valuable tool for disease treatment and control.

HIV-1, once it enters a cell, takes control of the cellular machinery and uses it to replicate its viral RNA and produce new viruses. This means the virus also takes over the spliceosomal components and uses them to produce its viral proteins. IDC16 is a molecule that was identified to inhibit splicing in HIV-1 by inhibiting the SR protein SRSF1 and preventing HIV-1 replication.

IDC16 is a suboptimal drug candidate because it is mildly cytotoxic on account of its ability to intercalate DNA. Therefore, in order to take advantage of its activity to produce a new anti-HIV/AIDS drug, a suitable mimic must be synthesized which is not cytotoxic. The goal of this project was to synthesize IDC16 mimics that do not intercalate DNA, are easier to synthesize than IDC16 and have the same protein target, SRSF1.

In order to build a diverse library of IDC16 mimics, five objectives were identified and pursued using a base 2-pyridinone scaffold. A library of amides was synthesized using peptide coupling of an acid chloride, synthesized using an excess of $SOCl_2$ at reflux, with various (hetero)aromatic amines in the presence of a base. The most effective procedure to accomplish this required use of K_2CO_3 as a base, THF as a solvent, and reaction conditions of 0°C under an N_2 atmosphere. The 1,2,4-oxadiazole library was the least problematic objective and resulted in the synthesis of 15 compounds in moderate yields. Synthesizing the isoxazolidinone 5-membered ring fused to the 2-pyridinone was not achieved but will be addressed in future work. The fourth and fifth objectives were successful with a small number of (hetero)aromatic compounds. Their syntheses need to be optimized to make them applicable to a wider scope of substrates.

This project successfully identified one active molecule, DGPS39/LB-45 (E5) able to inhibit HIV-1 replication. Furthermore, it was part of a larger effort to produce a total of four active molecules. Because of this activity, this project initiated a preliminary SAR investigation on the active compound. The work done can be applied to the other active molecules to produce a more complete SAR.

In general, using the biological results on hand, it appears that mimics that are almost identical in 2D structure to IDC16 do not provide optimal activity. Those compounds whereby the heteroaromatic substituent is projecting perpendicular to the D-ring of IDC16 appear to be the most active. This principle will need to be investigated further through the exploration and extension of objectives 4 and 5.

This project has limitations with regards to the biological testing. The data presented in this thesis is preliminary data; therefore any conclusions that have been drawn from it are subject to scrutiny. It is necessary to do further testing in order to obtain definitive data that the compounds are inhibiting a process or protein involved in alternative splicing and not through the same traditional mechanisms used by HAART drugs. This is an ongoing process that will be developed and optimized to obtain conclusive data.

Ultimately, this project has the potential to make a large impact on our understanding of the involvement of SR proteins in HIV-1 splicing. It also represents an entirely new strategy for HIV/AIDS treatment.

5.1 Future directions: This project has instigated an interest into an exciting area of research. An active molecule has been identified and it now gives this project more focus and direction. From here, there are many areas that need be addressed with regards to the specific objectives and the SAR work. The isoxazolidin-6-one ring of objective 3 was not synthesized; the problems need to be addressed and the synthesis needs to be completed successfully. The procedures presented in objectives 4 and 5 need to be optimized so they are more widely applicable to various aromatic and heteroaromatic substrates. The amine silylation procedure is a novel and logical idea, but needs more work with regards to both experimental technique and procedural optimization. Finally, there needs to be a more extensive SAR with regards to compound DGPS39/LB-45 (E5).

6 Experimental

Reagents and solvents were purchased from Sigma Aldrich or Fisher Scientific. All reagents and solvents were used without further purification unless otherwise stated. Reactions were monitored by TLC. TLC was performed using aluminum plates pre-coated with silica gel (Manufacturer: EMD Chemicals Inc., Silica Gel 60 F_{254}). Flash column chromatography was performed using silica gel (Manufacturer: Silicycle, Siliaflash® F60, 40-63μm, 230-400 mesh) or on a Biotage Isolera Four System (Manufacturer: PartnerTech Åtvidaberg AB) with pre-packed silica gel columns (Manufacturer: Biotage, part no. FSKO-1107-0010, FSKO-1107-0025, or FSKO-1107-0050). Microwave reactions were performed on a Biotage Initiator Robot Eight System (Manufacture: PartnerTech Åtvidaberg AB). Mass spectra were recorded on Quatrro Premier XE (Manufacture: Waters). ^{1}H-NMR spectra were recorded on a Bruker AVII+ (400 MHz) NMR spectrometer with a 5mm TXI or BBOF with z-gradients. Chemical shifts are expressed in ppm, δ scale using tetramethylsilane as the reference standard. When peak multiplicities are reported, the following abbreviations are used: s (singlet), d (doublet), t (triplet), q (quartet), m (multiplet), dd (doublet of doublet), dt (doublet of triplet). Coupling constants are reported in Hertz (Hz).

Please note that the C-6 substituted 3-aminopyridines synthesized by Dr. Mitra Matloobi (**6b, 6e, 6f** and **10d**) were unstable and were used in the amide coupling reactions immediately following their synthesis. Because of this, decomposition was observed and the resulting NMR spectra were not clean in the alkyl region but clean in the aromatic region. The NMR spectra have been included even though the alkyl region is not clean. The desired compounds were confirmed by mass spectrometry.

Preparation of Ethyl 4-hydroxy-1-methyl-6-oxo-1,6-dihydropyridine-3-carboxylate from diethyl 1,3-diacetonedicarboxylate **2**:

Acetic anhydride (26.05ml, 276mmol) was added to a solution of diethyl 1,3-acetonedicarboxylate (25ml, 138mmol) and triethyl orthoformate (22.9ml, 138mmol). The mixture was heated at 130°C for 1 hr. The yellow solution was then concentrated in vacuo to remove excess acetic anhydride. The resulting mixture was cooled to 0ºC and methylamine (26.5ml, 138mmol) was added followed by water (100ml). The solution was stirred at room temperature overnight. The solution was then washed with EtOAc (150 ml) and the aqueous

layer was acidified to pH 2 using conc. HCl and cooled to 0ºC. A white precipitate formed and was isolated by vacuum filtration. The filtrate was extracted with ethyl acetate (4 x 50mL) and the combined organic layers were dried over sodium sulfate and concentrated in vacuo to yield a yellow solid from which a further crop of white solid product was obtained by crystallization from H_2O followed by filtration. The remaining filtrate was concentrated and silica gel flash column chromatography was performed (DCM/MeOH; 98:2). The tubes containing the desired product were combined and concentrated in vacuo. The desired product, obtained from all methods of isolation and purification were combined, the product was a white solid; 20g, 74%. MS APCI (+) *m/z* 198 (M+) detected; ^{1}H NMR (400 MHz, $CDCl_3$) δ 8.15 (s, 1H), 5.94 (s, 1H), 4.38 (q, 2H, J=7.1Hz), 1.40 (t, 3H, J=7.1Hz).

Preparation of Ethyl 4-methoxy-1-methyl-6-oxo-1,6-dihydropyridine-3-carboxylate from ethyl 4-hydroxy-1-methyl-6-oxo-1,6-dihydropyridine-3-carboxylate **3**:

Ethyl 4-hydroxy-1-methyl-6-oxo-1,6-dihydropyridine-3-carboxylate (3.00g, 15.2mmol) was dissolved in dry DMF (100ml). Cesium carbonate (6.44g, 19.76mmol) and dimethyl sulfate (1.89ml, 19.76mmol) were added. The colourless reaction mixture was stirred overnight at room temperature. The mixture was diluted with water (35ml) and the aqueous layer extracted with DCM. The combined organic layers were washed with brine, dried over sodium sulfate and concentrated in vacuo to yield compound the desired compound as a white solid; 2.78g, 87%. MS APCI (+) *m/z* 212.1 (M+) detected; ^{1}H NMR (400 MHz, $CDCl_3$) δ 8.11 (s, 1H), 5.93 (s, 1H), 4.32 (q, 2H, J=7.1Hz), 3.87 (s, 3H), 3.56 (s, 3H), 1.36 (t, 3H, J=7.1Hz).

Preparation of 4-methoxy-1-methyl-6-oxo-1,6-dihydropyridine-3-carboxylic acid from ethyl 4-methoxy-1-methyl-6-oxo-1,6-dihydropyridine-3-carboxylate **4**:

Ethyl 4-methoxy-1-methyl-6-oxo-1,6-dihydropyridine-3-carboxylate (1g, 4.73mmol) was dissolved in THF:MeOH:H_2O (2:2:1, 120ml). Lithium hydroxide (0.340g, 14.20mmol) was then added. The transparent, yellow solution was stirred overnight at room temperature. The reaction mixture was acidified with concentrated HCl. The aqueous layer was extracted with DCM (3 x 50ml) and the combined organic layers were dried over sodium sulfate, filtered and concentrated in vacuo to yield the desired compound as a white solid; 736mg, 85% MS APCI (-) *m/z* 182.0

(M-) detected; ^{1}H NMR (400 MHz, MeOD) δ 8.37 (s, 1H), 5.98 (s, 1H), 3.88 (s, 3H), 3.55 (s, 3H).

Preparation N-(2-chloropyridin-4-yl)-4-methoxy-1-methyl-6-oxo-1,6-dihydropyridine-3-carboxamide from 4-methoxy-1-methyl-6-oxo-1,6-dihydropyridine-3- carboxylic acid **5k**:
4-methoxy-1-methyl-6-oxo-1,6-dihydropyridine-3-carboxylic acid (100mg, 0.546mmol) was dissolved in an excess of thionyl chloride (2ml) and the reaction mixture was stirred at room temperature for 1 hour. The excess thionyl chloride was removed in vacuo. 4-methoxy-1-methyl-6-oxo-1,6-dihydropyridine-3-carbonyl chloride was dissolved in pyridine (3ml). 2-chloropyridin-4-amine (103mg, 0.8mmol) was added at 0°C and the reaction mixture was stirred at room temperature overnight. The pyridine was removed in vacuo. The crude mixture was purified by washing with acetone followed by vacuum filteration. The final product was isolated as a beige solid; 136mg, 58%. MS APCI (-) *m/z* 292.0 (M-) detected; ^{1}H NMR (400 MHz, DMSO) δ 10.22 (s, 1H), 8.31 (s, 1H), 8.29 (d, 1H, J=5.7Hz), 7.84 (d, 1H, J=1.7Hz), 7.67 (d, 1H, J=1.9Hz), 5.95 (s, 1H), 3.88 (s, 3H), 3.45 (s, 3H).

Preparation of N-(2-hydroxyphenyl)-4-methoxy-1-methyl-6-oxo-1,6-dihydropyridine-3-carboxamide from 4-methoxy-1-methyl-6-oxo-1,6-dihydropyridine-3-carboxylic acid **5a**:
Prepared as described for **5k** from **4** (100mg, 0.546mmol) using 2-aminophenol (55mg, 0.5mmol). The compound was purified by silica gel flash column chromatography. The fractions containing the pure product were combined and concentrated in vacuo. The desired compound was obtained as a white solid; 57mg, 52%. MS APCI (-) *m/z* 273.0 (M-) detected; ^{1}H NMR (400 MHz, DMSO) δ 8.48 (s, 1H), 8.28 (d, 1H, J=7.6Hz), 6.91 (d, 1H, J=1.4Hz), 6.00 (s 1H), 3.98, (s, 3H), 3.49 (s, 3H).

Preparation of 4-methoxy-1-methyl-6-oxo-N-phenyl-1,6-dihydropyridine-3-carboxamide from 4-methoxy-1-methyl-6-oxo-1,6-dihydropyridine-3-carboxylic acid **5b**:
Prepared as described for **5k**, from **4** (100mg, 0.546mmol) using aniline (47mg, 0.5mmol). The desired compound was isolated as a white solid; 5mg, 4%. MS APCI (+) *m/z* 259.4 (M+) detected. ^{1}H NMR (400 MHz, $CDCl_3$) δ 9.24 (s, 1H), 8.44 (s, 1H), 7.61 (dd, 2H, J=0.9Hz, J=8.5Hz), 7.39 (t, 2H, J=8.0Hz), 7.17 (t, 1H, J=7.4Hz), 6.05 (s, 1H), 4.05 (s, 3H), 3.62 (s, 3H).

Preparation of N-(3-cyanophenyl)-4-methoxy-1-methyl-6-oxo-1,6-dihydropyridine-3-carboxamide from 4-methoxy-1-methyl-6-oxo-1,6-dihydropyridine-3-carboxylic acid **5c**:

Prepared as described for **24b**, from **4** (70mg, 0.38mmol) using 3-aminobenzonitrile (45mg, 0.38mmol). The desired compound was isolated as a peach-brown solid; 98mg, 92%. MS APCI (-) *m/z* 282.0 (M-) detected; ^{1}H NMR (400 MHz, $CDCl_3$) δ 9.37 (s, 1H), 8.45 (s, 1H), 8.03 (s, 1H), 7.82 (dt, J=8.0Hz, J=1.6Hz), 7.49 (t, 1H, J=7.8Hz), 7.45 (td, 1H, J=1.4Hz, J=7.7Hz), 6.05 (s, 1H), 4.08 (s, 3H), 3.64 (s, 3H).

Preparation of methyl 4-(4-methoxy-1-methyl-6-oxo-1,6-dihydropyridine-3-carboxamido)benzoate from 4-methoxy-1-methyl-6-oxo-1,6-dihydropyridine-3-carboxylic acid **5d**:

Prepared as described for **5k**, from **4** (100mg, 0.546mmol) using methyl 4-aminobenzoate (76mg, 0.5mmol). The desired product was isolated as a white solid; 88mg, 45%. MS APCI (+) *m/z* 315.1 (M+) detected; ^{1}H NMR (400 MHz, DMSO) δ 10.05 (s, 1H), 8.28 (s, 1H), 7.94 (d, 1H, J=8.8Hz), 7.83 (d, 1H, J=8.8Hz), 5.95 (s, 1H), 3.88 (s, 3H), 3.83 (s, 3H), 3.45 (s, 3H).

Preparation of 4-(4-methoxy-1-methyl-6-oxo-1,6-dihydropyridine-3-carboxamido)benzoic acid from methyl 4-(4-methoxy-1-methyl-6-oxo-1,6-dihydropyridine-3-carboxamido)benzoate **5e**:

Methyl 4-(4-methoxy-1-methyl-6-oxo-1,6-dihydropyridine-3-carboxamido)benzoate (100mg, 0.3mmol) was dissolved in THF:MeOH:H_2O (2:2:1, 5ml). Lithium hydroxide (23mg, 0.9mmol) was added to the suspension and the reaction mixture was heated at 40°C overnight. The mixture was acidified dropwise with concentrated HCl until a precipitate started to form. A pink solid was collected following filtration. The final product was isolated as a pink solid; 70mg, 77%. MS APCI (+) *m/z* 301 (M+) detected; ^{1}H NMR (400 MHz, $CDCl_3$) δ 9.97 (s, 1H), 8.24 (s, 1H), 7.87 (d, 2H, J= 8.74Hz), 7.77 (d, 2H, J= 8.77Hz), 5.91 (s, 1H), 3.85 (s, 3H), 3.41 (s, 3H)

Preparation of 4-methoxy-N-(4-methoxyphenyl)-1-methyl-6-oxo-1,6-dihydropyridine-3-carboxamide from 4-methoxy-1-methyl-6-oxo-1,6-dihydropyridine-3-carboxylic acid **5f**:

Prepared as described for **24b**, from **4** (80mg, 0.5mmol) using 4-methoxyaniline (57µl, 0.4mmol) with changes to the purification procedure. The crude mixture was purified using silica gel flash

column chromatography on Isolera (EtOAc:MeOH, 0:1). The desired fractions were combined and concentrated in vacuo. The desired compound was isolated as a white solid; 86mg, 68%. MS APCI (+) *m/z* 289.4 (M+) detected; ^{1}H NMR (400 MHz, DMSO) 10.02 (s, 1H), 8.24 (s, 1H), 7.90 (d, 2H, J=8.8Hz), 7.79 (d, 2H, J=8.8Hz), 5.91 (s, 1H), 3.85 (s, 3H), 3.79 (s, 3H), 3.41 (s, 3H).

Preparation of ethyl 3-(4-methoxy-1-methyl-6-oxo-1,6-dihydropyridine-3-carboxamido)benzoate from 4-methoxy-1-methyl-6-oxo-1,6-dihydropyridine-3-carboxylic acid **5g**:

Prepared as described for **5k**, from **4** (800mg, 0.44mmol) using ethyl 3-aminobenzoate (522µl, 0.44mmol). The desired product was isolated as a white solid; 300mg, 26%. MS APCI (+) *m/z* 331.2 (M+) detected; ^{1}H NMR (400 MHz, DMSO) δ 9.94 (s, 1H), 8.36 (m, 1H), 8.27 (s, 1H), 7.91 (d, 1H, J=8.13Hz), 7.69 (d, 1H, J=7.84Hz), 7.48 (t, 1H, J= 7.92Hz), 5.93 (s, 1H), 4.31 (q, 2H, J=7.10Hz), 3.88 (s, 3H), 3.45 (s, 3H), 3.31 (s, 1H), 3.17 (d, 2H, J=5.26Hz), 1.31 (t, 3H, J=7.10Hz).

Preparation of N-(6-chloropyridin-3-yl)-4-methoxy-1-methyl-6-oxo-1,6-dihydropyridine-3-carboxamide from 4-methoxy-1-methyl-6-oxo-1,6-dihydropyridine-3-carboxylic acid **5h**:

Prepared as described for **5k**, from **4** (183mg, 1.0mmol) using 6-chloropyridin-3-amine (103mg, 0.8mmol). The desired product was isolated as a pale pink solid; 234mg, 58%. MS APCI (+) *m/z* 292.1 (M+) detected; ^{1}H NMR (400 MHz, DMSO). δ 9.99 (s, 1H), 8.71 (d, 1H, J=2.65Hz), 8.31 (s, 1H), 8.18 (dd, 1H, J=2.78Hz, J=8.69Hz), 7.52 (d, 1H, J=8.68Hz), 5.95 (s, 1H), 3.89 (s, 2H), 3.45 (s, 2H), 3.31 (s, 2H)

Preparation of 4-methoxy-N-(6-methoxypyridin-3-yl)-1-methyl-6-oxo-1,6-dihydropyridine-3-carboxamide from 4-methoxy-1-methyl-6-oxo-1,6-dihydropyridine-3-carboxylic acid **5i**:

Prepared as described for **24b**, from **4** (93mg, 0.51mmol) using 6-methoxypyridin-3-amine (63mg, 0.51mmol). The desired product was isolated as a pink-purple solid; 93mg, 62%. MS APCI (+) *m/z* 290.3 (M+) detected; ^{1}H NMR (400 MHz, DMSO) δ 9.71 (s, 1H), 8.45 (d, 1H, J=2.5Hz), 8.31 (s, 1H), 7.97 (dd, 1H, J=2.7Hz, J=8.9Hz), 6.84 (d, 1H, J=8.8Hz), 5.95 (s, 1H), 3.91 (s, 3H), 3.85 (s, 3H), 3.46 (s, 3H).

Preparation of N-(6-cyanopyridin-3-yl)-4-methoxy-1-methyl-6-oxo-1,6-dihydropyridine-3-carboxamide from 4-methoxy-1-methyl-6-oxo-1,6-dihydropyridine-3-carboxylic acid **5j**:

Prepared as described for **5k**, from **4** (1g, 5.5mmol) using 5-amino-2-pyridinecarbonitrile (553mg, 4.6mmol). The desired product was isolated as a solid; 200mg, 15%. MS APCI (+) *m/z* 285.1 (M+) detected; ^{1}H NMR (400 MHz, DMSO) δ 10.28 (s, 1H), 8.98 (d, 1H, J=2.0Hz), 8.38 (dd, 1H, J=2.5Hz, J=8.6Hz), 8.35 (s, 1H), 8.02 (d, 1H, J=8.6Hz), 5.96 (s, 1H), 3.90 (s, 3H), 3.46 (s, 3H).

Preparation of N-((6-chloropyridin-3-yl)methyl)-4-methoxy-1-methyl-6-oxo-1,6-dihydropyridine-3-carboxamide from 4-methoxy-1-methyl-6-oxo-1,6-dihydropyridine-3-carboxylic acid **5l**:

Prepared as described for **5k**, from **4** (100mg, 0.5mmol) using (6-chloropyridin-3-yl)methanamine (57mg, 0.4mmol). The desired product was isolated as a white solid; 18mg, 15%. MS APCI (+) *m/z* 308.1 (M+) detected; ^{1}H NMR (400 MHz, DMSO) δ 8.50 (t, 1H, J=5.8Hz), 8.35 (d, 1H, J=2.0Hz), 8.26 (s, 1H), 7.76 (dd, 1H, J=2.5Hz, J=8.3Hz), 7.47 (d, 1H, J=8.4Hz), 5.89 (s, 1H), 4.45 (d, 2H, J=6.0Hz), 3.85 (s, 3H), 3.42 (s, 3H).

Preparation of 4-methoxy-1-methyl-6-oxo-N-(pyridin-2-ylmethyl)-1,6-dihydropyridine-3-carboxamide from 4-methoxy-1-methyl-6-oxo-1,6-dihydropyridine-3-carboxylic acid **5m**:

Prepared as described for **24b**, from **4** (100mg, 0.5mmol) using pyridin-2-ylmethanamine (43mg, 0.4mmol) with changes to the work up procedure. Following removal of THF, water was added and the desired compound was extracted with EtOAc 3 times. The combined organic extracts were dried over Na_2SO_4, filtered and concentrated in vacuo. The desired product was isolated as a pale yellow solid; 110mg, 96%. MS APCI (+) *m/z* 274.3 (M+) detected; ^{1}H NMR (400 MHz, DMSO) δ 8.66 (t, 1H, J=5.4Hz), 8.55 (d, 1H, J=4.8Hz), 8.33 (s, 1H), 7.78 (dt, 1H, J=1.8Hz, J=7.7Hz), 7.33 (d, 1H, J=7.9Hz), 7.29 (dd, 1H, J=5.2Hz, J=7.2Hz), 5.94 (s, 1H), 4.58 (d, 2H, J=5.6Hz), 3.92 (s, 3H), 3.46 (s, 3H).

Preparation of 4-methoxy-1-methyl-N-(4-methylthiazol-2-yl)-6-oxo-1,6-dihydropyridine-3-carboxamide from 4-methoxy-1-methyl-6-oxo-1,6-dihydropyridine-3-carboxylic acid **5n**:

Prepared as described for **5k**, from **4** (100mg, 0.5mmol) using 2-Amino-4-methylthiazole (46mg, 0.4mmol). The desired compound was isolated at a pale yellow solid; 20mg, 14%. MS APCI (+) *m/z* 280.0 (M+) detected; ^{1}H NMR (400 MHz, DMSO) δ 11.27 (s, 1H), 8.36 (s, 1H), 6.78 (s, 1H), 5.96 (s, 1H), 3.90 (s, 3H), 3.46 (s, 3H), 2.28 (s, 3H).

Preparation of 4-methoxy-1-methyl-N-(5-methylisoxazol-3-yl)-6-oxo-1,6-dihydropyridine-3-carboxamide from 4-methoxy-1-methyl-6-oxo-1,6-dihydropyridine-3-carboxylic acid **5o**:

Prepared as described for **5k**, from **4** (100mg, 0.5mmol) using 3-Amino-5-methylisoxazole (49mg, 0.5mmol). The desired compound was isolated as a white solid; 79mg, 60%. MS APCI (-) *m/z* 262.0 (M-) detected; ^{1}H NMR (400 MHz, DMSO) δ 10.31 (s, 1H), 8.30 (s, 1H), 6.68 (d, 1H, J=0.7Hz), 5.93 (s, 1H), 3.86 (s, 3H), 3.44 (s, 3H), 2.40 (d, 3H, J=0.7Hz)

Preparation of 4-methoxy-1-methyl-N-(4-(2-morpholinoethylcarbamoyl)phenyl)-6-oxo-1,6-dihydropyridine-3-carboxamide from 4-(4-methoxy-1-methyl-6-oxo-1,6-dihydropyridine-3-carboxamido)benzoic acid **5p**:

Dissolved **3** (200mg, 0.66mmol) in thionyl chloride (3ml, excess). The reaction mixture was stirred at 80°C for 45 minutes. The excess $SOCl_2$ was evaporated in vacuo. The solid acid chloride was dissolved in pyridine (4ml, excess) followed by the addition of 2-(4-morpholinyl)ethanamine (68.7µl, 0.528mmol). The red solution was stirred at room temperature overnight. The mixture was filtered, and washed with acetone to yield the desired product as a white solid; 140mg, 64%. MS APCI (+) *m/z* 415.5 (M+) detected; ^{1}H NMR (400 MHz, DMSO) δ 9.92 (s, 1H), 8.75 (s, 1H), 8.24 (s, 1H), 7.87 (d, 2H, J=8.8Hz), 7.75 (d, 1H, J=8.8Hz), 5.92 (s, 1H), 3.95 (d, 2H, J=11.7Hz), 3.86 (s, 3H), 3.74 (t, 2H, J=12.2Hz), 3.63 (dd, 2H, J=5.9Hz, J=11.8Hz), 3.51 (d, 2H, J=12.2Hz), 3.41 (s, 3H).

Preparation of N-(4-(2-(dimethylamino)ethylcarbamoyl)phenyl)-4-methoxy-1-methyl-6-oxo-1,6-dihydropyridine-3-carboxamide from 4-methoxy-1-methyl-6-oxo-1,6-dihydropyridine-3-carboxylic acid **6i**:

4-(4-methoxy-1-methyl-6-oxo-1,6-dihydropyridine-3-carboxamido)benzoic acid (148mg, 0.490mmol) was dissolved in DMF (5ml). N,N-Dimethylethylenediamine (58µl, 0.54mmol) was added followed by bis(2-oxo-3-oxazolidinyl)phosphonic chloride (217mg, 0.490mmol), 4-

(dimethylamino)pyridine (3.3mg, 0.027mmol), and triethylamine (0.206ml, 1.469mmol). The reaction mixture was stirred at room temperature overnight. A white precipitate was removed by vacuum filtration. The filtrate was concentrated in vacuo to yield a yellow-white solid. The solid was washed with acetone, and the desired product was isolated by vacuum filtration as a white solid; 64mg, 35%. MS APCI (+) *m/z* 372.8 (M+) detected; ^{1}H NMR (400 MHz, DMSO) δ 9.40 (s, 1H), 8.20 (s, 1H), 7.44 (d, 2H, J=9.0Hz), 6.66 (d, 2H, J=9.1Hz), 5.89 (s, 1H), 3.85 (s, 3H), 3.40 (s, 3H), 2.82 (s, 6H).

Preparation of 4-methoxy-1-methyl-N-(4-(4-methylpiperazine-1-carbonyl)phenyl)-6-oxo-1,6-dihydropyridine-3-carboxamide from 4-(4-methoxy-1-methyl-6-oxo-1,6-dihydropyridine-3-carboxamido)benzoic acid **5q**:

Prepared as described for **6i** from **5e** (150mg, 0.5mmol) using 1-methylpiperazine (56µl, 0.55mmol). After washing with acetone, compound **5q** was obtained as a solid; 38mg, 20%. MS APCI (+) *m/z* 385.5 (M+) detected; ^{1}H NMR (400 MHz, DMSO) δ 9.92 (s, 1H), 8.27 (s, 1H), 7.76 (d, 2H, J=8.4Hz), 7.41 (d, 2H, J=8.4Hz), 5.95 (s, 1H), 4.16 (t, 2H, J=8.0Hz), 3.89 (s, 3H), 3.75 (t, 2H, J=8.0Hz), 3.45 (s, 3H), 3.05 (s, 3H).

Preparation of N-(6-(dimethylamino)pyridin-3-yl)-4-methoxy-1-methyl-6-oxo-1,6-dihydropyridine-3-carboxamide from 4-methoxy-1-methyl-6-oxo-1,6-dihydropyridine-3-carboxylic acid **6a**:

4-methoxy-1-methyl-6-oxo-1,6-dihydropyridine-3-carboxylic acid (100mg, 0.546mmol) was dissolved in an excess of thionyl chloride (1ml). The reaction mixture was stirred at room temperature for 1 hour. Thionyl chloride was removed in vacuo. 2-(N,N-dimethylamino)-5-aminopyridine (75mg, 0.546mmol) was added and the flask was flushed with nitrogen. THF (3ml) and triethylamine (0.077ml, 0.548mmol) were added. The reaction was stirred at room temperature overnight. A precipitate formed and was isolated by vacuum filtration. The purple solid was dissolved in methanol, $KHCO_3$ was added and the mixture was filtered through celite using vacuum filtration. The celite was washed with methanol, and the filtrate was concentrated in vacuo. The final product was isolated as a purple solid; 150mg, 88%. MS APCI (+) *m/z* 303.0 (M+) detected; ^{1}H NMR (400 MHz, MeOD) δ 8.34 (s, 1H), 8.29 (d, 1H, J=2.3Hz), 7.77 (d, 1H, J=2.7Hz), 6.69 (d, 1H, J=9.0Hz), 6.07 (s, 1H), 4.03 (s, 3H), 3.59 (s, 3H), 3.09 (s, 6H).

Preparation of 4-methoxy-N-(6-(2-methoxyethoxy)pyridin-3-yl)-1-methyl-6-oxo-1,6-dihydropyridine-3-carboxamide from 4-methoxy-1-methyl-6-oxo-1,6-dihydropyridine-3-carboxylic acid **6b**:

Prepared as described for **6a**, from **4** (100mg, 0.5mmol) using 2-(2-methoxyethoxy)-5-aminopyridine (92mg, 0.546mmol), with changes to the work up procedure. The reaction mixture was filtered using vacuum filtration to yield the desired product as a light purple solid; 154mg, 85%. MS APCI (-) *m/z* 332.2 (M-) detected; ^{1}H NMR (400 MHz, MeOD) δ 8.39 (d, 1H, J=2.4Hz), 8.38 (s, 1H), 7.95 (dd, 1H, J=2.7Hz, J=8.9Hz), 6.84 (d, 1H, J=9.1Hz), 6.07 (s, 1H), 4.42 (t, 2H, J=4.8Hz), 4.03 (s, 3H), 3.76 (t, 2H, J=4.8Hz), 3.59 (s, 3H), 3.43 (s, 3H).

Preparation of 4-methoxy-1-methyl-N-(5-nitrobenzoisothiazol-3-yl)-6-oxo-1,6-dihydropyridine-3-carboxamide from 4-methoxy-1-methyl-6-oxo-1,6-dihydropyridine-3-carboxylic acid **6c**:

Prepared as described for **6a**, from **4** (100mg, 0.5mmol) using 3-amino-5-nitrobenzisothiazole (107mg, 0.546mmol), with changes to the work up procedure. The reaction mixture was filtered using vacuum filtration to give a yellow solid. The solid was washed with acetone, and the desired product was isolated as a yellow solid; quantitative yield 220mg, 109%. MS APCI (-) *m/z* 359.4 (M-) detected; ^{1}H NMR (400 MHz, MeOD) δ 8.58 (d, 1H, J=2.4Hz), 8.20 (d, 1H, J=2.3Hz), 7.97 (s, 1H), 7.45 (d, 1H, J=9.0Hz), 5.94 (s, 1H), 3.85 (s, 3H), 3.52 (s, 3H).

Preparation of N-(4-(dimethylamino)phenyl)-4-methoxy-1-methyl-6-oxo-1,6-dihydropyridine-3-carboxamide from 4-methoxy-1-methyl-6-oxo-1,6-dihydropyridine-3-carboxylic acid **6d**:

Prepared as described for **6a**, from **4** (150mg, 0.8mmol) using N,N-dimethyl-p-phenylenediamine (93mg, 0.68mmol), with the following changes. A solution of 4-methoxy-1-methyl-6-oxo-1,6-dihydropyridine-3-carboxylic acid (100mg, 0.546mmol) in $SOCl_2$ (2ml) was heated at 85°C for 1 hour. N,N-dimethyl-p-phenylenediamine was dissolved in THF (5ml) then added to the acid chloride. The solution was filtered using vacuum filtration to yield a grey solid which was washed with $KHCO_{3(aq)}$. The desired product was isolated as a grey solid; 100mg, 49%. MS APCI (+) *m/z* 302.5 (M+) detected; ^{1}H NMR (400 MHz, DMSO) δ 9.39 (s, 1H), 8.20 (s, 1H), 7.44 (d, 2H, J=9.03Hz), 6.67 (d, 2H, J=9.08Hz), 5.89 (s, 1H), 3.85 (s, 3H), 3.40 (s, 3H), 2.82 (s, 6H).

Preparation of N-(6-(2-(dimethylamino)ethoxy)pyridin-3-yl)-4-methoxy-1-methyl-6-oxo-1,6-dihydropyridine-3-carboxamide from 4-methoxy-1-methyl-6-oxo-1,6-dihydropyridine-3-carboxylic acid **6e**:

Prepared as described for **6d**, from **4** (100mg, 0.5mmol) using 2-(N –dimethylaminoethoxy)-5-aminopyridine (99mg, 0.546mmol). Final product was isolated as a pale yellow solid; 15mg, 9%. MS APCI (+) *m/z* 347.9 (M+) detected; ^{1}H NMR (400 MHz, MeOD) δ 8.40 (d, 1H, J=2.6Hz), 8.37 (s, 1H), 7.96 (dd, 1H, J=2.7Hz, J=8.9Hz), 6.85 (d, 1H, J=8.9Hz), 6.07 (s, 1H), 4.44 (t, 2H, J=5.6Hz), 4.03 (s, 3H), 3.59 (s, 3H), 2.84 (t, 2H, J=5.6Hz), 2.40 (s, 6H).

Preparation of 4-methoxy-1-methyl-N-(6-(4-methylpiperazin-1-yl)pyridin-3-yl)-6-oxo-1,6-dihydropyridine-3-carboxamide from 4-methoxy-1-methyl-6-oxo-1,6-dihydropyridine-3-carboxylic acid **6f**:

Compound **4** (100mg, 0.5mmol) was dissolved in 2ml SOCl2 and heated at 85°C for 1 hour. A ball of unidentifiable sticky substance formed in the mixture. The excess SOCl2 was removed and K_2CO_3 was added to the flask. The amine was suspended in 3ml THF and poured over the acid chloride and the flask was flushed with nitrogen. The reaction was stirred at room temperature overnight. The brown suspension was filtered and washed with acetone. A mixture of EtOAc/MeOH (1:1) was added and the solid filtered. The desired compound was isolated as a light brown solid; 65mg, 34%. MS APCI (+) *m/z* 358.2 (M+) detected; ^{1}H NMR (400 MHz, MeOD) δ 9.21 (s, 1H), 9.0 (s, 1H), 8.70 (dd, 1H, J=2.3Hz, J=9.1Hz), 7.82 (d, 1H, J=9.2Hz), 6.74 (s, 1H), 4.67 (s, 3H), 4.24 (s, 3H), 3.92 (s, 3H), 3.62 (s, 4H), 3.32 (s, 4H).

Preparation of N-(5-chlorobenzo[d]thiazol-2-yl)-4-methoxy-1-methyl-6-oxo-1,6-dihydropyridine-3-carboxamide from 4-methoxy-1-methyl-6-oxo-1,6-dihydropyridine-3-carboxylic acid **6g**:

Prepared as described for **6d**, from **4** (100mg, 0.5mmol) using 2-amino-4-chlorobenzothiazole (101mg, 0.546mmol), with changes to the work up procedure. The reaction mixture was filtered using vacuum filtration to yield 199mg of a beige solid. The crude mixture was purified using silica flash column chromatography; (EtOAc/MeOH; 8:2). The fractions containing the desired product were combined and concentrated in vacuo. The desired product was isolated as a white

solid; 20mg, 10%. MS APCI (-) *m/z* 348.1 (M-) detected; ^{1}H NMR (400 MHz, DMSO) δ 8.61 (s, 1H), 7.50 (dd, 1H, J=1.0Hz, J=1.9Hz), 7.32 (t, 1H, J=7.9Hz), 7.02 (t, 1H, J=7.9Hz), 6.11 (s, 1H), 4.16 (s, 3H), 3.63 (s, 3H).

Preparation of 4-methoxy-1-methyl-N-(6-nitrobenzothiazol-2-yl)-6-oxo-1,6-dihydropyridine-3-carboxamide from 4-methoxy-1-methyl-6-oxo-1,6-dihydropyridine-3-carboxylic acid **6h**:

Prepared as described for **6d**, from **4** (100mg, 0.56mmol) using 6-nitrobenzothiazol-2-amine (109mg, 0.56mmol), with changes to the work up procedure. The yellow precipitate was filtered and washed with acetone to yield the desired product as a yellow solid; quantitative yield 220mg, 109%. MS APCI (-) *m/z* 359.0 (M-) detected; ^{1}H NMR (400 MHz, MeOD) δ 8.58 (d, 1H, J=2.4Hz), 8.18 (dd, 1H, J=2.4Hz, J=8.9Hz), 7.97 (s, 1H), 7.45 (d, 1H, J=9.0Hz), 5.94 (s, 1H), 3.85 (s, 3H), 3.52 (s, 3H).

Preparation of ethyl 4-chloro-1-methyl-6-oxo-1,6-dihydropyridine-3-carboxylate from ethyl 4-hydroxy-1-methyl-6-oxo-1,6-dihydropyridine-3-carboxylate **7**:

Phosphorus oxylchloride (3.0ml, 32.2mmol) and triethyl amine (356µl, 2.54mmol) were added to ethyl 4-hydroxy-1-methyl-6-oxo-1,6-dihydropyridine-3-carboxylate (500mg, 2.54mmol), resulting in gas evolution. The yellow solution was stirred at room temperature overnight. The phosphorus oxylchloride was removed in vacuo to yield a red-orange oil. Ice was added to the oil followed by saturated K_2CO_3 until the solution reached pH 8. The aqueous suspension was extracted with EtOAc, the organic layers were combined, dried over sodium sulfate, filtered and concentrated in vacuo to yield a dark red solid. The crude mixture was purified using silica gel flash column chromatography (DCM/MeOH; 98:2). The fractions containing the desired product were combined and concentrated in vacuo. The desired product was obtained as an orange solid; 379mg, 69%. MS APCI (+) *m/z* 216.2 (M+) detected; ^{1}H NMR (400 MHz, $CDCl_3$) δ 8.22 (s, 1H), 6.67 (s, 1H), 4.36 (q, 2H, J=7.1Hz), 3.60 (s, 3H), 1.39 (t, 3H, J=7.1Hz).

Preparation of 4-chloro-1-methyl-6-oxo-1,6-dihydropyridine-3-carboxylic acid from ethyl 4-chloro-1-methyl-6-oxo-1,6-dihydropyridine-3-carboxylate **8**:

Prepared as described for **4** from **7** (500mg, 2.49mmol). The desired compound was isolated as a white solid; 440mg, 94%. MS APCI (-) *m/z* 188.1 (M-) detected; ^{1}H NMR (400 MHz, MeOD) δ 8.56 (s, 1H), 6.64 (s, 1H), 3.60 (s, 3H).

Preparation of 4-chloro-1-methyl-6-oxo-1,6-dihydropyridine-3-carbonyl fluoride from 4 4-chloro-1-methyl-6-oxo-1,6-dihydropyridine-3-carboxylic acid **8b**:

8 (100mg, 0.53mmol) was dissolved in a DCM (4ml) under a nitrogen atmosphere. The flask was cooled to 0°C and Hunig's base (279µl, 1.60mmol) was added and the solution became transparent. Cyanuric fluoride (69µl, 0.80mmol) was added dropwise and the solution was allowed to stir at 0°C for 30 minutes. The solution was then allowed to reach room temperature and stirred overnight. Aqueous Na_2CO_3 (6ml) was added to the red-brown solution and an extraction using DCM was performed and the combined organic extracts were dried over sodium sulfate, filtered and concentrated in vacuo. The desired compound was isolated as a brown semi-solid; 81mg, 85%. MS APCI (+) *m/z* 190.0 (M+) detected.

Preparation of 4-(2-methoxyethoxy)-1-methyl-6-oxo-1,6-dihydropyridine-3-carboxylic acid from 4-chloro-1-methyl-6-oxo-1,6-dihydropyridine-3-carboxylic acid **9**:

Under nitrogen at room temperature, a solution of sodium (283mg, 12.3mmol) in an excess of 2-ethoxyethanol (8ml) was prepared. The solution was added to **8** (460mg, 2.49mmol). The reaction mixture was stirred at 90°C for 2.5 hours. The reaction mixture was acidified with aqueous citric acid (3g in 50ml), and the aqueous layer was extracted with DCM, dried over Na_2SO_4 and concentrated in vacuo to give the desired compound as a white solid; 260mg, 46%. MS APCI (-) 226.4 *m/z* (M-) detected; ^{1}H NMR (400 MHz, DMSO) δ 12.39 (s, 1H), 8.35 (s, 1H), 5.86 (s, 1H), 4.11 (quartet, 2H, J=3.4Hz, J= 4.6Hz), 3.67 (quartet, 2H, J=3.2Hz, J=4.6Hz), 3.43 (s, 3H).

Preparation of N-(2-hydroxyphenyl)-4-(2-methoxyethoxy)-1-methyl-6-oxo-1,6-dihydropyridine-3-carboxamide from 4-(2-methoxyethoxy)-1-methyl-6-oxo-1,6-dihydropyridine-3-carboxylic acid **10a**:

Prepared as described for **6a** from **9** (100mg, 0.4mmol) using 2-aminophenol (65mg, 0.6mmol) with the following adjustments to the procedure. To form the acid chloride, the reaction mixture

was heated at 85°C for 1 hour. The isolated product was washed with KHCO in MeOH. The desired product was isolated as a tan solid; quantitative yield 145mg, 113%. MS APCI (-) *m/z* 319.3 (M-) detected; ^{1}H NMR (400 MHz, DMSO) δ 10.20 (s, 1H), 9.85 (s, 1H), 8.52 (s, 1H), 8.30 (d, 1H, J=7.9Hz), 6.94 (d, 2H, J=3.8Hz), 6.81 (pd, 1H, J=4.1Hz, J=8.5Hz), 6.03 (s, 1H), 4.33 (t, 2H, J=4.4Hz), 3.86 (t, 2H, J=4.4Hz), 3.50 (s, 3H), 3.32 (s, 3H).

Preparation of methyl 4-(4-(2-methoxyethoxy)-1-methyl-6-oxo-1,6-dihydropyridine-3-carboxamido)benzoate from 4-(2-methoxyethoxy)-1-methyl-6-oxo-1,6-dihydropyridine-3-carboxylic acid **10b**:

Prepared as described for **10a** from **9** (100mg, 0.44mmol) using methyl 4-aminobenzoate (60mg, 0.40mmol) with the following adjustments to the work up. The precipitate was filtered using vacuum filtration. The desired compound was isolated as a white solid; 90 mg, 63%. MS APCI (+) *m/z* 361.1 (M+) detected; ^{1}H NMR (400 MHz, DMSO) δ 10.00 (s, 1H), 8.40 (s, 1H), 7.97 (d, 2H, J=8.8Hz), 7.78 (d, 2H, J=8.8Hz), 6.00 (s, 1H), 4.28 (t, 2H, J=4.6Hz), 3.84 (s, 3H), 3.79 (t, 2H, J=4.4Hz), 3.47 (s, 3H), 3.36 (s, 3H).

Preparation of 4-(4-(2-methoxyethoxy)-1-methyl-6-oxo-1,6-dihydropyridine-3-carboxamido)benzoic acid from 4-(2-methoxyethoxy)-1-methyl-6-oxo-1,6-dihydropyridine-3-carboxylic acid **10c**:

Prepared as described for **5g** from **10b** (210mg, 0.583mmol). The precipitate was filtered. The desired compound was isolated as a white solid, 145 mg, 72%. MS APCI (+) *m/z* 347.4 (M+) detected; ^{1}H NMR (400 MHz, DMSO) δ 12.78 (s, 1H), 9.99 (s, 1H), 8.42 (s, 1H), 7.96 (d, 2H, J=8.6Hz), 7.77 (d, 2H, J=8.4Hz), 6.01 (s, 1H), 4.29 (t, 2H, J=4Hz), 3.81 (t, 2H, J=4Hz), 3.49 (s, 3H), 3.37 (s, 3H).

Preparation of 4-(2-methoxyethoxy)-1-methyl-N-(6-(4-methylpiperazin-1-yl)pyridin-3-yl)-6-oxo-1,6-dihydropyridine-3-carboxamide from 4-(2-methoxyethoxy)-1-methyl-6-oxo-1,6-dihydropyridine-3-carboxylic acid **10d**:

Prepared as described for **10a** from **9** (120mg, 0.5mmol) using 6-(4-methylpiperazin-1-yl)pyridin-3-amine (123mg, 0.64mmol) with the following adjustments to the work up. The precipitate was filtered using vacuum filtration and the filtrate was concentrated in vacuo.

Purification was done by silica gel flash column chromatography (EtOAc/MeOH; 1:1). The fractions containing the desired product were combined and concentrated in vacuo. The desired product was isolated as a beige solid; 88mg, 44%. MS APCI (+) *m/z* 402.3 (M+) detected; ^{1}H NMR (400 MHz, MeOD) δ 8.42 (s, 1H), 8.39 (d, 1H, J=2.4Hz), 7.93 (dd, 1H, J=2.7Hz, J=9.1Hz), 6.89 (d, 1H, J=9.1Hz), 6.08 (s, 1H), 4.36 (t, 2H, J=4.6Hz), 3.89 (t, 2H, J=4.4Hz), 3.60 (s, 3H), 3.58 (t, 4H), 3.48 (s, 3H), 2.69 (t, 4H, J=5.0Hz), 2.44 (s, 3H).

Preparation of 4-(2-methoxyethoxy)-1-methyl-6-oxo-N-(4-((2-(pyrrolidin-1-yl)ethyl)carbamoyl)phenyl)-1,6-dihydropyridine-3-carboxamide from 4 methyl 4-(4-(2-methoxyethoxy)-1-methyl-6-oxo-1,6-dihydropyridine-3-carboxamido)benzoate **10e**:

Prepared as described for **10a** from **10c** (100mg, 0.288mmol) using 2-(pyrrolidin-1-yl)ethanamine (37µl, 0.274mmol) with the following adjustments to the procedure. Potassium carbonate (120mg, 0.867mmol) was used instead of Et_3N. The precipitate was filtered using vacuum filtration and the filtrate was concentrated in vacuo. The crude mixture was purified using silica gel flash column chromatography (EtOAc/MeOH; 1:1). The desired compound was isolated as a red solid; 48mg, 39%. MS APCI (+) *m/z* 443.6 (M+) detected; ^{1}H NMR (400 MHz, MeOD) δ 8.45 (s, 1H), 7.91 (d, 2H, J=8.8Hz), 7.80 (d, 2H, J=8.8Hz), 6.07 (s, 1H), 4.37 (t, 2H, J=4.4 Hz), 4.92 (t, 2H, J=4.4 Hz), 3.60 (s, 3H), 3.51 (s, 3H).

Preparation of 4-(2-methoxyethoxy)-1-methyl-N-(5-nitrobenzoisothiazol-3-yl)-6-oxo-1,6-dihydropyridine-3-carboxamide from 4-(2-methoxyethoxy)-1-methyl-6-oxo-1,6-dihydropyridine-3-carboxylic acid **10f**:

Prepared as described for **10a** from **9** (100mg, 0.4mmol) using 3-amino-5-nitrobenzisothiazole (66mg, 0.34mmol) with the following adjustments to the work up. The precipitate was filtered and the filtrate was concentrated in vacuo. The concentrated filtrate was washed with acetone. Purification was done by silica gel flash column chromatography (EtOAc/MeOH; 9:1). The fractions containing the desired product were combined and concentrated in vacuo. The desired product was isolated as a yellow solid; 80mg, 58%. MS APCI (-) *m/z* 403.4 (M-) detected; ^{1}H NMR (400 MHz, DMSO) δ 9.30 (d, 1H, J=2.50 Hz), 9.29 (s, 1H), 8.67 (dd, 1H, J=2.56 Hz, 9.36 Hz), 8.39 (d, 1H, J=9.36 Hz), 8.36 (s, 1H), 6.02 (s, 1H), 4.19 (t, 2H, J=4.8 Hz), 3.73 (t, 2H, J=4.4 Hz), 3.47 (s, 3H), 3.34 (s, 3H).

Preparation 4-methoxy-1-methyl-6-oxo-1,6-dihydropyridine-3-carboxamide from ethyl 4-methoxy-1-methyl-6-oxo-1,6-dihydropyridine-3-carboxylate **11a**:

A solution of ethyl 4-methoxy-1-methyl-6-oxo-1,6-dihydropyridine-3-carboxylate (200mg, 0.95mmol) in ammonia 7M MeOH (7ml, 323mmol) was prepared and transferred to pressure apparatus. The reaction mixture was stirred at 57°C for 48 h. The methanol was removed in vacuo to yield a white solid, quantitative yield 183mg, 106%. MS APCI (+) *m/z* 183.0 (M+) detected; ^{1}H NMR (400 MHz, MeOD) δ 8.37 (s, 1H), 6.03 (s, 1H), 3.98 (s, 3H), 3.57 (s, 3H).

Preparation of 1-methyl-6-oxo-4-phenoxy-1,6-dihydropyridine-3-carboxamide from ethyl 1-methyl-6-oxo-4-phenoxy-1,6-dihydropyridine-3-carboxylate **11b**:

Prepared as described for **11a** from **17** (110mg, 0.40mmol). The desired product was isolated as a white solid, quantitative yield 100mg, 102%. MS APCI (+) *m/z* 245.5 (M+) detected; ^{1}H NMR (400 MHz, MeOD) 8.46 (s, 1H), 7.55 (t, 2H, J=7.9Hz), 7.40 (t, 1H, J=7.5Hz), 7.26 (d, 2H, J=7.8Hz), 5.50 (s, 1H), 3.58 (s, 3H).

Preparation 1-methyl-6-oxo-4-phenoxy-N-phenyl-1,6-dihydropyridine-3-carboxamide from 1-methyl-6-oxo-4-phenoxy-1,6-dihydropyridine-3-carboxamide **12b**:

DMF (2ml) was added to a mixture of 1-methyl-6-oxo-4-phenoxy-1,6-dihydropyridine-3-carboxamide (100mg, 0.409mmol), potassium phosphate (145mg, 0.682mmol), and copper(I) iodide (32.5mg, 0.171mmol) under N_2. Iodobenzene (0.038ml, 0.341mmol) and N,N,N',N'-Tetramethylethylenediamine (0.051ml, 0.341mmol) were added to the blue suspension. The green/blue reaction mixture was heated at 111ºC for 24 hours. DMF was removed in vacuo to yield a brown solid. Water (25ml), DMC (25ml), and 1 spatula EDTA were added and the organic layer was separated. The aqueous layer was extracted with DCM, the organic layers were combined, dried over Na_2SO_4, and concentrated in vacuo. A burgundy solid was obtained which was purified by silica gel flash column chromatography (EtOAc/MeOH; 9:1). The fractions containing the desired product were combined and concentrated in vacuo. The desired compound was isolated as a white solid; 83mg, 76%. MS APCI (+) *m/z* 321.1 (M+) detected; ^{1}H NMR (400 MHz, MeOD) δ 8.41 (s, 1H), 7.63 (d, 2H, J=8.0Hz), 7.55 (t, 2H, J=7.9Hz), 7.40 (d, 1H, J=7.4Hz), 7.36 (m, 2H), 7.31 (d, 2H, J=8.0Hz), 7.15 (t, 1H, J=7.4Hz), 5.58 (s, 1H), 3.60 (s, 3H).

Preparation 4-methoxy-1-methyl-6-oxo-5-phenyl-1,6-dihydropyridine-3-carboxamide from 4-methoxy-1-methyl-6-oxo-1,6-dihydropyridine-3-carboxamide **12a**:

Prepared as described for **12a** from **11a** (70mg, 0.38mmol). A red semi-solid was obtained after extraction. The aqueous layer was extracted with DCM again, dried over Na_2SO_4, filtered and concentrated in vacuo to yield a white solid. Both crude compounds were combined and purified using silica gel flash column chromatography (EtOAc/MeOH; 7:3). The fractions containing the desired product were combined and concentrated in vacuo. The desired product was isolated as a white solid; 10mg, 10%. MS APCI (+) *m/z* 259.2 (M+) detected; ^{1}H NMR (400 MHz, DMSO) δ 8.46 (s, 1H), 7.64 (dd, 2H, J=1.0Hz, J=8.5Hz), 7.35 (t, 2H, J=7.9Hz), 7.10 (t, 1H, J=7.4Hz), 4.03 (s, 3H), 3.44 (s, 3H).

Preparation 4-methoxy-5-(3-(4-methoxyphenyl)-1,2,4-oxadiazol-5-yl)-1-methylpyridin-2(1H)-one from 4-methoxy-1-methyl-6-oxo-1,6-dihydropyridine-3-carboxylic acid **13a**: Dissolved 4-methoxy-1-methyl-6-oxo-1,6-dihydropyridine-3-carboxylic acid (100mg, 0.546mmol) in an excess of thionyl chloride (1.5ml) at room temperature. The reaction mixture was stirred for 1 hour at room temperature. The excess thionyl chloride was removed in vacuo. N'-hydroxy-4-methoxybenzimidamide (91mg, 0.546mmol) and potassium carbonate (113mg, 0.819mmol) were added, the vessel was flushed with N_2, and THF (5ml) was added. The solution was stirred at room temperature overnight. THF was removed in vacuo, the vessel was flushed with N_2 and dry DMF (5ml) was added. The reaction mixture was stirred at 111°C for 5 hours. DMF was removed in vacuo, and water was added to the resulting solid. A precipitate formed and it was isolated by vacuum filtration. The crude solid was purified using silica gel flash column chromatography (EtOAc/MeOH; 9:1). The fractions containing the desired product were combined and concentrated in vacuo. The desired product was isolated as a pale yellow solid: 98mg, 63%. MS APCI (+) *m/z* 314.0 (M+) detected; ^{1}H NMR (400 MHz, $CDCl_3$) δ 8.36 (s, 1H), 8.05 (d, 2H, J=8.9Hz), 7.00 (d, 2H, J=8.9Hz), 6.03 (s, 1H), 3.95 (s, 3H), 3.88 (s, 3H), 3.62 (s, 3H).

Preparation of 5-(3-(3,5-dichlorophenyl)-1,2,4-oxadiazol-5-yl)-4-methoxy-1-methylpyridin-2(1H)-one from 4-methoxy-1-methyl-6-oxo-1,6-dihydropyridine-3-carboxylic acid **13b**:

Prepared as described for **13a** from **4** (100mg, 0.5mmol) using 3,5-dichloro-N'-hydroxybenzimidamide (103mg, 0.5mmol). The desired product was isolated as a white solid; 45mg, 26%. MS APCI (+) *m/z* 351.9 (M+) detected; ^{1}H NMR (400 MHz, $CDCl_3$) δ 8.41 (s, 1H), 8.04 (d, 1H, J=1.4Hz), 7.53 (s, 1H), 6.06 (s, 1H), 3.98 (s, 3H), 3.66 (s, 3H).

Preparation of 5-(3-(3-bromophenyl)-1,2,4-oxadiazol-5-yl)-4-methoxy-1-methylpyridin-2(1H)-one from 4-methoxy-1-methyl-6-oxo-1,6-dihydropyridine-3-carboxylic acid **13c**:

Prepared as described for **13a** from **4** (100mg, 0.5mmol) using 3-bromo-N'-hydroxybenzimidamide (107mg, 0.5mmol) with the following change to the purification procedure. Following vacuum filtration, the solid was collected and methanol (3ml) was added to the solid. The suspension was filtered using vacuum filtration. The desired product was obtained as a light pink solid; 52mg, 29%. MS APCI (+) *m/z* 363.9 (M+) detected; ^{1}H NMR (400 MHz, $CDCl_3$) δ 8.41 (s, 1H), 8.30 (s, 1H), 8.08 (d, 1H, J = 7.81 Hz), 7.67 (d, 1H, J = 8.03 Hz), 7.39 (t, 1H, 7.90 Hz), 6.05 (s, 1H), 3.98 (s, 3H), 3.65 (s, 3H).

Preparation of 4-methoxy-1-methyl-5-(3-(4-phenoxyphenyl)-1,2,4-oxadiazol-5-yl)pyridin-2(1H)-one from 4-methoxy-1-methyl-6-oxo-1,6-dihydropyridine-3-carboxylic acid **13d**:

Prepared as described for **13a** from **4** (100mg, 0.5mmol) using N'-hydroxy-4-phenoxybenzimidamide (114mg, 0.5mmol) with the following changes to the procedure. After removal of THF in vacuo, NMP (2ml) was added and the reaction mixture was stirred at 99°C for 5 hours. The solution was cooled to room temperature and water (4ml) was added. The resulting precipitate was filtered by vacuum filtration. The crude solid was purified using silica gel flash column chromatography (EtOAc/MeOH; 95:5). The fractions containing the desired product were combined and concentrated in vacuo. The desired product was obtained as a white solid; 20mg, 11%. MS APCI (+) *m/z* 376.1 (M+) detected; ^{1}H NMR (400 MHz, $CDCl_3$) δ 8.39 (s, 1H), 8.10 (d, 2H, J=8.9Hz), 7.41 (dd, 2H, J=7.5Hz, J=8.4Hz), 7.20 (t, 1H, J=7.4Hz), 7.11 (dd, 4H, J=3.8Hz, J=5.1Hz), 6.05 (s, 1H), 3.97 (s, 3H), 3.64 (s, 3H).

Preparation of 5-(3-(5-bromopyridin-2-yl)-1,2,4-oxadiazol-5-yl)-4-methoxy-1-methylpyridin-2(1H)-one from 4-methoxy-1-methyl-6-oxo-1,6-dihydropyridine-3-carboxylic acid **13e**:

Prepared as described for **13a** from **4** (100mg, 0.5mmol) using 5-bromo-N'-hydroxypicolinimidamide (108mg, 0.5mmol) with the following change to the purification procedure. The crude solid isolated from vacuum filtration was, dissolved in EtOAc/MeOH (9:1). A white precipitate formed which was isolated using vacuum filtration. The desired product was isolated as a beige solid; 43mg, 24%. MS APCI (+) *m/z* 362.9 (M+) detected; ^{1}H NMR (400 MHz, DMSO) δ 8.92 (d, 1H), 8.79 (s, 1H), 8.33 (dd, 1H), 8.09 (t, 1H), 6.06 (s, 1H), 3.917 (s, 1H), 3.523 (s, 1H).

Preparation of 5-(3-(2,4-dimethoxyphenyl)-1,2,4-oxadiazol-5-yl)-4-methoxy-1-methylpyridin-2(1H)-one from 4-methoxy-1-methyl-6-oxo-1,6-dihydropyridine-3-carboxylic acid **13f**:

Prepared as described for **13d** from **4** (120mg, 0.66mmol) using N'-hydroxy-2,4-dimethoxybenzimidamide (129mg, 0.66mmol) with the following change to the purification procedure. Vacuum filtration isolated the product as a pure white solid; 60mg, 27%. MS APCI (+) *m/z* 344.1 (M+) detected; ^{1}H NMR (400 MHz, $CDCl_3$) δ 8.35 (s, 1H), 8.01 (d, 1H, J=8.5Hz), 6.63 (dd, 1H, J=2.3Hz, J=8.5Hz), 6.60 (d, 1H, J=2.2Hz), 6.03 (s, 1H), 3.98 (s, 3H), 3.95 (s, 3H), 3.90 (s, 3H), 3.62 (s, 3H).

Preparation of 4-methoxy-1-methyl-5-(3-(3,4,5-trimethoxyphenyl)-1,2,4-oxadiazol-5-yl)pyridin-2(1H)-one from 4-methoxy-1-methyl-6-oxo-1,6-dihydropyridine-3-carboxylic acid **13g**:

Prepared as described for **13a** from **4** (100mg, 0.5mmol) using N'-hydroxy-3,4,5-trimethoxybenzimidamide (113mg, 0.5mmol) with the following changes to the procedure. The DMF solution was stirred at 103°C for 4.5 hours. The DMF was evaporated in vacuo then water was added to the solid and a brown precipitate formed. The brown solid was isolated by vacuum filtration and purified using Isolera (EtOAc/MeOH 99→90:1→10). The fractions containing the desired product were combined and concentrated in vacuo. The desired product was isolated as a white solid; 74 mg 40%. MS APCI (+) *m/z* 374.2 (M+) detected; ^{1}H NMR (400 MHz, $CDCl_3$) δ 8.40 (s, 1H), 7.38 (s, 1H), 6.05 (s, 1H), 3.97 (d, 9H, J=2.7Hz), 3.94 (s, 3H), 3.65 (s, 3H).

Preparation of 4-methoxy-5-(3-(2-methoxyphenyl)-1,2,4-oxadiazol-5-yl)-1-methylpyridin-2(1H)-one from 4-methoxy-1-methyl-6-oxo-1,6-dihydropyridine-3-carboxylic acid **13h**:

Prepared as described for **13g** from **4** (100mg, 0.5mmol) using N'-hydroxy-2-methoxybenzimidamide (91mg, 0.5mmol). The crude solid was purified using silica gel flash column chromatography (EtOAc/MeOH, 9:1). The fractions containing the desired product were combined and concentrated in vacuo. The desired product was isolated as a brown solid; 66mg, 42%. MS APCI (+) *m/z* 314.0 (M+) detected; ^{1}H NMR (400 MHz, $CDCl_3$) δ 8.37 (s, 1H), 8.03 (dd, 1H, J=1.6Hz, J=7.7Hz), 7.51 (ddd, 1H, J=1.8Hz, J=7.5Hz, J=8.4Hz), 7.11 (dd, 1H, J=0.9Hz, J=7.6Hz), 7.08 (dd, 1H, J=3.7Hz, J=4.7Hz), 6.04 (s, 1H), 4.00 (s, 3H), 3.95 (s, 3H), 3.63 (s, 3H).

Preparation of 5-(3-(4-fluorophenyl)-1,2,4-oxadiazol-5-yl)-4-methoxy-1-methylpyridin-2(1H)-one from 4-methoxy-1-methyl-6-oxo-1,6-dihydropyridine-3-carboxylic acid **13i**:

4-methoxy-1-methyl-6-oxo-1,6-dihydropyridine-3-carboxylic acid (100mg, 0.546mmol) was dissolved in an excess of thionyl chloride (1.2ml) at room temperature. The reaction mixture was stirred for 1 hour. The excess thionyl chloride was removed in vacuo. 4-fluoro-N'-hydroxybenzimidamide (84mg, 0.546mmol) and potassium carbonate (113mg, 0.819mmol) were added, the vessel was flushed with N_2, and DMF (3ml) was added. The solution was stirred at room temperature overnight. The next day the reaction mixture was heated at 85°C for 5 hours. The DMF was removed in vacuo, water was added to the resulting solid and a brown precipitate formed that was isolated using vacuum filtration. The brown solid was purified using silica gel flash column chromatography (EtOAc/MeOH, 97:3). The fractions containing the desired product were combined and concentrated in vacuo. The desired product was isolated as a white solid; 60mg, 36%. MS APCI (+) *m/z* 302.1 (M+) detected; ^{1}H NMR (400 MHz, $CDCl_3$) δ 8.31 (s, 1H), 8.14 (dd, 2H, J=5.4Hz, J=8.9Hz), 7.21 (t, 2H, J=8.7Hz), 6.05 (s, 1H), 3.97 (s, 3H), 3.65 (s, 3H).

Preparation of 4-methoxy-1-methyl-5-(3-(o-tolyl)-1,2,4-oxadiazol-5-yl)pyridin-2(1H)-one from 4-methoxy-1-methyl-6-oxo-1,6-dihydropyridine-3-carboxylic acid **13j**:

Prepared as described for **13i** from **4** (100mg, 0.5mmol) using N'-hydroxy-2-methylbenzimidamide (82mg, 0.5mmol) with the following changes to the procedure. The next day the DMF was heated at 71°C for 5 hours. After removing the DMF in vacuo, the TLC showed the reaction was incomplete. The solid was dried, 1.5ml of DMF was added and the mixture was stirred at 83°C for 4 hours followed by removal of DMF in vacuo. Water was added

and the resulting solid was filtered using vacuum filtration and purified by silica gel flash column chromatography (EtOAC/MeOH, 100→95:0→5). The fractions containing the desired product were combined and concentrated in vacuo. The desired product was isolated as a white solid; 34mg, 23%. MS APCI (+) *m/z* 298.2 (M+) detected; ^{1}H NMR (400 MHz, $CDCl_3$) δ 8.41 (s, 1H), 8.03 (d, 1H, J=7.8Hz), 7.42 (t, 1H, J=7.4Hz), 7.36 (s, 1H), 7.34 (d, 1H, J=7.4Hz), 6.06 (s, 1H), 3.98 (s, 3H), 3.64 (s, 3H), 2.67 (s, 3H).

Preparation of 4-methoxy-1-methyl-5-(3-(4-(trifluoromethyl)phenyl)-1,2,4-oxadiazol-5-yl)pyridin-2(1H)-one from 4-methoxy-1-methyl-6-oxo-1,6-dihydropyridine-3-carboxylic acid **13k**:

Prepared as described for **13a** from **4** (100mg, 0.5mmol) using N'-hydroxy-4-(trifluoromethyl)benzimidamide (111mg, 0.5mmol) with the following changes to the procedure. **4** was dissolved in $SOCl_2$ and stirred at 85°C for 3 hours. After removal of THF the solid was dissolved in DMF and stirred at 85°C for 5 hours. Following the removal of DMF in vacuo, water was added and extracted with DCM, dried over Na_2SO_4, filtered and concentrated in vacuo. The resulting red oil was purified using silica gel flash column chromatography (EtOAC/MeOH, 95:5). The fractions containing the desired product were combined and concentrated in vacuo. The desired product was isolated as a white solid; 78mg, 41%. MS APCI (+) *m/z* 351.1 (M+) detected; ^{1}H NMR (400 MHz, MeOD) δ 8.71 (s, 1H), 8.32 (d, 2H, J=8.1Hz), 7.87 (d, 2H, J=8.2Hz), 6.12 (s, 1H), 4.01 (s, 3H), 3.64 (s, 3H).

Preparation of 4-methoxy-1-methyl-5-(3-(3-(trifluoromethyl)phenyl)-1,2,4-oxadiazol-5-yl)pyridin-2(1H)-one from 4-methoxy-1-methyl-6-oxo-1,6-dihydropyridine-3-carboxylic acid **13l**:

Prepared as described for **13k** from **4** (100mg, 0.5mmol) using N'-hydroxy-3-(trifluoromethyl)benzimidamide (111mg, 0.5mmol) with the following changes to the procedure. After 24hours the THF was removed in vacuo then 5ml of THF was added and the solution was stirred at reflux overnight. The THF was removed in vacuo, water was added and extracted with DCM. The combined organic layers were dried over Na_2SO_4, filtered and concentrated in vacuo. The desired compound was isolated as a white solid; 30mg, 17%. MS APCI (+) *m/z* (M+)

detected; ^{1}H NMR (400 MHz, MeOD) δ 8.55 (s, 1H), 8.15 (s, 1H), 8.07 (d, 1H, J=7.9Hz), 7.85 (d, 1H, J=7.9Hz), 7.70 (d, 1H, J=8.0Hz), 6.04 (s, 1H), 3.96 (s, 3H), 3.60 (s, 3H).

Preparation of 4-methoxy-1-methyl-5-(3-(3-nitrophenyl)-1,2,4-oxadiazol-5-yl)pyridin-2(1H)-one from 4-methoxy-1-methyl-6-oxo-1,6-dihydropyridine-3-carboxylic acid **13m**:
Prepared as described for **8k** from **3** (100mg, 0.5mmol) using N'-hydroxy-3-nitrobenzimidamide (99mg, 0.5mmol). After filtration, the solid was purified using Isolera (EtOAc/MeOH, 95:5). The fractions containing the desired product were combined and concentrated in vacuo. The desired product was isolated as a pale yellow solid; 56mg, 33%. MS APCI (+) *m/z* 344.3 (M+) detected; ^{1}H NMR (400 MHz, DMSO) δ 8.83 (s, 1H), 8.77 (s,1H), 8.48 (dd, 1H, J=1.2Hz, J=3.4Hz), 8.46 (d, 1H, J=1.8Hz), 7.91 (t, 1H, J=8.0Hz), 6.06 (s, 1H), 3.93 (s, 3H), 3.54 (s, 3H).

Preparation of 4-chloro-1-methyl-6-oxo-N'-phenyl-1,6-dihydropyridine-3-carbohydrazide from 4-chloro-1-methyl-6-oxo-1,6-dihydropyridine-3-carboxylic acid **14a**:
8 (180mg, 0.9mmol) was dissolved in $SOCl_2$ and heated at reflux for 1 hour. The excess $SOCl_2$ was removed in vacuo. Potassium carbonate (146mg, 1.06mmol) was added to the dry acid chloride. THF (3ml) was added and the solution was cooled to 0°C and placed under N_2. Phenylhydrazine (95µl, 0.9mmol) was added and a pink precipitate formed immediately. The suspension was stirred at 0°C for 10 minutes then allowed to warm to room temperature and stir overnight. In the morning, 15ml of water was added and the aqueous layer was extracted with EtOAc. The combined organic layers were dried over Na_2SO_4, filtered and concentrated in vacuo. A yellow-orange solid was obtained which was purified by silica gel flash column chromatography (EtOAc/MeOH; 9:1). The fractions containing the desired product were combined and concentrated in vacuo. The desired hydrazide was obtained as a yellow solid; 138 mg, 55%. MS APCI (+) *m/z* 278.1 (M+) detected; ^{1}H NMR (400 MHz, MeOD) δ 8.13 (s, 1H), 7.22 (dd, 2H, J=7.4Hz, J=8.5Hz), 6.93 (dd, 2H, J=0.9Hz, J=8.6Hz), 6.85 (t, 1H, J=7.3Hz), 6.70 (s, 1H), 3.61 (s, 3H).

Preparation of N'-(benzothiophen-2-yl)-4-chloro-1-methyl-6-oxo-1,6-dihydropyridine-3-carbohydrazide from 4-chloro-1-methyl-6-oxo-N'-phenyl-1,6-dihydropyridine-3-carbohydrazide **14b**:

Prepared as described for **14a** from **8** (100mg, 0.54mmol) and (3a,7a-dihydrobenzothiophen-2-yl)hydrazine (88mg, 0.54mmol). The desired compound was isolated as a yellow solid; 40mg, 22%. MS APCI (+) *m/z* 335.2 (M2+) detected; ^{1}H NMR (400 MHz, DMSO) δ 10.71 (s, 1H), 10.08 (s, 1H), 8.20 (s, 1H), 7.77 (d, 1H, J=7.6Hz), 7.50 (d, 1H, J=7.7Hz), 7.31 (t, 1H, J=8.2Hz), 7.12 (t, 1H, J=7.5Hz), 6.66 (s, 1H), 3.50 (s, 3H).

Preparation of 5-methyl-1-phenyl-1H-pyrazolo[4,3-c]pyridine-3,6(2H,5H)-dione from 4-chloro-1-methyl-6-oxo-N'-phenyl-1,6-dihydropyridine-3-carbohydrazide **15a**:

Compound **14a** (50mg, 0.18mmol) was combined with K_2CO_3 in a microwave vial. DMF (1ml) was added and the vial was flushed with N_2. The reaction was stirred at 200°C for 20 minutes in the MW. TLC indicated the reaction was incomplete. The reaction was stirred at 200°C for 25 additional minutes. The DMF was removed in vacuo. EtOAc was added and an orange solid was collected and washed with methanol. The filtrate was concentrated in vacuo to give a yellow solid which was purified by silica gel flash column chromatography (EtOAc/MeOH; 100→50:0→50). The fractions containing the desired product were combined and concentrated in vacuo. The desired compound was obtained as a yellow solid; 28 mg, 65%. MS APCI (+) *m/z* 242.3 (M+) detected; ^{1}H NMR (400 MHz, MeOD) δ 8.47 (s, 1H), 7.53 (m, 4H), 7.30 (t, 1H, J=7.1Hz), 6.31 (s, 1H), 3.72 (s, 3H).

Preparation of 1-(benzo[b]thiophen-2-yl)-5-methyl-1H-pyrazolo[4,3-c]pyridine-3,6(2H,5H)-dione from N'-(benzo[b]thiophen-2-yl)-4-chloro-1-methyl-6-oxo-1,6-dihydropyridine-3-carbohydrazide **15b**:

The hydrazide **14b** (40mg, 0.12mmol) was dissolved in DMF (1ml) and K_2CO_3 (50mg, 0.36mmol) was added. The solution was stirred in the microwave at 200°C for 30 minutes. The DMF was removed in vacuo. The crude solid was purified using silica gel flash column chromatography (EtOAc/MeOH; 9:1). The fractions containing the desired product were combined and concentrated in vacuo. The desired compound was isolated as a yellow solid; 17mg, 48%. MS APCI (+) *m/z* 299.3 (M2+) detected; ^{1}H NMR (400 MHz, MeOD) δ 8.19 (s, 1H), 7.82 (d, 1H, J=7.7Hz), 7.77 (d, 1H, J=8.1Hz), 7.41 (t, 2H), 7.24 (t, 1H, J=7.6Hz), 3.72 (s, 1H).

Preparation of 5-methyl-1-(3-(trifluoromethyl)phenyl)-1H-pyrazolo[4,3-c]pyridine-3,6(2H,5H)-dione from 4-chloro-1-methyl-6-oxo-N'-phenyl-1,6-dihydropyridine-3-carbohydrazide **15c**:

8 (75mg, 0.4mmol) was dissolved in $SOCl_2$ (2ml) and refluxed at 85°C for 1 hour. The thionyl chloride was removed in vacuo. K_2CO_3 (61mg, 0.44mmol) was added and the flask was flushed with N_2. THF (2ml) was added and the suspension was cooled to 0°C. (3-(trifluoromethyl)phenyl)hydrazine (52µl, 0.4mmol) was added. The orange translucent solution was stirred at room temperature overnight. The THF was removed in vacuo. The crude mixture was purified using silica gel flash column chromatography on Isolera (EtOAc/MeOH; gradient 10→5:0→5). The fractions containing the desired product were combined and concentrated in vacuo. The desired product was isolated as an orange-yellow solid; 70mg, 57%. MS APCI (+) *m/z* 310.2 (M+) detected; ^{1}H NMR (400 MHz, MeOD) δ 8.16 (s, 1H), 7.40 (t, 1H, J=7.9Hz), 7.18 (s, 1H), 7.12 (dd, 2H, J=7.9Hz, J=15.2Hz), 6.71 (s, 1H), 3.61 (s, 3H).

Preparation of ethyl 1-methyl-6-oxo-4-(phenylamino)-1,6-dihydropyridine-3-carboxylate from ethyl 4-chloro-1-methyl-6-oxo-1,6-dihydropyridine-3-carboxylate **16a**:

7 (76mg, 0.35mmol) and aniline (64µl, 0.70mmol) were dissolved in isopropanol (2.75ml) in a microwave vial, under N_2. The reaction mixture was stirred in the microwave for 7 hours at 175°C, TLC monitoring at 4 hours showed the reaction was incomplete. The isopropanol was removed in vacuo to yield a purple-pink oil. The crude product was purified using silica gel flash column chromatography on Isolera (EtOAc/MeOH; gradient 10→9:0→10). The fractions containing the desired product were combined and concentrated in vacuo. The desired product was isolated as white crystals; 85mg, 89%. MS APCI (+) *m/z* 273.4 (M+) detected; ^{1}H NMR (400 MHz, MeOD) δ 8.48 (s, 1H), 7.44 (dd, 2H, J=7.5Hz, J=8.3Hz), 7.27 (m, 3H), 5.86 (s, 1H), 4.38 (q, 2H, J=7.1Hz), 3.53 (s, 3H), 1.41 (t, 3H, J=7.1Hz).

Preparation of 3-((5-(ethoxycarbonyl)-1-methyl-2-oxo-1,2-dihydropyridin-4-yl)amino)benzoic acid from ethyl 4-chloro-1-methyl-6-oxo-1,6-dihydropyridine-3-carboxylate **16b**:

Prepared according to **16a** from **7** (100mg, 0.46mmol) and 3-aminobenzoic acid (127mg, 0.93mmol), with the following changes. The reaction time was 8 hours. Work up and purification were the same. The desired product was isolated as a yellow solid; 24mg, 16%. MS APCI (+) *m/z* 317.2 (M+) detected; ^{1}H NMR (400 MHz, MeOD) δ 8.44 (s, 1H), 7.89 (s, 1H), 7.84 (d, 1H,

J=6.6Hz), 7.45 (t, 1H), 7.39 (s, 1H), 5.86 (s, 1H), 4.35 (q, 2H, J=7.0Hz), 3.50 (s, 3H), 1.38 (t, 3H, J=7.1Hz).

Preparation of ethyl 4-((3-cyanophenyl)amino)-1-methyl-6-oxo-1,6-dihydropyridine-3-carboxylate from ethyl 4-chloro-1-methyl-6-oxo-1,6-dihydropyridine-3-carboxylate **16c**:
Prepared according to **16a** from **7** (100mg, 0.46mmol) and 3-aminobenzonitrile (110mg, 0.93mmol). Reaction time was 14 hours. The desired compound was isolated as an orange-white solid; 5mg, 4%. MS APCI (+) *m/z* 298.2 (M+) detected; ^{1}H NMR (400 MHz, MeOD) δ 8.53 (s, 1H), 7.69 (s, 1H), 7.62 (m, 2H), 7.59 (m, 1H), 5.91 (s, 1H), 4.39 (q, 2H, J=7.1Hz), 3.55 (s, 1H), 1.41 (t, 3H, J=7.1Hz).

Preparation of ethyl 4-((2,3-dimethylphenyl)amino)-1-methyl-6-oxo-1,6-dihydropyridine-3-carboxylate from ethyl 4-chloro-1-methyl-6-oxo-1,6-dihydropyridine-3-carboxylate **16d**:
Prepared according to **16a** from **7** (90mg, 0.42mmol) and 2,3-dimethylaniline (51µl, 0.42mmol). Reaction time was 8 hours. The crude purple oil was purified using silica gel flash column chromatography on Isolera (EtOAc/MeOH; gradient 10→9.2:0→0.8). The fractions containing the desired product were combined and concentrated in vacuo. The desired product was isolated as a pale yellow solid; 12mg, 10%. MS APCI (+) *m/z* 301.2 (M+) detected; ^{1}H NMR (400 MHz, MeOD) δ 8.46 (s, 1H), 7.14 (m, 2H), 7.07 (dd, 1H, J=2.4Hz, J=6.6Hz), 5.28 (s, 1H), 4.38 (q, 2H, J=7.1Hz), 3.51 (s, 3H), 2.33 (s, 3H), 2.14 (s, 3H), 1.40 (t, 3H, J=7.1Hz).

Preparation of 1-methyl-4-((5-nitrobenzo[d]isothiazol-3-yl)amino)-6-oxo-1,6-dihydropyridine-3-carboxylic acid from 4-chloro-1-methyl-6-oxo-1,6-dihydropyridine-3-carboxylic acid **16e**:
5-nitrobenzoisothiazol-3-amine (261mg, 1.34mmol) was suspended in 7ml THF and cooled to -78°C. LDA (1.5M in THF, 1.2ml, 1.87mmol) was added dropwise to the suspension. The dark purple suspension was stirred at -78°C for 15 minutes. **8** (100mg, 0.53mmol), in 6ml of THF, was added to the suspension in two portions of 3ml, at -78°C. The reaction mixture was stirred at -78°C for 30 minutes and then was allowed to warm to room temperature and stirred overnight. Saturated $NaHCO_3$ was added and the aqueous layer was extracted with DCM. The combined organic layers were dried over Na_2SO_4, filtered and concentrated in vacuo. A dark purple solid was obtained which was purified by silica gel flash column chromatography (EtOAc/MeOH;

1:1). The fractions containing the desired product were combined and concentrated in vacuo. The desired compound was obtained as a yellow-orange solid; 7 mg, 4%. MS APCI (-) *m/z* 351.0(M-) detected.

Preparation of ethyl 1-methyl-6-oxo-4-phenoxy-1,6-dihydropyridine-3-carboxylate from ethyl 4-chloro-1-methyl-6-oxo-1,6-dihydropyridine-3-carboxylate **17**:

A solution of **7** (110mg, 0.927mmol), phenol (96mg, 1.10mmol) and cesium carbonate (333mg, 1.10mmol) in DMF (2ml) was prepared. The colorless solution was stirred at 100°C overnight. Water (30ml) was added and the solution extracted with DCM. The combined organic extracts were washed with brine and aqueous NaOH, dried over Na_2SO_4, and concentrated in vacuo. The solid was purified by silica gel flash column chromatography (DCM/MeOH; 97:3). The fractions containing the desired product were combined and concentrated in vacuo. The desired compound was obtained as yellow-white needle-like crystals; 110mg, 77%. MS APCI (+) *m/z* 274.1 (M+) detected; ^{1}H NMR (400 MHz, $CDCl_3$) δ 8.22 (s, 1H), 7.43 (dd, 2H, J=7.6Hz, J=8.3Hz), 7.25 (d, 1H, J=7.4Hz), 7.11 (dd, 2H, J=1.0Hz, J=8.6Hz), 5.68 (s, 1H), 4.35 (q, 2H, J=7.1Hz), 3.57 (s, 3H), 1.36 (t, 3H, J=7.1Hz).

Preparation of ethyl 1-methyl-6-oxo-4-(pyridin-4-yloxy)-1,6-dihydropyridine-3-carboxylate from ethyl 4-chloro-1-methyl-6-oxo-1,6-dihydropyridine-3-carboxylate **18a**:

Prepared as described for **17** from **7** (100mg, 0.465mmol) using 4-hydroxypyridine (88mg, 0.93mmol) with the following changes to the procedure. The reaction mixture was heated at 85°C overnight. The desired product was obtained without purification as a yellow-white solid; 100mg, 78%. MS APCI (+) *m/z* 275.2 (M+) detected; ^{1}H NMR (400 MHz, $CDCl_3$) δ 8.40 (s, 1H), 7.31 (m, 1H), 6.51 (s, 1H), 6.45 (d, 2H, J=7.8Hz), 4.23 (q, 2H, J=7.15), 3.69 (s, 3H), 1.63 (s, 3H), 1.22 (t, 3H, J=7.15)

Preparation of ethyl 1-methyl-6-oxo-4-(pyridin-2-yloxy)-1,6-dihydropyridine-3-carboxylate from ethyl 4-chloro-1-methyl-6-oxo-1,6-dihydropyridine-3-carboxylate **18b**:

Prepared as described for **17** from **7** (80mg, 0.37mmol) using 2-hydroxypyridine (71mg, 0.74mmol) with the following changes to the procedure. The reaction mixture was heated at 85°C for 24 hours. The crude mixture was purified by silica gel flash column chromatography

(DCM/MeOH; 95:5). The fractions containing the desired product were combined and concentrated in vacuo. The desired product was obtained as a white solid; 10mg, 10%. MS APCI (+) *m/z* 275.3 (M+) detected; ^{1}H NMR (400 MHz, $CDCl_3$) δ 8.27 (s, 1H), 8.16 (ddd, 1H, J=0.7Hz, J=1.9Hz, J=5.0Hz), 7.77 (ddd, 1H, J=2.0Hz, J=7.3Hz, J=8.3Hz), 7.05 (m, 2H), 6.24 (s, 1H), 4.12 (q, 2H, J=7.1Hz), 3.62 (s, 3H), 1.11 (t, 3H, J=7.1Hz).

Preparation of benzophenone oxime from benzophenone **19**:

Benzophenone (3g, 16.5mmol) and hydroxylamine hydrochloride (3g, 43.2mmol) were dissolved in 15ml of pyridine and 15ml of ethanol at 60°C for 2 hours. The solvents were removed en vacuo. 15ml of water was added and the mixture was filtered by vacuum filtration to yield a white solid. The desired product was recrystallized from ethanol to yield white crystals; 2.73g, 84%. MS APCI (+) *m/z* 198.2 (M+) detected; ^{1}H NMR (400 MHz, $CDCl_3$) δ 8.36 (s, 1H), 7.44 (m, 9H).

Preparation of 2-chloro-5-nitrobenzonitrile from 2-chlorobenzonitrile **20**:

2-chlorobenzonitrile (13.7g, 99.6mmol) was added to H_2SO_4 (80ml) and the mixture was cooled to 8°C. HNO_3 (30ml) was added dropwise, making sure the solution stayed below 20°C. The reaction mixture was then stirred at 20°C for 1 hour. The mixture was then slowly poured onto 800g of ice water. The product precipitated out of solution and was isolated by vacuum filtration and washed with cold water. The desired product was isolated as a white solid; 16.4g, 90%. MS APCI (+) *m/z* 183.2 (M+) detected; ^{1}H NMR (400 MHz, DMSO) δ 8.93 (d, 1H, J=2.72Hz), 8.54 (dd, 1H, J=2.75Hz, J=8.96Hz), 8.07 (d, 1H, J=8.95Hz).

Preparation of 2-(((diphenylmethylene)amino)oxy)-5-nitrobenzonitrile from 2-chloro-5-nitrobenzonitrile **21a**:

19 (985mg, 5mmol) and K^{t}OBu (662mg, 5.9mmol) were stirred at room temperature in THF (65ml) for 30 minutes. **20** (913mg. 5mmol) was added to the suspension and it slowly became a red solution. The reaction mixture was stirred for 24 hours at 55°C. The THF was then removed in vacuo. Water (20ml) was added and extracted with DCM. The organic layers were collected, dried over Na_2SO_4, filtered and concentrated in vacuo to yield an orange-brown solid. The solid was washed with Hex/DCM (95:5) twice to yield the desired intermediate as a beige solid;

1.308g, 76%. MS APCI (+) *m/z* 344.2 (M+) detected; ^{1}H NMR (400 MHz, $CDCl_3$) δ 8.50 (d, 1H, J=1.44Hz), 8.49 (d, 1H, J=3.64Hz), 7.97 (d, 1H, J=10.0Hz), 7.68 (t, 1H, J=1.3Hz), 7.66 (d, 1H, J=1.5Hz), 7.58 (d, 2H, J=2.7Hz), 7.57 (d, 2H, J=0.9Hz), 7.55 (d, 2H, J=1.5Hz), 7.49 (dd, 2H, J=1.4Hz, J=6.3Hz).

Preparation of 2-(((diphenylmethylene)amino)oxy)benzonitrile from 2-fluorobenzonitrile **21b**:
Prepared as described for **21a** using 2-fluorobenzonitrile (543µl, 5mmol). The reaction mixture was stirred at 55°C for 42 hours. The THF was removed in vacuo. An extraction from water using DCM was performed and the combined organic extracts were dried over sodium sulfate, filtered and concentrated in vacuo. Flash column chromatography using Isolera was performed using Hex/EtOAc (gradient; 10→8:0→2). The fractions containing the desired product were combined and concentrated in vacuo. The desired product was isolated as a white solid; 1.437g, 96%. MS APCI (+) *m/z* 344.2 (M+) detected; ^{1}H NMR (400 MHz, DMSO) δ 7.78 (dd, 3H, J=6.6Hz, J=8.2Hz), 7.61 (s, 1H), 7.59 (d, 1H, J=1.5Hz), 7.57 (dd, 4H, J=2.4Hz, J=6.9Hz), 7.52 (dd, 4H, J=2.6Hz, J=4.9Hz), 7.25 (td, 1H, J=1.2Hz, J=7.4Hz).

Preparation of 5-nitrobenzisoxazol-3-amine from 2-(((diphenylmethylene)amino)oxy)-5-nitrobenzonitrile **22a**:
21a (303mg, 0.88mmol) was dissolved in TFA/HCl (4:1, 2.5ml) and stirred at 55°C for 2 hours. Aqueous K_2CO_3 was added until the pH reached 7. The water layer was extracted with EtOAc, the organic layer was then washed with water, dried over Na_2SO_4, filtered and concentrated in vacuo. The solid was then washed with hexanes. The desired product was isolated as a yellow solid; 132mg, 84%. MS APCI (+) *m/z* 180.2 (M+) detected; ^{1}H NMR (400 MHz, DMSO) δ 8.97 (d, 1H, J=2.2Hz), 8.41 (dd, 1H, J=2.3Hz, J=9.2Hz), 7.70 (d, 1H, J=9.2Hz), 6.86 (s, 2H).

Preparation of benzisoxazol-3-amine from 2-(((diphenylmethylene)amino)oxy)benzonitrile **22b**:
Prepared as described for **22a** from **21b** (230mg, 0.77mmol). The desired product was isolated as a beige solid; 96mg, 93%. MS APCI (+) *m/z* 135.1 (M+) detected; ^{1}H NMR (400 MHz, MeOD) δ 7.78 (d, 1H, J=7.9Hz), 7.56 (t, 1H, J=8.3Hz), 7.41 (d, 1H, J=8.5Hz), 7.28 (t, 1H, J=7.5Hz).

Preparation of 1-indazol-3-amine from 2-fluorobenzonitrile **23a**:

2-fluorobenzonitrile (217µl, 2mmol) was dissolved in BuOH (5ml) and hydrazine in H_2O (10ml, 10mmol) was added. The reaction mixture was stirred at 140°C for 48 hours. The reaction mixture was cooled to room temperature and 25 ml H_2O and 50ml EtOAc were added. The water layer was extracted with EtOAc, the organic layers were washed 2 times with brine, dried over Na_2SO_4, filtered and concentrated in vacuo. The desired product was isolated as a white solid; 215mg, 81%. MS APCI (+) *m/z* 134.4 (M+) detected; ^{1}H NMR (400 MHz, DMSO) δ 11.37 (s, 1H), 7.70 (d, 1H, J=8.0Hz), 7.23 (m, 2H), 6.91 (ddd, 1H, J=2.5Hz, J=5.2Hz, J=7.9Hz), 5.33 (s, 2H).

Preparation of 5-nitro-1-indazol-3-amine from 2-chloro-5-nitrobenzonitrile **23b**:
Prepared as described for **23a** using **20** (363mg, 2mmol). The reaction mixture was stirred at 65°C overnight. The work up procedure was the same as **23a**. The reaction was purified using flash column chromatography on Isolera DCM/MeOH (gradient; 10→9:0→10). The fractions containing the desired product were combined and concentrated in vacuo. The desired product was isolated as a red solid; 348mg, 97%. MS APCI (+) *m/z* 179.2 (M+) detected; ^{1}H NMR (400 MHz, DMSO) δ 12.19 (s, 1H), 8.91 (d, 1H, J=2.1Hz), 8.07 (dd, 1H, J=2.0Hz, J=9.2Hz), 7.36 (d, 1H, J=9.2Hz), 6.00 (s, 2H).

Preparation of N-(benzisoxazol-3-yl)-4-methoxy-1-methyl-6-oxo-1,6-dihydropyridine-3-carboxamide from 4-methoxy-1-methyl-6-oxo-1,6-dihydropyridine-3-carboxylic acid **24a**:
4 (99.8mg, 0.54mmol) was dissolved in 3ml thionyl chloride and stirred at 90°C for 1 hour. The $SOCl_2$ was removed in vacuo. The flask was purged with nitrogen, THF (3ml) was added and the flask was cooled to 0°C. Benzoisoxazol-3-amine (73mg, 0.54mmol) and K_2CO_3 (113mg, 0.82mmol) were added at 0°C. The flask was allowed to warm to room temperature and the reaction mixture was stirred overnight. The THF was removed in vacuo. MeOH (1.5ml) and DCM (1.5ml) were added and a white solid was isolated by vacuum filtration. The solid was washed with water to obtain a pure product. The filtrate was evaporated and the procedure was repeated using 0.5ml of both DCM and MeOH. The desired product was isolated from both filtrations as a white solid; 160mg, 99%. MS APCI (+) *m/z* 300.4 (M+) detected; ^{1}H NMR (400 MHz, DMSO) δ 10.59 (s, 1H), 8.43 (s, 1H), 7.99 (d, 1H, J=8.0Hz), 7.75 (d, 1H, J=8.5Hz), 7.69 (t, 1H, J=8.2Hz), 7.41 (t, 1H, J=7.8Hz), 5.99 (s, 1H), 3.91 (s, 3H), 3.49 (s, 3H).

Preparation of N-(benzisoxazol-3-yl)-4-(2-methoxyethoxy)-1-methyl-6-oxo-1,6-dihydropyridine-3-carboxamide from 4-(2-methoxyethoxy)-1-methyl-6-oxo-1,6-dihydropyridine-3-carboxylic acid **24b**:

Prepared as described for **24a** from **9** (105mg, 0.46mmol) using benzoisoxazol-3-amine (62mg, 0.46mmol) and K_2CO_3 (96mg, 0.69mmol). The work up procedure was changed and EtOAc (3ml) and H_2O (2ml) were added instead of DCM and MeOH. A beige solid was isolated following vacuum filtration of EtOAc/H_2O suspension. The desired product was isolated as a beige solid; 100mg, 63%. MS APCI (+) *m/z* 344.3 (M+) detected; ^{1}H NMR (400 MHz, $CDCl_3$) δ 10.22 (s, 1H), 8.51 (s, 1H), 8.20 (d, 1H, J=8.12Hz), 7.59 (dd, 1H, J=1.0Hz, J=6.5Hz), 7.35 (ddd, 1H, J=1.4Hz, J=6.5Hz, J=8.0Hz), 6.04 (s, 1H), 4.33 (t, 2H, J=4.2Hz), 3.92 (t, 2H, J=3.8Hz), 3.65 (s, 3H), 3.55 (s, 3H).

Preparation of 4-methoxy-1-methyl-N-(6-nitrobenzisoxazol-3-yl)-6-oxo-1,6-dihydropyridine-3-carboxamide from 4-methoxy-1-methyl-6-oxo-1,6-dihydropyridine-3-carboxylic acid **24c**:

Prepared as described for **24a** from **4** (100mg, 0.55mmol) using 6-nitrobenzoisoxazol-3-amine (98mg, 0.55mmol) and K_2CO_3 (113mg, 0.82mmol). The work up procedure was changed. THF was removed in vacuo, water (5ml) and 3ml DCM/MeOH mixture (1:1) was added and a yellow solid was isolated by vacuum filtration. The solid was washed with EtOAc/MeOH (9:1). The desired product was isolated as a yellow solid; 16mg, 8.5%. MS APCI (+) *m/z* 345.4 (M+) detected; ^{1}H NMR (400 MHz, DMSO) δ 8.67 (s, 1H), 8.66 (s, 1H), 7.80 (dd, 1H, J=3.2Hz, J=9.6Hz), 6.14 (d, 1H, J=9.6Hz), 6.04 (s, 1H), 3.91 (s, 3H), 3.53 (s, 3H).

Preparation of 4-(2-methoxyethoxy)-1-methyl-N-(6-nitrobenzisoxazol-3-yl)-6-oxo-1,6-dihydropyridine-3-carboxamide from 4-(2-methoxyethoxy)-1-methyl-6-oxo-1,6-dihydropyridine-3-carboxylic acid **24d**:

Prepared as described for **24b** from **9** (81mg, 0.36mmol) using 6-nitrobenzoisoxazol-3-amine (64mg, 0.36mmol) and K_2CO_3 (74mg, 0.54mmol). Isolated as a white solid following vacuum filtration which was purified using Isolera; gradient EtOAc/MeOH ((10→9:0→1). The fractions containing the desired product were combined and concentrated in vacuo. The desired product was isolated as a white solid; 26mg, 19%. MS APCI (+) *m/z* 389.4 (M+) detected; ^{1}H NMR (400

MHz, $CDCl_3$) δ 10.42 (s, 1H), 9.32 (d, 1H, J=2.3Hz), 8.56 (s, 1H), 8.50 (dd, 1H, J=2.3Hz, J=9.2Hz), 7.66 (d, 1H, J=9.2Hz), 6.04 (s, 1H), 4.34 (t, 2H, J=4.6Hz), 3.93 (t, 2H, J=4.4Hz), 3.68 (s, 3H), 3.57 (s, 3H).

Preparation of N-(1H-indazol-3-yl)-4-methoxy-1-methyl-6-oxo-1,6-dihydropyridine-3-carboxamide from 4-methoxy-1-methyl-6-oxo-1,6-dihydropyridine-3-carboxylic acid **24e**:
Prepared as described for **24b** from **4** (75mg, 0.41mmol) using 1H-indazol-3-amine (54mg, 0.41mmol) and potassium carbonate (85mg, 0.61mmol). The desired product was isolated, following vacuum filtration as a pink solid; 47mg, 38%. MS APCI (+) *m/z* 299.3 (M+) detected; ^{1}H NMR (400 MHz, DMSO) δ 12.77 (s, 1H), 9.94 (s, 1H), 8.42 (s, 1H), 7.79 (d, 1H, J=8.2Hz), 7.50 (d, 1H, J=8.1Hz), 7.36 (t, 1H, J=7.4Hz), 7.09 (t, 1H, J=7.6Hz), 5.99 (s, 1H), 3.95 (s, 3H), 3.49 (s, 3H).

Preparation of N-(1H-indazol-3-yl)-4-(2-methoxyethoxy)-1-methyl-6-oxo-1,6-dihydropyridine-3-carboxamide from 4-(2-methoxyethoxy)-1-methyl-6-oxo-1,6-dihydropyridine-3-carboxylic acid **24f**:
Dissolved **9** (113.5mg, 0.50mmol) in an excess, 3ml, of $SOCl_2$. The yellow solution was stirred at 90°C for 1 hour. The thionyl chloride was removed en vacuo. 4-(2-methoxyethoxy)-1-methyl-6-oxo-1,6-dihydropyridine-3-carbonyl chloride was dissolved in THF (3ml) and cooled to 0°C. 1H-indazol-3-amine (67mg, 0.50mmol) and potassium carbonate (104mg, 0.75mmol) were added. The white suspension was stirred overnight at room temperature. After 16 hours the THF was removed in vacuo. 5 ml of water and EtOAc were added to the flask and a white solid was isolated by filtration. Flash column chromatography on Isolera was performed (EtOAc 100→90/MeOH 0→10). The fractions containing the desired product were combined and concentrated in vacuo. The desired product was isolated as a white solid; 80mg, 47%. MS APCI (+) *m/z* 343.4 (M+) detected; ^{1}H NMR (400 MHz, DMSO) δ 12.77 (s, 1H), 9.99 (s, 1H), 8.49 (s 1H), 7.86 (d, 1H, J=8.16Hz), 7.48 (d, 1H, J=8.45Hz), 7.37 (ddd, 1H, J=0.8Hz, J=6.8Hz, J=7.2Hz), 7.09 (ddd 1H, J=0.76Hz, J=6.81Hz, J=7.95Hz), 6.04 (s, 1H), 4.32 (t, 2H, J=4.0Hz), 3.78 (t, 2H, J=3.6), 3.51 (s, 3H), 3.32 (s, 3H).

Preparation of 4-methoxy-1-methyl-N-(6-nitro-1H-indazol-3-yl)-6-oxo-1,6-dihydropyridine-3-carboxamide from 4-methoxy-1-methyl-6-oxo-1,6-dihydropyridine-3-carboxylic acid **24g**:

Prepared as described for **24b** from **4** (90mg, 0.49mmol) using 5-nitro-1H-indazol-3-amine (65mg, 0.37mmol) and potassium carbonate (102mg, 0.74mmol). The desired product was isolated, following vacuum filtration as an orange solid; 79mg, 62%. MS APCI (+) *m/z* 344.2 (M+) detected; ^{1}H NMR (400 MHz, DMSO) δ 13.49 (s, 1H), 10.32 (s, 1H), 9.07 (d, 1H, J=2.1Hz), 8.52 (s, 1H), 8.21 (dd, 1H, J=2.2Hz, J=9.2Hz), 7.68 (d, 1H, J=9.2Hz), 6.01 (s, 1H), 3.95 (s, 3H), 3.51 (s, 3H).

Preparation of 4-(2-methoxyethoxy)-1-methyl-N-(5-nitro-1H-indazol-3-yl)-6-oxo-1,6-dihydropyridine-3-carboxamide from 4-(2-methoxyethoxy)-1-methyl-6-oxo-1,6-dihydropyridine-3-carboxylic acid **24h**:

9 (92mg, 0.41mmol) was dissolved in an excess of $SOCl_2$ (2.5ml). The yellow solution was stirred at 90°C for 1 hour. The thionyl chloride was removed in vacuo. 4-(2-methoxyethoxy)-1-methyl-6-oxo-1,6-dihydropyridine-3-carbonyl chloride was dissolved in 3ml of THF and cooled to 0°C. 5-nitro-1H-indazol-3-amine (72mg, 0.41mmol) and potassium carbonate (84mg, 0.61mmol) were added. The red suspension was stirred overnight at room temperature. After about 1 hour it became a yellow suspension. After 16 hours the THF was removed in vacuo. 5 ml of water and EtOAc were added to the flask and the desired product was isolated by vacuum filtration as an orange-yellow solid; 110mg, 69%. MS APCI (+) *m/z* 388.5 (M+) detected; ^{1}H NMR (400 MHz, DMSO) δ 13.49 (s, 1H), 10.35 (s, 1H), 9.15 (d, 1H, J=2.03Hz), 8.61 (s 1H), 8.20, (dd, 1H, J=2.24Hz, J=9.24Hz), 7.66 (d, 1H, J=9.26Hz), 6.05 (s, 1H), 4.33 (t, 2H, J=4.2Hz), 3.80 (t, 2H, J=3.8Hz), 3.52 (s, 3H), 3.36 (s, 3H).

6.1 NMR data

2

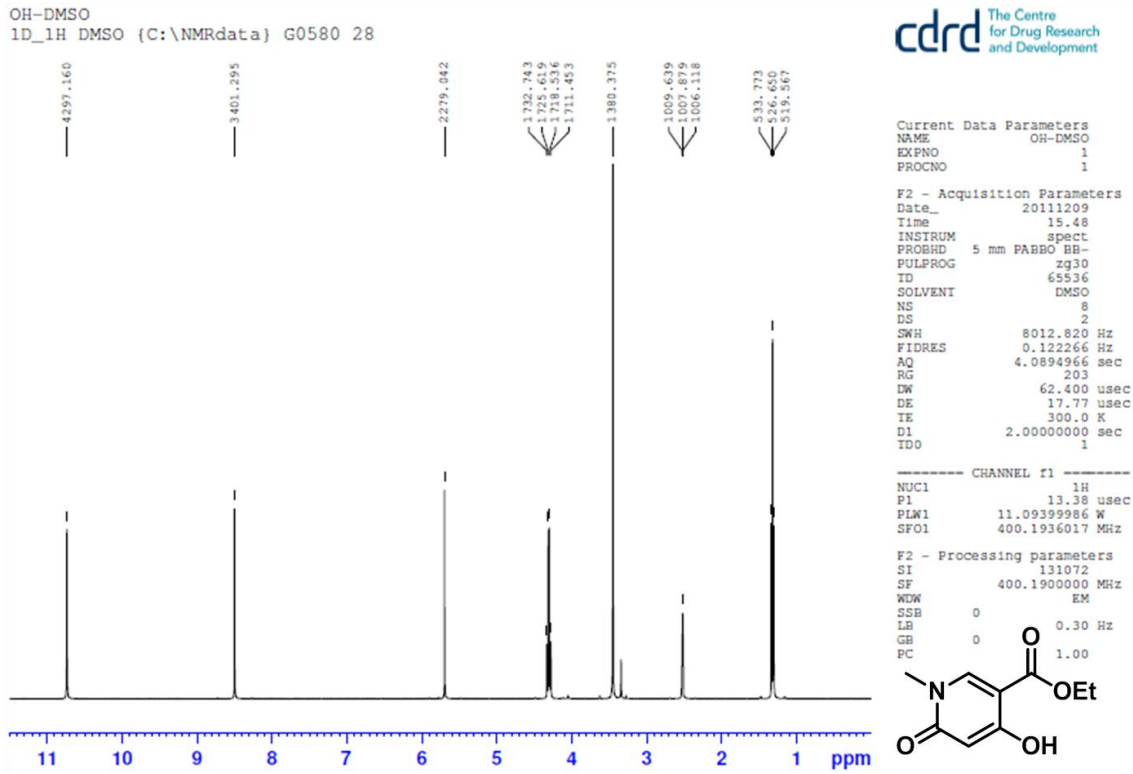

3

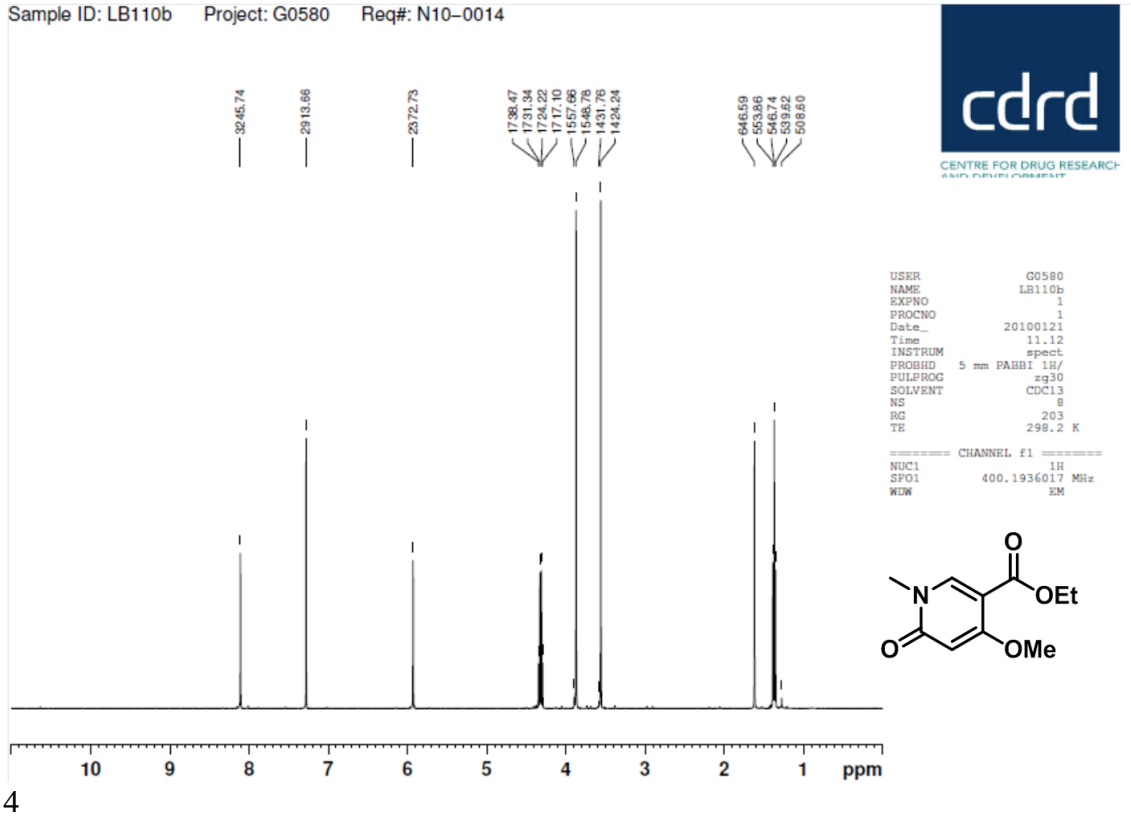

4

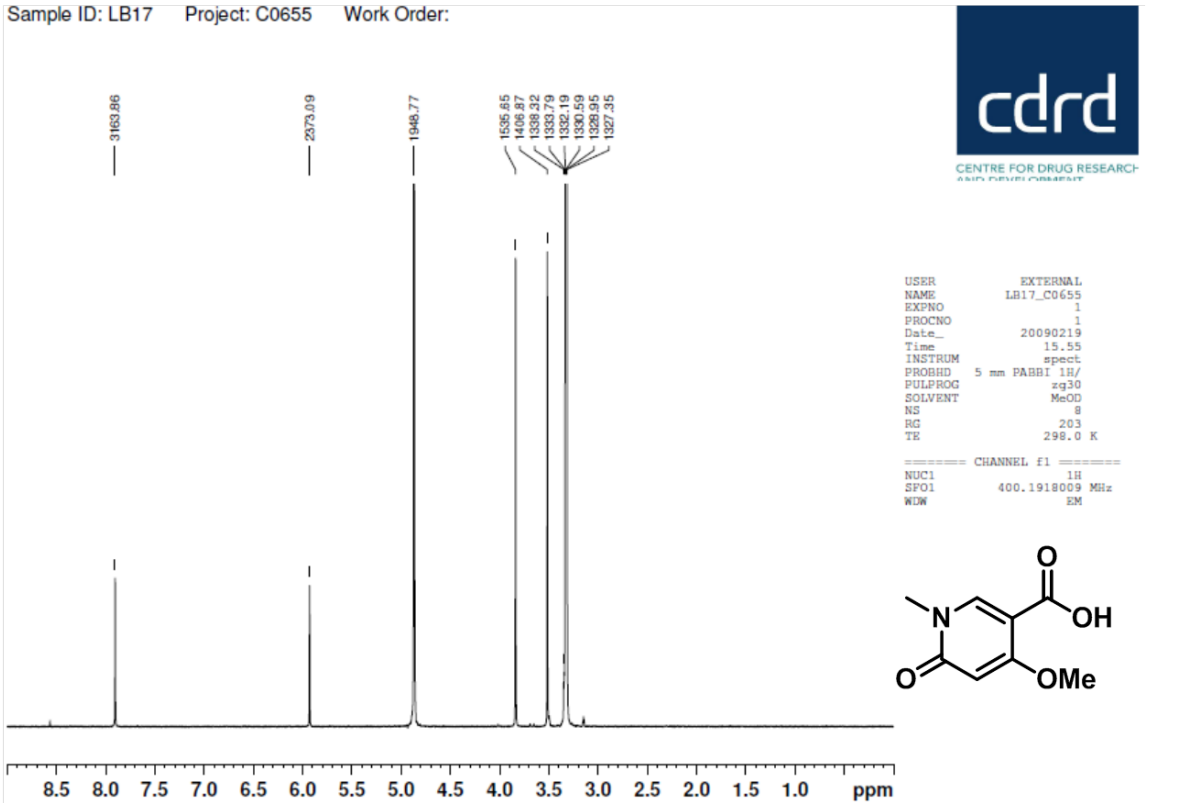
Sample ID: LB17 Project: C0655 Work Order:
3163.86
2373.09
1948.77
1535.65
1406.87
1338.32
1333.79
1332.19
1330.59
1328.95
1327.35
USER EXTERNAL
NAME LB17_C0655
EXPNO 1
PROCNO 1
Date_ 20090219
Time 15.55
INSTRUM spect
PROBHD 5 mm PABBI 1H/
PULPROG zg30
SOLVENT MeOD
NS 8
RG 203
TE 298.0 K
======= CHANNEL f1 =======
NUC1 1H
SFO1 400.1918009 MHz
WDW EM
8.5 8.0 7.5 7.0 6.5 6.0 5.5 5.0 4.5 4.0 3.5 3.0 2.5 2.0 1.5 1.0 ppm

5a

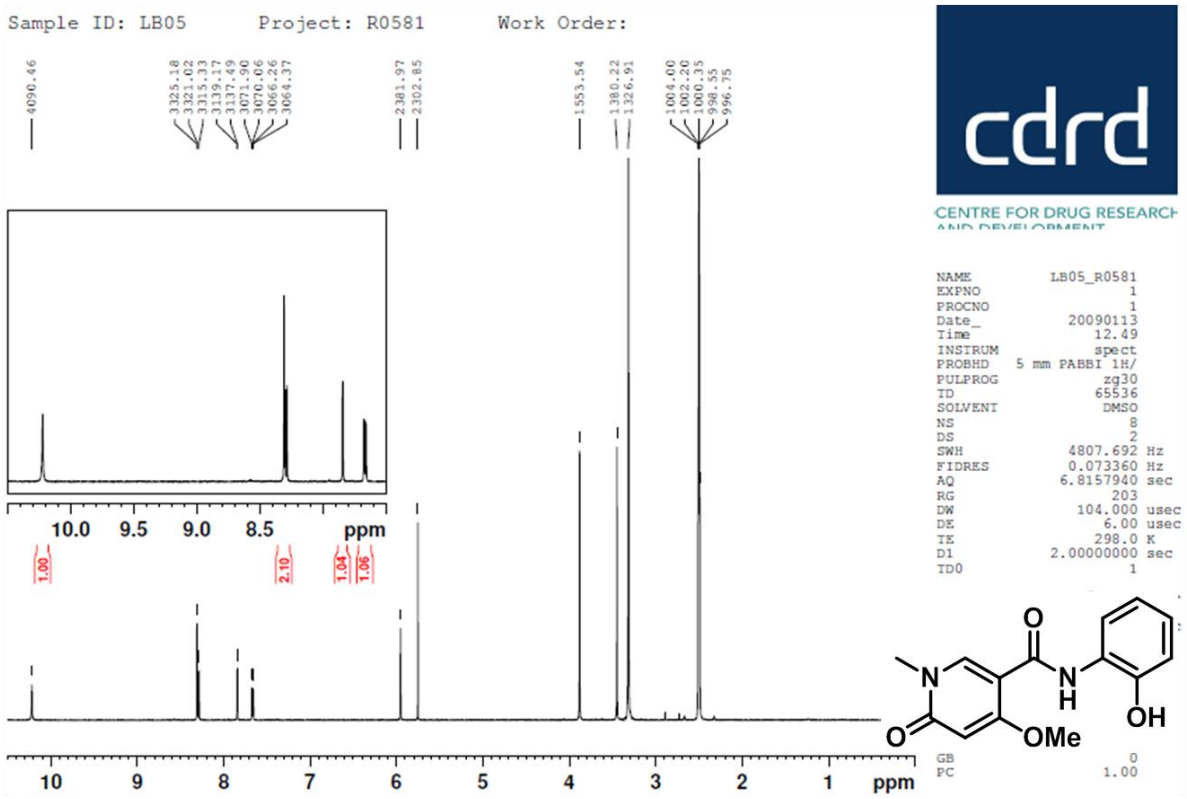
Sample ID: LB05 Project: R0581 Work Order:
4090.46
3325.18
3321.02
3315.33
3139.17
3137.49
3071.90
3070.06
3066.26
3064.37
2381.97
2302.85
1553.54
1380.22
1326.91
1004.00
1002.20
1000.35
998.55
996.75
10.0 9.5 9.0 8.5 ppm
1.00
2.10
1.04
1.06
10 9 8 7 6 5 4 3 2 1 ppm
NAME LB05_R0581
EXPNO 1
PROCNO 1
Date_ 20090113
Time 12.49
INSTRUM spect
PROBHD 5 mm PABBI 1H/
PULPROG zg30
TD 65536
SOLVENT DMSO
NS 8
DS 2
SWH 4807.692 Hz
FIDRES 0.073360 Hz
AQ 6.8157940 sec
RG 203
DW 104.000 usec
DE 6.00 usec
TE 298.0 K
D1 2.00000000 sec
TD0 1
GB 0
PC 1.00

5b

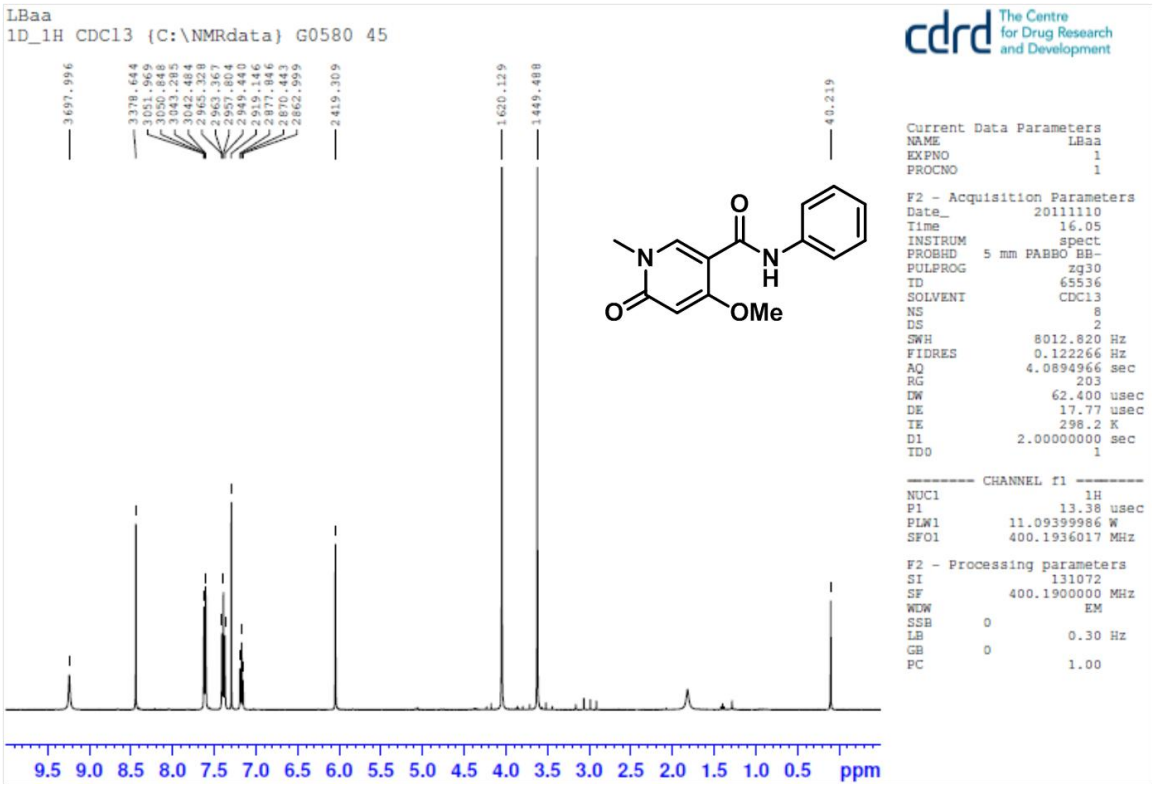
LBaa
1D_1H CDCl3 (C:\NMRdata) G0580 45
3697.996
3378.644
3051.969
3050.848
3043.285
3042.484
2965.328
2963.367
2957.804
2949.440
2919.146
2877.846
2870.443
2862.999
2419.309
1620.129
1449.488
40.219
O
N
H
O
N
OMe
9.5 9.0 8.5 8.0 7.5 7.0 6.5 6.0 5.5 5.0 4.5 4.0 3.5 3.0 2.5 2.0 1.5 1.0 0.5 ppm
cdrd The Centre for Drug Research and Development
Current Data Parameters
NAME LBaa
EXPNO 1
PROCNO 1
F2 - Acquisition Parameters
Date_ 20111110
Time 16.05
INSTRUM spect
PROBHD 5 mm PABBO BB-
PULPROG zg30
TD 65536
SOLVENT CDCl3
NS 8
DS 2
SWH 8012.820 Hz
FIDRES 0.122266 Hz
AQ 4.0894966 sec
RG 203
DW 62.400 usec
DE 17.77 usec
TE 298.2 K
D1 2.00000000 sec
TD0 1
CHANNEL f1
NUC1 1H
P1 13.38 usec
PLW1 11.09399986 W
SFO1 400.1936017 MHz
F2 - Processing parameters
SI 131072
SF 400.1900000 MHz
WDW EM
SSB 0
LB 0.30 Hz
GB 0
PC 1.00

5c

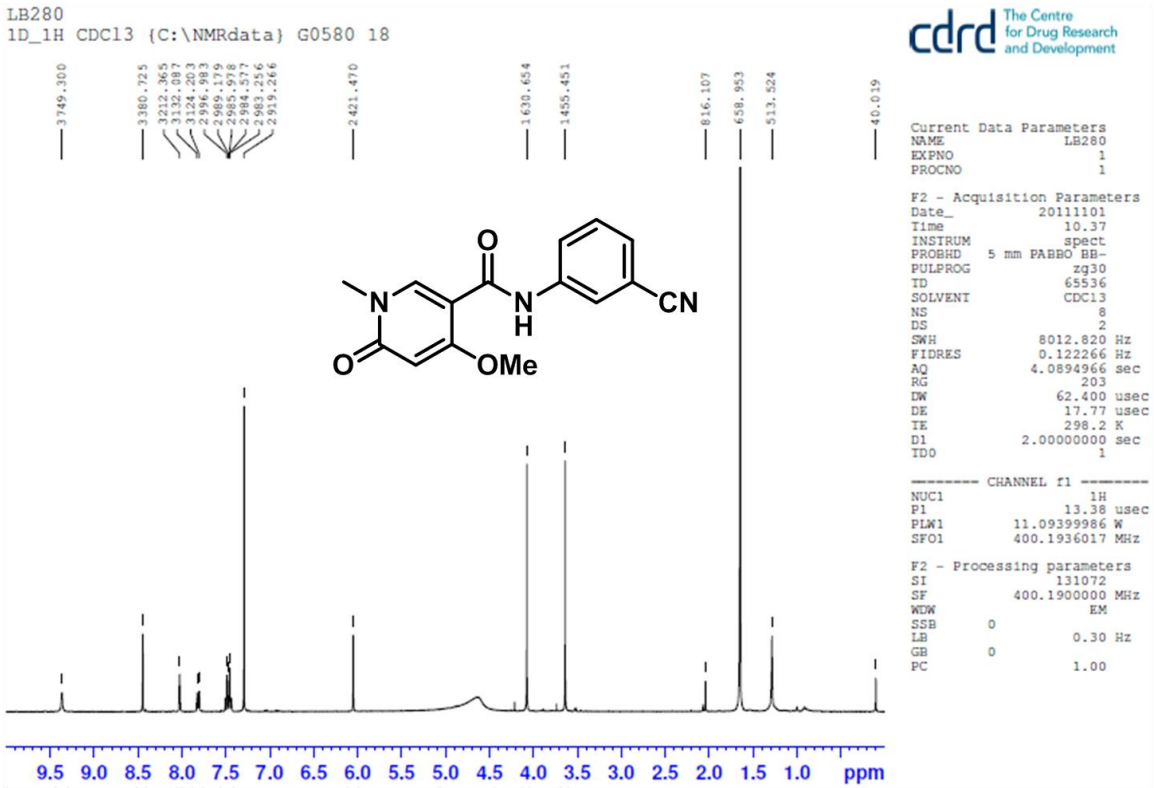
LB280
1D_1H CDCl3 (C:\NMRdata) G0580 18
3749.300
3360.725
3212.365
3132.087
3124.203
2996.983
2989.179
2985.978
2984.577
2983.256
2919.266
2421.470
1630.654
1455.451
816.107
658.953
513.524
40.019
O
N
H
CN
O
N
OMe
9.5 9.0 8.5 8.0 7.5 7.0 6.5 6.0 5.5 5.0 4.5 4.0 3.5 3.0 2.5 2.0 1.5 1.0 ppm
cdrd The Centre for Drug Research and Development
Current Data Parameters
NAME LB280
EXPNO 1
PROCNO 1
F2 - Acquisition Parameters
Date_ 20111101
Time 10.37
INSTRUM spect
PROBHD 5 mm PABBO BB-
PULPROG zg30
TD 65536
SOLVENT CDCl3
NS 8
DS 2
SWH 8012.820 Hz
FIDRES 0.122266 Hz
AQ 4.0894966 sec
RG 203
DW 62.400 usec
DE 17.77 usec
TE 298.2 K
D1 2.00000000 sec
TD0 1
CHANNEL f1
NUC1 1H
P1 13.38 usec
PLW1 11.09399986 W
SFO1 400.1936017 MHz
F2 - Processing parameters
SI 131072
SF 400.1900000 MHz
WDW EM
SSB 0
LB 0.30 Hz
GB 0
PC 1.00

5d

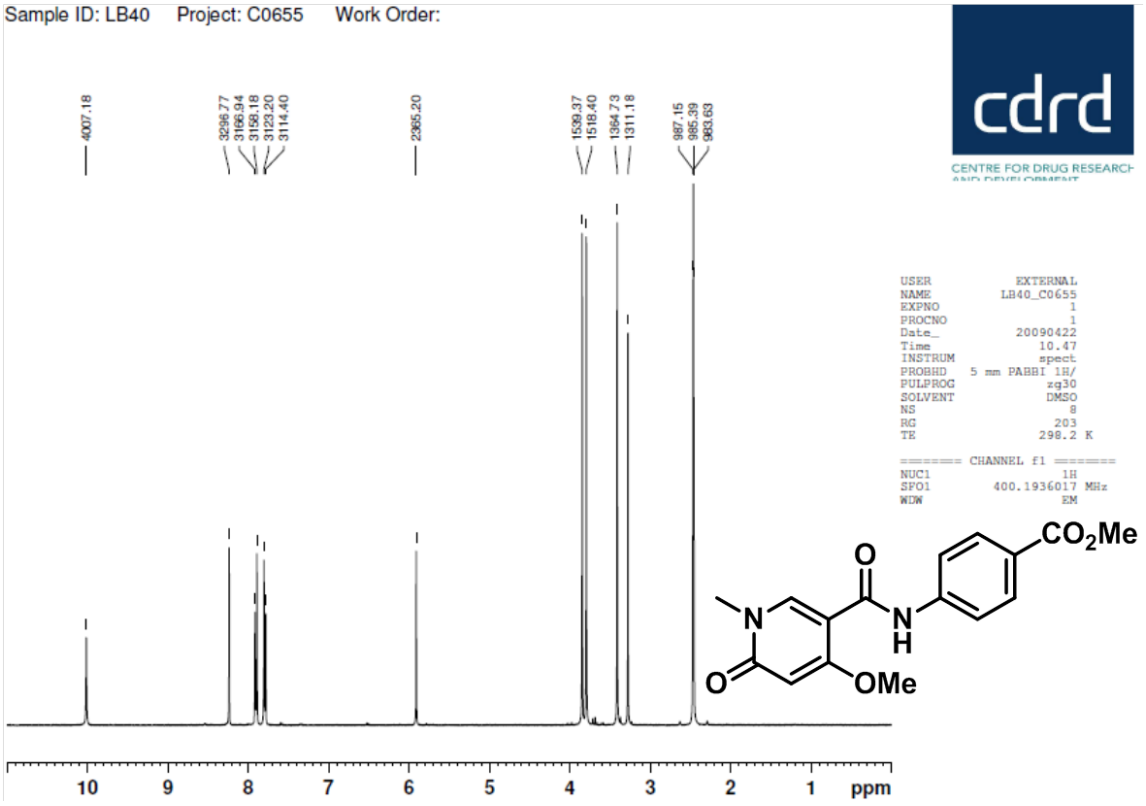
Sample ID: LB40 Project: C0655 Work Order:
4007.18
3296.77
3166.94
3158.18
3123.20
3114.40
2965.20
1539.37
1518.40
1364.73
1311.18
987.15
985.39
983.63
CENTRE FOR DRUG RESEARCH
USER EXTERNAL
NAME LB40_C0655
EXPNO 1
PROCNO 1
Date_ 20090422
Time 10.47
INSTRUM spect
PROBHD 5 mm PABBI 1H/
PULPROG zg30
SOLVENT DMSO
NS 8
RG 203
TE 298.2 K
CHANNEL f1
NUC1 1H
SFO1 400.1936017 MHz
WDW EM
CO2Me
O
N
H
N
O
OMe
10 9 8 7 6 5 4 3 2 1 ppm

5e

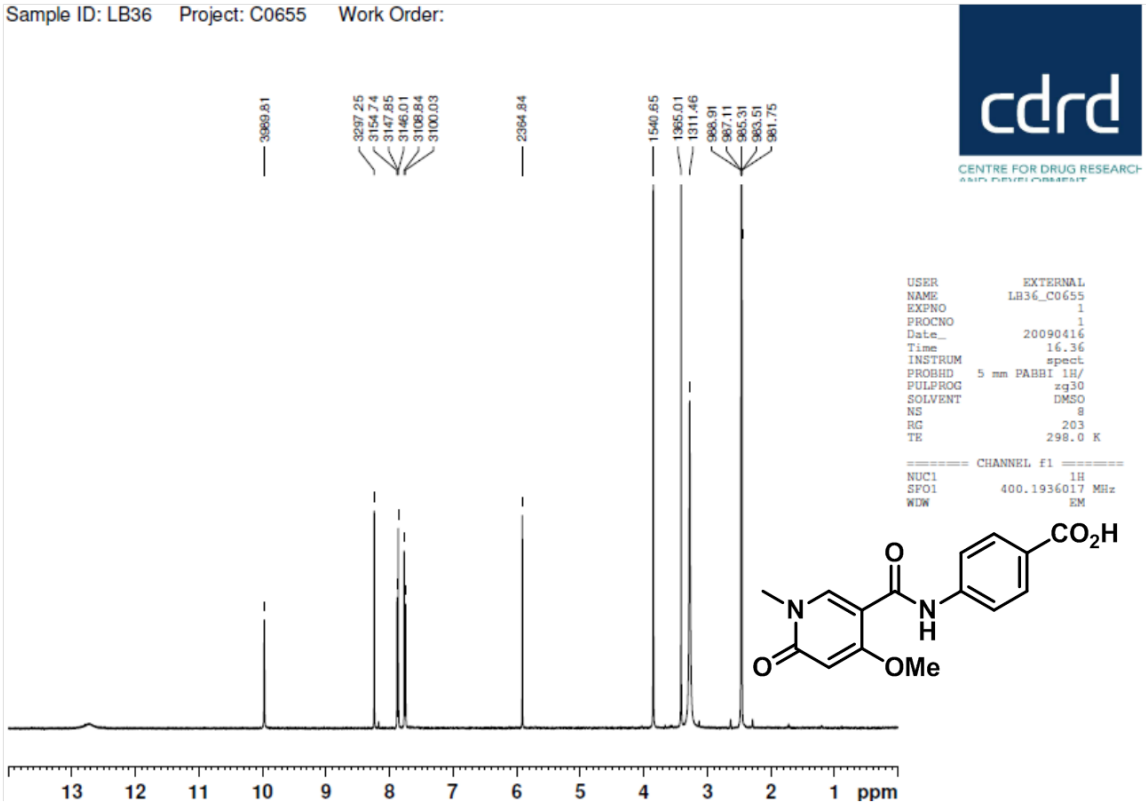
Sample ID: LB36 Project: C0655 Work Order:
3989.81
3297.25
3154.74
3147.85
3146.01
3106.84
3100.03
2364.84
1540.65
1365.01
1311.46
998.91
967.11
965.31
963.51
961.75
CENTRE FOR DRUG RESEARCH
USER EXTERNAL
NAME LB36_C0655
EXPNO 1
PROCNO 1
Date_ 20090416
Time 16.36
INSTRUM spect
PROBHD 5 mm PABBI 1H/
PULPROG zg30
SOLVENT DMSO
NS 8
RG 203
TE 298.0 K
CHANNEL f1
NUC1 1H
SFO1 400.1936017 MHz
WDW EM
CO2H
O
N
H
N
O
OMe
13 12 11 10 9 8 7 6 5 4 3 2 1 ppm

5f

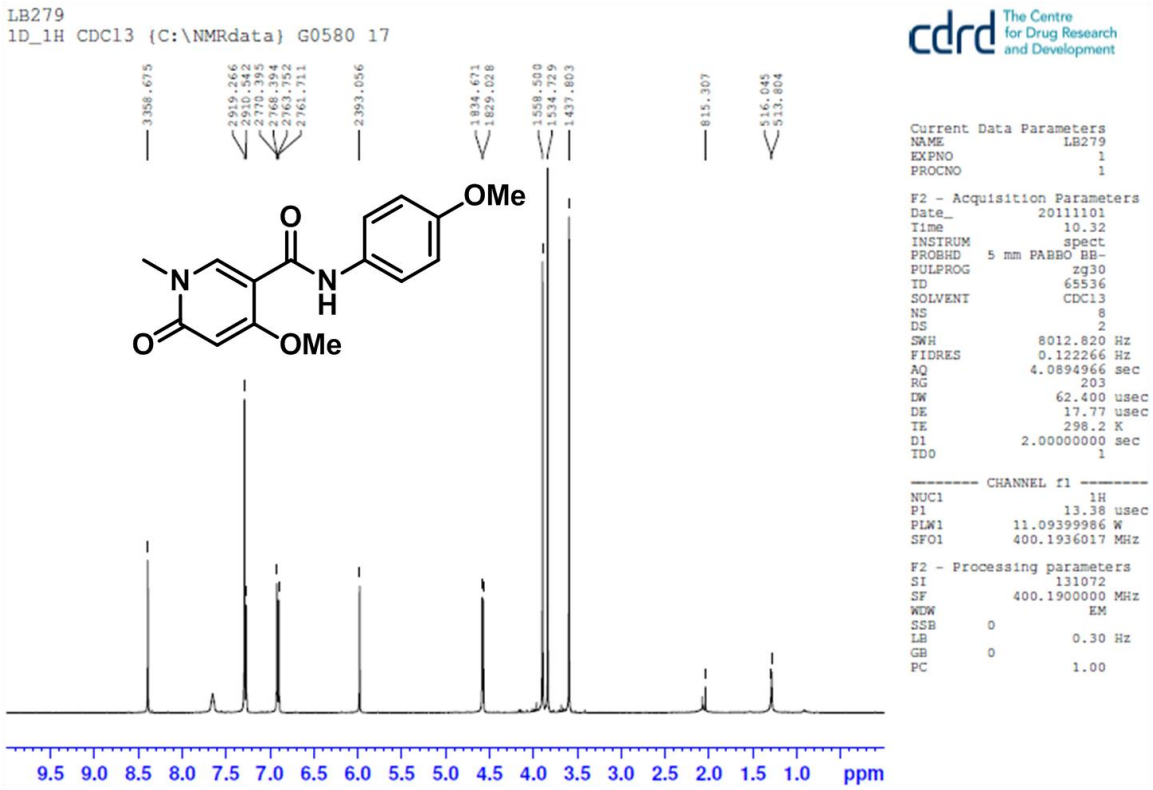
LB279
1D_1H CDCl3 {C:\NMRdata} G0580 17
3358.675
2919.266
2910.542
2770.395
2768.394
2763.752
2761.711
2393.056
1834.671
1829.028
1558.500
1534.729
1437.803
815.307
516.045
513.804
OMe
O
N
H
O
OMe
Current Data Parameters
NAME LB279
EXPNO 1
PROCNO 1
F2 - Acquisition Parameters
Date_ 20111101
Time 10.32
INSTRUM spect
PROBHD 5 mm PABBO BB-
PULPROG zg30
TD 65536
SOLVENT CDCl3
NS 8
DS 2
SWH 8012.820 Hz
FIDRES 0.122266 Hz
AQ 4.0894966 sec
RG 203
DW 62.400 usec
DE 17.77 usec
TE 298.2 K
D1 2.00000000 sec
TD0 1
CHANNEL f1
NUC1 1H
P1 13.38 usec
PLW1 11.09399986 W
SFO1 400.1936017 MHz
F2 - Processing parameters
SI 131072
SF 400.1900000 MHz
WDW EM
SSB 0
LB 0.30 Hz
GB 0
PC 1.00
9.5 9.0 8.5 8.0 7.5 7.0 6.5 6.0 5.5 5.0 4.5 4.0 3.5 3.0 2.5 2.0 1.5 1.0 ppm

5g

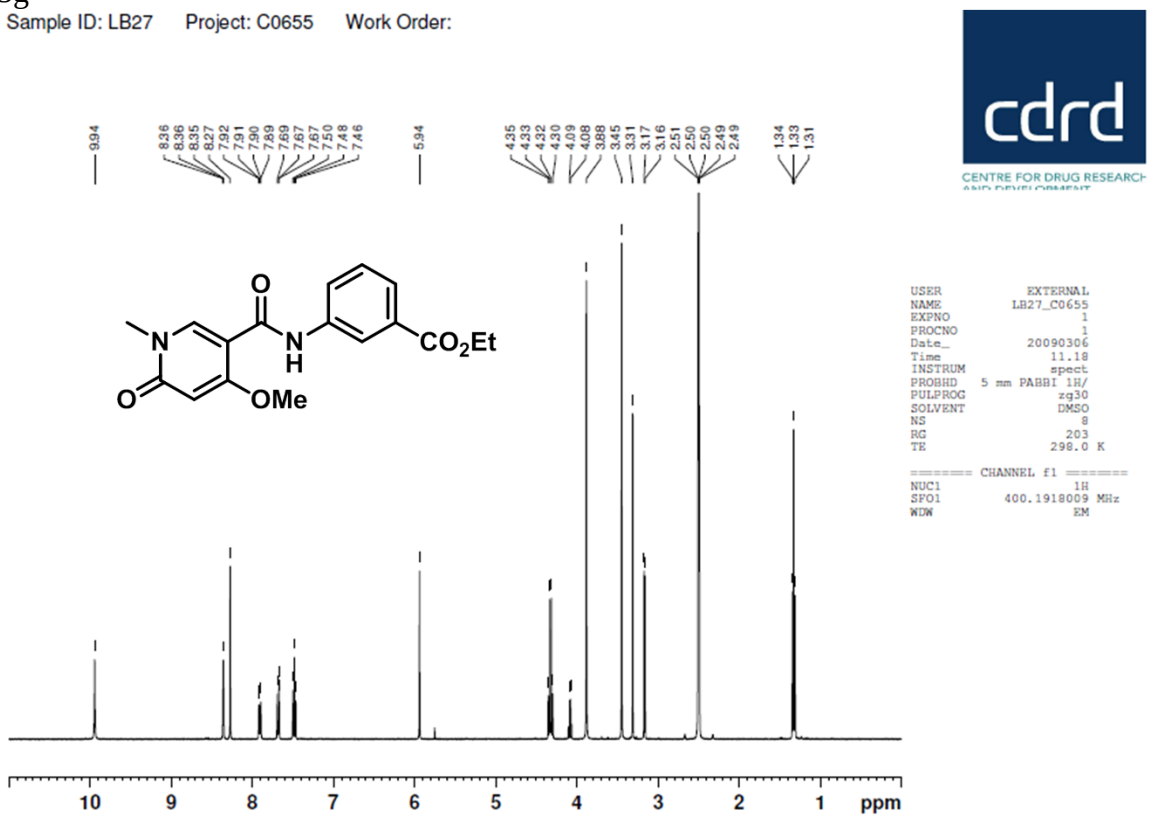
Sample ID: LB27 Project: C0655 Work Order:
CENTRE FOR DRUG RESEARCH
9.94
8.36
8.36
8.35
8.27
7.92
7.91
7.90
7.89
7.89
7.87
7.87
7.50
7.48
7.46
5.94
4.35
4.33
4.32
4.30
4.09
4.08
3.88
3.45
3.31
3.17
3.16
2.51
2.50
2.50
2.49
2.49
1.34
1.33
1.31
O
N
H
O
OMe
CO2Et
USER EXTERNAL
NAME LB27_C0655
EXPNO 1
PROCNO 1
Date_ 20090306
Time 11.18
INSTRUM spect
PROBHD 5 mm PABBI 1H/
PULPROG zg30
SOLVENT DMSO
NS 8
RG 203
TE 298.0 K
CHANNEL f1
NUC1 1H
SFO1 400.1918009 MHz
WDW EM
10 9 8 7 6 5 4 3 2 1 ppm

5h

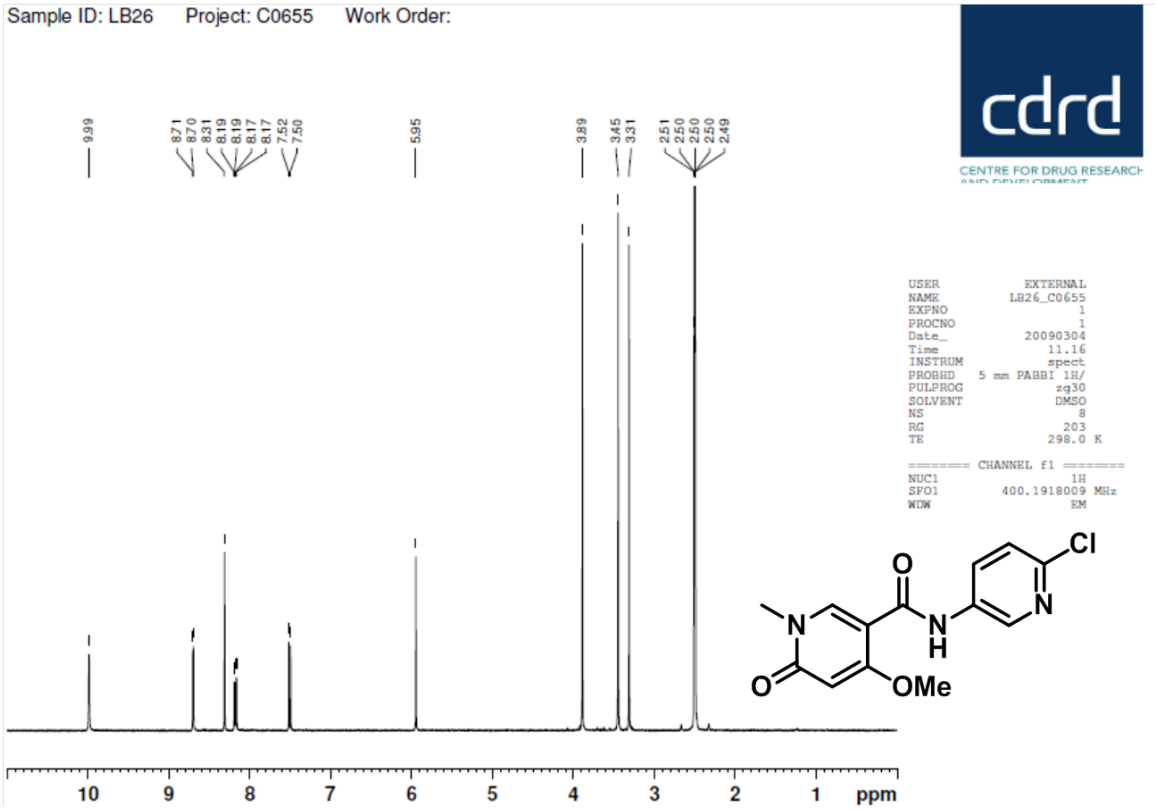
Sample ID: LB26 Project: C0655 Work Order:
cdrd
CENTRE FOR DRUG RESEARCH
9.99
8.71
8.70
8.31
8.19
8.19
8.17
8.17
7.52
7.50
5.95
3.89
3.45
3.31
2.51
2.50
2.50
2.50
2.49
USER EXTERNAL
NAME LB26_C0655
EXPNO 1
PROCNO 1
Date_ 20090304
Time 11.16
INSTRUM spect
PROBHD 5 mm PABBI 1H/
PULPROG zg30
SOLVENT DMSO
NS 8
RG 203
TE 298.0 K
CHANNEL f1
NUC1 1H
SFO1 400.1918009 MHz
WDW EM
Cl
O
N
N
H
O
OMe
10 9 8 7 6 5 4 3 2 1 ppm

5i

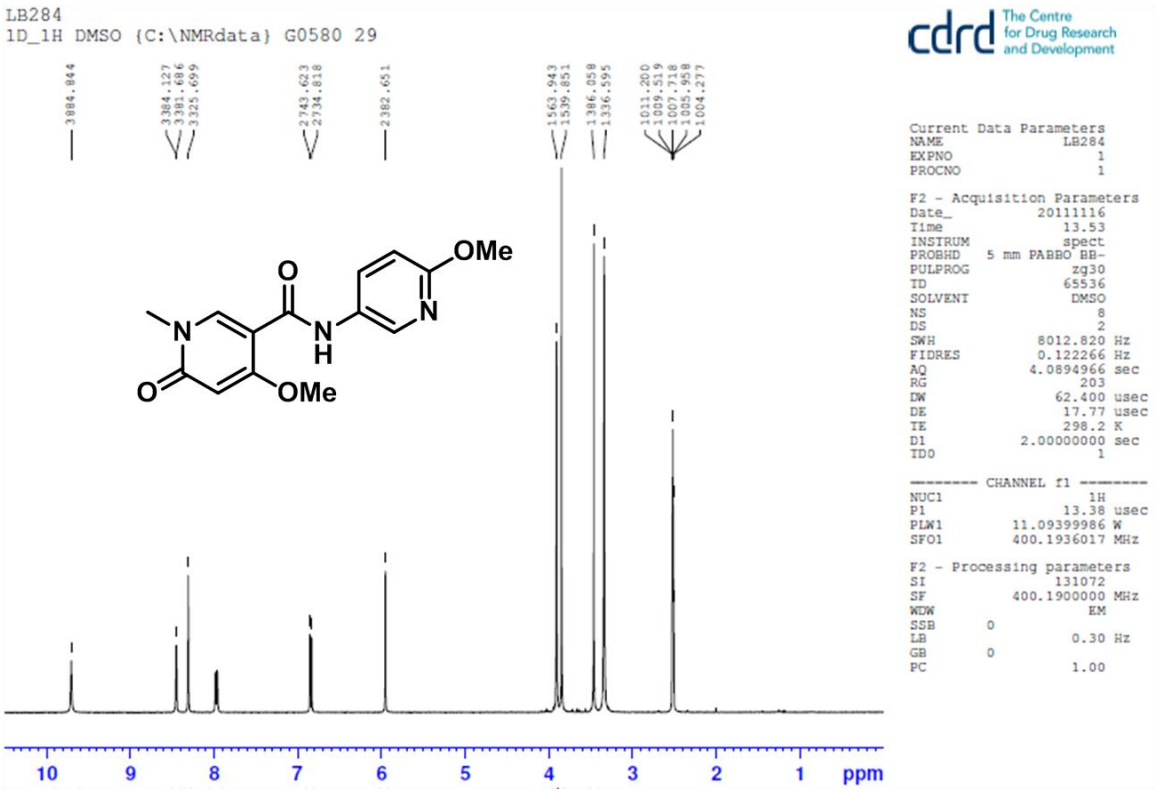
LB284
1D_1H DMSO {C:\NMRdata} G0580 29
cdrd The Centre for Drug Research and Development
8.844
8.127
8.086
8.025
7.623
7.818
7.651
6.943
6.851
6.058
5.595
1.200
1.519
1.718
1.958
1.277
OMe
O
N
N
H
O
OMe
Current Data Parameters
NAME LB284
EXPNO 1
PROCNO 1
F2 - Acquisition Parameters
Date_ 20111116
Time 13.53
INSTRUM spect
PROBHD 5 mm PABBO BB-
PULPROG zg30
TD 65536
SOLVENT DMSO
NS 8
DS 2
SWH 8012.820 Hz
FIDRES 0.122266 Hz
AQ 4.0894966 sec
RG 203
DW 62.400 usec
DE 17.77 usec
TE 298.2 K
D1 2.00000000 sec
TD0 1
CHANNEL f1
NUC1 1H
P1 13.38 usec
PLW1 11.09399986 W
SFO1 400.1936017 MHz
F2 - Processing parameters
SI 131072
SF 400.1900000 MHz
WDW EM
SSB 0
LB 0.30 Hz
GB 0
PC 1.00
10 9 8 7 6 5 4 3 2 1 ppm

5j

Sample ID: LB28 Project: C0655 Work Order:

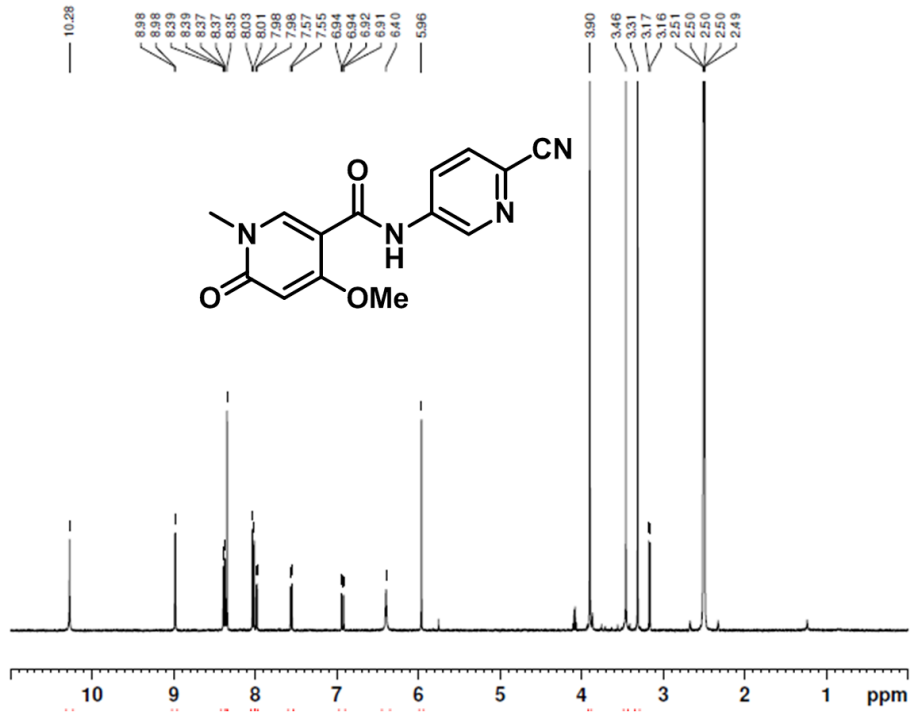


```
USER            EXTERNAL
NAME          LB28_C0655
EXPNO                  1
PROCNO                 1
Date_           20090306
Time               12.50
INSTRUM            spect
PROBHD   5 mm PABBI 1H/
PULPROG             zg30
SOLVENT             DMSO
NS                     8
RG                   203
TE                298.0 K

======= CHANNEL f1 =======
NUC1                  1H
SFO1       400.1918009 MHz
WDW                   EM
```

5k

Sample ID: LB20 Project: C0655 Work Order:

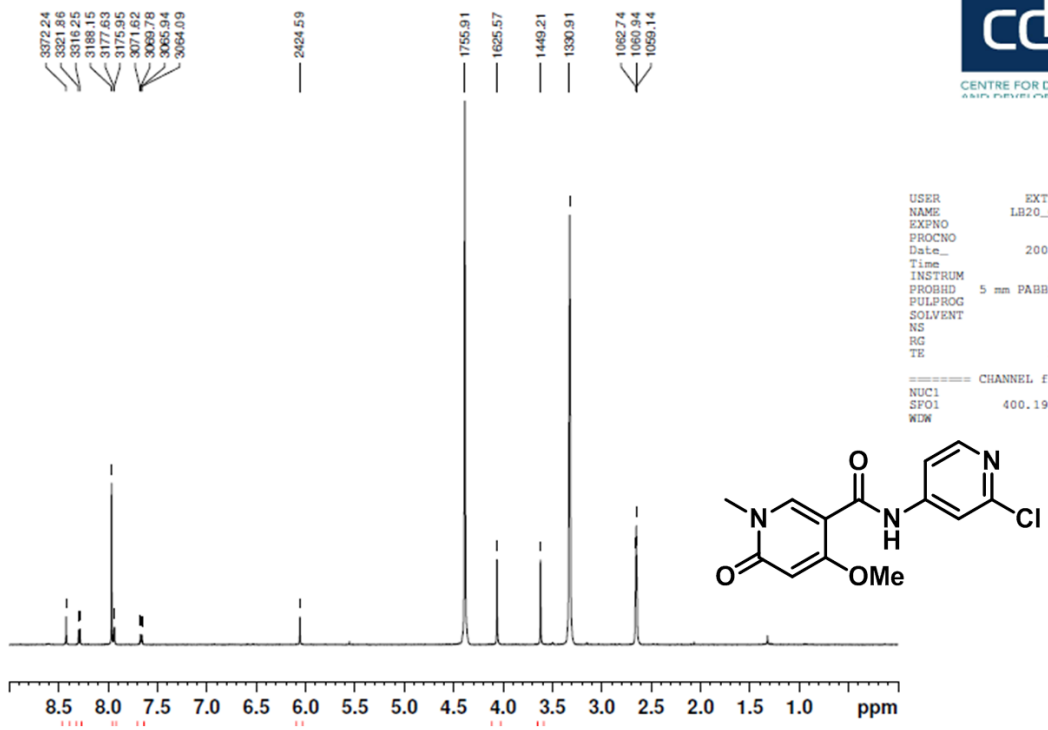


```
USER            EXTERNAL
NAME          LB20_C0655
EXPNO                  1
PROCNO                 1
Date_           20090223
Time               10.54
INSTRUM            spect
PROBHD   5 mm PABBI 1H/
PULPROG             zg30
SOLVENT             MeOD
NS                     8
RG                   203
TE                298.0 K

======= CHANNEL f1 =======
NUC1                  1H
SFO1       400.1918009 MHz
WDW                   EM
```

5l

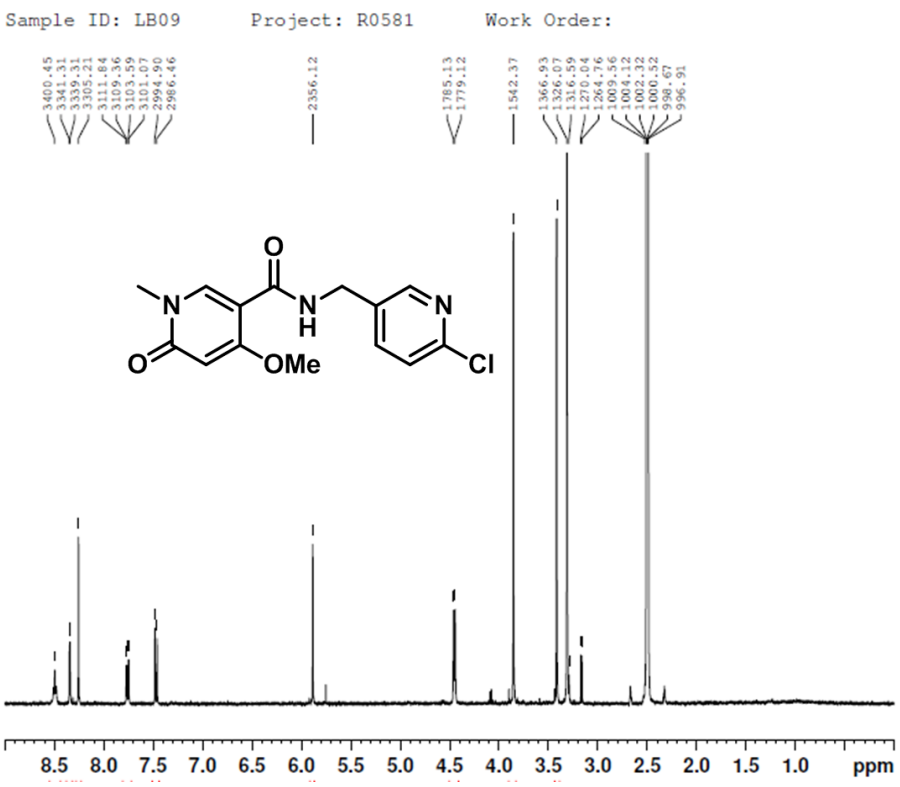

CENTRE FOR DRUG RESEARCH AND DEVELOPMENT

NAME	LB09_R0581
EXPNO	1
PROCNO	1
Date_	20090119
Time	10.32
INSTRUM	spect
PROBHD	5 mm PABBI 1H/
PULPROG	zg30
TD	65536
SOLVENT	DMSO
NS	8
DS	2
SWH	5597.015 Hz
FIDRES	0.085404 Hz
AQ	5.8545995 sec
RG	203
DW	89.333 usec
DE	6.00 usec
TE	298.0 K
D1	2.00000000 sec
TD0	1
-------- CHANNEL f1 --------	
NUC1	1H
P1	8.18 usec
PL1	0.00 dB
PL1W	9.01767254 W
SFO1	400.1918009 MHz
SI	131072
SF	400.1900011 MHz
WDW	EM
SSB	0
LB	0.30 Hz
GB	0
PC	1.00

5m

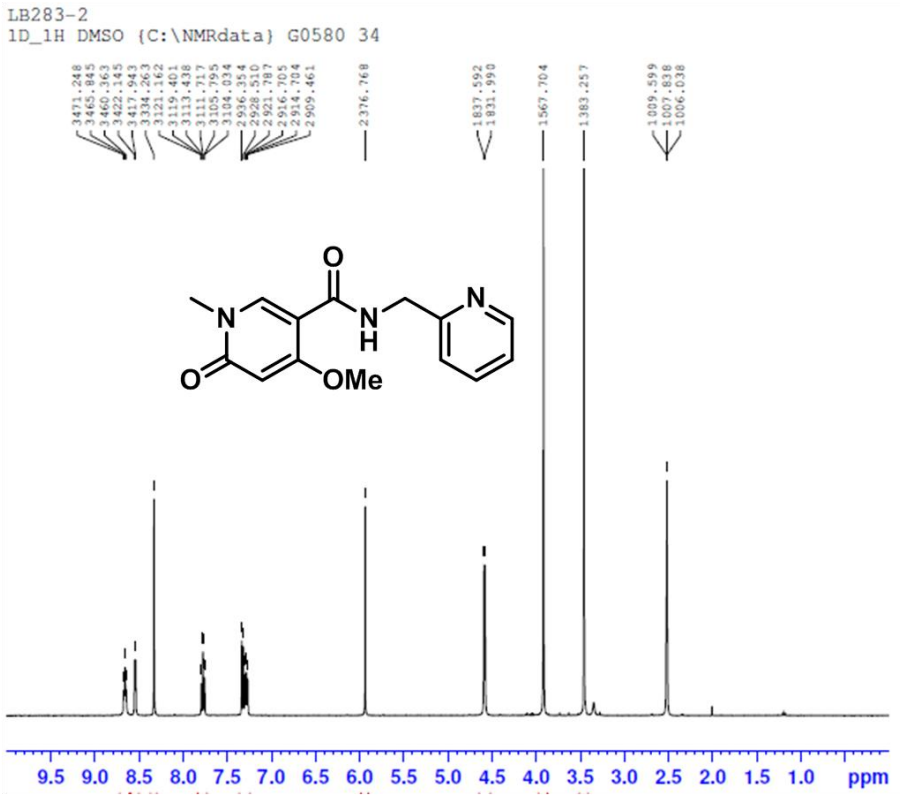

cdrd The Centre for Drug Research and Development

Current Data Parameters	
NAME	LB283-2
EXPNO	1
PROCNO	1
F2 - Acquisition Parameters	
Date_	20111125
Time	15.58
INSTRUM	spect
PROBHD	5 mm PABBO BB-
PULPROG	zg30
TD	65536
SOLVENT	DMSO
NS	8
DS	2
SWH	8012.820 Hz
FIDRES	0.122266 Hz
AQ	4.0894966 sec
RG	203
DW	62.400 usec
DE	17.77 usec
TE	298.2 K
D1	2.00000000 sec
TD0	1
-------- CHANNEL f1 --------	
NUC1	1H
P1	13.38 usec
PLW1	11.09399986 W
SFO1	400.1936017 MHz
F2 - Processing parameters	
SI	131072
SF	400.1900000 MHz
WDW	EM
SSB	0
LB	0.30 Hz
GB	0
PC	1.00

5n

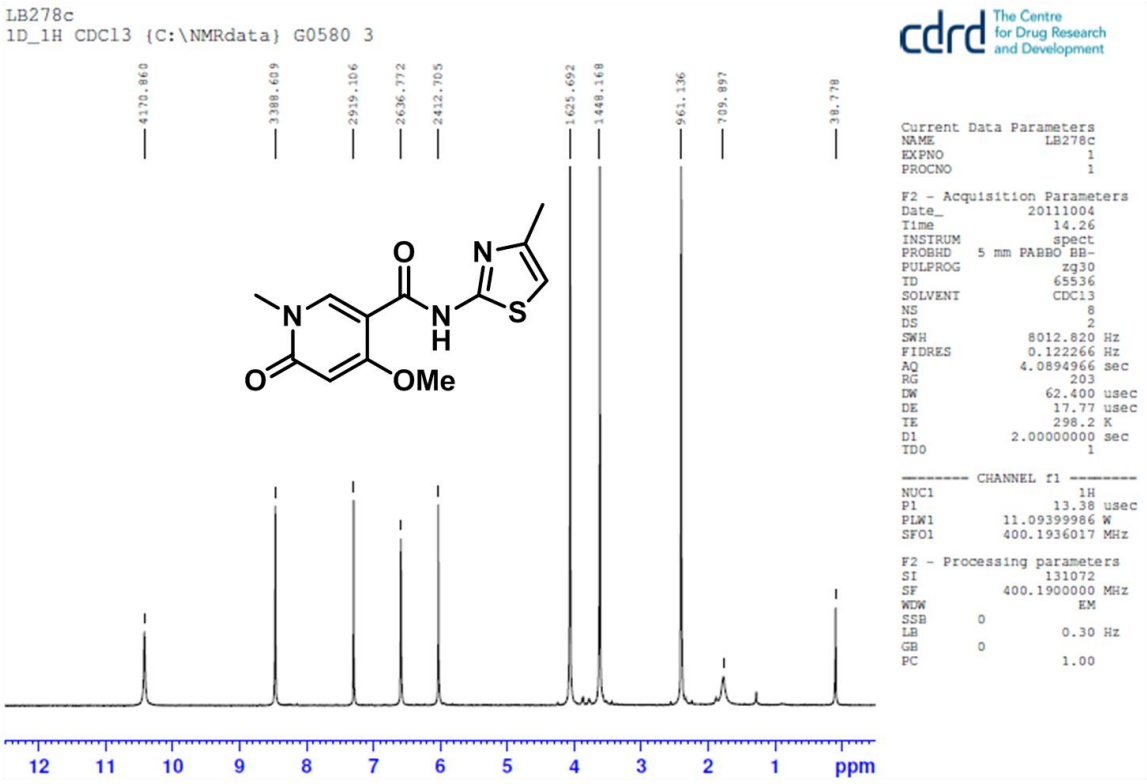
LB278c
1D_1H CDCl3 (C:\NMRdata) G0580 3
4170.860
3388.609
2919.106
2636.772
2412.705
1625.692
1448.168
961.136
709.897
38.778
O
N
N
H
S
O
OMe
12
11
10
9
8
7
6
5
4
3
2
1
ppm
The Centre for Drug Research and Development
Current Data Parameters
NAME LB278c
EXPNO 1
PROCNO 1
F2 - Acquisition Parameters
Date_ 20111004
Time 14.26
INSTRUM spect
PROBHD 5 mm PABBO BB-
PULPROG zg30
TD 65536
SOLVENT CDCl3
NS 8
DS 2
SWH 8012.820 Hz
FIDRES 0.122266 Hz
AQ 4.0894966 sec
RG 203
DW 62.400 usec
DE 17.77 usec
TE 298.2 K
D1 2.00000000 sec
TD0 1
CHANNEL f1
NUC1 1H
P1 13.38 usec
PLW1 11.09399986 W
SFO1 400.1936017 MHz
F2 - Processing parameters
SI 131072
SF 400.1900000 MHz
WDW EM
SSB 0
LB 0.30 Hz
GB 0
PC 1.00

5o

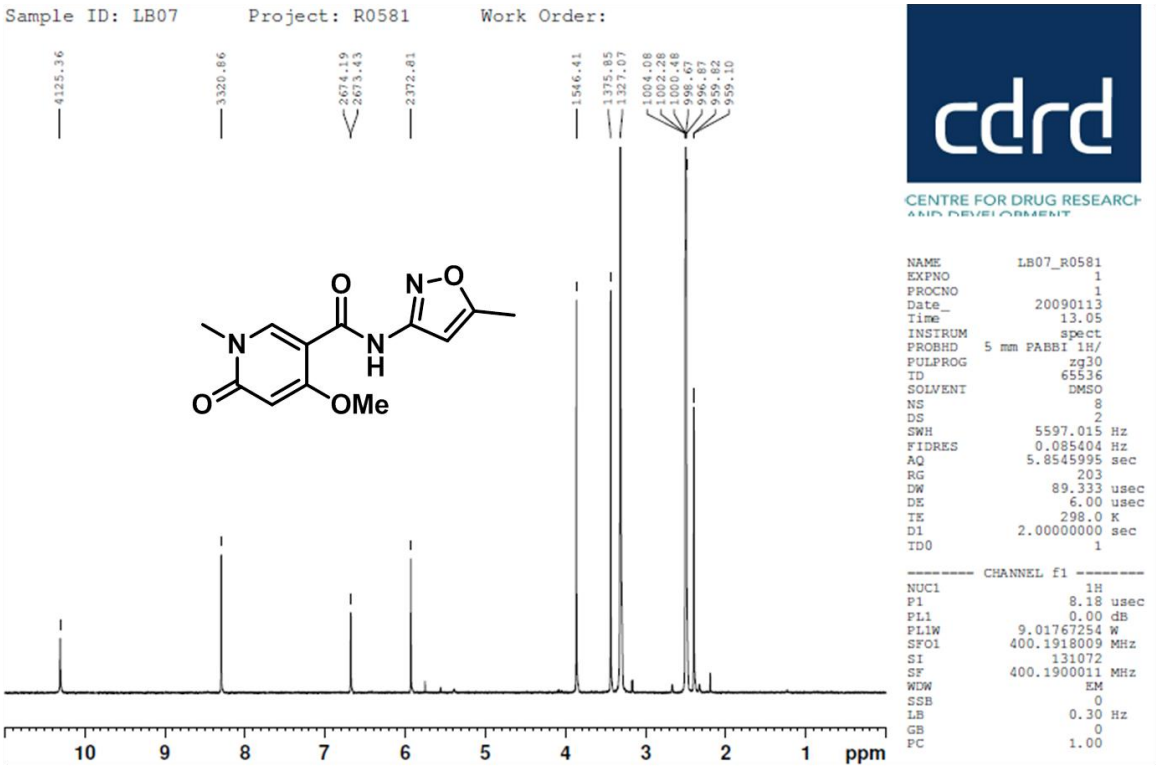
Sample ID: LB07
Project: R0581
Work Order:
4125.36
3320.86
2674.19
2673.43
2372.81
1546.41
1375.85
1327.07
1004.08
1002.28
1000.48
998.67
996.87
996.82
959.10
O
N
O
N
H
O
OMe
10
9
8
7
6
5
4
3
2
1
ppm
CENTRE FOR DRUG RESEARCH
NAME LB07_R0581
EXPNO 1
PROCNO 1
Date_ 20090113
Time 13.05
INSTRUM spect
PROBHD 5 mm PABBI 1H/
PULPROG zg30
TD 65536
SOLVENT DMSO
NS 8
DS 2
SWH 5597.015 Hz
FIDRES 0.085404 Hz
AQ 5.8545995 sec
RG 203
DW 89.333 usec
DE 6.00 usec
TE 298.0 K
D1 2.00000000 sec
TD0 1
CHANNEL f1
NUC1 1H
P1 8.18 usec
PL1 0.00 dB
PL1W 9.01767254 W
SFO1 400.1918009 MHz
SI 131072
SF 400.1900011 MHz
WDW EM
SSB 0
LB 0.30 Hz
GB 0
PC 1.00

5p

Sample ID: LB41 Project: C0655 Work Order:

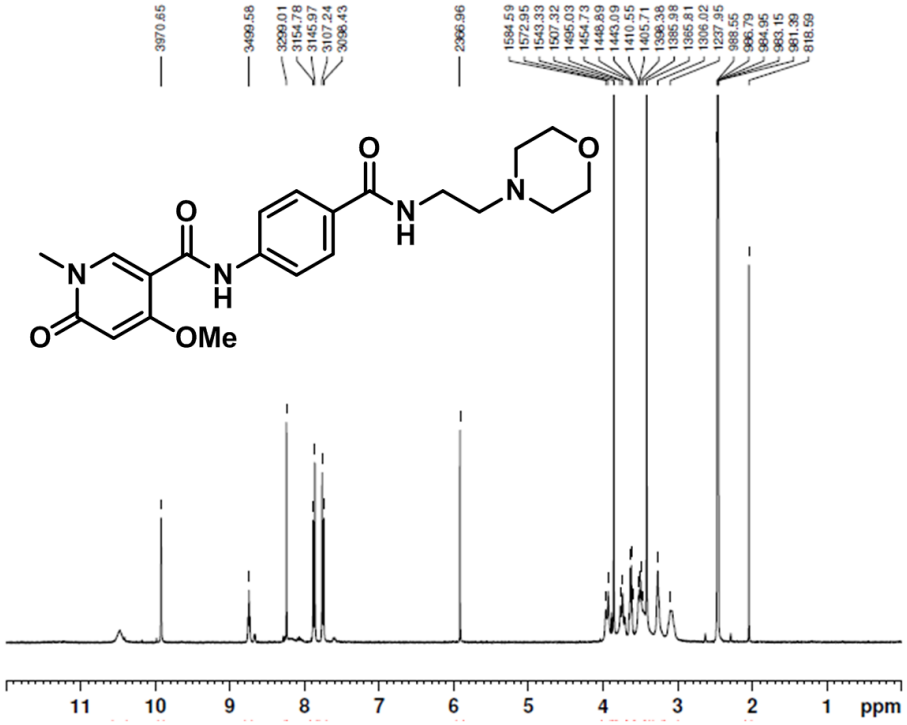


```
USER            EXTERNAL
NAME          LB41_C0655
EXPNO                  1
PROCNO                 1
Date_           20090423
Time               16.33
INSTRUM            spect
PROBHD   5 mm PABBI 1H/
PULPROG             zg30
SOLVENT             DMSO
NS                     8
RG                   203
TE                298.0 K

======= CHANNEL f1 =======
NUC1                1H
SFO1     400.1936017 MHz
WDW                 EM
```

5q

Sample ID: LB46 Project: C0655 Work Order:

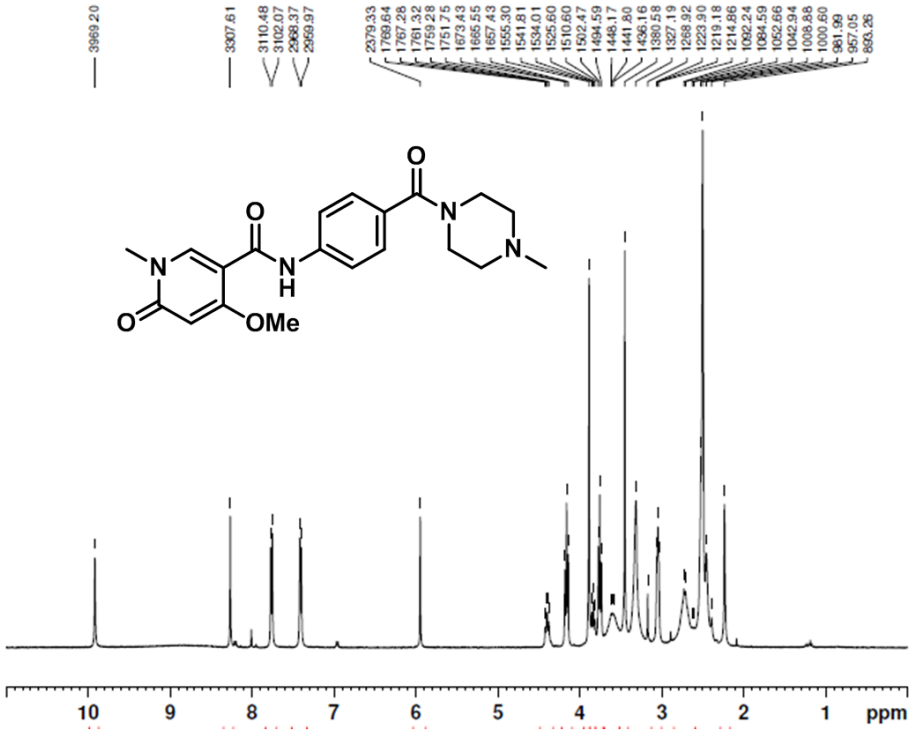


```
USER                C0655
NAME                LB46
EXPNO                  2
PROCNO                 1
Date_           20090522
Time               10.24
INSTRUM            spect
PROBHD   5 mm PABBI 1H/
PULPROG             zg30
SOLVENT             DMSO
NS                     8
RG                   203
TE                299.2 K

======= CHANNEL f1 =======
NUC1                1H
SFO1     400.1936017 MHz
WDW                 EM
```

6a

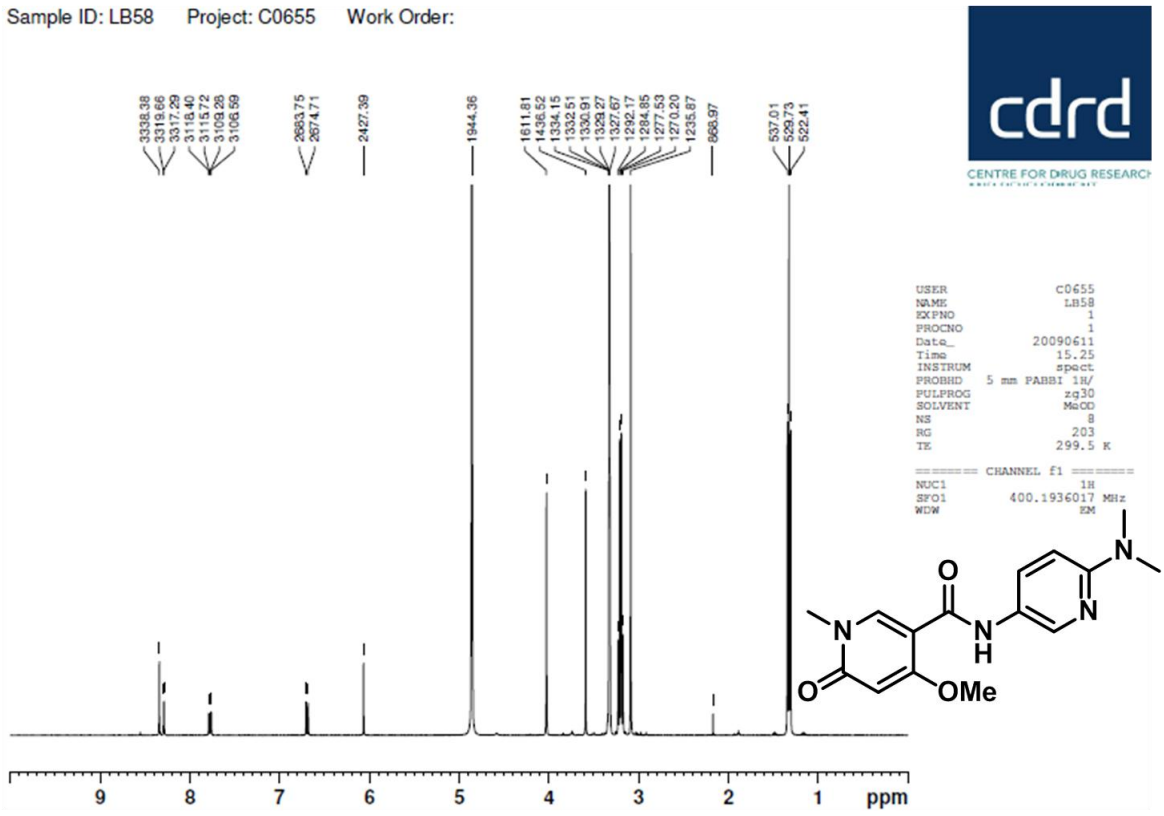
Sample ID: LB58 Project: C0655 Work Order:
3338.38
3319.66
3317.29
3116.40
3115.72
3109.28
3106.59
2683.75
2674.71
2427.39
1944.36
1611.81
1436.52
1334.15
1332.51
1330.91
1329.27
1327.67
1292.17
1284.85
1277.53
1270.20
1235.87
868.97
537.01
529.73
522.41
USER C0655
NAME LB58
EXPNO 1
PROCNO 1
Date_ 20090611
Time 15.25
INSTRUM spect
PROBHD 5 mm PABBI 1H/
PULPROG zg30
SOLVENT MeOD
NS 8
RG 203
TE 299.5 K
CHANNEL f1
NUC1 1H
SFO1 400.1936017 MHz
WDW EM
CENTRE FOR DRUG RESEARCH
9 8 7 6 5 4 3 2 1 ppm

6b

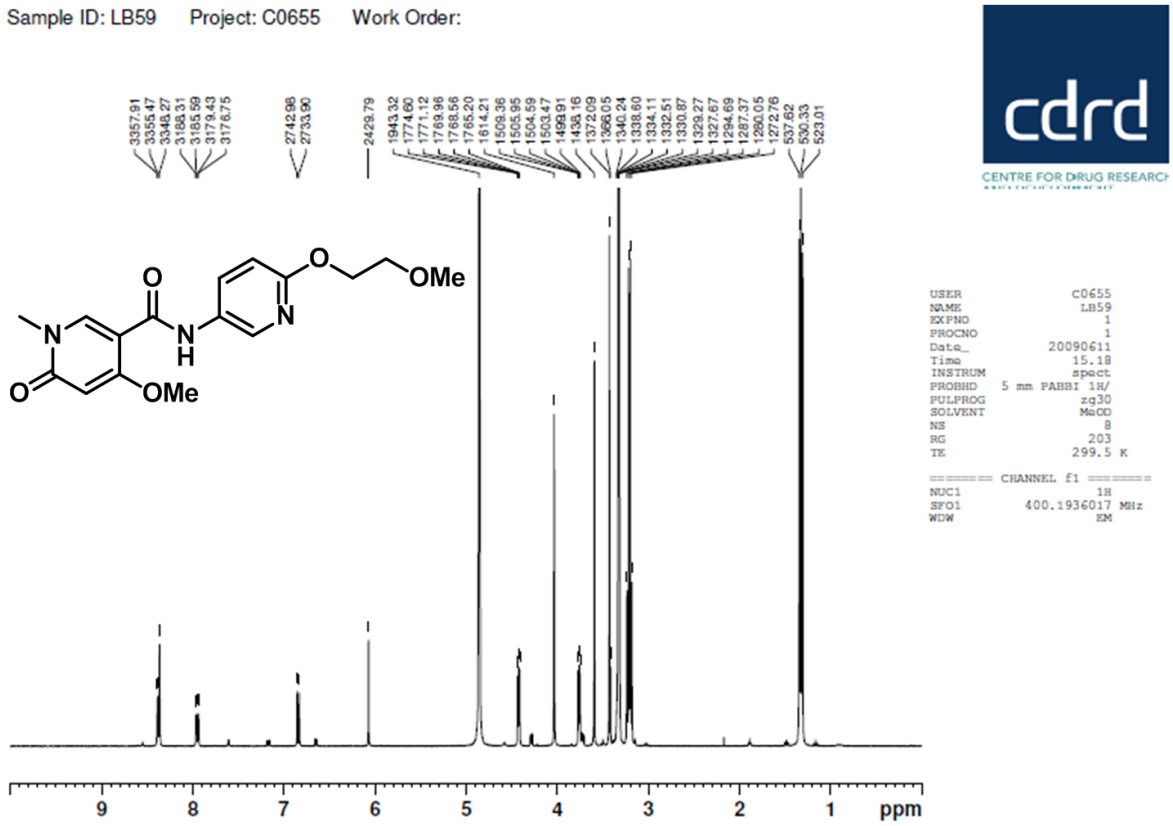
Sample ID: LB59 Project: C0655 Work Order:
3357.91
3355.47
3348.27
3188.31
3185.59
3179.43
3176.75
2742.98
2733.90
2429.79
1943.32
1774.60
1771.12
1769.96
1768.56
1765.20
1614.21
1509.36
1505.95
1504.59
1503.47
1499.91
1438.16
1372.09
1366.05
1340.24
1338.60
1334.11
1332.51
1330.87
1329.27
1327.67
1294.69
1287.37
1280.05
1272.76
537.62
530.33
523.01
USER C0655
NAME LB59
EXPNO 1
PROCNO 1
Date_ 20090611
Time 15.18
INSTRUM spect
PROBHD 5 mm PABBI 1H/
PULPROG zg30
SOLVENT MeOD
NS 8
RG 203
TE 299.5 K
CHANNEL f1
NUC1 1H
SFO1 400.1936017 MHz
WDW EM
CENTRE FOR DRUG RESEARCH
9 8 7 6 5 4 3 2 1 ppm

6c

Sample ID: LB45 Project: C0655 Work Order:
precipitate visible

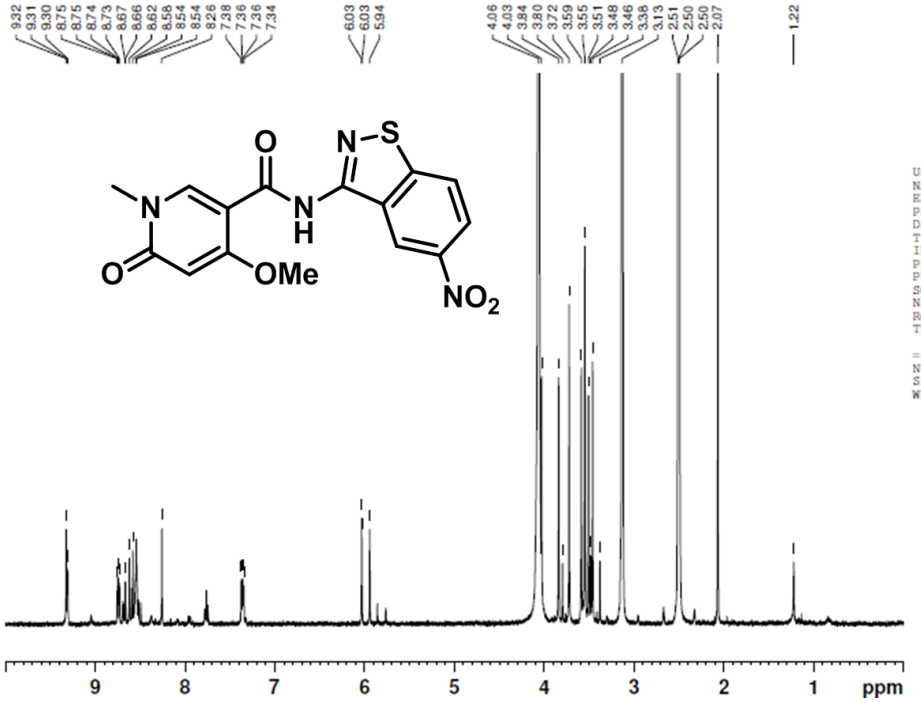

USER	C0655
NAME	LB47
EXPNO	1
PROCNO	1
Date_	20090514
Time	14.00
INSTRUM	spect
PROBHD	5 mm PABBI 1H/
PULPROG	zg30
SOLVENT	DMSO
NS	8
RG	203
TE	298.6 K
======= CHANNEL f1 =======	
NUC1	1H
SFO1	400.1936017 MHz
WDW	EM

6d

Sample ID: LB37 Project: C0655 Work Order:

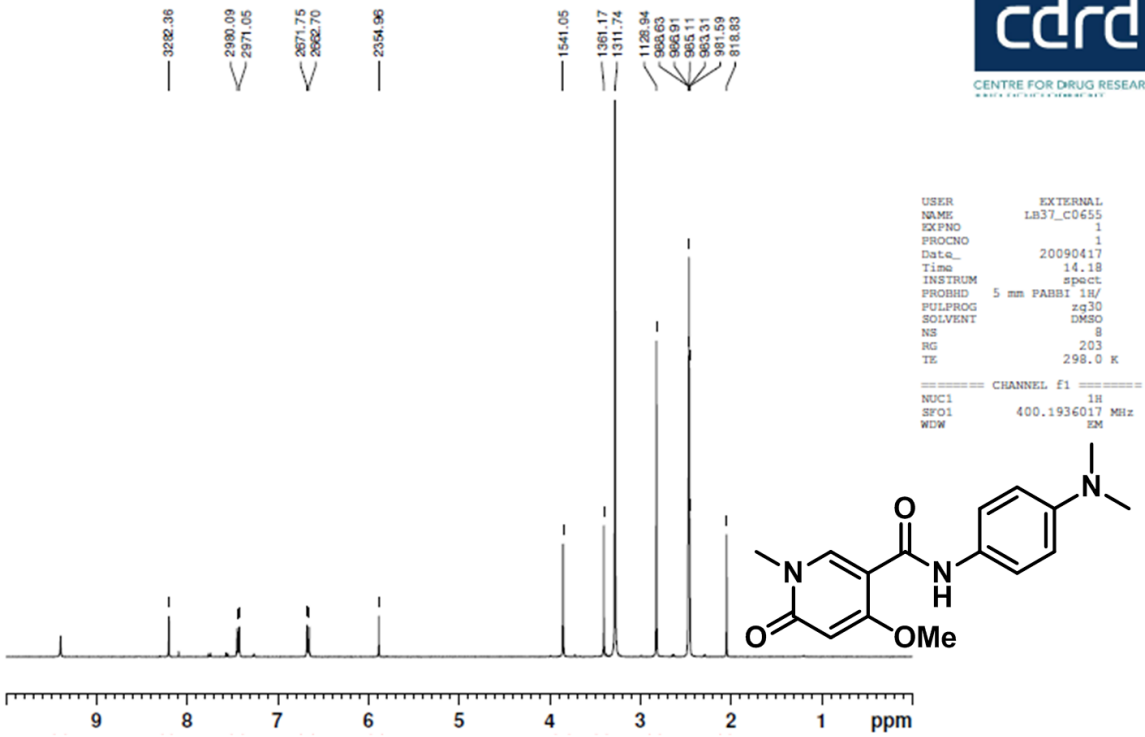

USER	EXTERNAL
NAME	LB37_C0655
EXPNO	1
PROCNO	1
Date_	20090417
Time	14.18
INSTRUM	spect
PROBHD	5 mm PABBI 1H/
PULPROG	zg30
SOLVENT	DMSO
NS	8
RG	203
TE	298.0 K
======= CHANNEL f1 =======	
NUC1	1H
SFO1	400.1936017 MHz
WDW	EM

6e

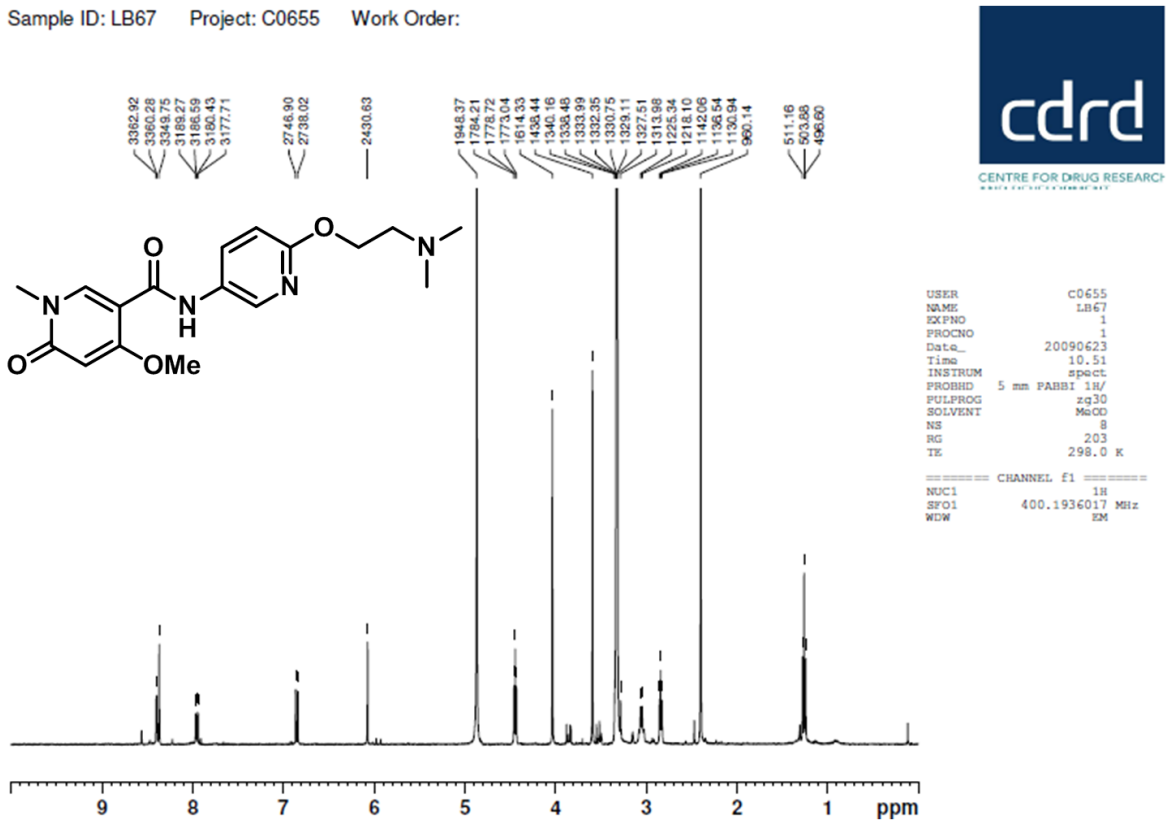
Sample ID: LB67 Project: C0655 Work Order:
3362.92
3360.28
3349.75
3189.27
3186.59
3180.43
3177.71
2746.90
2738.02
2430.63
1948.37
1784.21
1778.72
1773.04
1614.33
1438.44
1340.16
1336.48
1333.99
1332.35
1330.75
1329.11
1327.51
1313.98
1225.34
1218.10
1142.06
1136.54
1130.94
960.14
511.16
503.88
496.60
O
N
H
N
O
N
O
OMe
USER C0655
NAME LB67
EXPNO 1
PROCNO 1
Date_ 20090623
Time 10.51
INSTRUM spect
PROBHD 5 mm PABBI 1H/
PULPROG zg30
SOLVENT MeOD
NS 8
RG 203
TE 298.0 K
CHANNEL f1
NUC1 1H
SFO1 400.1936017 MHz
WDW EM
9
8
7
6
5
4
3
2
1
ppm

6f

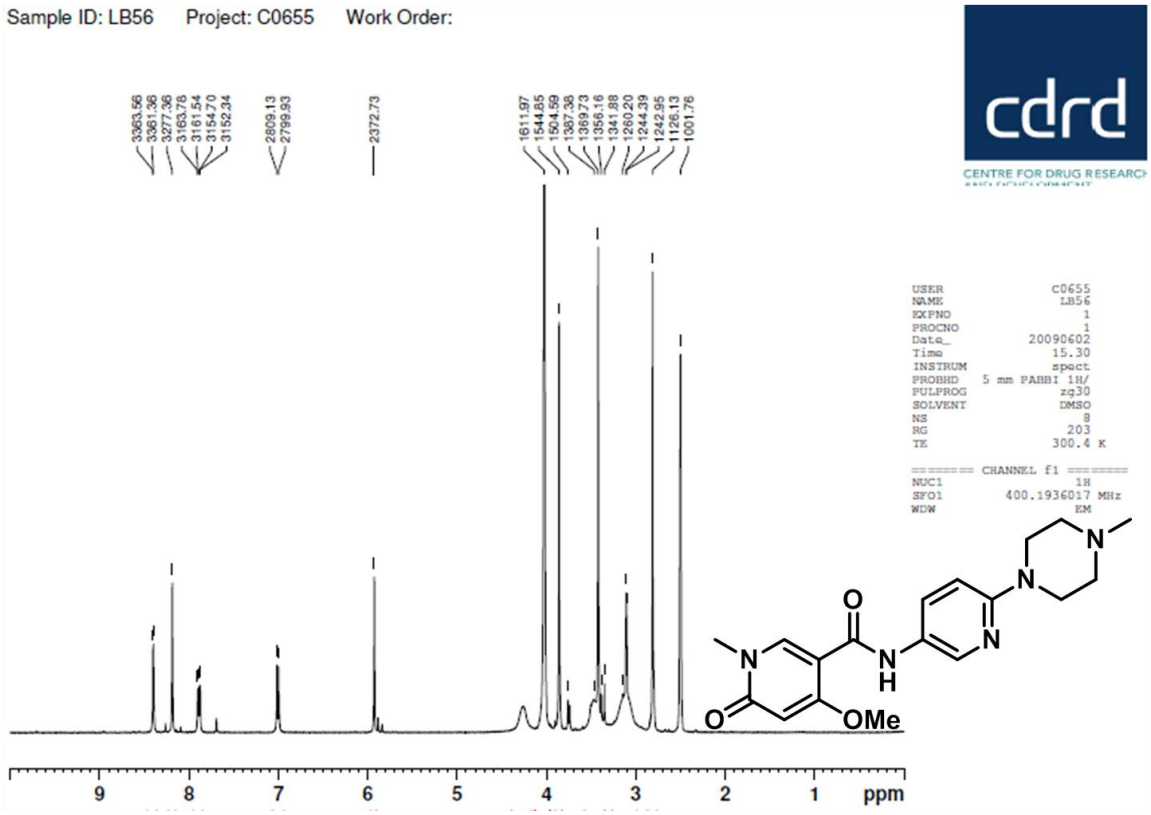
Sample ID: LB56 Project: C0655 Work Order:
3363.56
3361.36
3277.36
3163.78
3161.54
3154.70
3152.34
2809.13
2799.93
2372.73
1611.97
1544.85
1504.59
1387.38
1369.73
1356.16
1341.88
1260.20
1244.39
1242.95
1126.13
1001.76
O
N
H
N
N
N
O
OMe
USER C0655
NAME LB56
EXPNO 1
PROCNO 1
Date_ 20090602
Time 15.30
INSTRUM spect
PROBHD 5 mm PABBI 1H/
PULPROG zg30
SOLVENT DMSO
NS 8
RG 203
TE 300.4 K
CHANNEL f1
NUC1 1H
SFO1 400.1936017 MHz
WDW EM
9
8
7
6
5
4
3
2
1
ppm

6g

Sample ID: LB72 Project: C0655 Req#: N09–0039

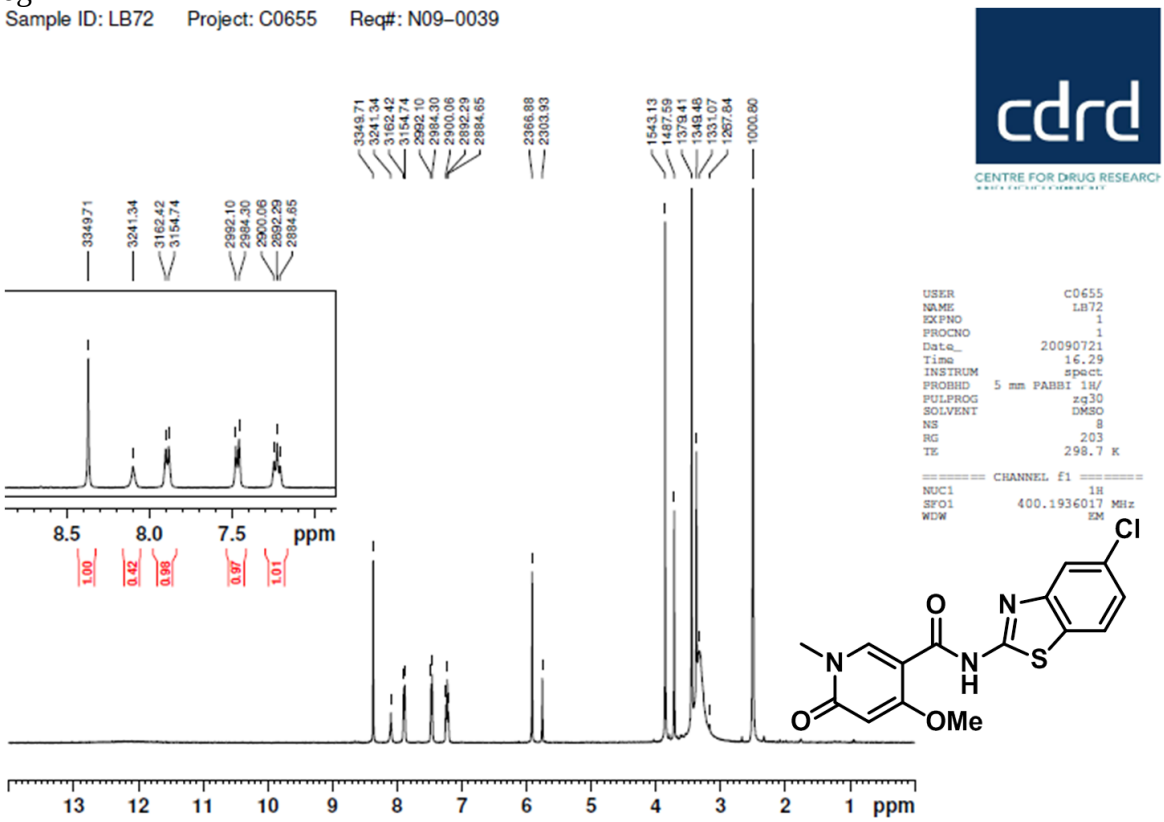

6h

Sample ID: LB70b Project: C0655 Req#: N09–0040
precipitation visible!

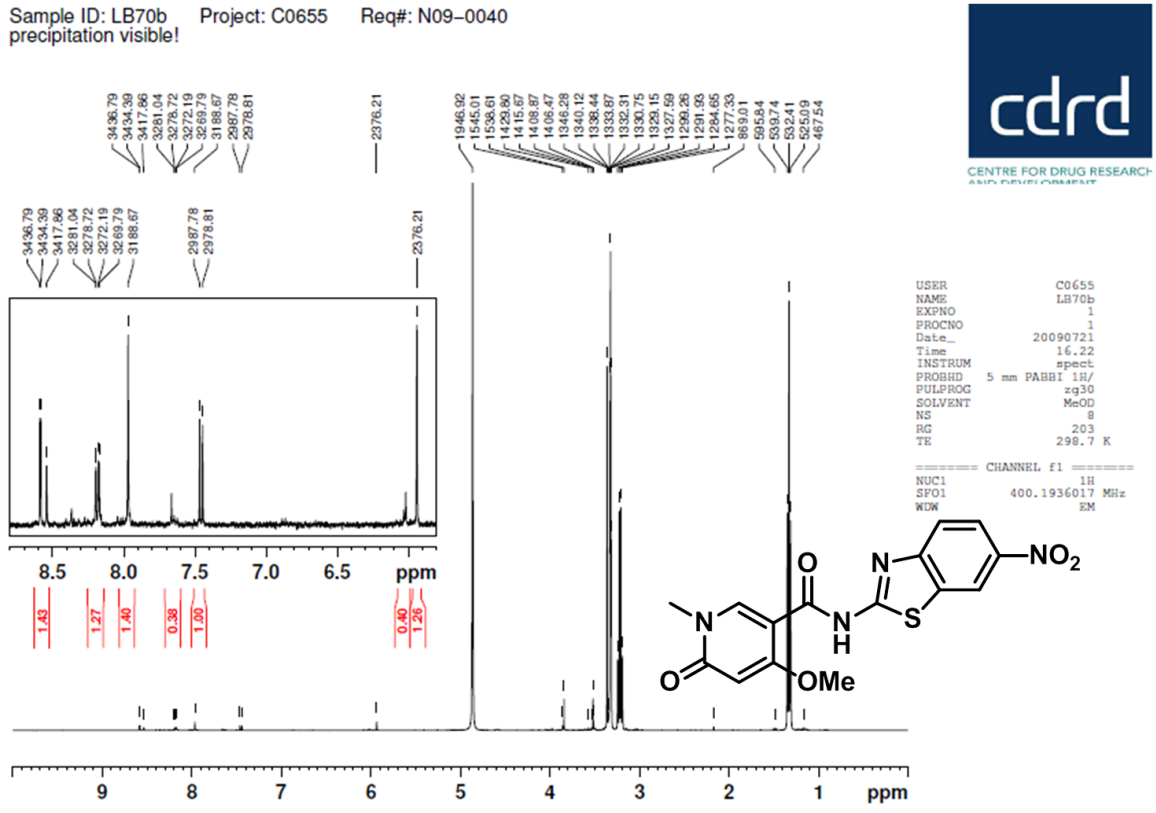

6i

Sample ID: LB38b Project: C0655 Work Order:

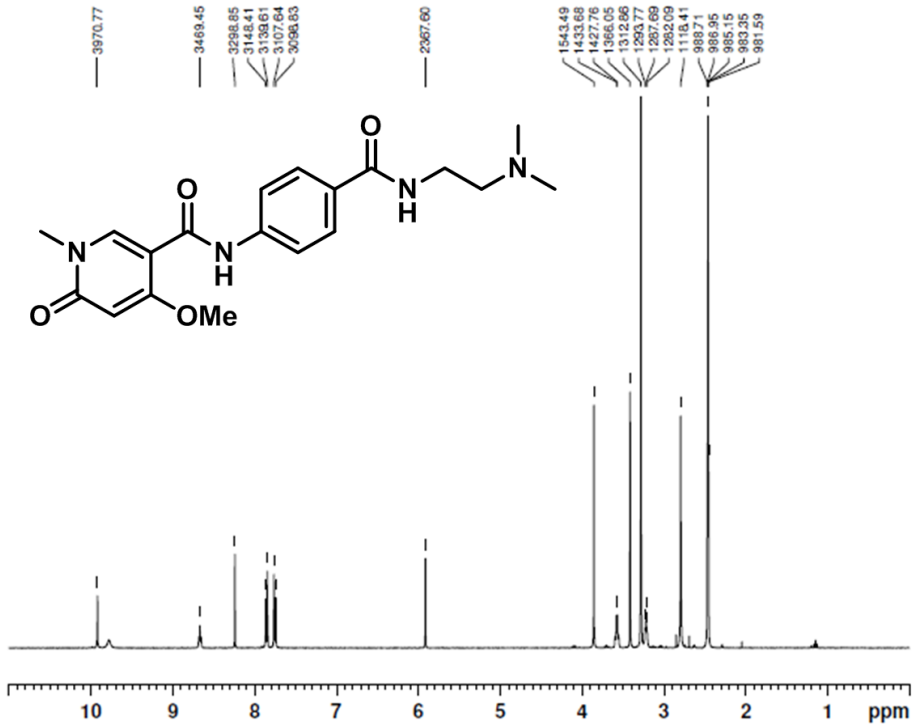


```
USER            EXTERNAL
NAME         LB38b_C0655
EXPNO                  1
PROCNO                 1
Date_           20090423
Time               16.39
INSTRUM            spect
PROBHD   5 mm PABBI 1H/
PULPROG             zg30
SOLVENT             DMSO
NS                     8
RG                   203
TE                298.0 K

======== CHANNEL f1 ========
NUC1                 1H
SFO1      400.1936017 MHz
WDW                  EM
```

7

ClEt-D
1D_1H DMSO {C:\NMRdata} G0580 34

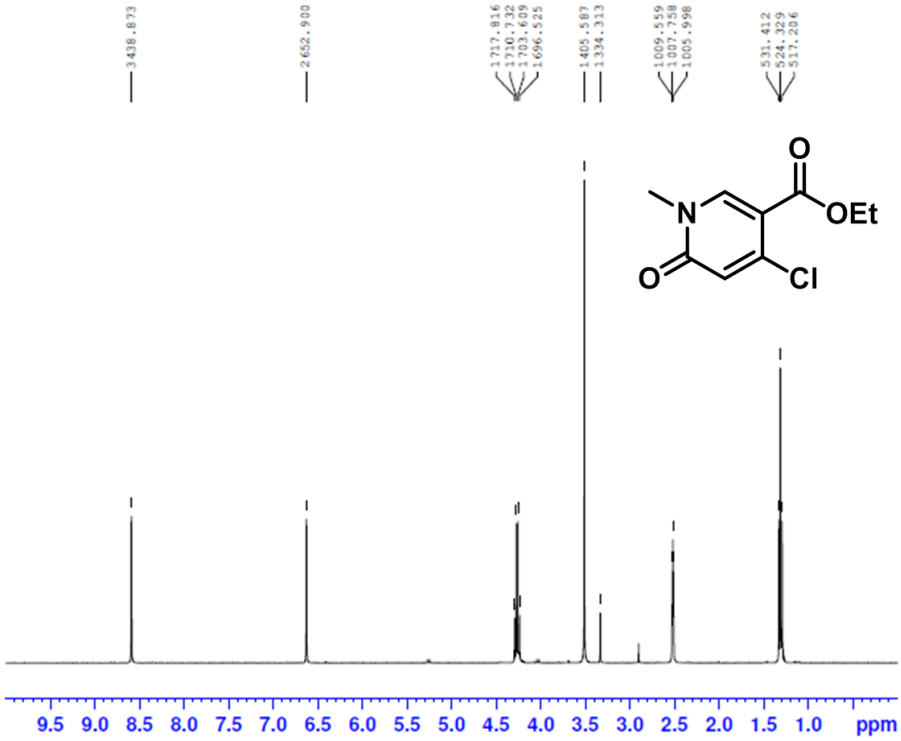


```
Current Data Parameters
NAME                 ClEt-D
EXPNO                     1
PROCNO                    1

F2 - Acquisition Parameters
Date_             20111209
Time                 16.16
INSTRUM              spect
PROBHD    5 mm PABBO BB-
PULPROG               zg30
TD                   65536
SOLVENT               DMSO
NS                       8
DS                       2
SWH               8012.820 Hz
FIDRES            0.122266 Hz
AQ                4.0894966 sec
RG                     203
DW                  62.400 usec
DE                  17.77 usec
TE                  298.2 K
D1               2.00000000 sec
TD0                      1

======== CHANNEL f1 ========
NUC1                   1H
P1                  13.38 usec
PLW1           11.09399986 W
SFO1           400.1936017 MHz

F2 - Processing parameters
SI                   131072
SF             400.1900000 MHz
WDW                    EM
SSB          0
LB                  0.30 Hz
GB           0
PC                  1.00
```

8

Sample ID: LBbs Project: G0580 Req#: N10–0522

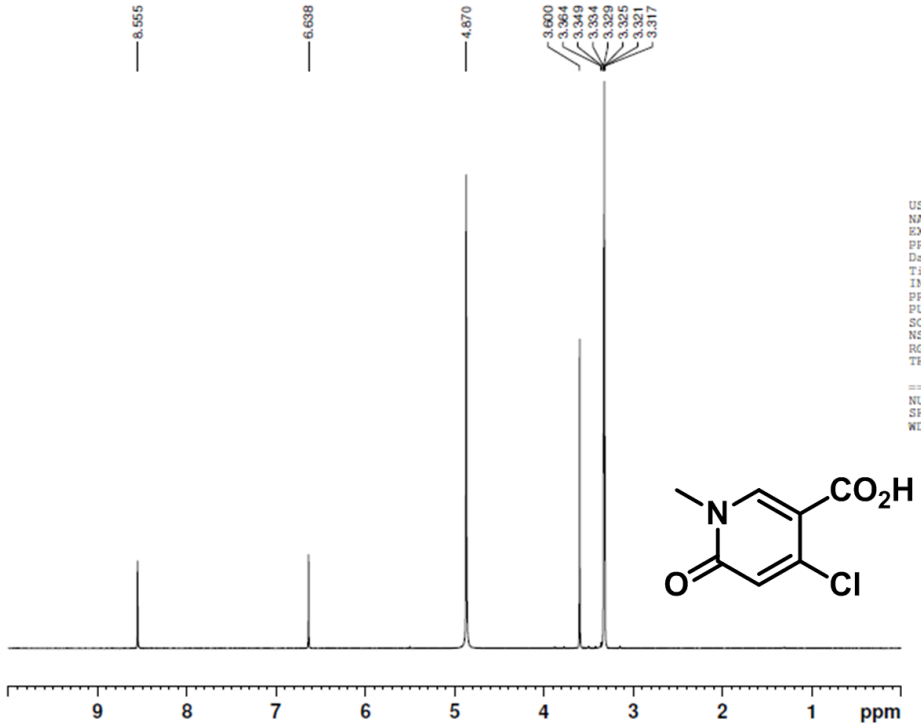

USER	G0580
NAME	LBbs
EXPNO	1
PROCNO	1
Date_	20101112
Time	13.52
INSTRUM	spect
PROBHD	5 mm PABBI 1H/
PULPROG	zg30
SOLVENT	MeOD
NS	8
RG	203
TE	298.2 K
======= CHANNEL f1 =======	
NUC1	1H
SFO1	400.1936017 MHz
WDW	EM

9

Sample ID: LB43 Project: C0655 Work Order:

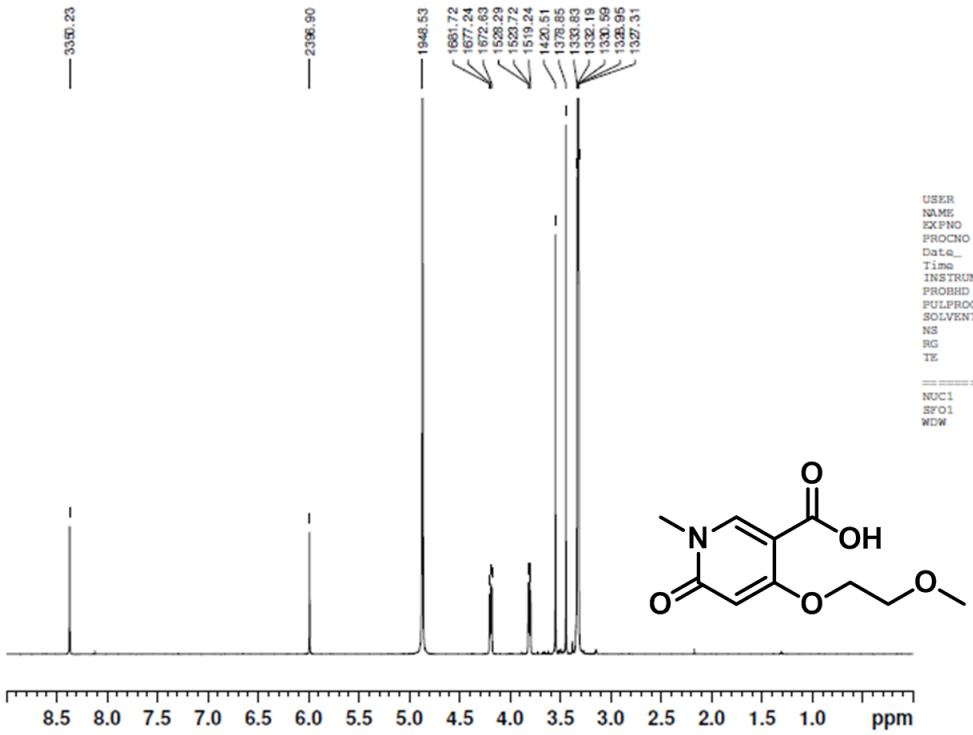

USER	C0655
NAME	LB43
EXPNO	1
PROCNO	1
Date_	20090501
Time	12.22
INSTRUM	spect
PROBHD	5 mm PABBI 1H/
PULPROG	zg30
SOLVENT	MeOD
NS	8
RG	203
TE	298.0 K
======= CHANNEL f1 =======	
NUC1	1H
SFO1	400.1936017 MHz
WDW	EM

10a

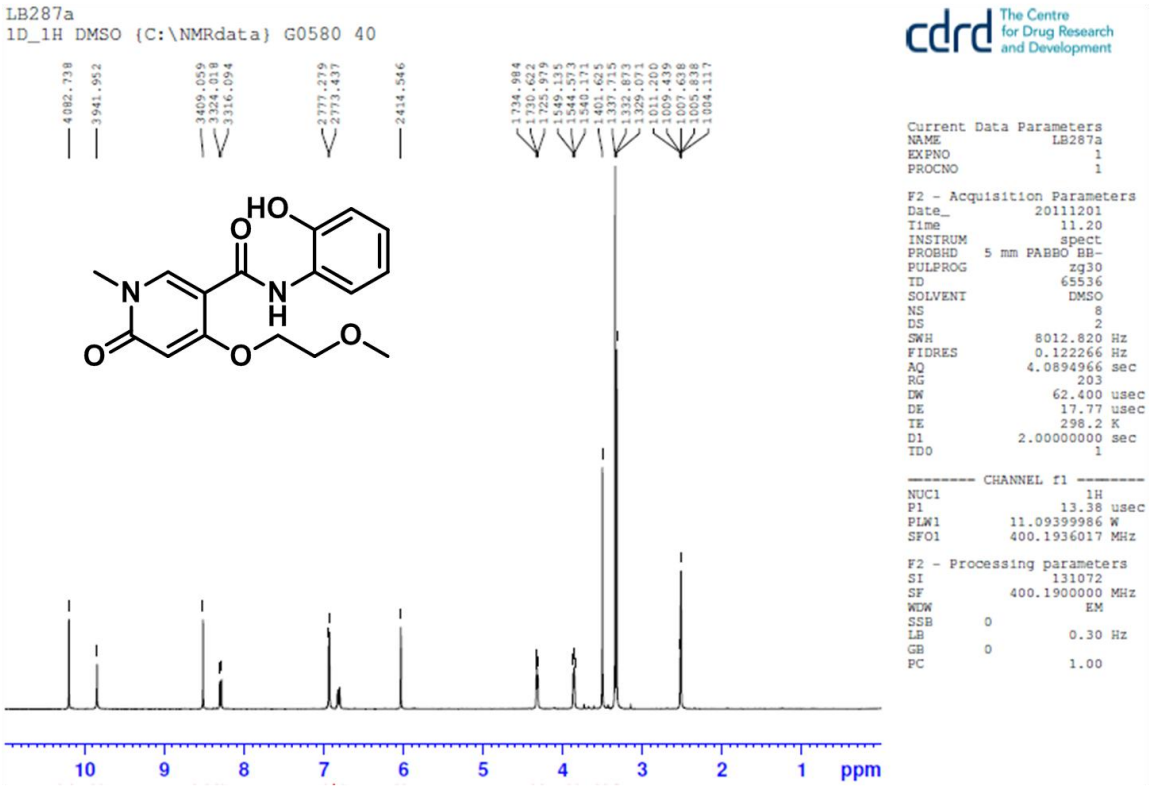
LB287a
1D_1H DMSO {C:\NMRdata} G0580 40
4082.738
3941.952
3409.059
3324.018
3316.094
2777.279
2773.437
2414.546
1734.984
1730.622
1725.979
1549.135
1544.573
1540.171
1401.625
1337.715
1332.873
1329.071
1011.200
1009.439
1007.638
1005.838
1004.117
HO
O
N
H
N
O
O
O
The Centre for Drug Research and Development
Current Data Parameters
NAME LB287a
EXPNO 1
PROCNO 1
F2 - Acquisition Parameters
Date_ 20111201
Time 11.20
INSTRUM spect
PROBHD 5 mm PABBO BB-
PULPROG zg30
TD 65536
SOLVENT DMSO
NS 8
DS 2
SWH 8012.820 Hz
FIDRES 0.122266 Hz
AQ 4.0894966 sec
RG 203
DW 62.400 usec
DE 17.77 usec
TE 298.2 K
D1 2.00000000 sec
TD0 1
CHANNEL f1
NUC1 1H
P1 13.38 usec
PLW1 11.09399986 W
SFO1 400.1936017 MHz
F2 - Processing parameters
SI 131072
SF 400.1900000 MHz
WDW EM
SSB 0
LB 0.30 Hz
GB 0
PC 1.00
10 9 8 7 6 5 4 3 2 1 ppm

10b

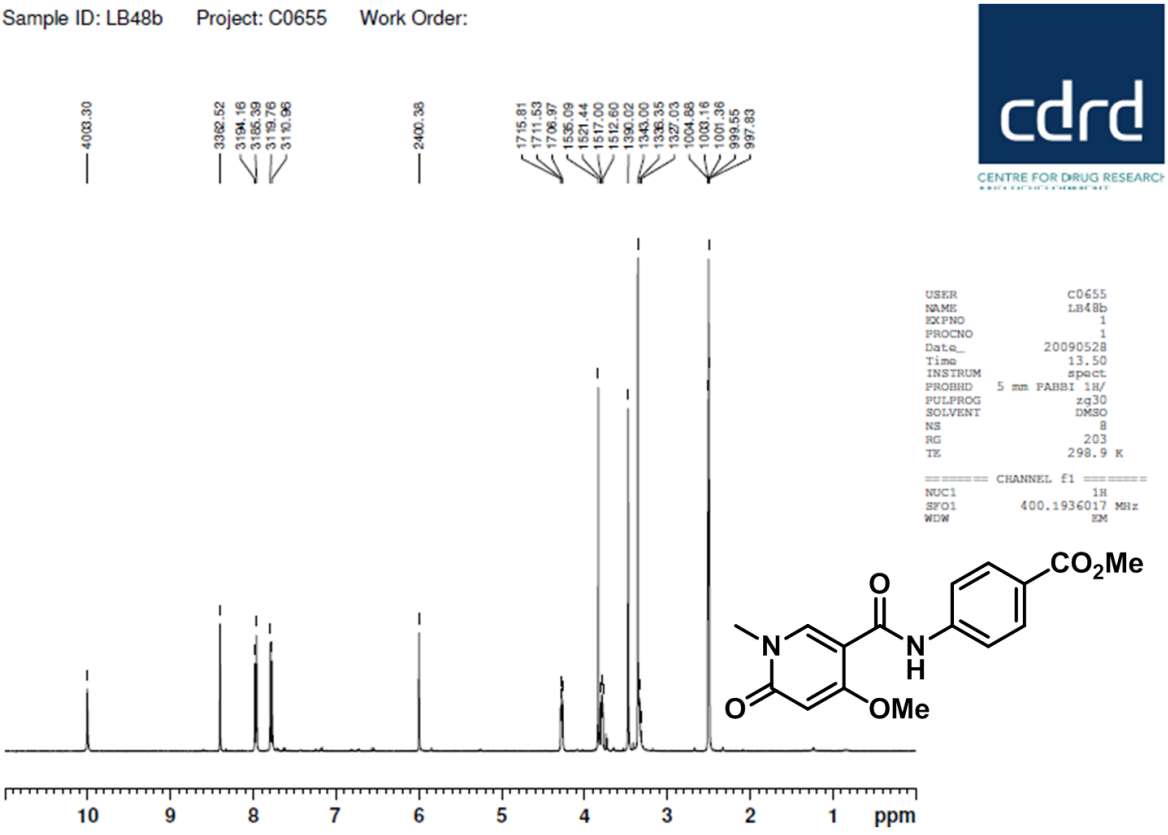
Sample ID: LB48b Project: C0655 Work Order:
4003.30
3382.52
3194.16
3165.39
3119.76
3110.96
2400.38
1715.81
1711.53
1706.97
1535.09
1521.44
1517.00
1512.60
1390.02
1343.00
1336.35
1327.03
1004.88
1003.16
1001.36
999.55
997.83
cdrd
CENTRE FOR DRUG RESEARCH
USER C0655
NAME LB48b
EXPNO 1
PROCNO 1
Date_ 20090528
Time 13.50
INSTRUM spect
PROBHD 5 mm PABBI 1H/
PULPROG zg30
SOLVENT DMSO
NS 8
RG 203
TE 298.9 K
CHANNEL f1
NUC1 1H
SFO1 400.1936017 MHz
WDW EM
CO2Me
O
N
H
N
O
OMe
10 9 8 7 6 5 4 3 2 1 ppm

10c

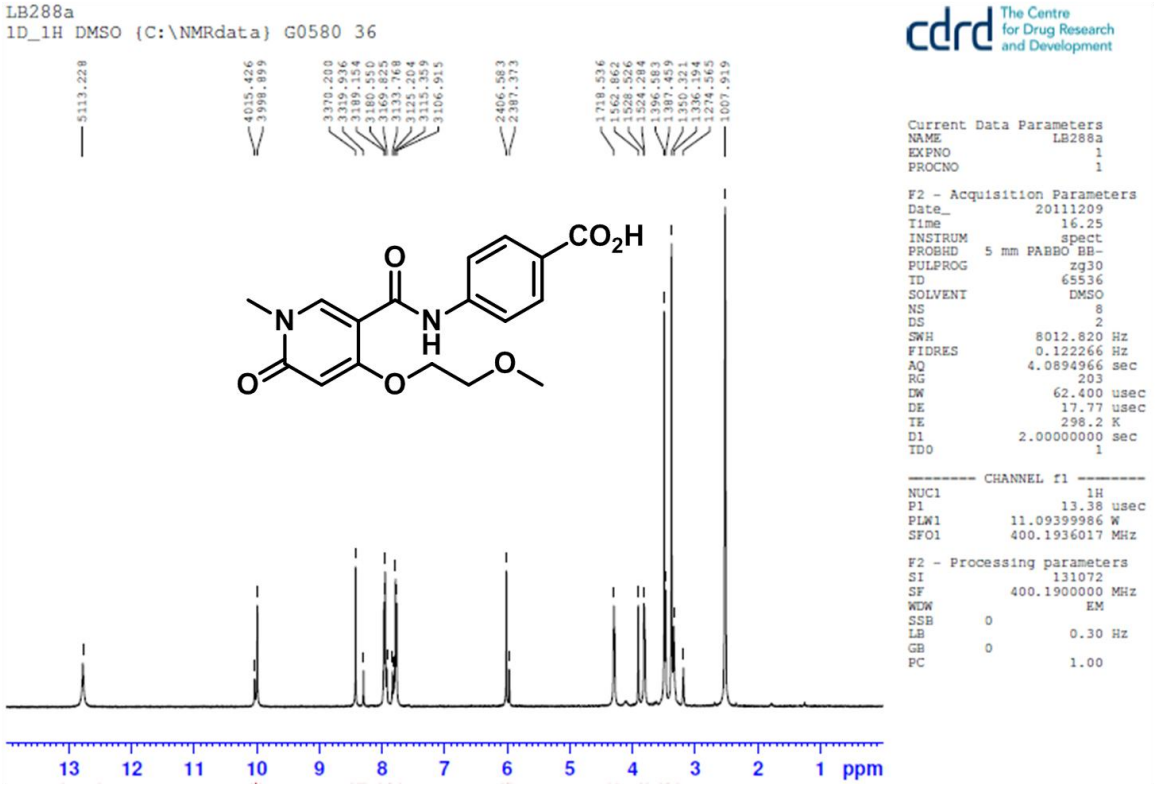

cdrd The Centre for Drug Research and Development

```
Current Data Parameters
NAME                  LB288a
EXPNO                      1
PROCNO                     1

F2 - Acquisition Parameters
Date_              20111209
Time                  16.25
INSTRUM               spect
PROBHD   5 mm PABBO BB-
PULPROG                zg30
TD                    65536
SOLVENT                DMSO
NS                         8
DS                         2
SWH                8012.820 Hz
FIDRES            0.122266 Hz
AQ                4.0894966 sec
RG                       203
DW                  62.400 usec
DE                  17.77 usec
TE                   298.2 K
D1                2.00000000 sec
TD0                        1

======== CHANNEL f1 ========
NUC1                      1H
P1                    13.38 usec
PLW1             11.09399986 W
SFO1             400.1936017 MHz

F2 - Processing parameters
SI                       131072
SF                400.1900000 MHz
WDW                        EM
SSB          0
LB                    0.30 Hz
GB           0
PC                    1.00
```

10d

Sample ID: LB56-2 Project: C0655 Work Order:

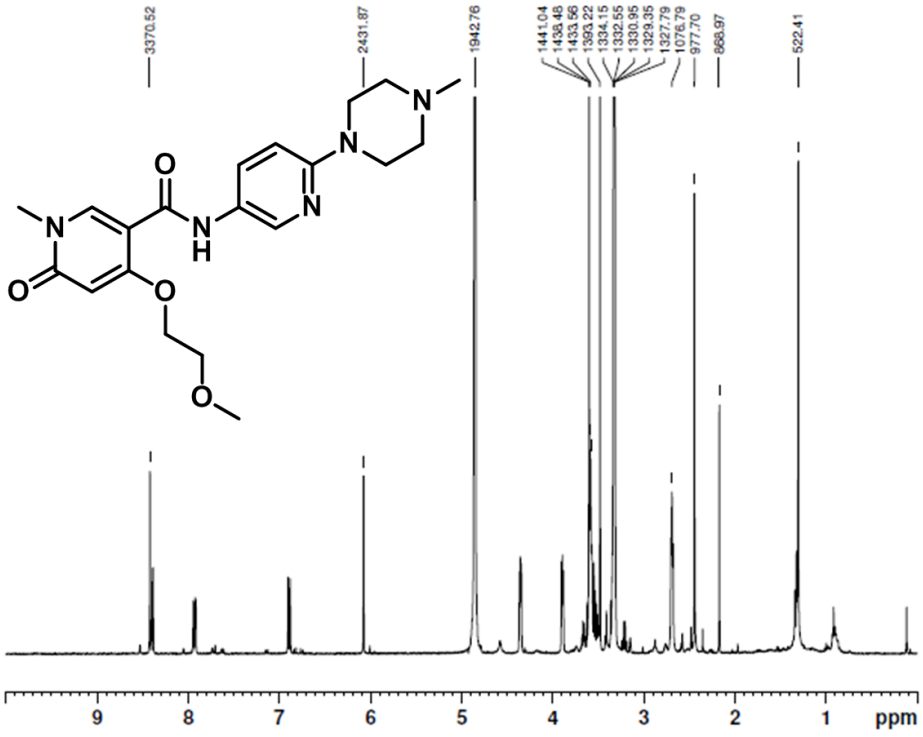

CENTRE FOR DRUG RESEARCH

```
USER                   C0655
NAME                LB56-2
EXPNO                      1
PROCNO                     1
Date_              20090611
Time                  15.35
INSTRUM               spect
PROBHD   5 mm PABBI 1H/
PULPROG                zg30
SOLVENT                MeOD
NS                         8
RG                       203
TE                   299.6 K

======== CHANNEL f1 ========
NUC1                      1H
SFO1             400.1936017 MHz
WDW                        EM
```

10e

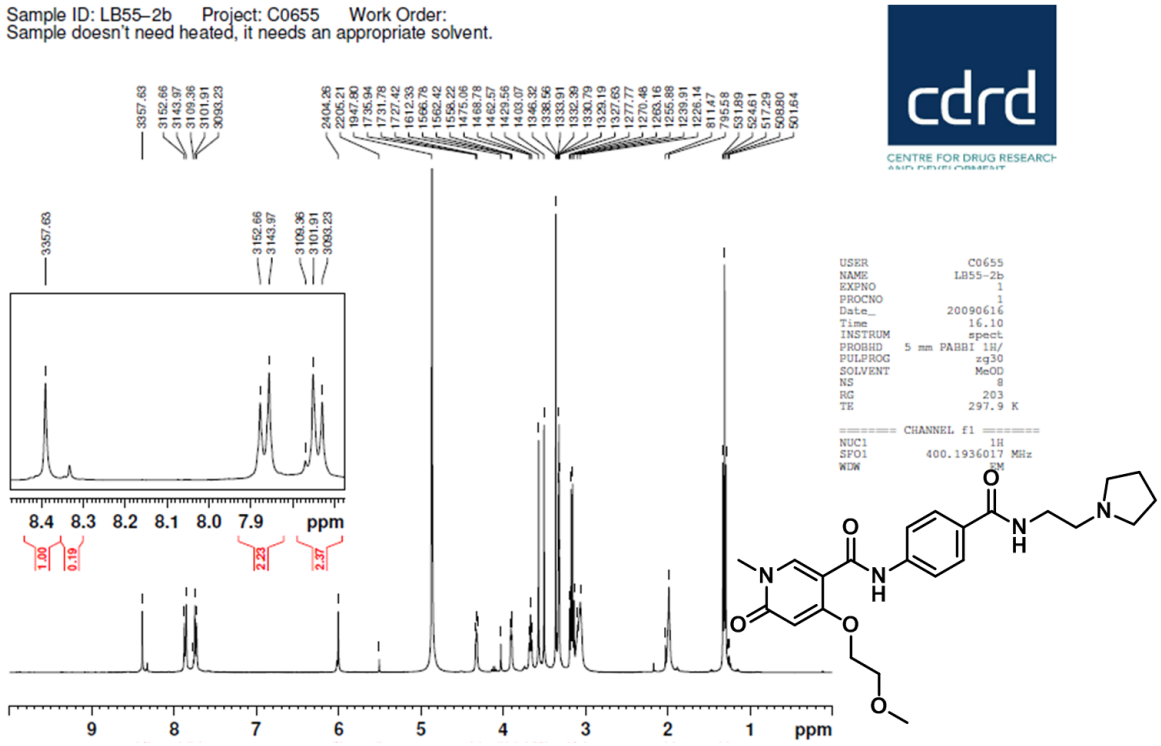
Sample ID: LB55–2b Project: C0655 Work Order:
Sample doesn't need heated, it needs an appropriate solvent.
cdrd
CENTRE FOR DRUG RESEARCH
3357.63
3152.66
3143.97
3109.36
3101.91
3093.23
8.4 8.3 8.2 8.1 8.0 7.9 ppm
1.00 0.19 2.23 2.37
USER C0655
NAME LB55-2b
EXPNO 1
PROCNO 1
Date_ 20090616
Time 16.10
INSTRUM spect
PROBHD 5 mm PABBI 1H/
PULPROG zg30
SOLVENT MeOD
NS 8
RG 203
TE 297.9 K
CHANNEL f1
NUC1 1H
SFO1 400.1936017 MHz
WDW EM
9 8 7 6 5 4 3 2 1 ppm

10f

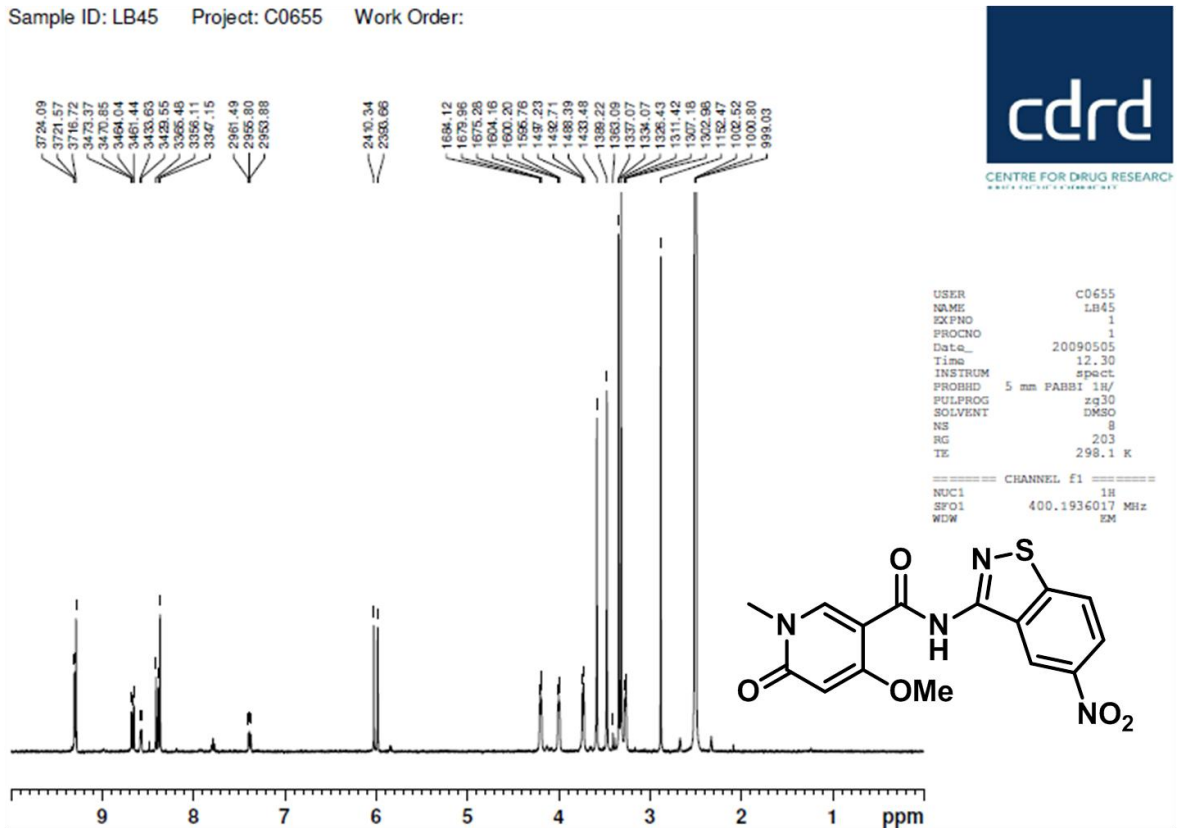
Sample ID: LB45 Project: C0655 Work Order:
cdrd
CENTRE FOR DRUG RESEARCH
3724.09
3721.57
3716.72
3473.37
3470.85
3464.04
3461.44
3433.63
3429.55
3365.48
3356.11
3347.15
2961.49
2955.80
2953.88
2410.34
2393.66
1684.12
1679.96
1675.28
1604.16
1600.20
1585.76
1497.23
1492.71
1488.39
1433.48
1389.22
1363.09
1337.07
1334.07
1326.43
1311.42
1307.18
1302.96
1152.47
1022.52
1000.80
999.03
USER C0655
NAME LB45
EXPNO 1
PROCNO 1
Date_ 20090505
Time 12.30
INSTRUM spect
PROBHD 5 mm PABBI 1H/
PULPROG zg30
SOLVENT DMSO
NS 8
RG 203
TE 298.1 K
CHANNEL f1
NUC1 1H
SFO1 400.1936017 MHz
WDW EM
9 8 7 6 5 4 3 2 1 ppm

11a

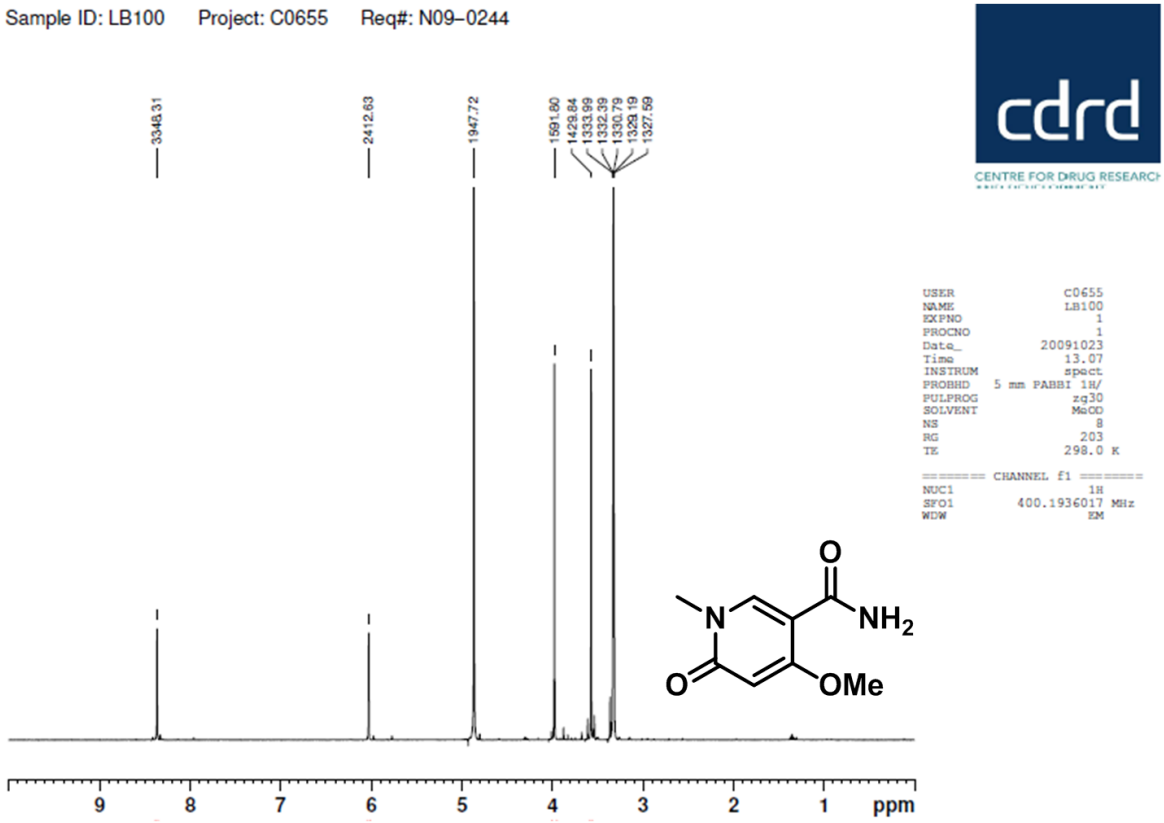
Sample ID: LB100 Project: C0655 Req#: N09–0244
3348.31
2412.63
1947.72
1591.80
1429.84
1333.99
1332.39
1330.79
1328.19
1327.59
CENTRE FOR DRUG RESEARCH
USER C0655
NAME LB100
EXPNO 1
PROCNO 1
Date_ 20091023
Time 13.07
INSTRUM spect
PROBHD 5 mm PABBI 1H/
PULPROG zg30
SOLVENT MeOD
NS 8
RG 203
TE 298.0 K
CHANNEL f1
NUC1 1H
SFO1 400.1936017 MHz
WDW EM
O
NH2
N
O
OMe
9 8 7 6 5 4 3 2 1 ppm

11b

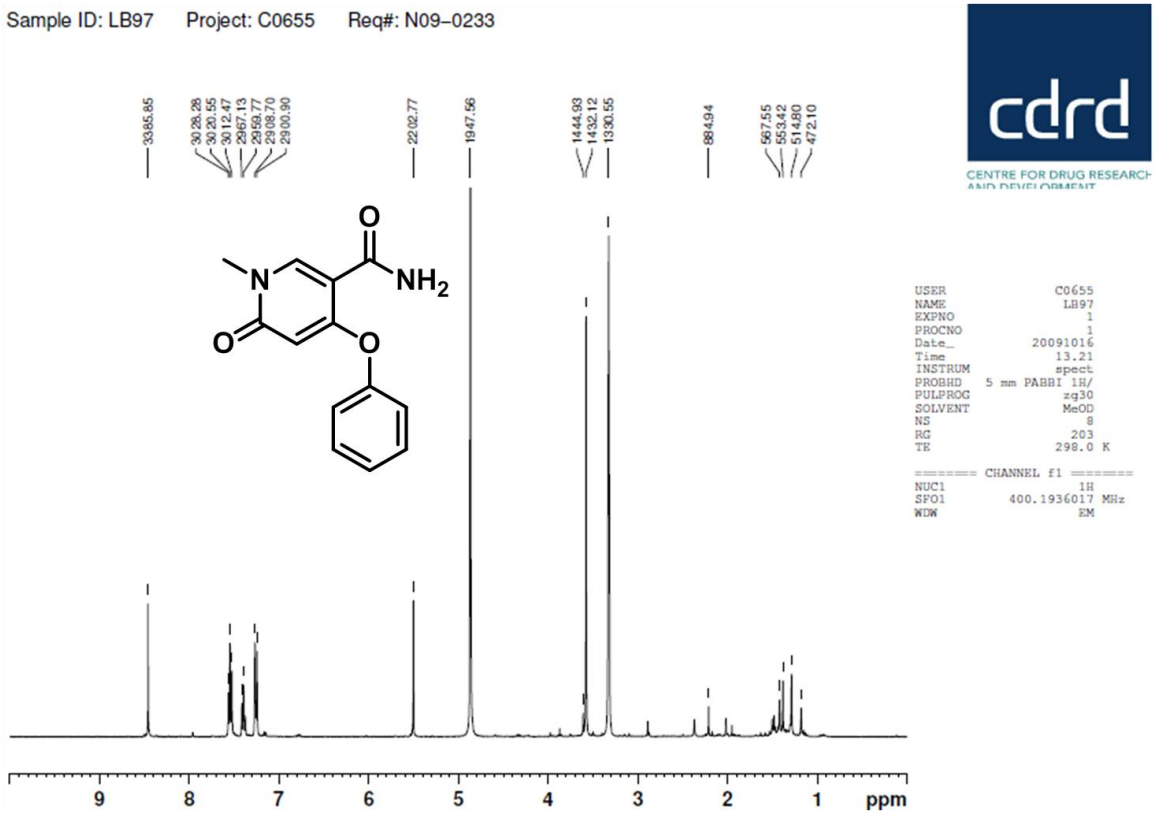
Sample ID: LB97 Project: C0655 Req#: N09–0233
3385.85
3028.28
3026.55
3012.47
2967.13
2959.77
2908.70
2900.90
2202.77
1947.56
1444.93
1432.12
1330.55
884.94
567.55
553.42
514.80
472.10
CENTRE FOR DRUG RESEARCH
USER C0655
NAME LB97
EXPNO 1
PROCNO 1
Date_ 20091016
Time 13.21
INSTRUM spect
PROBHD 5 mm PABBI 1H/
PULPROG zg30
SOLVENT MeOD
NS 8
RG 203
TE 298.0 K
CHANNEL f1
NUC1 1H
SFO1 400.1936017 MHz
WDW EM
O
NH2
N
O
O
9 8 7 6 5 4 3 2 1 ppm

12a

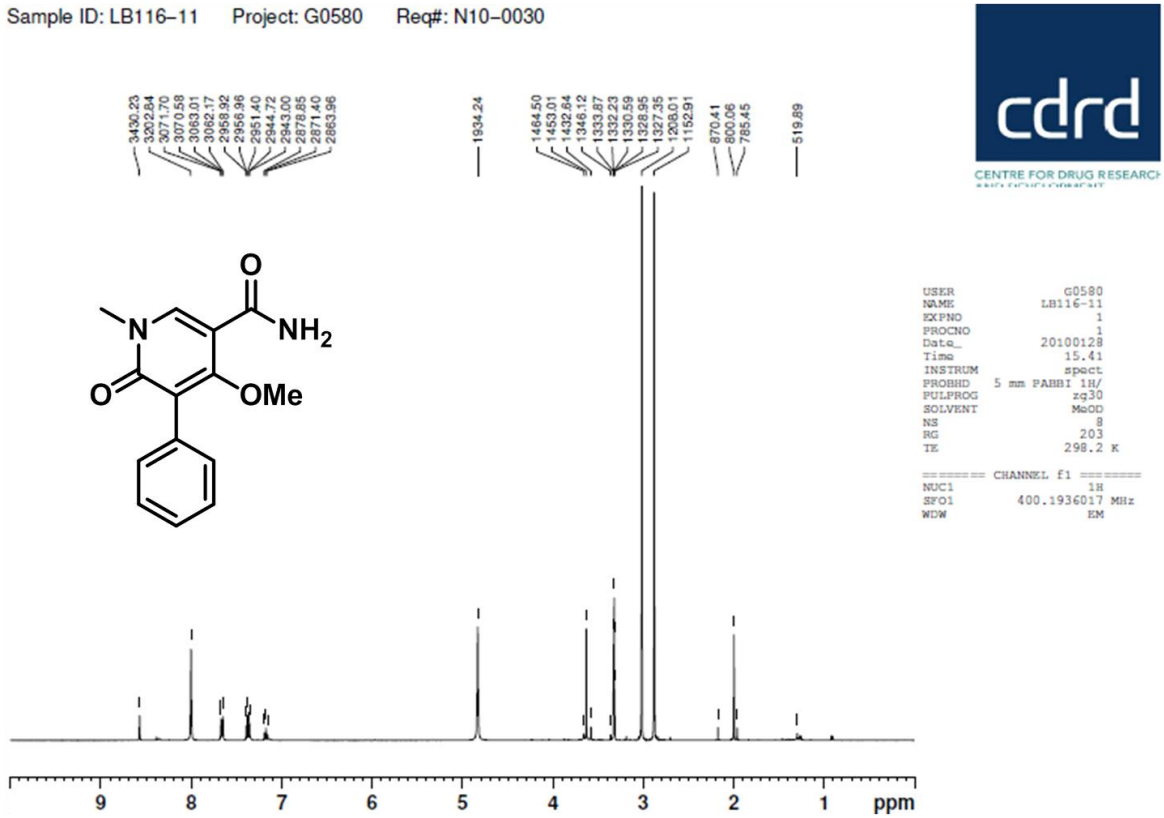
Sample ID: LB116-11 Project: G0580 Req#: N10-0030
3430.23
3202.84
3071.70
3070.58
3063.01
3062.17
2958.92
2956.96
2951.40
2944.72
2943.00
2878.85
2871.40
2863.96
1934.24
1464.50
1453.01
1432.84
1346.12
1333.87
1332.23
1330.59
1328.95
1327.35
1208.01
1152.91
870.41
800.06
785.45
519.89
O
N
NH2
O
OMe
USER G0580
NAME LB116-11
EXPNO 1
PROCNO 1
Date_ 20100128
Time 15.41
INSTRUM spect
PROBHD 5 mm PABBI 1H/
PULPROG zg30
SOLVENT MeOD
NS 8
RG 203
TE 298.2 K
CHANNEL f1
NUC1 1H
SFO1 400.1936017 MHz
WDW EM
9 8 7 6 5 4 3 2 1 ppm

12b

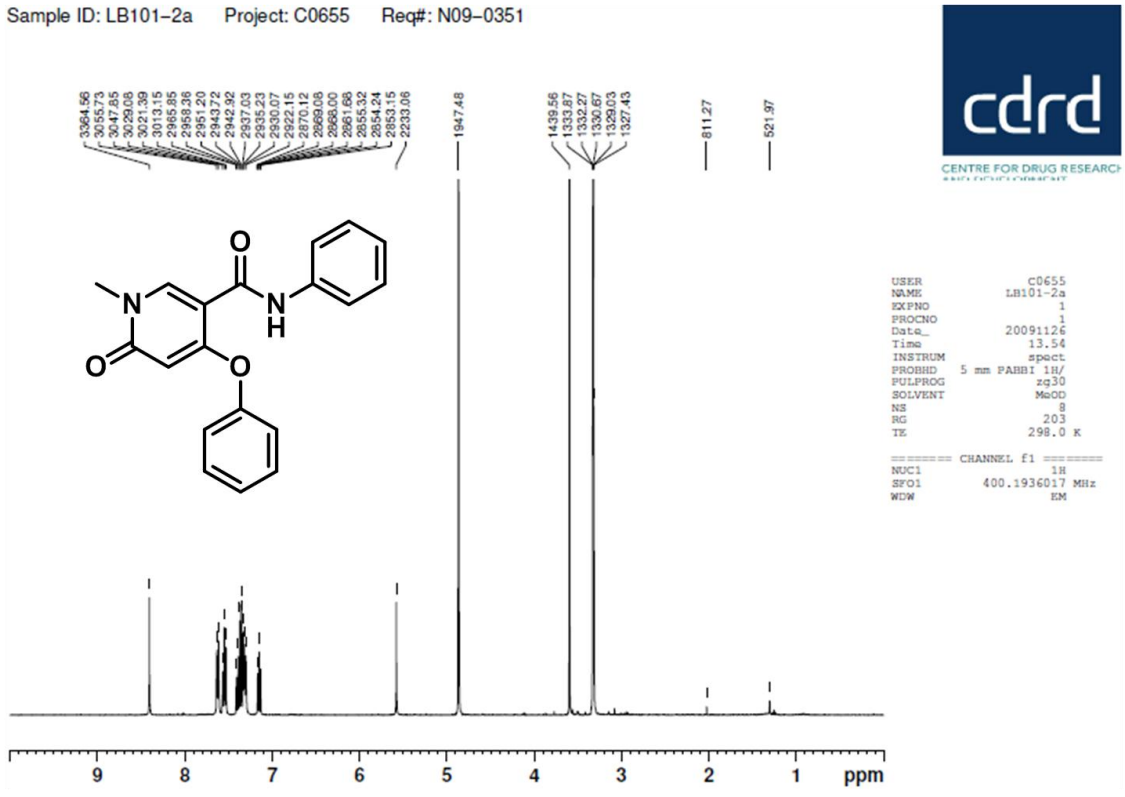
Sample ID: LB101-2a Project: C0655 Req#: N09-0351
3364.56
3055.73
3047.85
3029.08
3021.39
3013.15
2965.85
2958.36
2951.20
2943.72
2942.92
2937.03
2935.23
2930.07
2922.15
2870.12
2869.06
2868.00
2861.66
2855.32
2854.24
2853.15
2233.06
1947.48
1439.56
1333.87
1332.27
1330.67
1329.03
1327.43
811.27
521.97
O
N
H
N
O
O
USER C0655
NAME LB101-2a
EXPNO 1
PROCNO 1
Date_ 20091126
Time 13.54
INSTRUM spect
PROBHD 5 mm PABBI 1H/
PULPROG zg30
SOLVENT MeOD
NS 8
RG 203
TE 298.0 K
CHANNEL f1
NUC1 1H
SFO1 400.1936017 MHz
WDW EM
9 8 7 6 5 4 3 2 1 ppm

13a

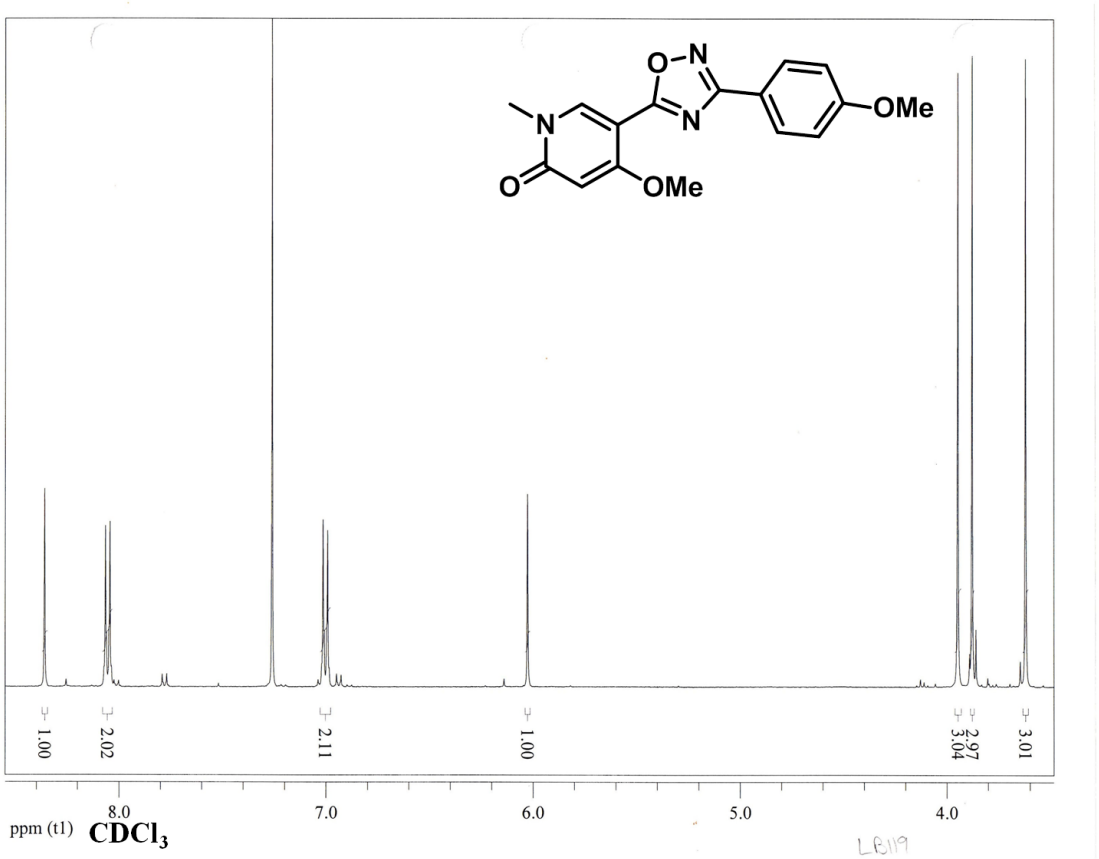
O
N
N
O
N
OMe
OMe
1.00
2.02
2.11
1.00
3.04
2.97
3.01
8.0
7.0
6.0
5.0
4.0
ppm (t1)
CDCl3

13b

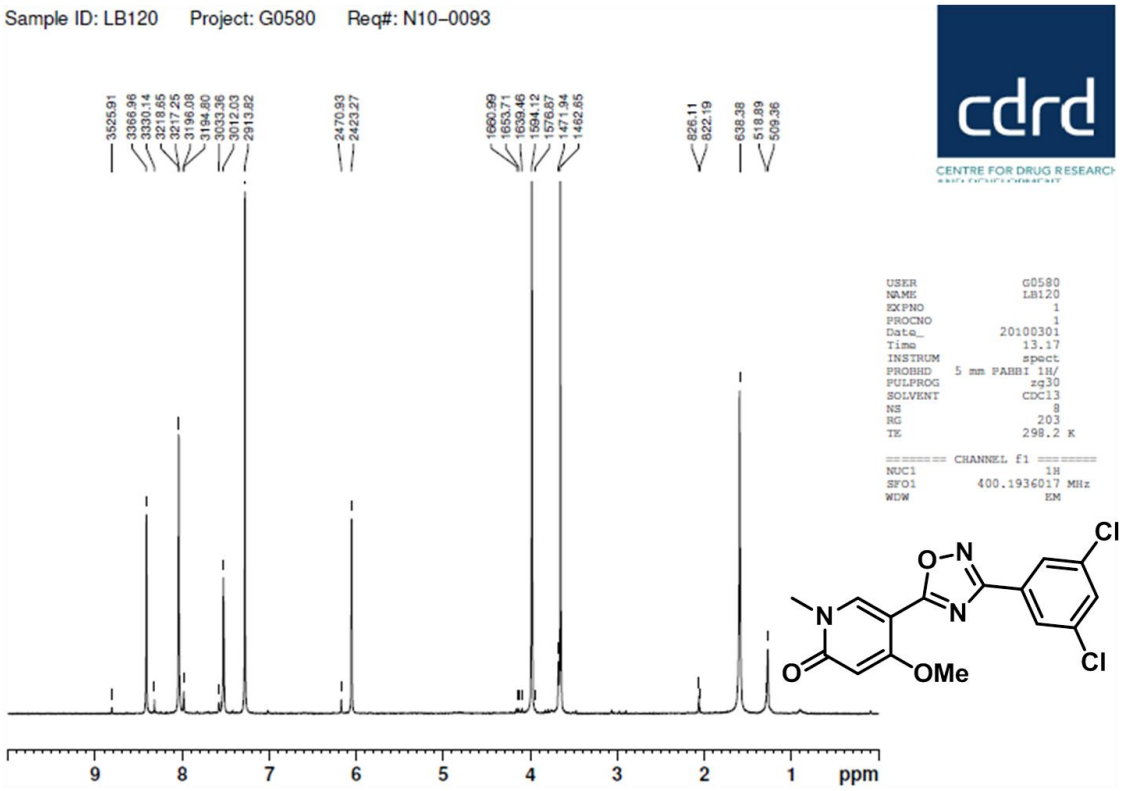
Sample ID: LB120 Project: G0580 Req#: N10–0093
3525.91
3366.96
3330.14
3218.65
3217.25
3196.08
3194.80
3033.36
3012.03
2913.82
2470.93
2423.27
1660.99
1653.71
1639.46
1594.12
1576.67
1471.34
1462.85
826.11
822.19
638.38
518.89
509.36
cdrd
CENTRE FOR DRUG RESEARCH
USER G0580
NAME LB120
EXPNO 1
PROCNO 1
Date_ 20100301
Time 13.17
INSTRUM spect
PROBHD 5 mm PABBI 1H/
PULPROG zg30
SOLVENT CDCl3
NS 8
RG 203
TE 298.2 K
CHANNEL f1
NUC1 1H
SFO1 400.1936017 MHz
WDW EM
O
N
N
O
N
OMe
Cl
Cl
9
8
7
6
5
4
3
2
1
ppm

13c

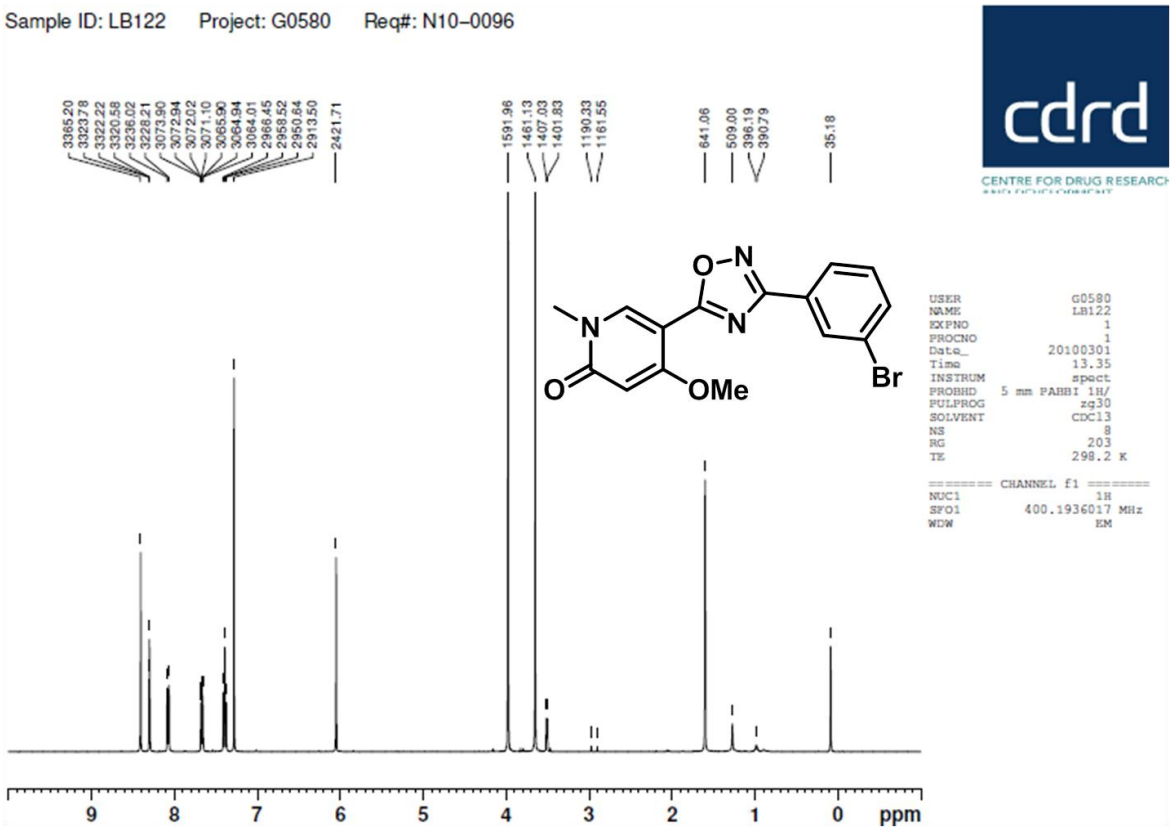
Sample ID: LB122 Project: G0580 Req#: N10–0096
3365.20
3323.78
3322.22
3320.58
3236.02
3228.21
3073.90
3072.94
3072.02
3071.10
3065.90
3064.94
3064.01
2968.45
2953.52
2950.64
2913.50
2421.71
1591.96
1461.13
1407.03
1401.83
1190.33
1161.55
641.06
509.00
396.19
390.79
35.18
USER G0580
NAME LB122
EXPNO 1
PROCNO 1
Date_ 20100301
Time 13.35
INSTRUM spect
PROBHD 5 mm PABBI 1H/
PULPROG zg30
SOLVENT CDCl3
NS 8
RG 203
TE 298.2 K
CHANNEL f1
NUC1 1H
SFO1 400.1936017 MHz
WDW EM
ppm

13d

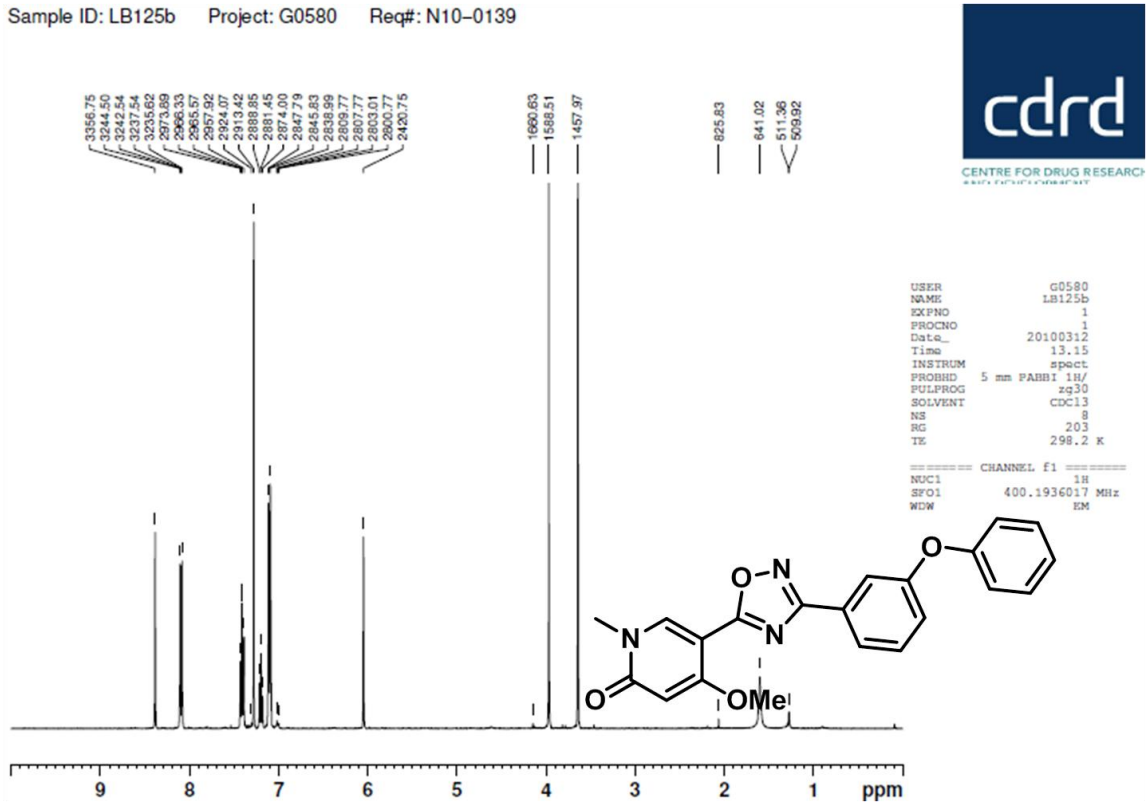
Sample ID: LB125b Project: G0580 Req#: N10–0139
3356.75
3244.50
3242.54
3237.54
3235.62
2973.89
2966.33
2965.57
2957.92
2924.07
2913.42
2888.85
2881.45
2874.00
2847.79
2845.83
2838.99
2809.77
2807.77
2803.01
2800.77
2420.75
1600.63
1588.51
1457.97
825.83
641.02
511.36
509.92
USER G0580
NAME LB125b
EXPNO 1
PROCNO 1
Date_ 20100312
Time 13.15
INSTRUM spect
PROBHD 5 mm PABBI 1H/
PULPROG zg30
SOLVENT CDCl3
NS 8
RG 203
TE 298.2 K
CHANNEL f1
NUC1 1H
SFO1 400.1936017 MHz
WDW EM
ppm

13e

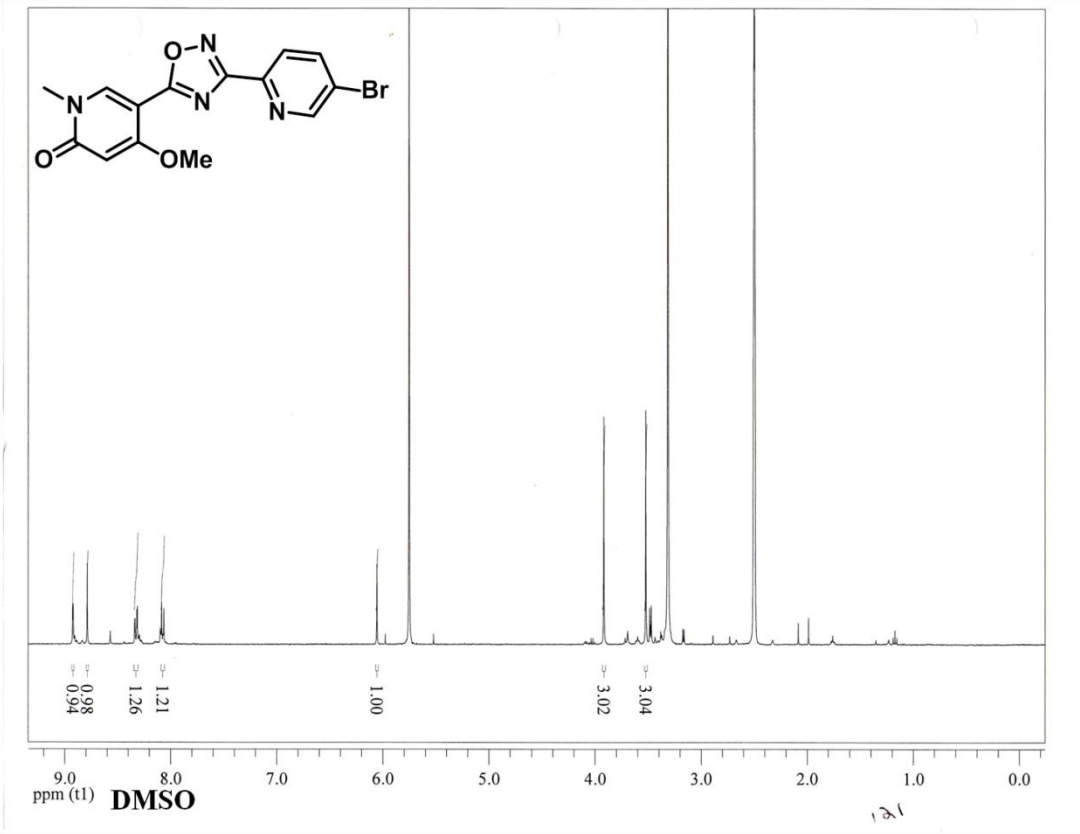
Br
OMe
0.94
0.98
1.26
1.21
1.00
3.02
3.04
9.0
8.0
7.0
6.0
5.0
4.0
3.0
2.0
1.0
0.0
ppm (t1)
DMSO

13f

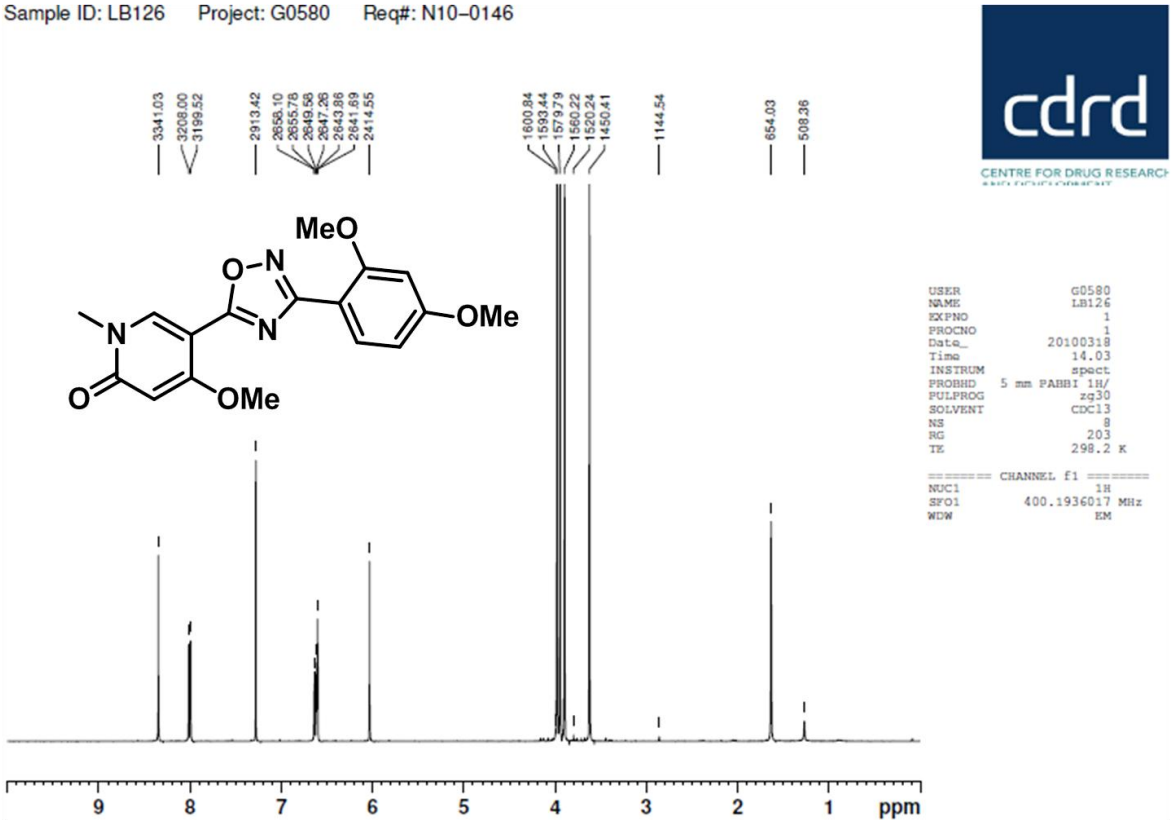
Sample ID: LB126
Project: G0580
Req#: N10-0146
3341.03
3208.00
3199.52
2913.42
2656.10
2655.78
2649.58
2647.26
2643.86
2641.69
2414.55
1600.84
1593.44
1579.79
1560.22
1520.24
1450.41
1144.54
654.03
508.36
MeO
OMe
OMe
CENTRE FOR DRUG RESEARCH
USER G0580
NAME LB126
EXPNO 1
PROCNO 1
Date_ 20100318
Time 14.03
INSTRUM spect
PROBHD 5 mm PABBI 1H/
PULPROG zg30
SOLVENT CDCl3
NS 8
RG 203
TE 298.2 K
======== CHANNEL f1 ========
NUC1 1H
SFO1 400.1936017 MHz
WDW EM
9
8
7
6
5
4
3
2
1
ppm

13g

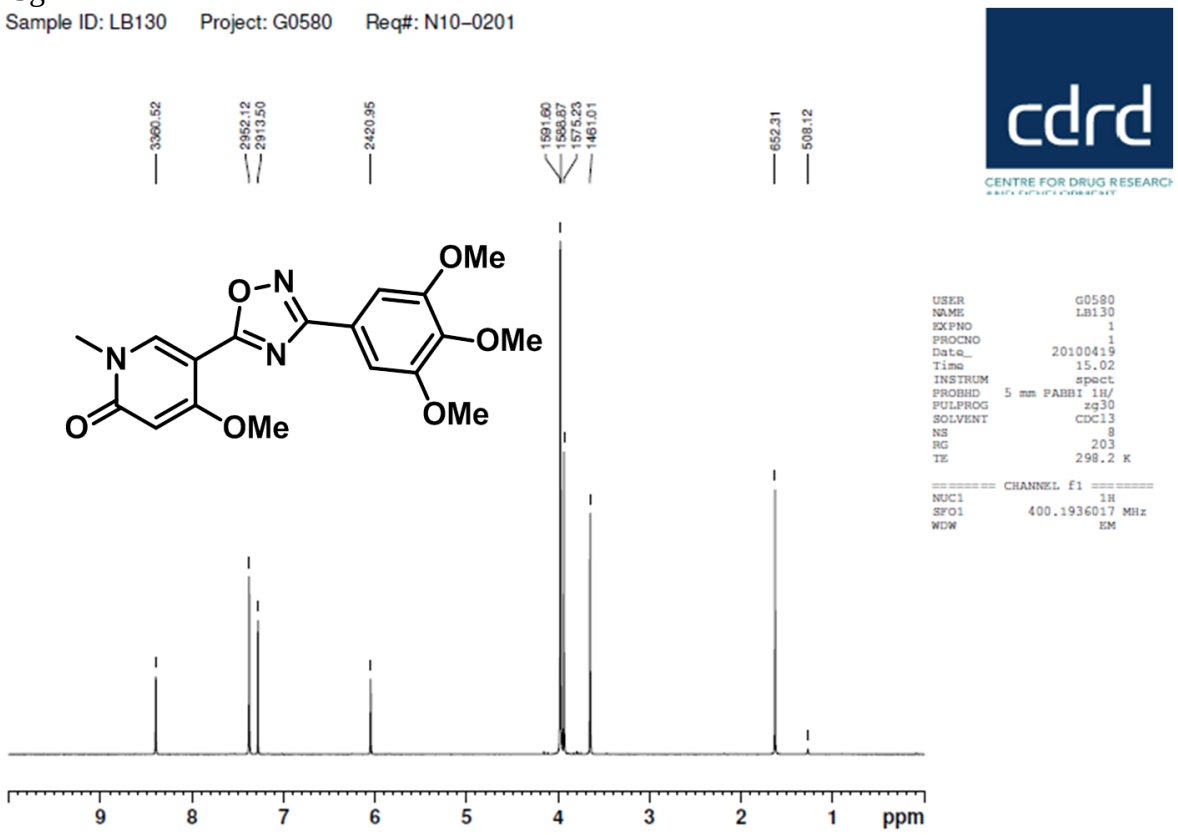
Sample ID: LB130 Project: G0580 Req#: N10–0201
3360.52
2952.12
2913.50
2420.95
1591.60
1588.87
1575.23
1461.01
652.31
508.12
OMe
OMe
OMe
OMe
O
N
N
O
USER G0580
NAME LB130
EXPNO 1
PROCNO 1
Date_ 20100419
Time 15.02
INSTRUM spect
PROBHD 5 mm PABBI 1H/
PULPROG zg30
SOLVENT CDCl3
NS 8
RG 203
TE 298.2 K
CHANNEL f1
NUC1 1H
SFO1 400.1936017 MHz
WDW EM
9 8 7 6 5 4 3 2 1 ppm

13h

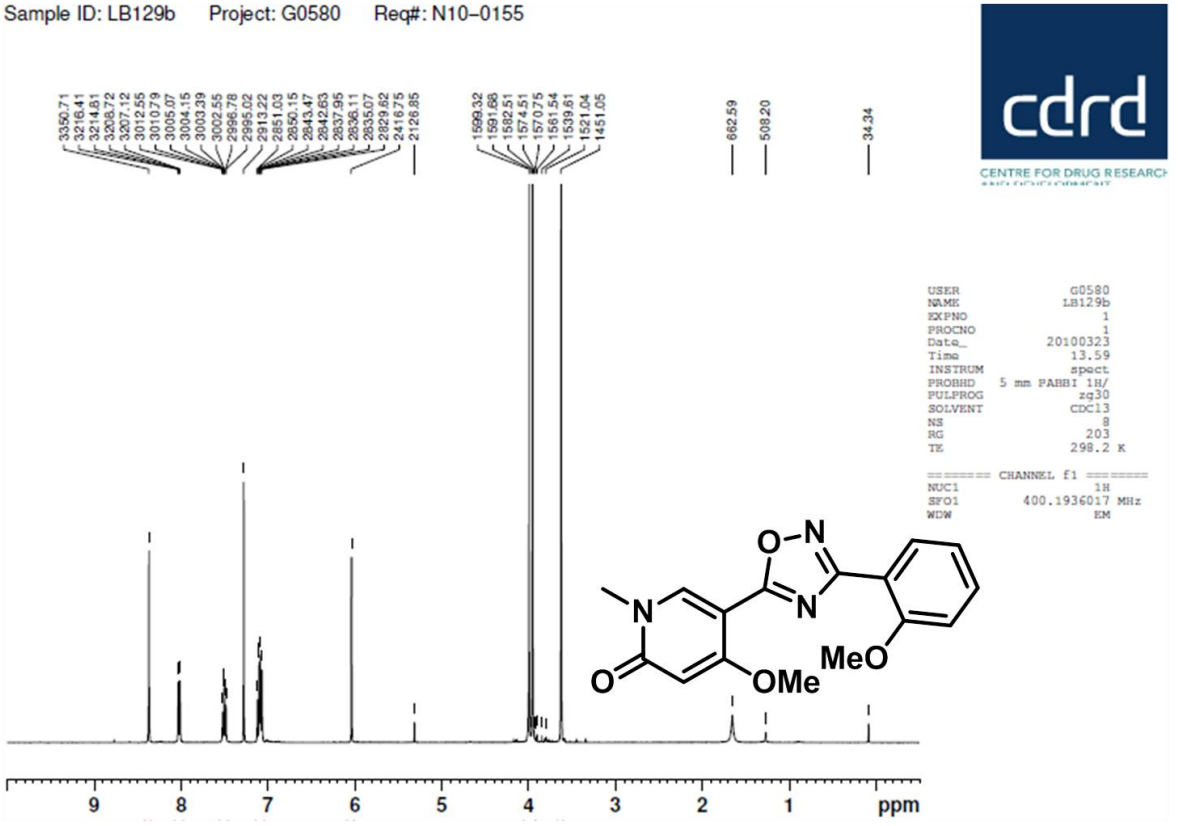
Sample ID: LB129b Project: G0580 Req#: N10–0155
3350.71
3216.41
3214.81
3208.72
3207.12
3012.55
3010.79
3005.07
3004.15
3003.39
3002.55
2996.78
2995.02
2913.22
2851.03
2850.15
2843.47
2842.63
2837.95
2836.11
2835.07
2829.62
2416.75
2126.85
1599.32
1591.68
1582.51
1574.51
1570.75
1561.54
1539.81
1521.04
1451.05
682.59
508.20
34.34
N
O
N
O
OMe
MeO
USER G0580
NAME LB129b
EXPNO 1
PROCNO 1
Date_ 20100323
Time 13.59
INSTRUM spect
PROBHD 5 mm PABBI 1H/
PULPROG zg30
SOLVENT CDCl3
NS 8
RG 203
TE 298.2 K
CHANNEL f1
NUC1 1H
SFO1 400.1936017 MHz
WDW EM
9 8 7 6 5 4 3 2 1 ppm

13i

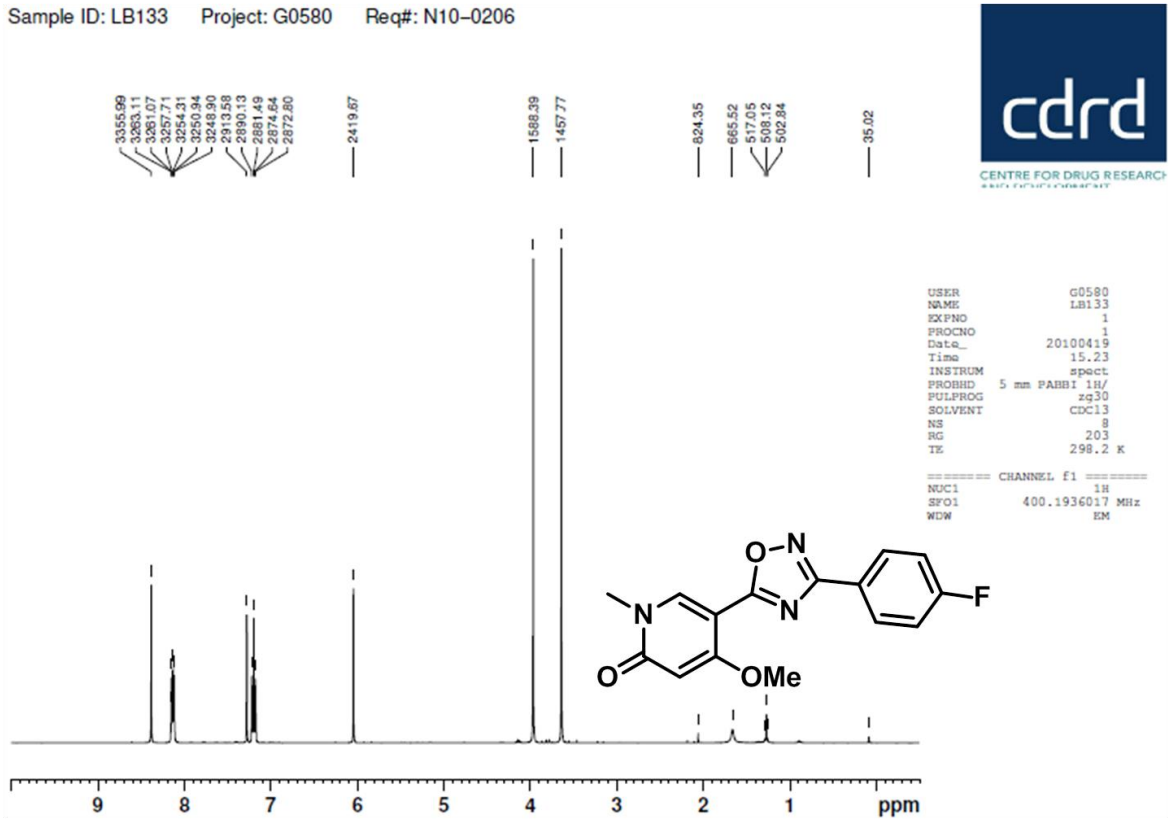
Sample ID: LB133 Project: G0580 Req#: N10–0206
3355.99
3283.11
3261.07
3257.71
3254.31
3250.94
3248.90
2913.58
2890.13
2881.49
2874.64
2872.80
2419.67
1588.39
1457.77
824.35
665.52
517.05
508.12
502.84
35.02
USER G0580
NAME LB133
EXPNO 1
PROCNO 1
Date_ 20100419
Time 15.23
INSTRUM spect
PROBHD 5 mm PABBI 1H/
PULPROG zg30
SOLVENT CDC13
NS 8
RG 203
TE 298.2 K
CHANNEL f1
NUC1 1H
SFO1 400.1936017 MHz
WDW EM
O-N
N
N
F
N
O
OMe
9 8 7 6 5 4 3 2 1 ppm

13j

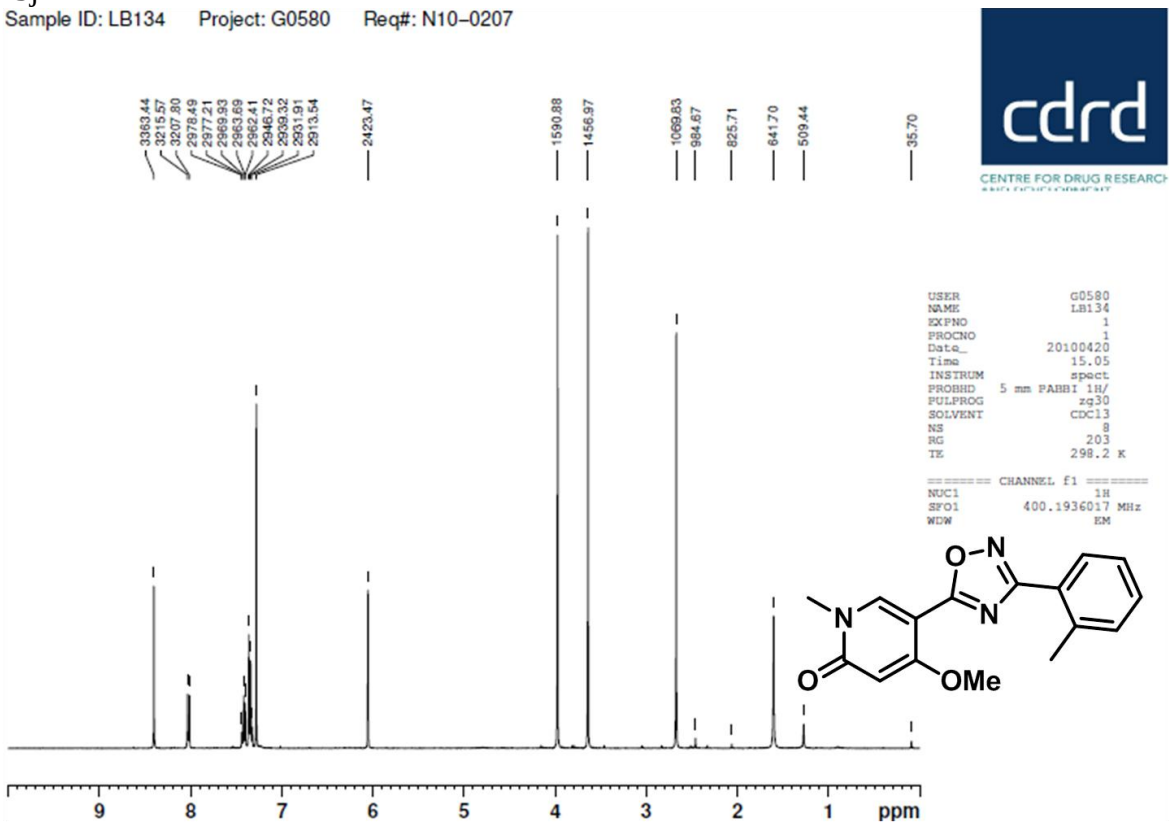
Sample ID: LB134 Project: G0580 Req#: N10–0207
3363.44
3215.57
3207.80
2978.49
2977.21
2969.93
2963.69
2962.41
2946.72
2939.32
2931.91
2913.54
2423.47
1590.88
1456.97
1069.83
984.67
825.71
641.70
509.44
35.70
USER G0580
NAME LB134
EXPNO 1
PROCNO 1
Date_ 20100420
Time 15.05
INSTRUM spect
PROBHD 5 mm PABBI 1H/
PULPROG zg30
SOLVENT CDC13
NS 8
RG 203
TE 298.2 K
CHANNEL f1
NUC1 1H
SFO1 400.1936017 MHz
WDW EM
O-N
N
N
N
O
OMe
9 8 7 6 5 4 3 2 1 ppm

13k

Sample ID: LB135 Project: G0580 Req#: N10–0219

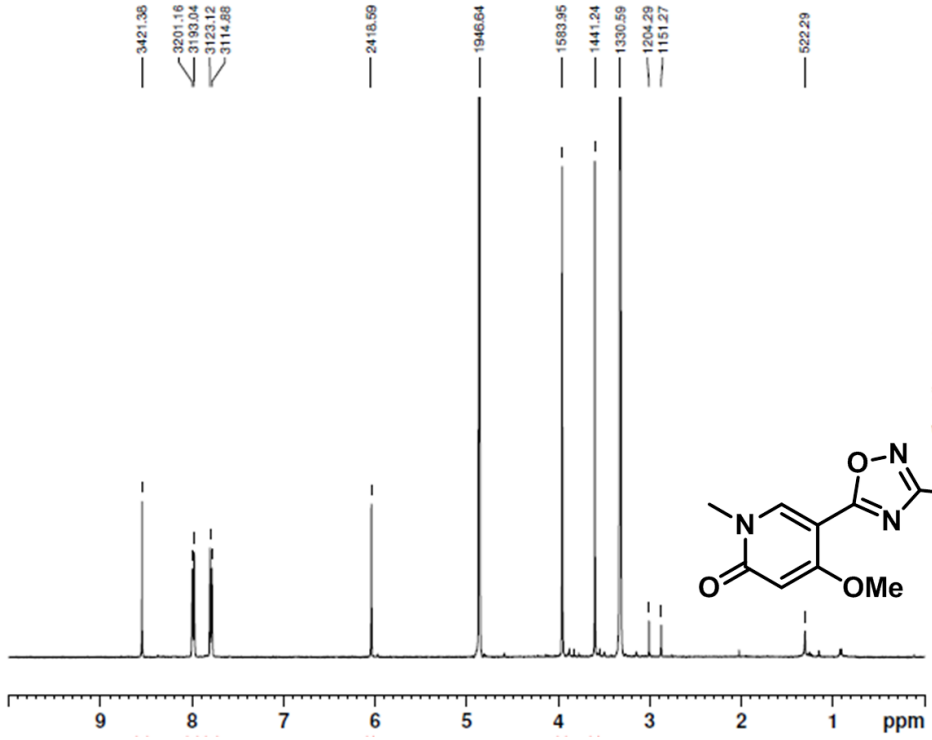

13l

Sample ID: LB136 Project: G0580 Req#: N10–0223

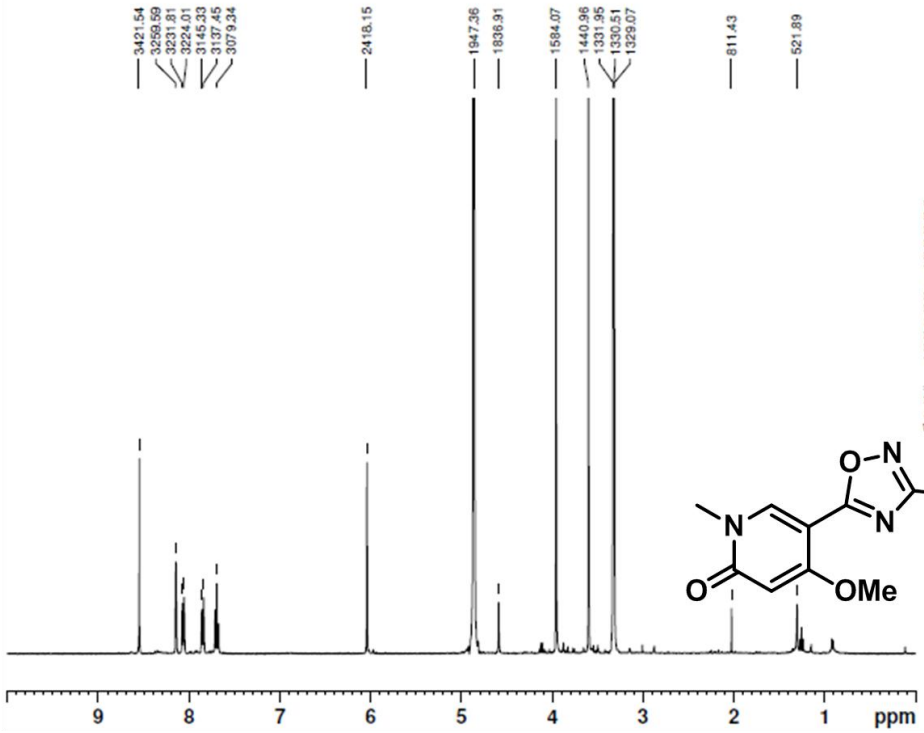

13m

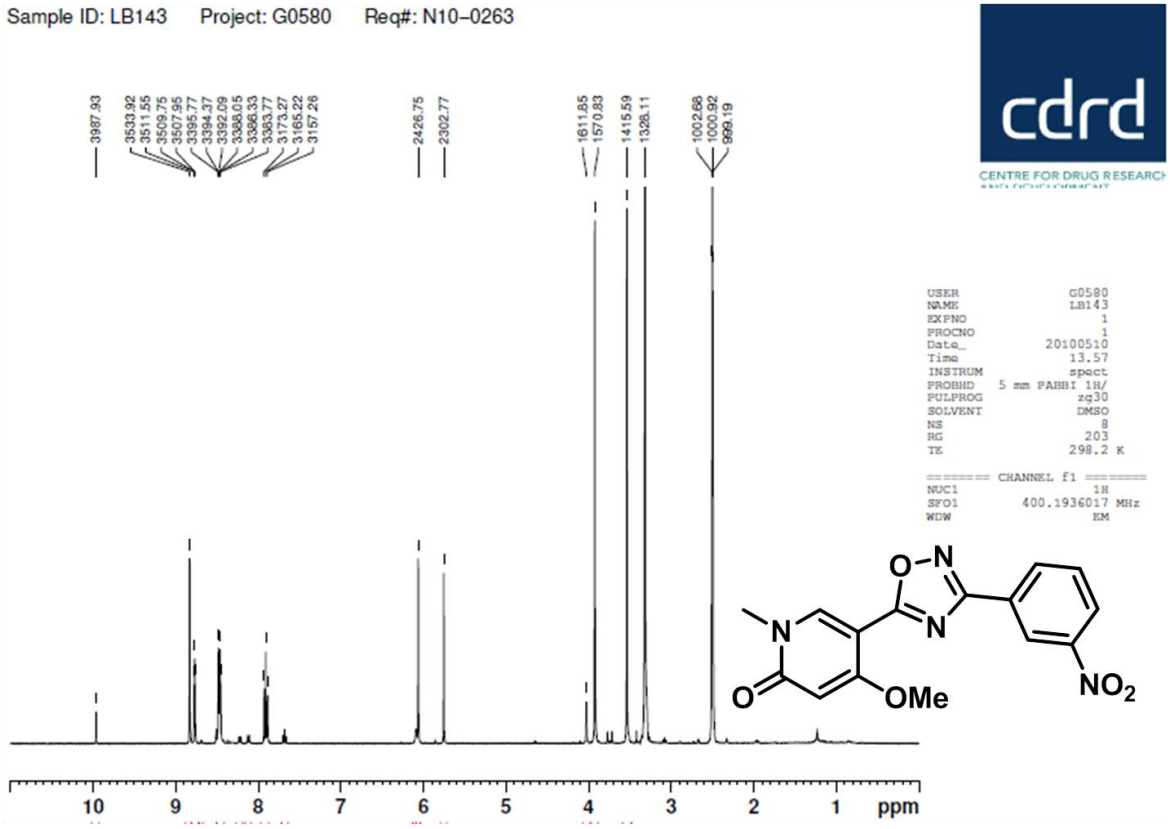
Sample ID: LB143 Project: G0580 Req#: N10-0263
3987.93
3533.92
3511.55
3509.75
3507.95
3395.77
3394.37
3392.09
3388.05
3386.33
3383.77
3173.27
3165.22
3157.26
2426.75
2302.77
1611.85
1570.83
1415.59
1328.11
1002.66
1000.92
998.19
USER G0580
NAME LB143
EXPNO 1
PROCNO 1
Date_ 20100510
Time 13.57
INSTRUM spect
PROBHD 5 mm PABBI 1H/
PULPROG zg30
SOLVENT DMSO
NS 8
RG 203
TE 298.2 K
CHANNEL f1
NUC1 1H
SFO1 400.1936017 MHz
WDW EM
OMe
NO2
10 9 8 7 6 5 4 3 2 1 ppm

14a

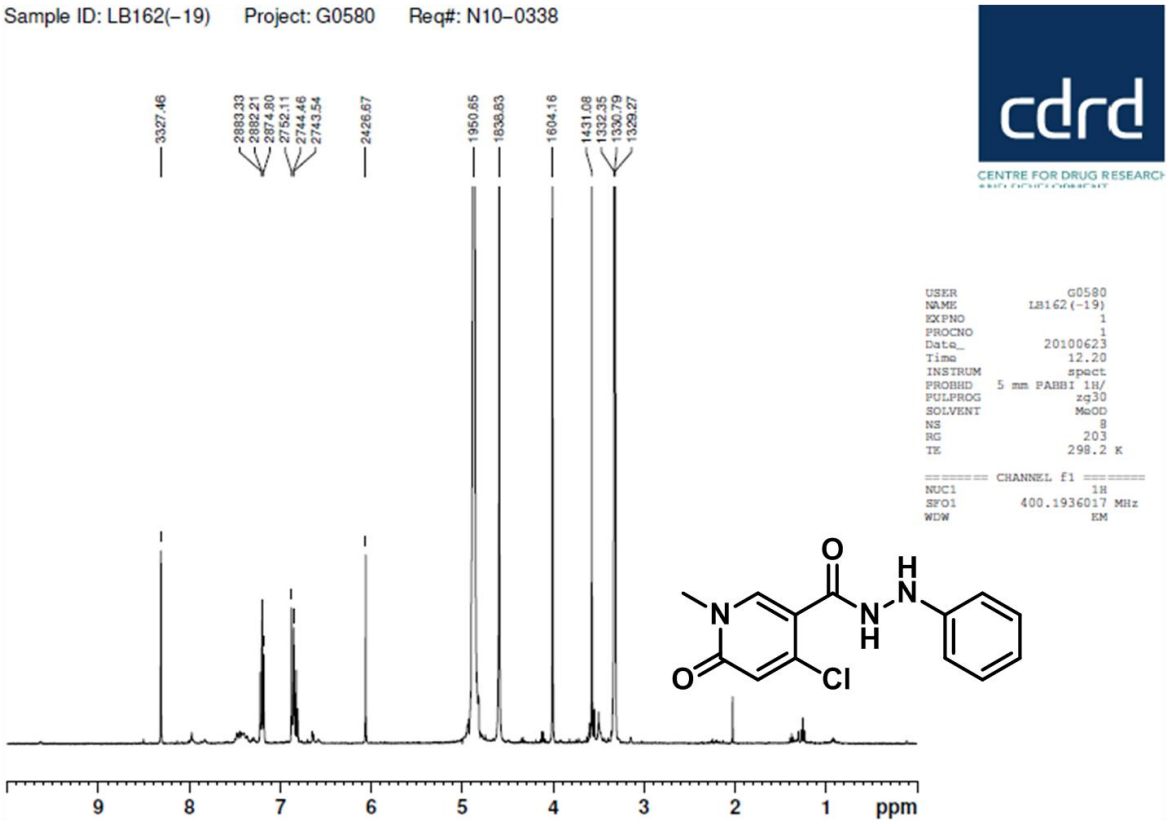
Sample ID: LB162(-19) Project: G0580 Req#: N10-0338
3327.46
2883.33
2882.21
2874.80
2752.11
2744.46
2743.54
2426.67
1950.65
1838.83
1604.16
1431.08
1332.35
1330.79
1329.27
USER G0580
NAME LB162(-19)
EXPNO 1
PROCNO 1
Date_ 20100623
Time 12.20
INSTRUM spect
PROBHD 5 mm PABBI 1H/
PULPROG zg30
SOLVENT MeOD
NS 8
RG 203
TE 298.2 K
CHANNEL f1
NUC1 1H
SFO1 400.1936017 MHz
WDW EM
Cl
9 8 7 6 5 4 3 2 1 ppm

14b

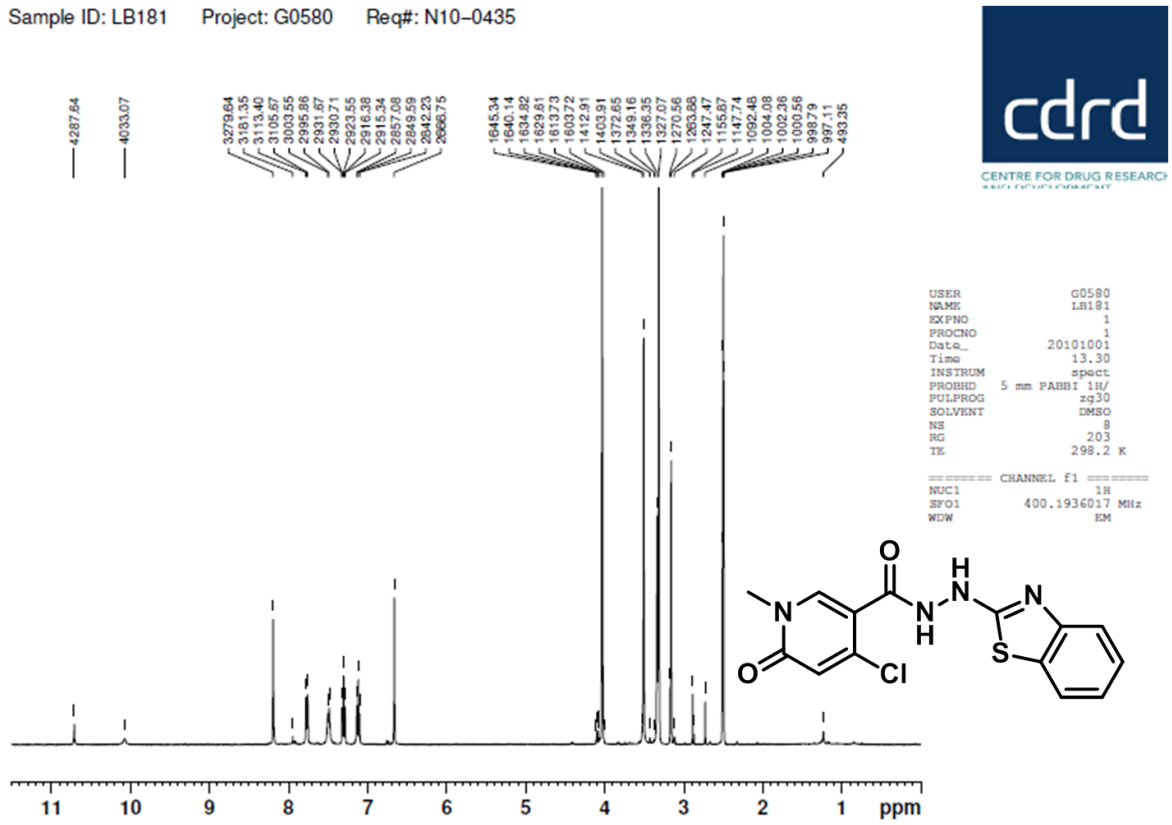
Sample ID: LB181 Project: G0580 Req#: N10-0435
4287.64
4033.07
3279.64
3161.35
3113.40
3105.67
3003.55
2995.86
2931.67
2930.71
2923.55
2916.38
2915.34
2857.08
2849.59
2842.23
2666.75
1645.34
1640.14
1634.82
1629.81
1613.73
1603.72
1412.91
1403.91
1372.65
1349.16
1336.35
1327.07
1270.56
1263.88
1247.47
1155.87
1147.74
1092.48
1004.08
1002.36
1000.56
998.79
997.11
493.35
USER G0580
NAME LB181
EXPNO 1
PROCNO 1
Date_ 20101001
Time 13.30
INSTRUM spect
PROBHD 5 mm PABBI 1H/
PULPROG zg30
SOLVENT DMSO
NS 8
RG 203
TE 298.2 K
CHANNEL f1
NUC1 1H
SFO1 400.1936017 MHz
WDW EM
11 10 9 8 7 6 5 4 3 2 1 ppm

15a

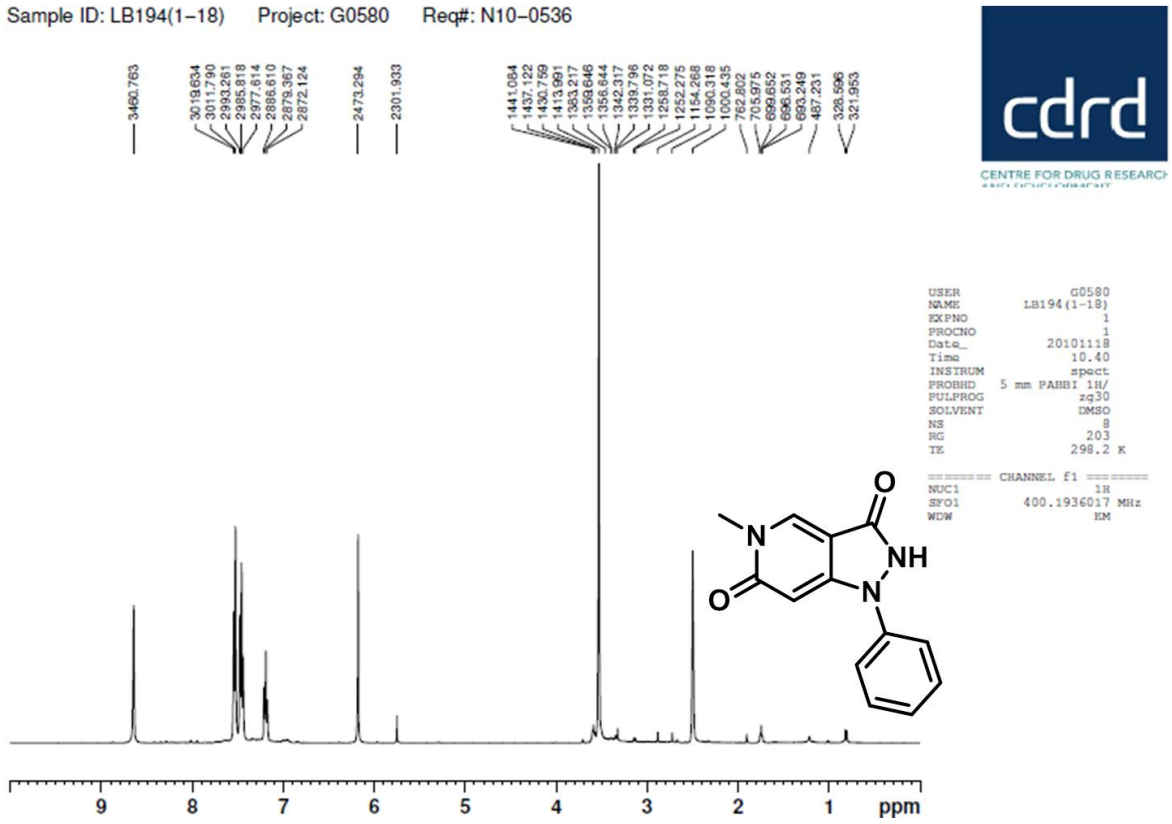
Sample ID: LB194(1-18) Project: G0580 Req#: N10-0536
3460.763
3019.634
3011.790
2993.261
2985.818
2977.614
2888.610
2879.367
2872.124
2473.294
2301.933
1441.084
1437.122
1430.759
1413.991
1383.217
1359.646
1356.644
1342.317
1339.796
1331.072
1258.718
1252.275
1154.268
1090.318
1000.435
762.802
705.975
699.652
696.531
693.249
487.231
328.596
321.953
USER G0580
NAME LB194(1-18)
EXPNO 1
PROCNO 1
Date_ 20101118
Time 10.40
INSTRUM spect
PROBHD 5 mm PABBI 1H/
PULPROG zg30
SOLVENT DMSO
NS 8
RG 203
TE 298.2 K
CHANNEL f1
NUC1 1H
SFO1 400.1936017 MHz
WDW EM
9 8 7 6 5 4 3 2 1 ppm

15b

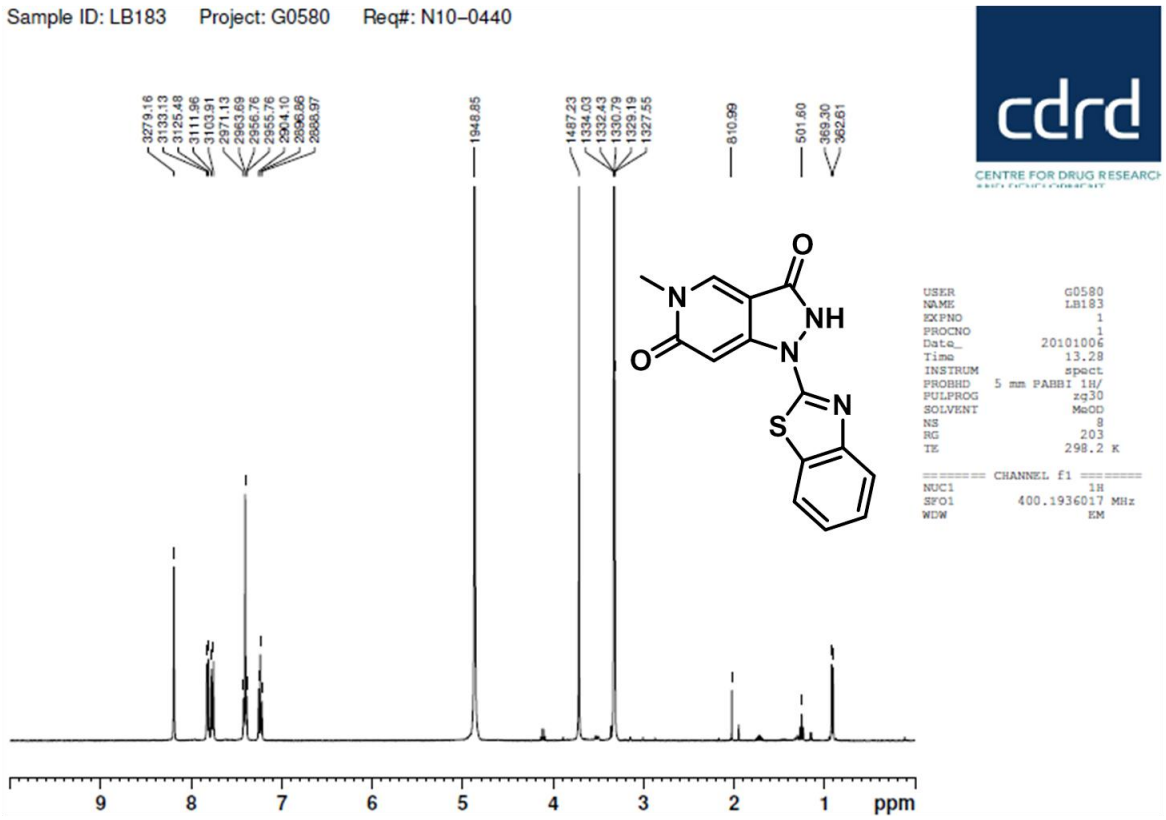
Sample ID: LB183 Project: G0580 Req#: N10–0440
3279.16
3133.13
3125.48
3111.96
3103.91
2971.13
2963.69
2956.76
2955.76
2904.10
2896.86
2868.97
1948.85
1487.23
1334.03
1332.43
1330.79
1329.19
1327.55
810.99
501.80
369.30
362.61
O
N
NH
O
N
N
S
USER G0580
NAME LB183
EXPNO 1
PROCNO 1
Date_ 20101006
Time 13.28
INSTRUM spect
PROBHD 5 mm PABBI 1H/
PULPROG zg30
SOLVENT MeOD
NS 8
RG 203
TE 298.2 K
CHANNEL f1
NUC1 1H
SFO1 400.1936017 MHz
WDW EM
9
8
7
6
5
4
3
2
1
ppm

15c

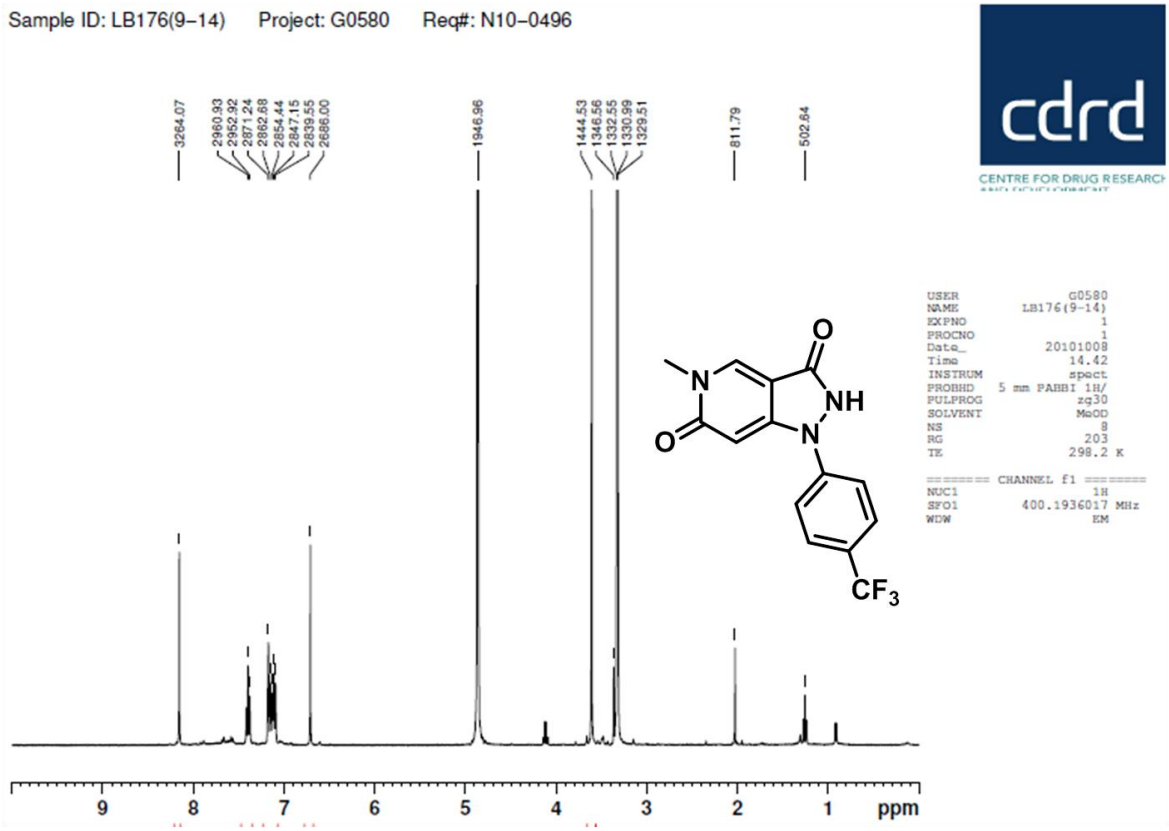
Sample ID: LB176(9–14) Project: G0580 Req#: N10–0496
3264.07
2960.93
2952.92
2871.24
2862.68
2854.44
2847.15
2839.55
2686.00
1946.96
1444.53
1346.56
1332.55
1330.99
1329.51
811.79
502.84
O
N
NH
O
N
CF3
USER G0580
NAME LB176(9-14)
EXPNO 1
PROCNO 1
Date_ 20101008
Time 14.42
INSTRUM spect
PROBHD 5 mm PABBI 1H/
PULPROG zg30
SOLVENT MeOD
NS 8
RG 203
TE 298.2 K
CHANNEL f1
NUC1 1H
SFO1 400.1936017 MHz
WDW EM
9
8
7
6
5
4
3
2
1
ppm

16a

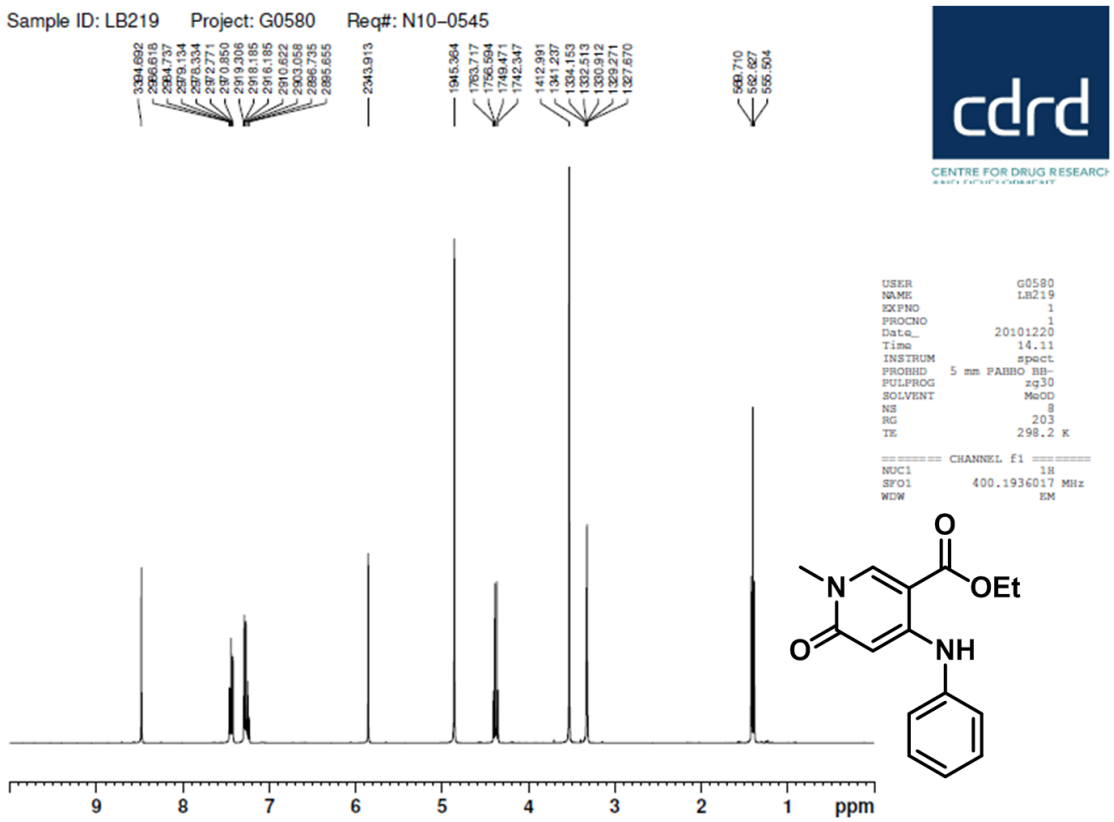
Sample ID: LB219 Project: G0580 Req#: N10–0545
cdrd
CENTRE FOR DRUG RESEARCH
USER G0580
NAME LB219
EXPNO 1
PROCNO 1
Date_ 20101220
Time 14.11
INSTRUM spect
PROBHD 5 mm PABBO BB-
PULPROG zg30
SOLVENT MeOD
NS 8
RG 203
TE 298.2 K
CHANNEL f1
NUC1 1H
SFO1 400.1936017 MHz
WDW EM
O
OEt
N
O
NH
9 8 7 6 5 4 3 2 1 ppm

16b

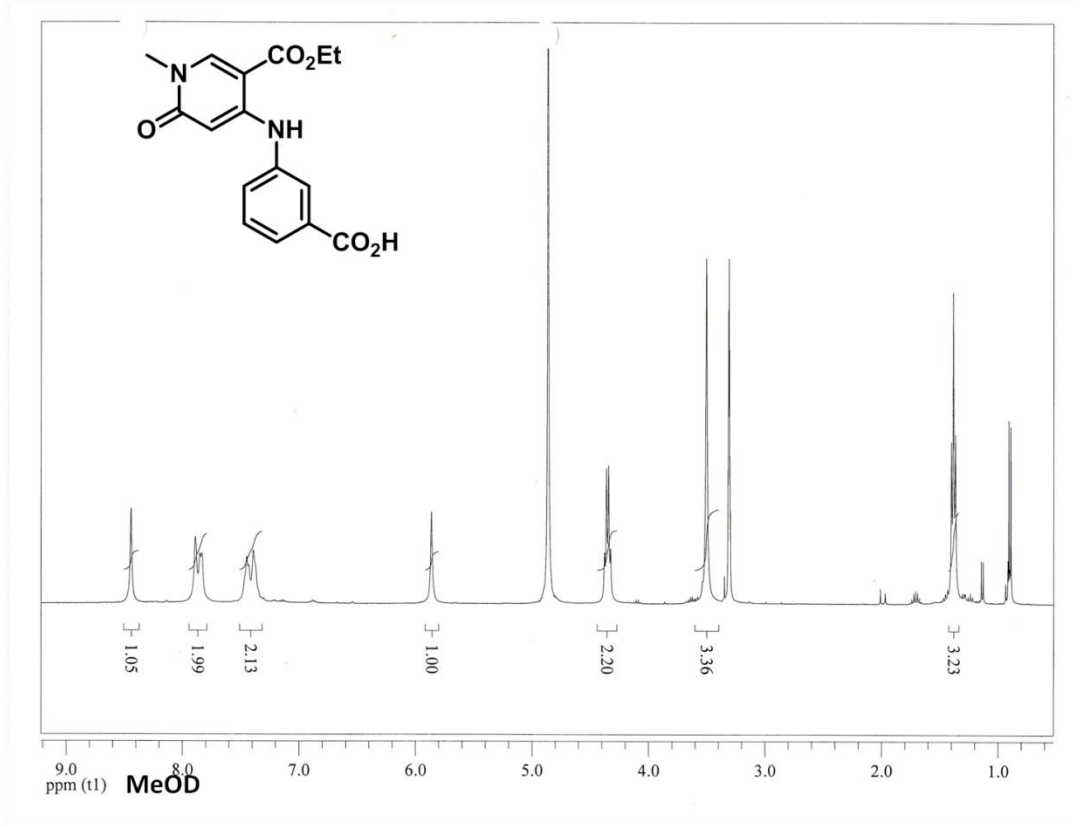
CO2Et
N
O
NH
CO2H
1.05
1.99
2.13
1.00
2.20
3.36
3.23
9.0 8.0 7.0 6.0 5.0 4.0 3.0 2.0 1.0
ppm (t1)
MeOD

16c

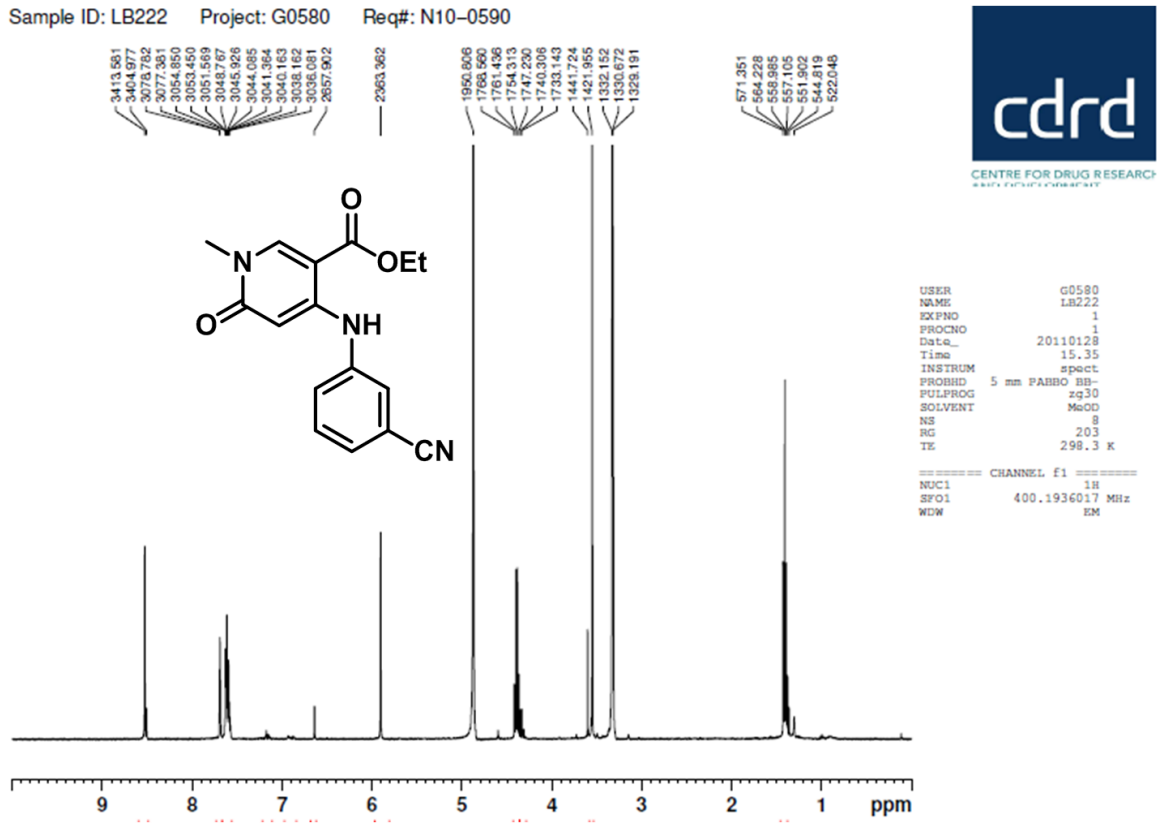
Sample ID: LB222 Project: G0580 Req#: N10–0590
3413.581
3404.977
3078.782
3077.381
3054.850
3053.450
3051.569
3048.767
3045.928
3044.085
3041.364
3040.163
3038.162
3036.081
2857.902
2363.362
1950.806
1768.560
1761.496
1754.313
1747.230
1740.306
1733.143
1441.724
1421.955
1332.152
1330.672
1329.191
571.351
564.228
558.985
557.105
551.902
544.819
522.048
O
OEt
N
O
NH
CN
USER G0580
NAME LB222
EXPNO 1
PROCNO 1
Date_ 20110128
Time 15.35
INSTRUM spect
PROBHD 5 mm PABBO BB-
PULPROG zg30
SOLVENT MeOD
NS 8
RG 203
TE 298.3 K
CHANNEL f1
NUC1 1H
SFO1 400.1936017 MHz
WDW EM
9
8
7
6
5
4
3
2
1
ppm

16d

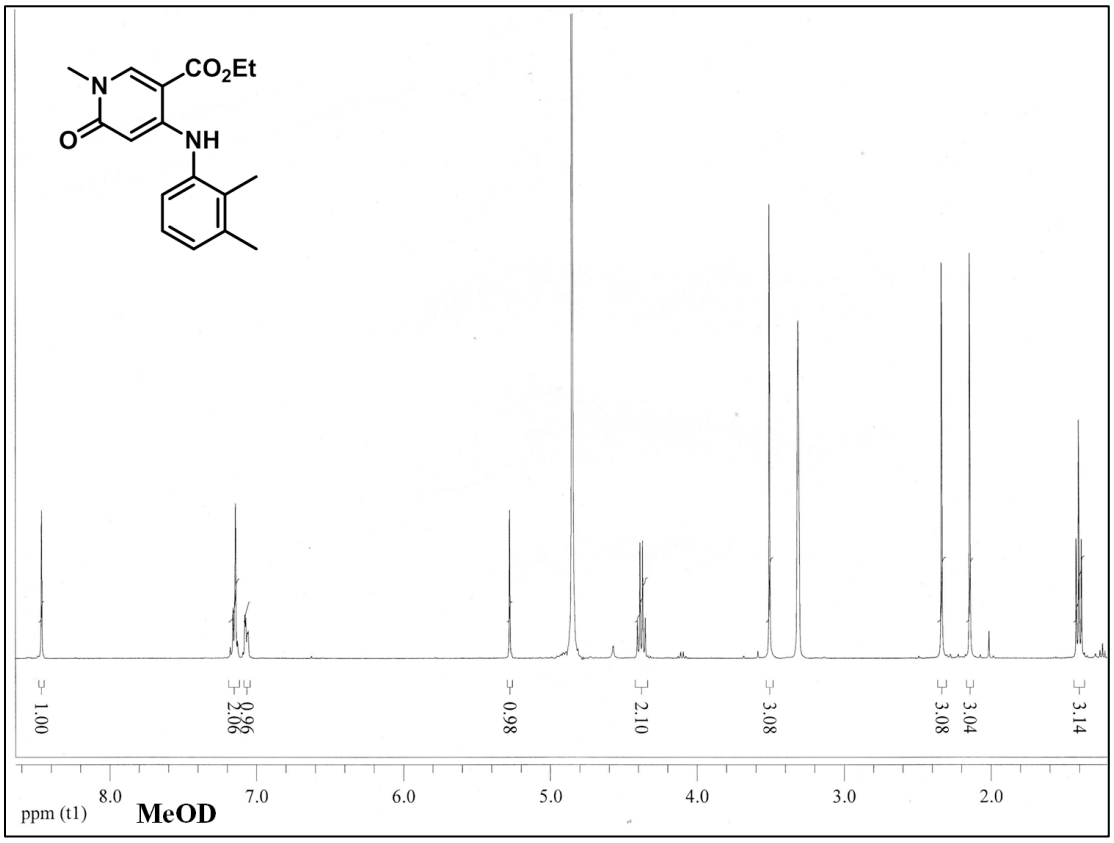
CO2Et
N
O
NH
1.00
0.96
2.06
0.98
2.10
3.08
3.08
3.04
3.14
8.0
7.0
6.0
5.0
4.0
3.0
2.0
ppm (t1)
MeOD

17

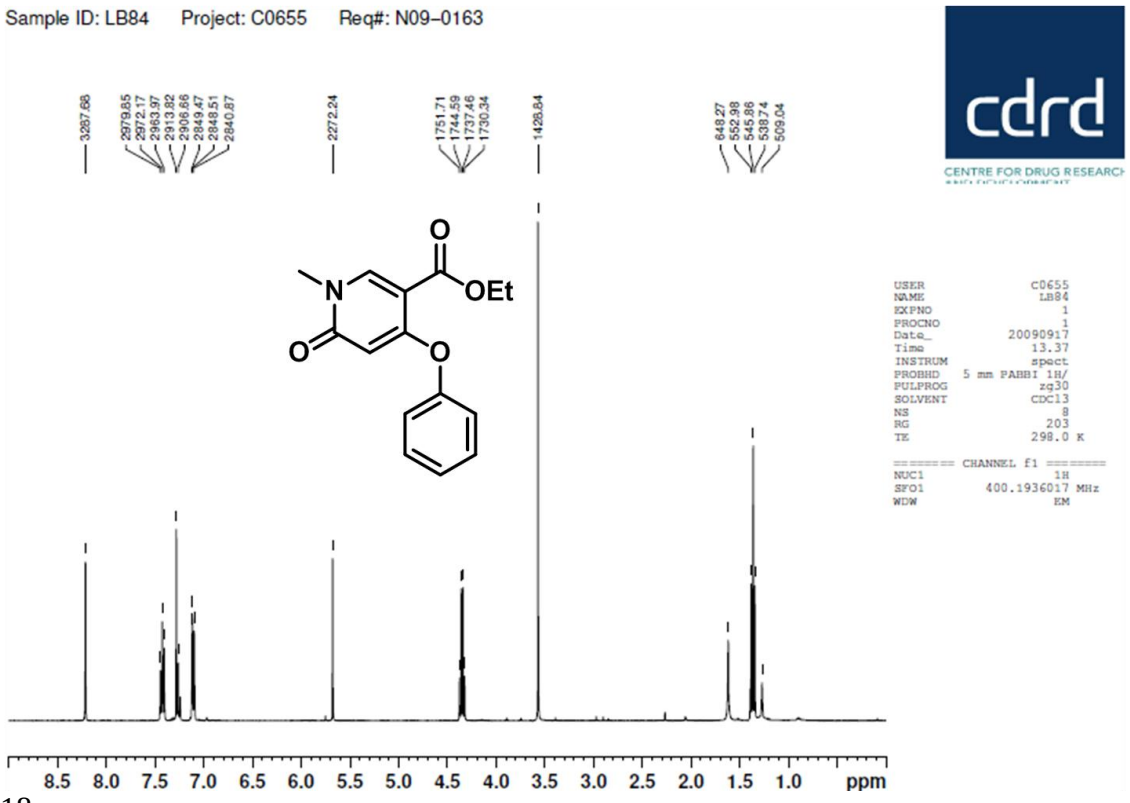
Sample ID: LB84 Project: C0655 Req#: N09-0163
3267.66
2979.85
2972.17
2963.97
2913.82
2906.66
2849.47
2848.51
2840.87
2272.24
1751.71
1744.59
1737.46
1730.34
1428.84
848.27
552.98
545.86
538.74
509.04
CENTRE FOR DRUG RESEARCH
O
N
OEt
O
O
USER C0655
NAME LB84
EXPNO 1
PROCNO 1
Date_ 20090917
Time 13.37
INSTRUM spect
PROBHD 5 mm PABBI 1H/
PULPROG zg30
SOLVENT CDCl3
NS 8
RG 203
TE 298.0 K
CHANNEL f1
NUC1 1H
SFO1 400.1936017 MHz
WDW EM
8.5 8.0 7.5 7.0 6.5 6.0 5.5 5.0 4.5 4.0 3.5 3.0 2.5 2.0 1.5 1.0 ppm

18a

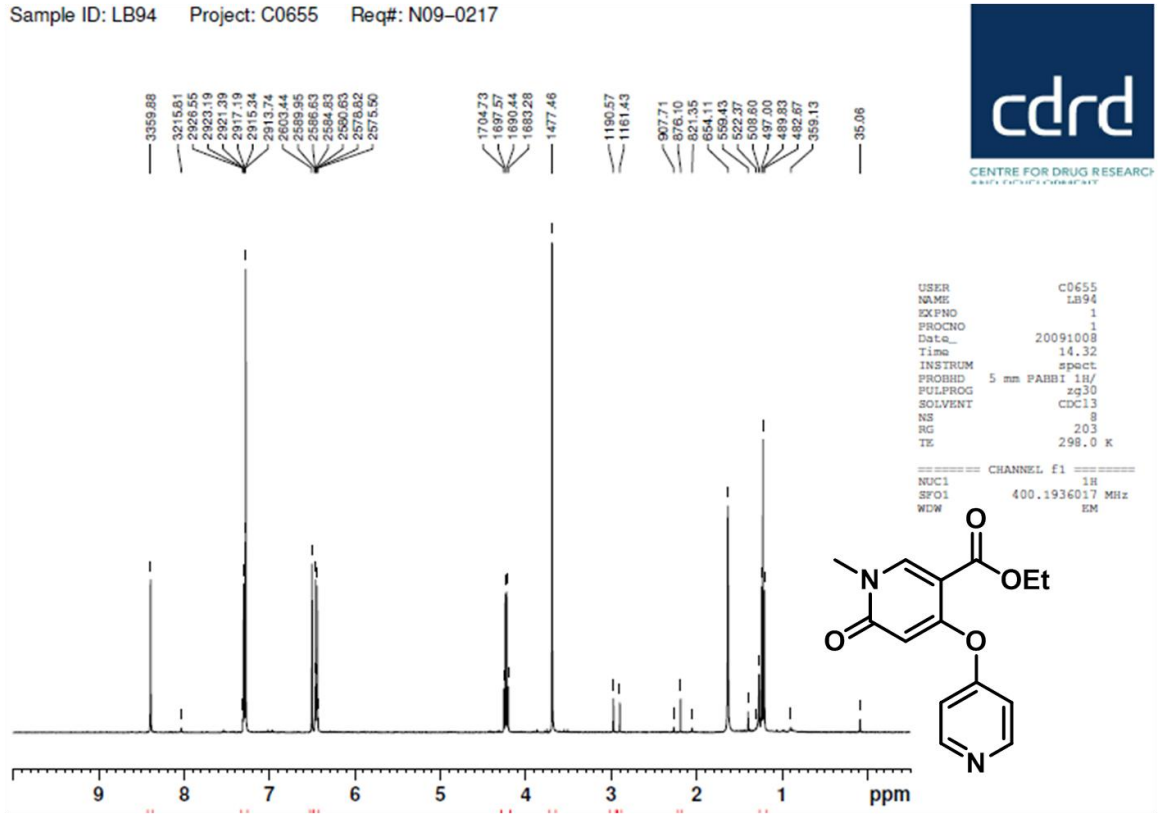
Sample ID: LB94 Project: C0655 Req#: N09-0217
3359.88
3215.81
2928.55
2923.19
2921.39
2917.19
2915.34
2913.74
2603.44
2589.95
2586.63
2584.83
2580.63
2578.82
2575.50
1704.73
1697.57
1690.44
1683.28
1477.46
1190.57
1161.43
907.71
876.10
821.35
654.11
599.43
522.37
508.60
497.00
489.83
482.67
359.13
35.06
CENTRE FOR DRUG RESEARCH
USER C0655
NAME LB94
EXPNO 1
PROCNO 1
Date_ 20091008
Time 14.32
INSTRUM spect
PROBHD 5 mm PABBI 1H/
PULPROG zg30
SOLVENT CDCl3
NS 8
RG 203
TE 298.0 K
CHANNEL f1
NUC1 1H
SFO1 400.1936017 MHz
WDW EM
O
N
OEt
O
O
N
9 8 7 6 5 4 3 2 1 ppm

18b

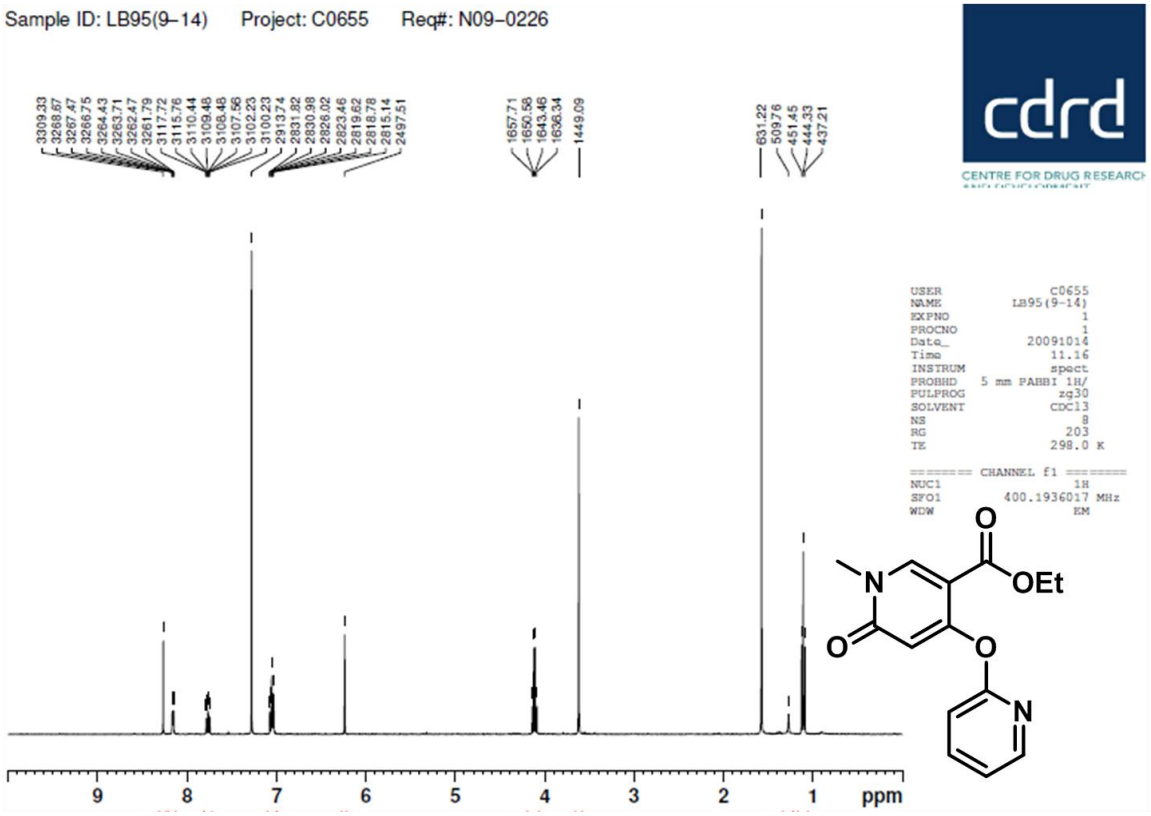
Sample ID: LB95(9–14) Project: C0655 Req#: N09–0226
cdrd
CENTRE FOR DRUG RESEARCH
3309.33
3268.67
3267.47
3266.75
3264.43
3263.71
3262.47
3261.79
3117.72
3115.76
3110.44
3109.48
3108.48
3107.56
3102.23
3100.23
2913.74
2831.82
2830.98
2826.02
2823.46
2819.62
2818.78
2815.14
2497.51
1657.71
1650.58
1643.46
1636.34
1449.09
631.22
509.76
451.45
444.33
437.21
USER C0655
NAME LB95(9-14)
EXPNO 1
PROCNO 1
Date_ 20091014
Time 11.16
INSTRUM spect
PROBHD 5 mm PABBI 1H/
PULPROG zg30
SOLVENT CDCl3
NS 8
RG 203
TE 298.0 K
CHANNEL f1
NUC1 1H
SFO1 400.1936017 MHz
WDW EM
O
OEt
N
O
O
N
9
8
7
6
5
4
3
2
1
ppm

19

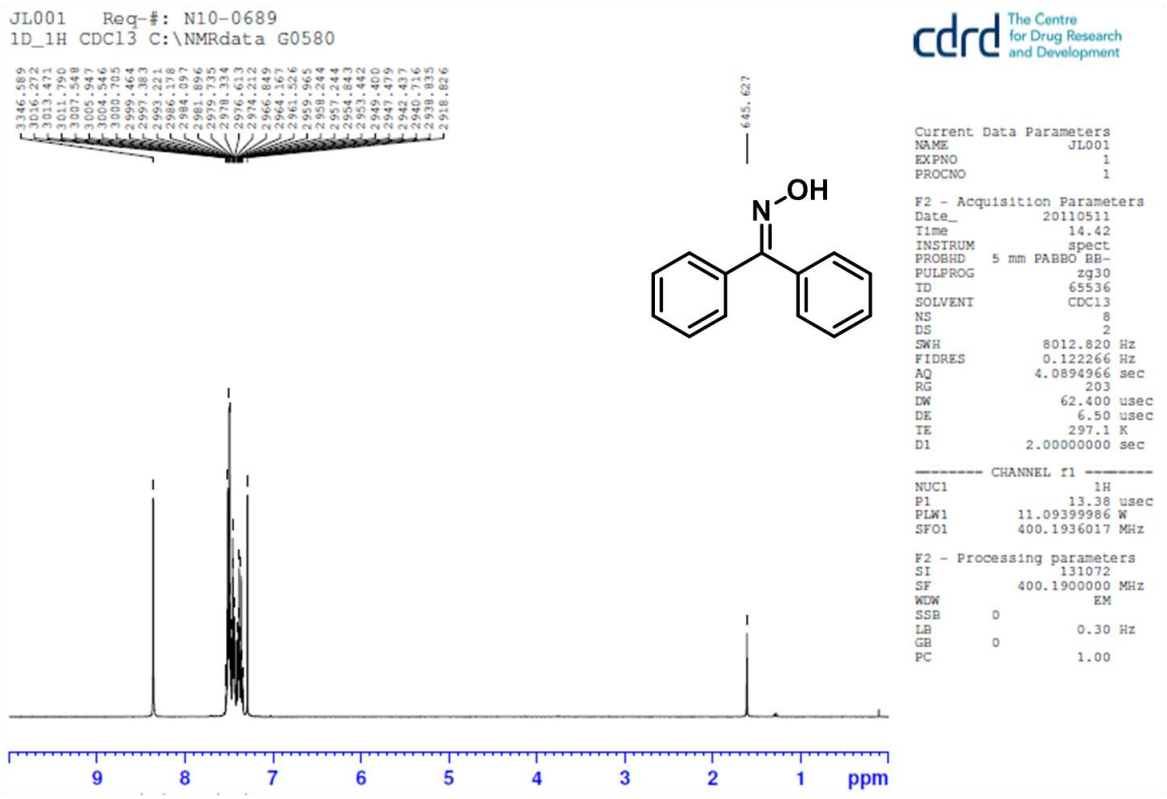
JL001 Req-#: N10-0689
1D_1H CDCl3 C:\NMRdata G0580
cdrd The Centre for Drug Research and Development
3346.589
3016.272
3013.471
3011.790
3007.548
3005.947
3004.546
3000.705
2999.464
2997.383
2993.221
2986.178
2984.097
2981.936
2979.735
2978.334
2976.613
2974.212
2966.849
2964.167
2961.526
2959.965
2958.244
2957.244
2954.843
2953.442
2949.400
2947.479
2942.437
2940.716
2938.835
2918.826
645.627
N
OH
Current Data Parameters
NAME JL001
EXPNO 1
PROCNO 1
F2 - Acquisition Parameters
Date_ 20110511
Time 14.42
INSTRUM spect
PROBHD 5 mm PABBO BB-
PULPROG zg30
TD 65536
SOLVENT CDCl3
NS 8
DS 2
SWH 8012.820 Hz
FIDRES 0.122266 Hz
AQ 4.0894966 sec
RG 203
DW 62.400 usec
DE 6.50 usec
TE 297.1 K
D1 2.00000000 sec
CHANNEL f1
NUC1 1H
P1 13.38 usec
PLW1 11.09399986 W
SFO1 400.1936017 MHz
F2 - Processing parameters
SI 131072
SF 400.1900000 MHz
WDW EM
SSB 0
LB 0.30 Hz
GB 0
PC 1.00
9
8
7
6
5
4
3
2
1
ppm

20

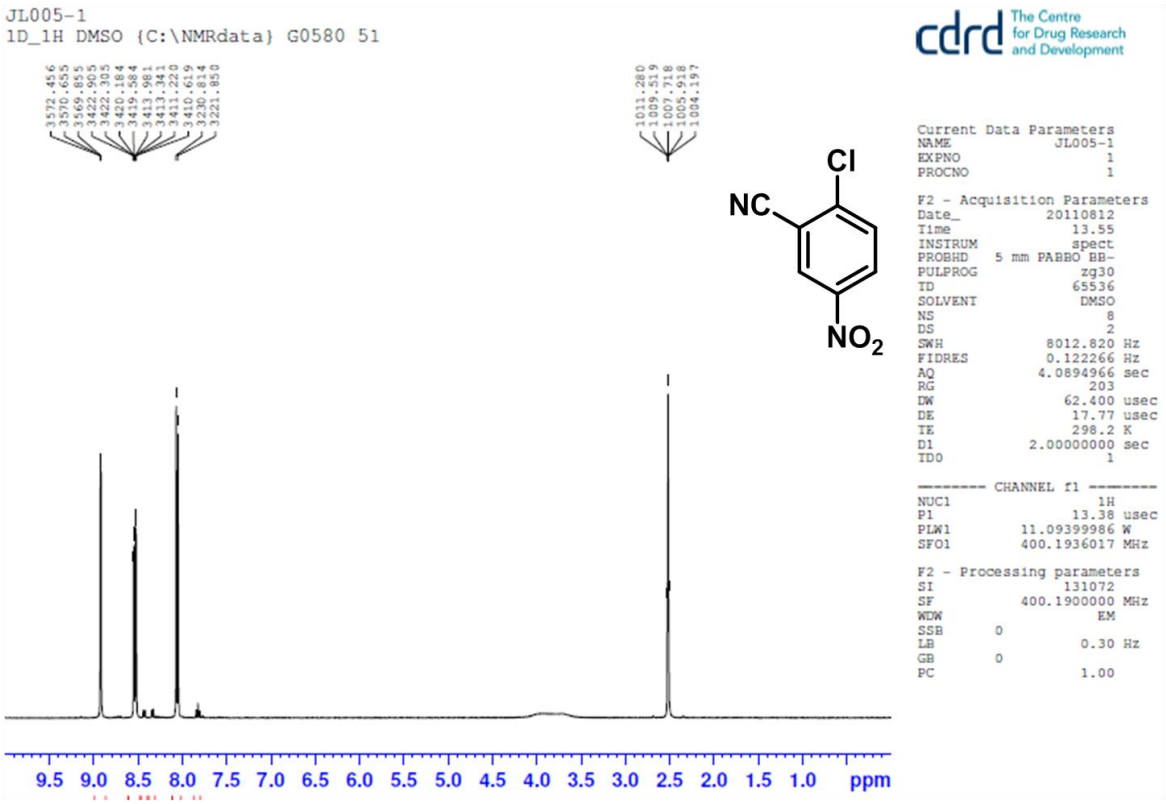

The Centre for Drug Research and Development

```
Current Data Parameters
NAME                  JL005-1
EXPNO                       1
PROCNO                      1

F2 - Acquisition Parameters
Date_              20110812
Time                  13.55
INSTRUM               spect
PROBHD    5 mm PABBO BB-
PULPROG                zg30
TD                    65536
SOLVENT                DMSO
NS                        8
DS                        2
SWH                8012.820 Hz
FIDRES            0.122266 Hz
AQ                4.0894966 sec
RG                      203
DW                   62.400 usec
DE                   17.77 usec
TE                   298.2 K
D1              2.00000000 sec
TD0                       1

======== CHANNEL f1 ========
NUC1                    1H
P1                   13.38 usec
PLW1           11.09399986 W
SFO1           400.1936017 MHz

F2 - Processing parameters
SI                   131072
SF              400.1900000 MHz
WDW                     EM
SSB          0
LB                    0.30 Hz
GB           0
PC                    1.00
```

21a

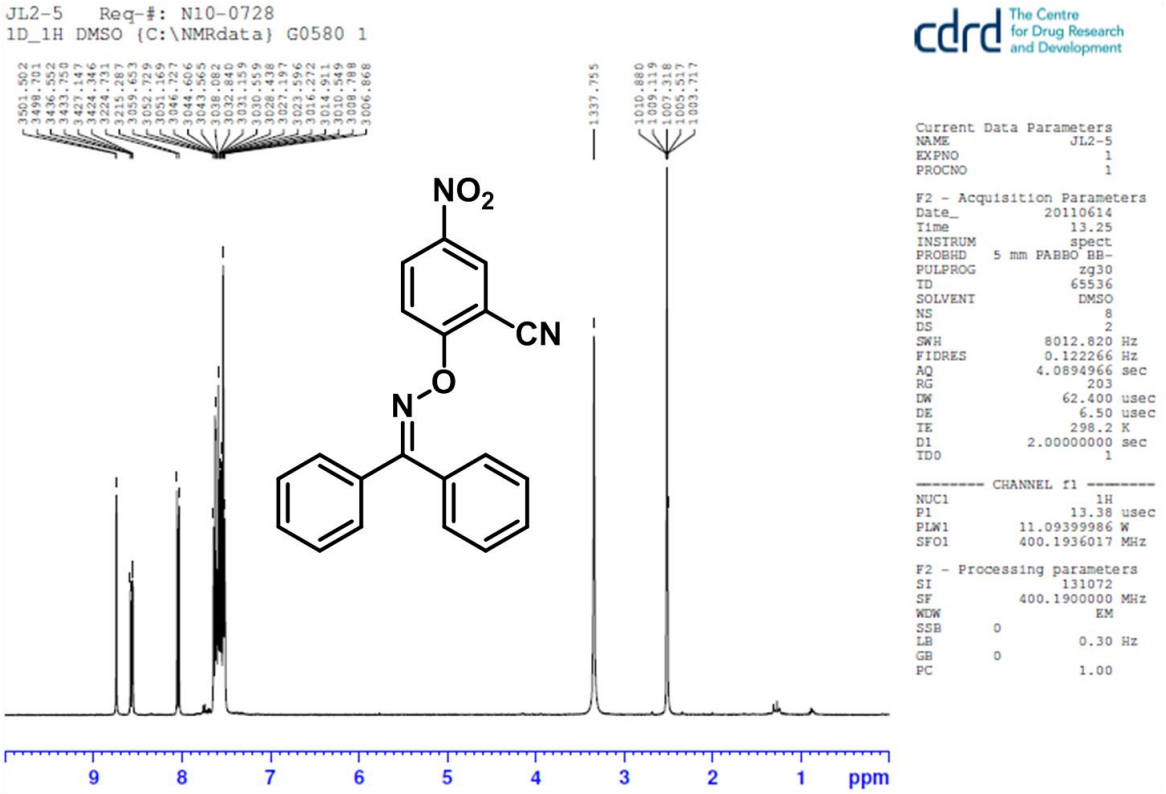

The Centre for Drug Research and Development

```
Current Data Parameters
NAME                  JL2-5
EXPNO                       1
PROCNO                      1

F2 - Acquisition Parameters
Date_              20110614
Time                  13.25
INSTRUM               spect
PROBHD    5 mm PABBO BB-
PULPROG                zg30
TD                    65536
SOLVENT                DMSO
NS                        8
DS                        2
SWH                8012.820 Hz
FIDRES            0.122266 Hz
AQ                4.0894966 sec
RG                      203
DW                   62.400 usec
DE                    6.50 usec
TE                   298.2 K
D1              2.00000000 sec
TD0                       1

======== CHANNEL f1 ========
NUC1                    1H
P1                   13.38 usec
PLW1           11.09399986 W
SFO1           400.1936017 MHz

F2 - Processing parameters
SI                   131072
SF              400.1900000 MHz
WDW                     EM
SSB          0
LB                    0.30 Hz
GB           0
PC                    1.00
```

21b

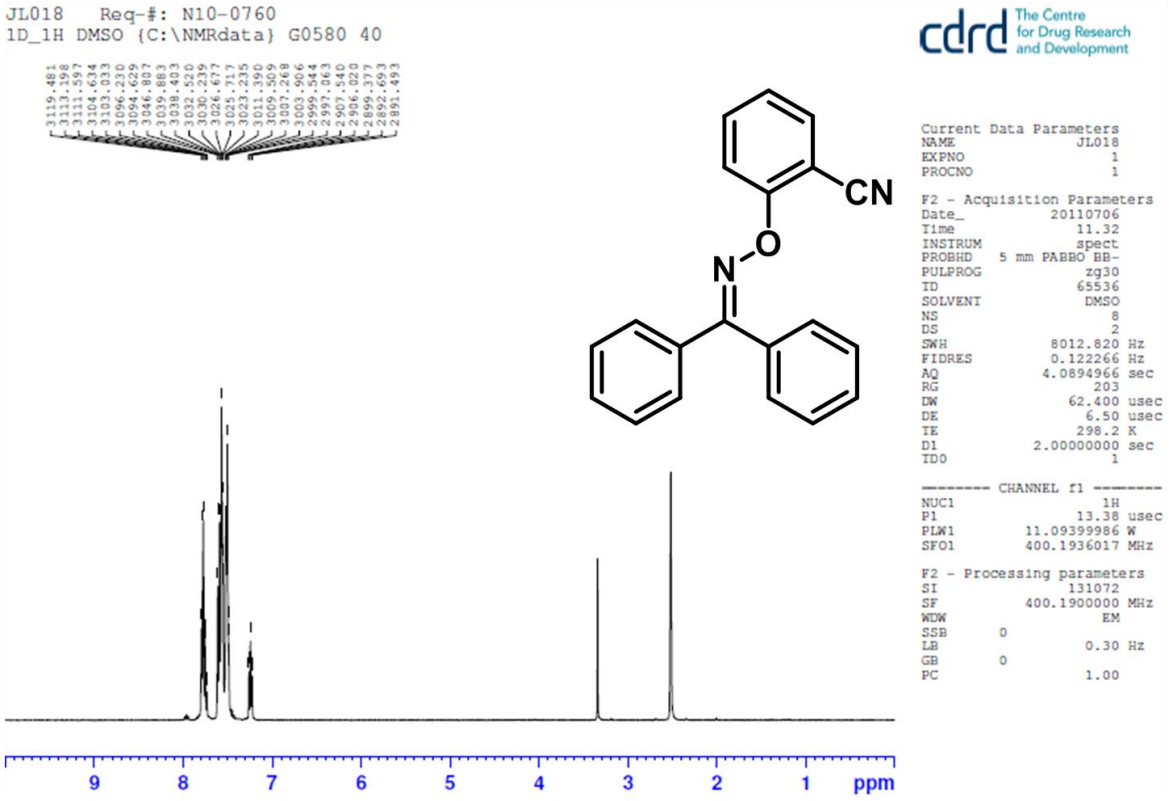

The Centre for Drug Research and Development

```
Current Data Parameters
NAME                  JL018
EXPNO                     1
PROCNO                    1

F2 - Acquisition Parameters
Date_              20110706
Time                  11.32
INSTRUM               spect
PROBHD    5 mm PABBO BB-
PULPROG                zg30
TD                    65536
SOLVENT                DMSO
NS                        8
DS                        2
SWH                8012.820 Hz
FIDRES            0.122266 Hz
AQ                4.0894966 sec
RG                      203
DW                   62.400 usec
DE                    6.50 usec
TE                   298.2 K
D1                2.00000000 sec
TD0                       1

======== CHANNEL f1 ========
NUC1                      1H
P1                    13.38 usec
PLW1           11.09399986 W
SFO1           400.1936017 MHz

F2 - Processing parameters
SI                      131072
SF              400.1900000 MHz
WDW                       EM
SSB          0
LB                    0.30 Hz
GB           0
PC                    1.00
```

22a

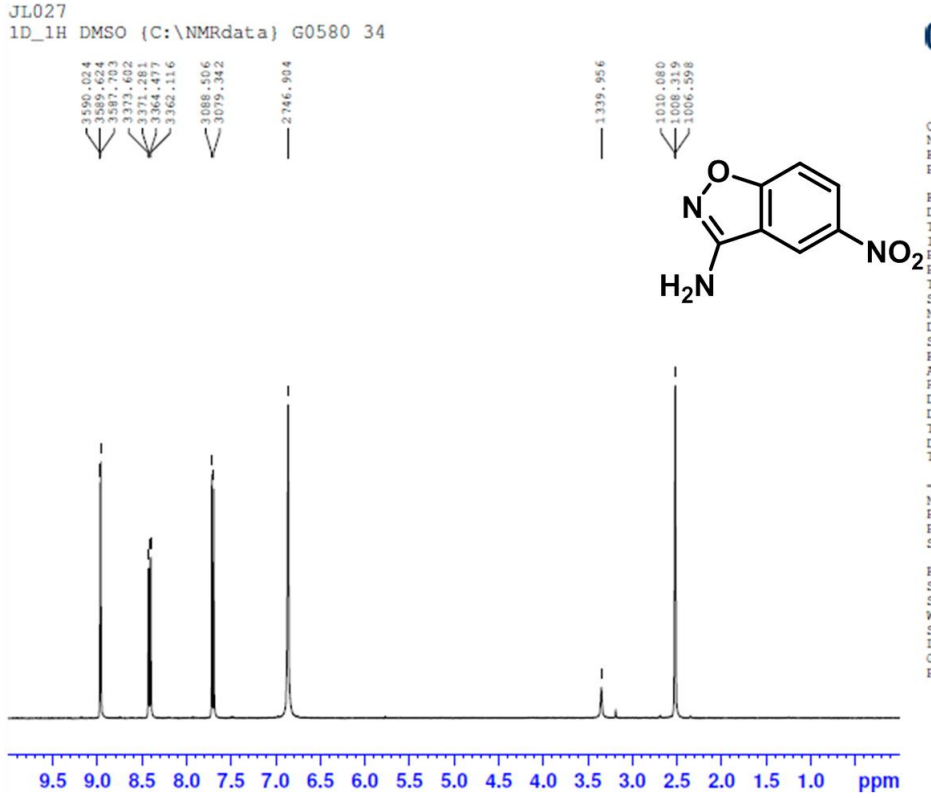

The Centre for Drug Research and Development

```
Current Data Parameters
NAME                  JL027
EXPNO                     1
PROCNO                    1

F2 - Acquisition Parameters
Date_              20110713
Time                  13.42
INSTRUM               spect
PROBHD    5 mm PABBO BB-
PULPROG                zg30
TD                    65536
SOLVENT                DMSO
NS                        8
DS                        2
SWH                8012.820 Hz
FIDRES            0.122266 Hz
AQ                4.0894966 sec
RG                      203
DW                   62.400 usec
DE                   16.66 usec
TE                   298.2 K
D1                2.00000000 sec
TD0                       1

======== CHANNEL f1 ========
NUC1                      1H
P1                    13.38 usec
PLW1           11.09399986 W
SFO1           400.1936017 MHz

F2 - Processing parameters
SI                      131072
SF              400.1900000 MHz
WDW                       EM
SSB          0
LB                    0.30 Hz
GB           0
PC                    1.00
```

22b

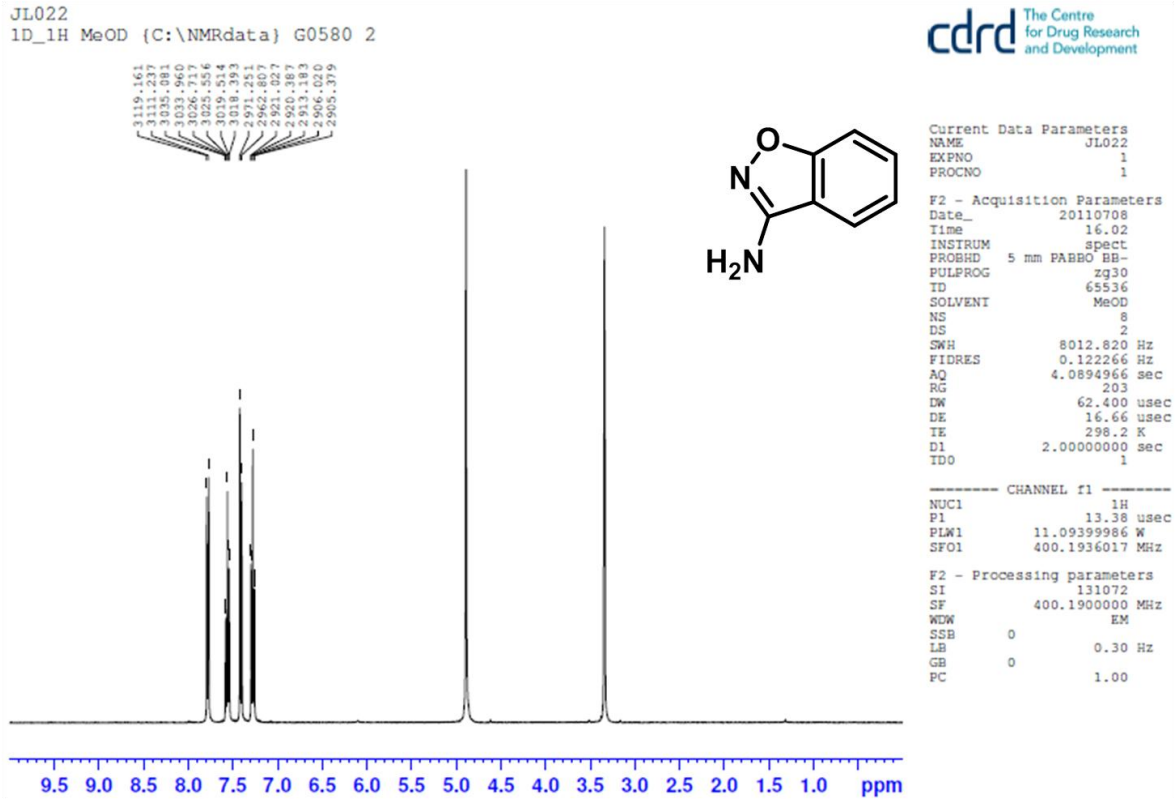

cdrd The Centre for Drug Research and Development

```
Current Data Parameters
NAME                   JL022
EXPNO                      1
PROCNO                     1

F2 - Acquisition Parameters
Date_               20110708
Time                   16.02
INSTRUM                spect
PROBHD    5 mm PABBO BB-
PULPROG                zg30
TD                    65536
SOLVENT                MeOD
NS                         8
DS                         2
SWH                8012.820 Hz
FIDRES            0.122266 Hz
AQ                4.0894966 sec
RG                       203
DW                  62.400 usec
DE                  16.66 usec
TE                  298.2 K
D1               2.00000000 sec
TD0                        1

======== CHANNEL f1 ========
NUC1                      1H
P1                    13.38 usec
PLW1           11.09399986 W
SFO1           400.1936017 MHz

F2 - Processing parameters
SI                    131072
SF             400.1900000 MHz
WDW                       EM
SSB       0
LB                  0.30 Hz
GB        0
PC                    1.00
```

23a

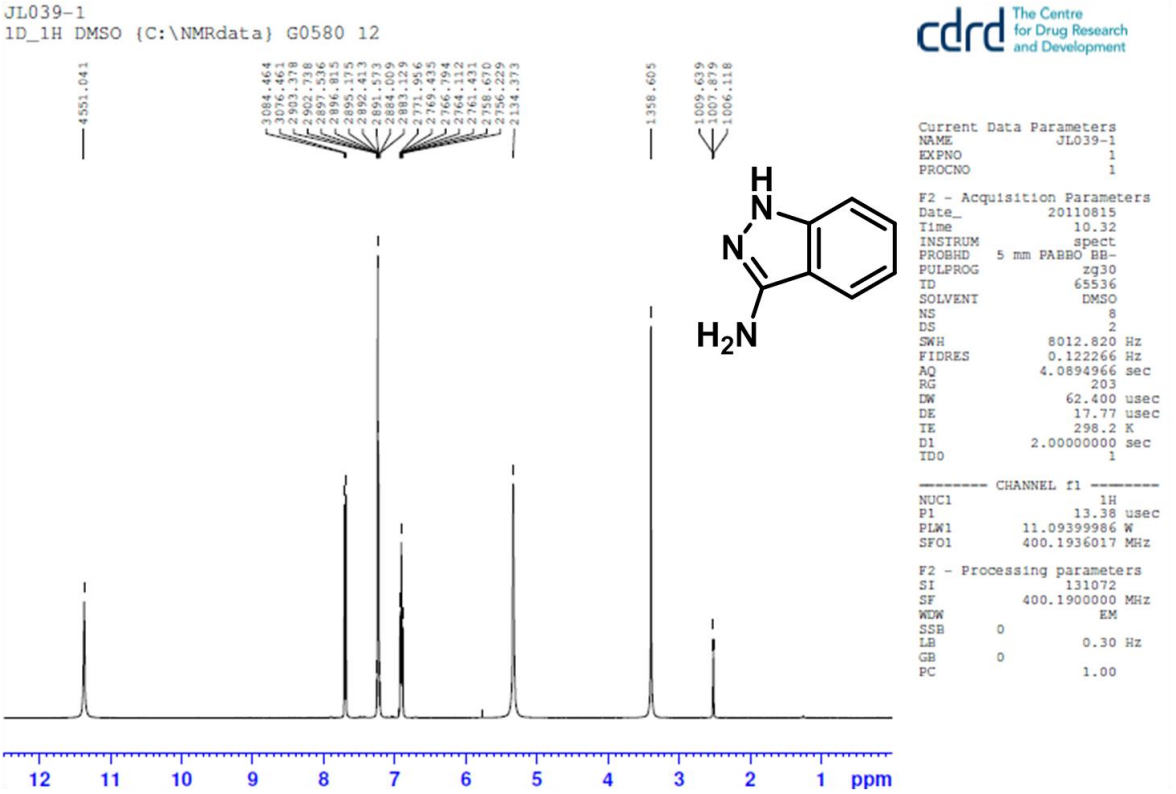

cdrd The Centre for Drug Research and Development

```
Current Data Parameters
NAME                 JL039-1
EXPNO                      1
PROCNO                     1

F2 - Acquisition Parameters
Date_               20110815
Time                   10.32
INSTRUM                spect
PROBHD    5 mm PABBO BB-
PULPROG                zg30
TD                    65536
SOLVENT                DMSO
NS                         8
DS                         2
SWH                8012.820 Hz
FIDRES            0.122266 Hz
AQ                4.0894966 sec
RG                       203
DW                  62.400 usec
DE                  17.77 usec
TE                  298.2 K
D1               2.00000000 sec
TD0                        1

======== CHANNEL f1 ========
NUC1                      1H
P1                    13.38 usec
PLW1           11.09399986 W
SFO1           400.1936017 MHz

F2 - Processing parameters
SI                    131072
SF             400.1900000 MHz
WDW                       EM
SSB       0
LB                  0.30 Hz
GB        0
PC                    1.00
```

23b

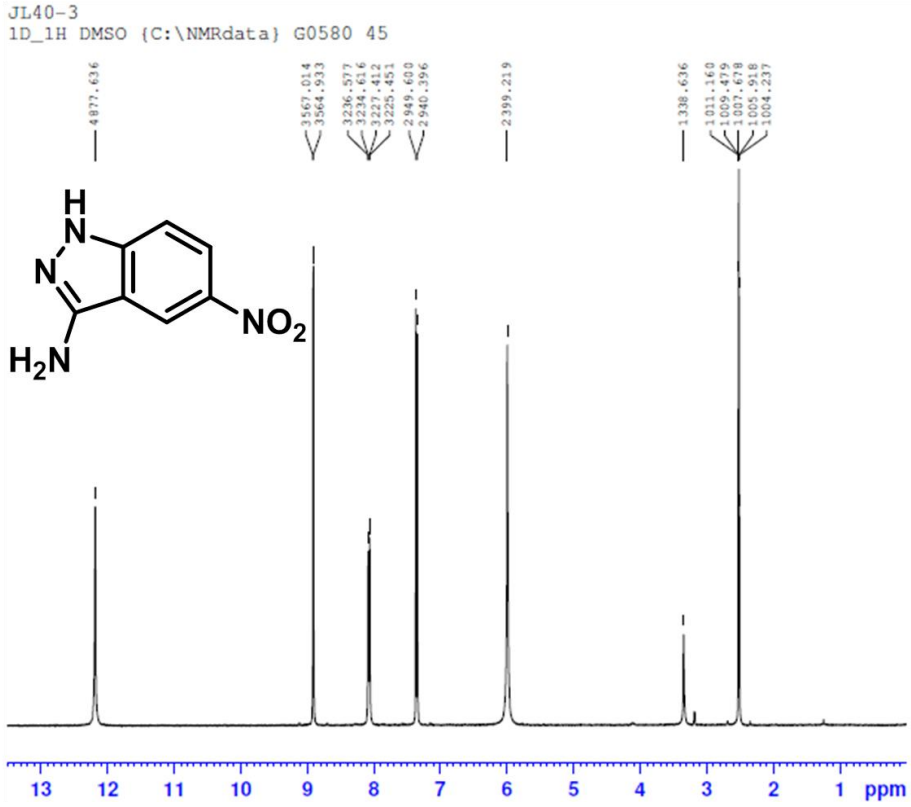

cdrd The Centre for Drug Research and Development

```
Current Data Parameters
NAME                  JL40-3
EXPNO                      1
PROCNO                     1

F2 - Acquisition Parameters
Date_              20110824
Time                  16.25
INSTRUM               spect
PROBHD   5 mm PABBO BB-
PULPROG                zg30
TD                    65536
SOLVENT                DMSO
NS                         8
DS                         2
SWH                8012.820 Hz
FIDRES            0.122266 Hz
AQ                4.0894966 sec
RG                       203
DW                  62.400 usec
DE                  17.77 usec
TE                  298.2 K
D1                2.00000000 sec
TD0                        1

======== CHANNEL f1 ========
NUC1                      1H
P1                    13.38 usec
PLW1           11.09399986 W
SFO1           400.1936017 MHz

F2 - Processing parameters
SI                       131072
SF              400.1900000 MHz
WDW                        EM
SSB          0
LB                    0.30 Hz
GB           0
PC                    1.00
```

24a

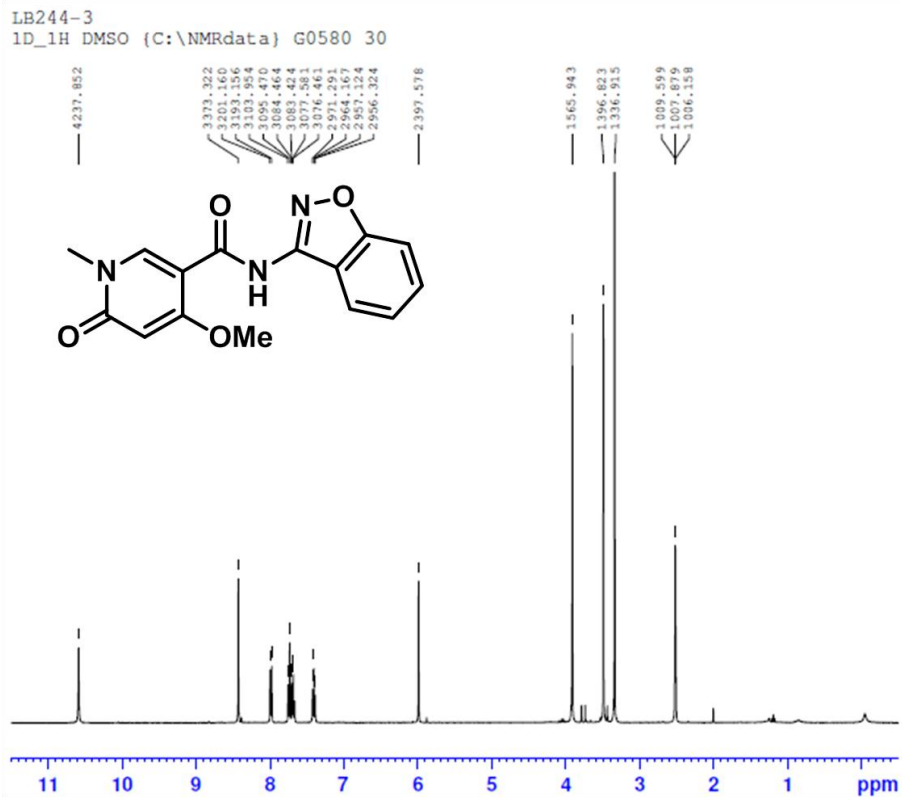

cdrd The Centre for Drug Research and Development

```
Current Data Parameters
NAME                  LB244-3
EXPNO                      1
PROCNO                     1

F2 - Acquisition Parameters
Date_              20111116
Time                  13.57
INSTRUM               spect
PROBHD   5 mm PABBO BB-
PULPROG                zg30
TD                    65536
SOLVENT                DMSO
NS                         8
DS                         2
SWH                8012.820 Hz
FIDRES            0.122266 Hz
AQ                4.0894966 sec
RG                       203
DW                  62.400 usec
DE                  17.77 usec
TE                  298.2 K
D1                2.00000000 sec
TD0                        1

======== CHANNEL f1 ========
NUC1                      1H
P1                    13.38 usec
PLW1           11.09399986 W
SFO1           400.1936017 MHz

F2 - Processing parameters
SI                       131072
SF              400.1900000 MHz
WDW                        EM
SSB          0
LB                    0.30 Hz
GB           0
PC                    1.00
```

24b

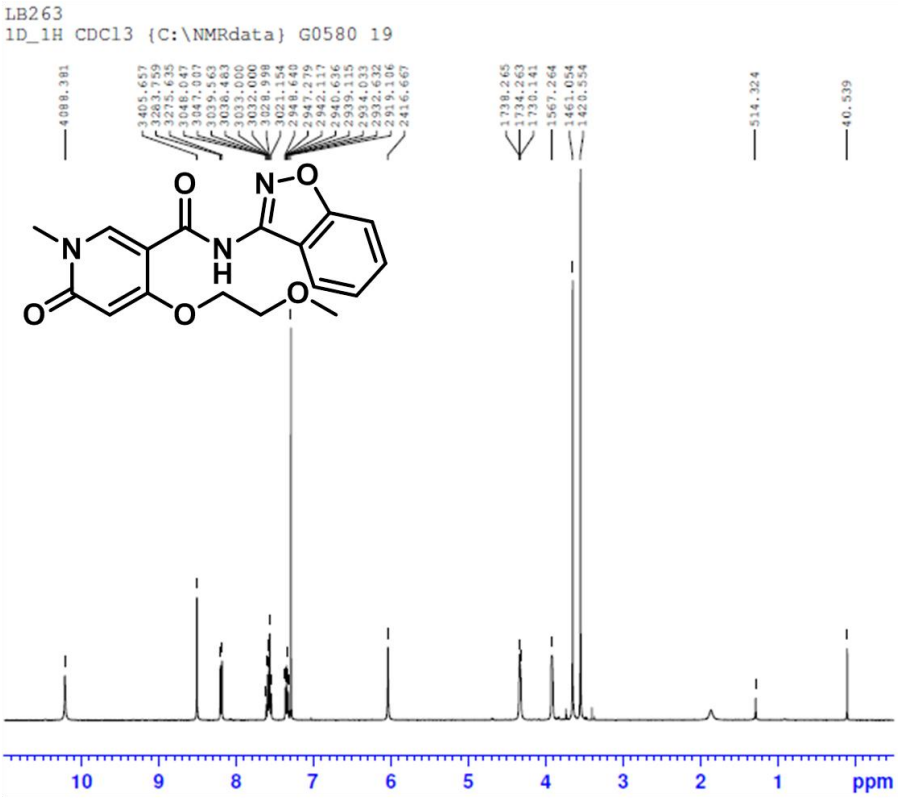

cdrd The Centre for Drug Research and Development

```
Current Data Parameters
NAME                  LB263
EXPNO                     1
PROCNO                    1

F2 - Acquisition Parameters
Date_              20110818
Time                  11.25
INSTRUM               spect
PROBHD    5 mm PABBO BB-
PULPROG                zg30
TD                    65536
SOLVENT               CDCl3
NS                        8
DS                        2
SWH                8012.820 Hz
FIDRES            0.122266 Hz
AQ                4.0894966 sec
RG                      203
DW                   62.400 usec
DE                   17.77 usec
TE                   298.2 K
D1              2.00000000 sec
TD0                       1

======== CHANNEL f1 ========
NUC1                      1H
P1                    13.38 usec
PLW1           11.09399986 W
SFO1           400.1936017 MHz

F2 - Processing parameters
SI                      131072
SF              400.1900000 MHz
WDW                       EM
SSB          0
LB                    0.30 Hz
GB           0
PC                    1.00
```

24c

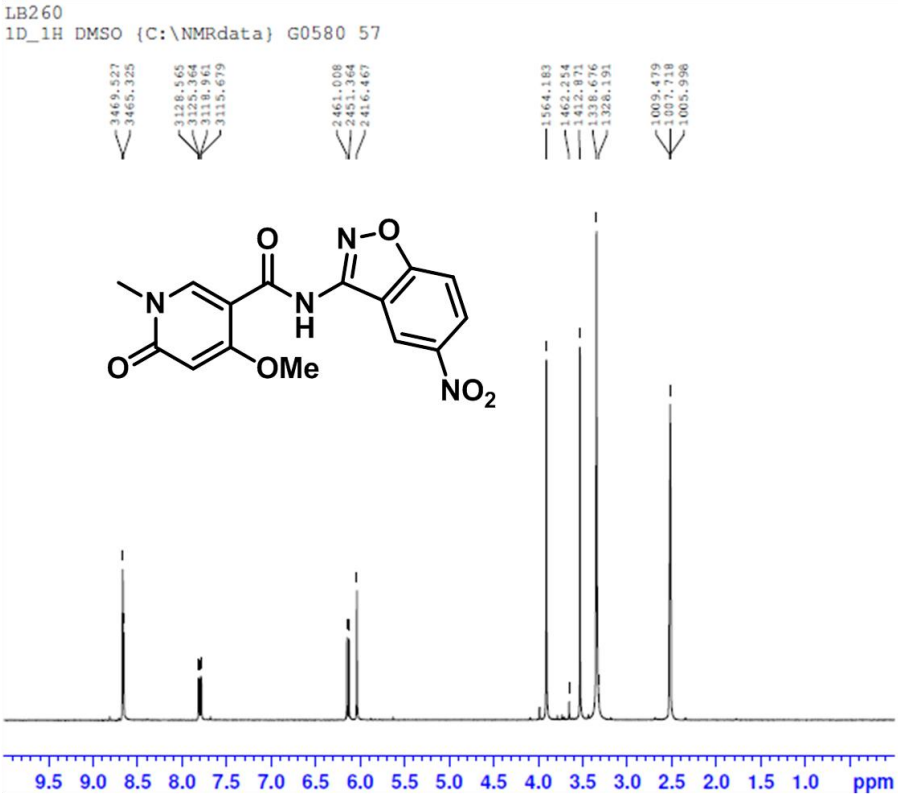

cdrd The Centre for Drug Research and Development

```
Current Data Parameters
NAME                  LB260
EXPNO                     1
PROCNO                    1

F2 - Acquisition Parameters
Date_              20110802
Time                  11.19
INSTRUM               spect
PROBHD    5 mm PABBO BB-
PULPROG                zg30
TD                    65536
SOLVENT                DMSO
NS                        8
DS                        2
SWH                8012.820 Hz
FIDRES            0.122266 Hz
AQ                4.0894966 sec
RG                      203
DW                   62.400 usec
DE                   13.41 usec
TE                   298.2 K
D1              2.00000000 sec
TD0                       1

======== CHANNEL f1 ========
NUC1                      1H
P1                    13.38 usec
PLW1           11.09399986 W
SFO1           400.1936017 MHz

F2 - Processing parameters
SI                      131072
SF              400.1900000 MHz
WDW                       EM
SSB          0
LB                    0.30 Hz
GB           0
PC                    1.00
```

24d

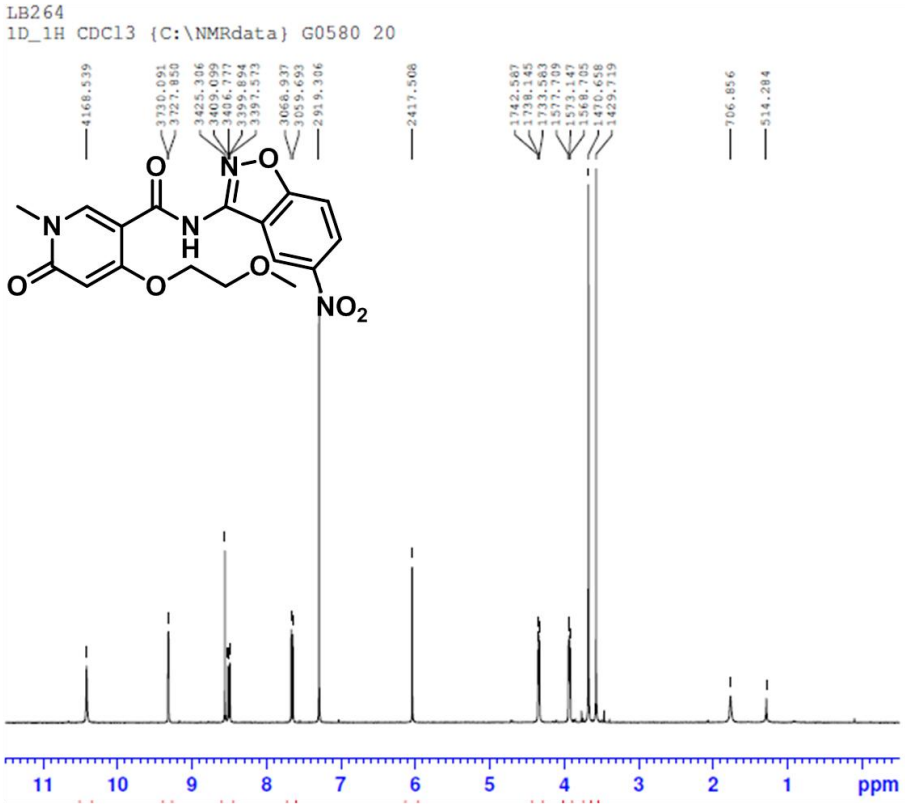

cdrd The Centre for Drug Research and Development

```
Current Data Parameters
NAME                  LB264
EXPNO                     1
PROCNO                    1

F2 - Acquisition Parameters
Date_              20110818
Time                  11.29
INSTRUM               spect
PROBHD    5 mm PABBO BB-
PULPROG                zg30
TD                    65536
SOLVENT               CDCl3
NS                        8
DS                        2
SWH                8012.820 Hz
FIDRES            0.122266 Hz
AQ                4.0894966 sec
RG                      203
DW                   62.400 usec
DE                   17.77 usec
TE                   298.2 K
D1              2.00000000 sec
TD0                       1

======== CHANNEL f1 ========
NUC1                      1H
P1                    13.38 usec
PLW1           11.09399986 W
SFO1           400.1936017 MHz

F2 - Processing parameters
SI                    131072
SF             400.1900000 MHz
WDW                       EM
SSB         0
LB                    0.30 Hz
GB          0
PC                    1.00
```

24e

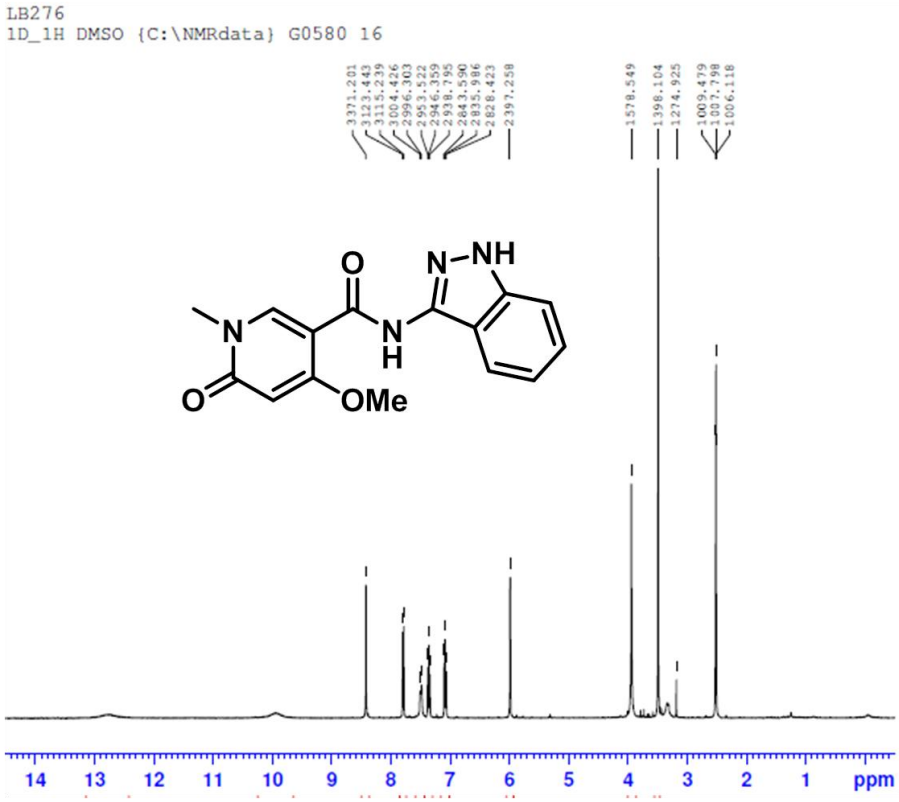

cdrd The Centre for Drug Research and Development

```
Current Data Parameters
NAME                  LB276
EXPNO                     1
PROCNO                    1

F2 - Acquisition Parameters
Date_              20110929
Time                  11.30
INSTRUM               spect
PROBHD    5 mm PABBO BB-
PULPROG                zg30
TD                    65536
SOLVENT                DMSO
NS                        8
DS                        2
SWH                8012.820 Hz
FIDRES            0.122266 Hz
AQ                4.0894966 sec
RG                      203
DW                   62.400 usec
DE                   17.77 usec
TE                   298.2 K
D1              2.00000000 sec
TD0                       1

======== CHANNEL f1 ========
NUC1                      1H
P1                    13.38 usec
PLW1           11.09399986 W
SFO1           400.1936017 MHz

F2 - Processing parameters
SI                    131072
SF             400.1900000 MHz
WDW                       EM
SSB         0
LB                    0.30 Hz
GB          0
PC                    1.00
```

24f

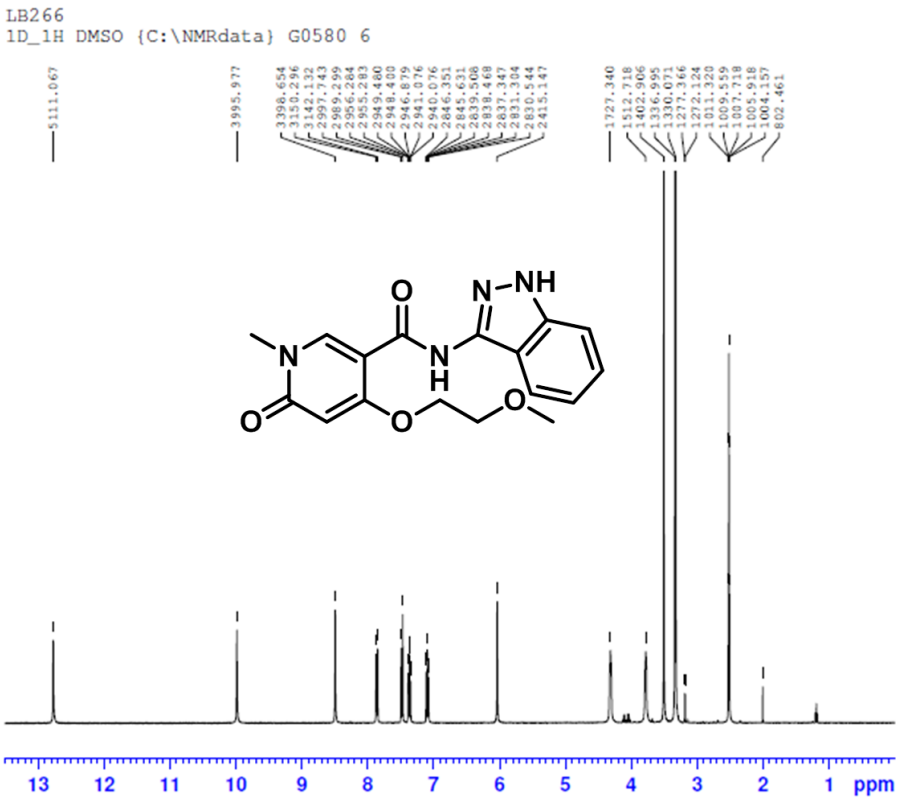


```
Current Data Parameters
NAME                  LB266
EXPNO                     1
PROCNO                    1

F2 - Acquisition Parameters
Date_              20110829
Time                  10.28
INSTRUM               spect
PROBHD    5 mm PABBO BB-
PULPROG               zg30
TD                   65536
SOLVENT               DMSO
NS                        8
DS                        2
SWH                8012.820 Hz
FIDRES            0.122266 Hz
AQ                4.0894966 sec
RG                      203
DW                   62.400 usec
DE                   17.77 usec
TE                   298.2 K
D1              2.00000000 sec
TD0                       1

======== CHANNEL f1 ========
NUC1                      1H
P1                   13.38 usec
PLW1           11.09399986 W
SFO1           400.1936017 MHz

F2 - Processing parameters
SI                   131072
SF             400.1900000 MHz
WDW                      EM
SSB          0
LB                    0.30 Hz
GB           0
PC                    1.00
```

24g

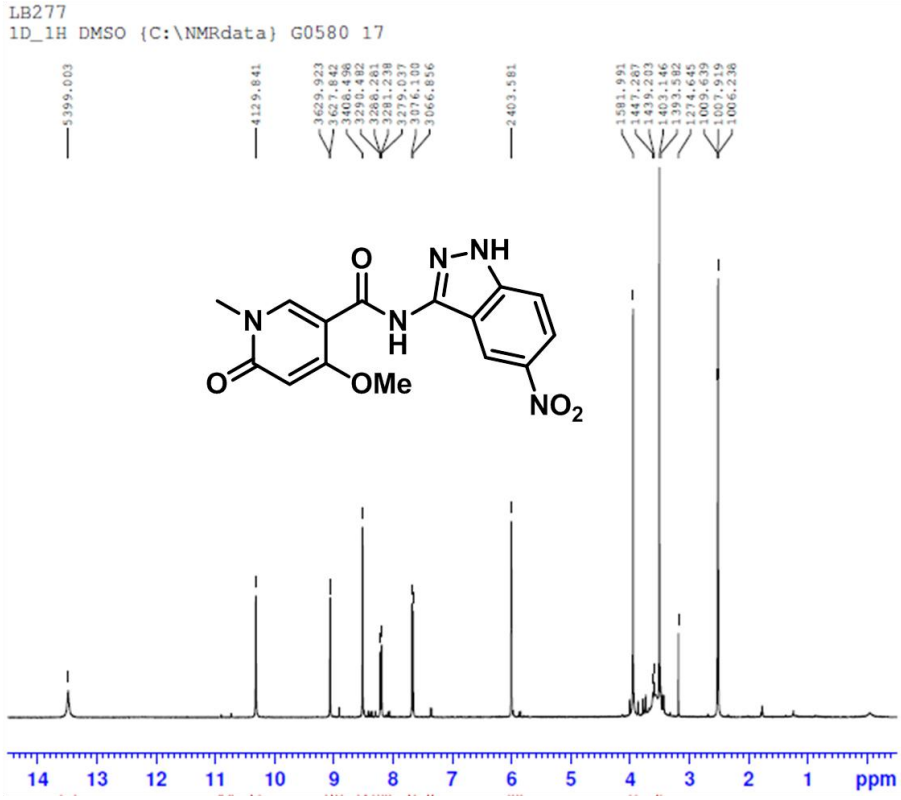


```
Current Data Parameters
NAME                  LB277
EXPNO                     1
PROCNO                    1

F2 - Acquisition Parameters
Date_              20110929
Time                  11.34
INSTRUM               spect
PROBHD    5 mm PABBO BB-
PULPROG               zg30
TD                   65536
SOLVENT               DMSO
NS                        8
DS                        2
SWH                8012.820 Hz
FIDRES            0.122266 Hz
AQ                4.0894966 sec
RG                      203
DW                   62.400 usec
DE                   17.77 usec
TE                   298.2 K
D1              2.00000000 sec
TD0                       1

======== CHANNEL f1 ========
NUC1                      1H
P1                   13.38 usec
PLW1           11.09399986 W
SFO1           400.1936017 MHz

F2 - Processing parameters
SI                   131072
SF             400.1900000 MHz
WDW                      EM
SSB          0
LB                    0.30 Hz
GB           0
PC                    1.00
```

24h

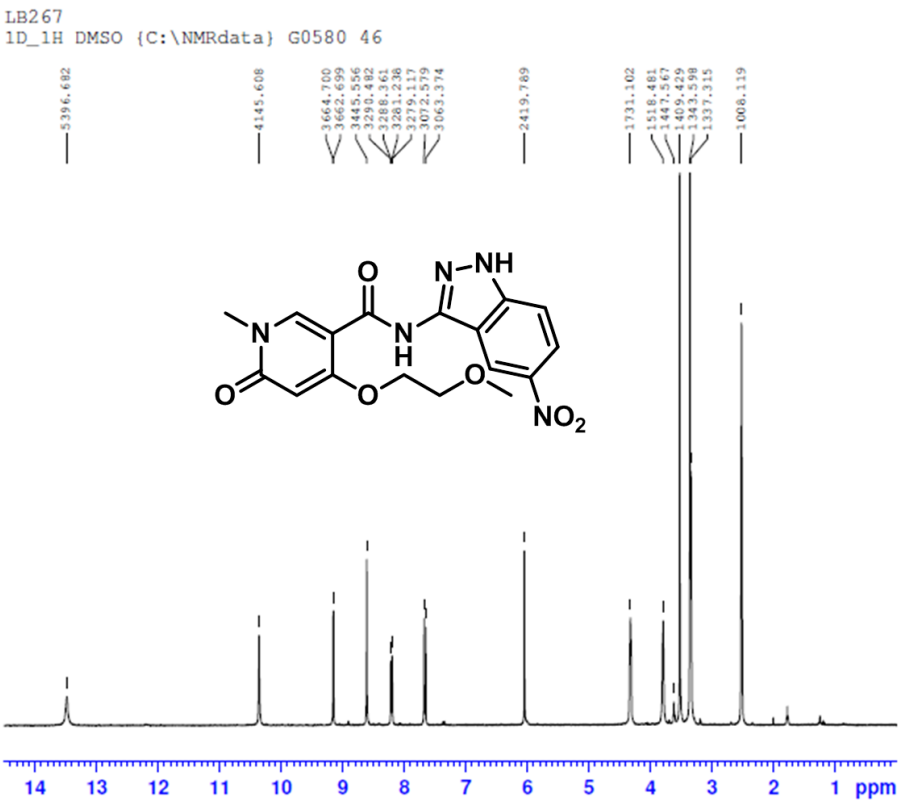

cdrd The Centre for Drug Research and Development

```
Current Data Parameters
NAME                  LB267
EXPNO                     1
PROCNO                    1

F2 - Acquisition Parameters
Date_              20110824
Time                  16.30
INSTRUM               spect
PROBHD   5 mm PABBO BB-
PULPROG                zg30
TD                    65536
SOLVENT                DMSO
NS                        8
DS                        2
SWH                8012.820 Hz
FIDRES            0.122266 Hz
AQ                4.0894966 sec
RG                      203
DW                   62.400 usec
DE                   17.77 usec
TE                   298.2 K
D1                2.00000000 sec
TD0                       1

======== CHANNEL f1 ========
NUC1                      1H
P1                    13.38 usec
PLW1           11.09399986 W
SFO1           400.1936017 MHz

F2 - Processing parameters
SI                      131072
SF             400.1900000 MHz
WDW                       EM
SSB       0
LB                    0.30 Hz
GB        0
PC                    1.00
```

References

[1] Grierson, D. *Medicinal chemistry Part I: Therapeutic targets and drug design. In: Pharmacy foundations review guide.* Vancouver: UBC Faculty of Pharmaceutical Sciences; 2011.

[2] Chothia, C., Lesk, A.M. *The relation between the divergence of sequence and structure in proteins*. **EMBO J**. 5, 823–826, 1986.

[3] Pan, Q., Shai, O., Lee, L.J., Frey, B.J., Blencowe, B.J. *Deep surveying of alternative splicing complexity in the human transcriptome by high-throughput sequencing*. **Nat. Genet**. 40, 1413-1415, 2008.

[4] UNAIDS Secretariat. Report of the global AIDS epidemic. *http://www.unaids.org/en/KnowledgeCentre/HIVData/default.asp* (accessed 15/10, 2011).

[5] Pommier, Y., Johnson, A.A., Marchand, C. *Integrase inhibitors to treat HIV/Aids*. **Nat. Rev. Drug. Discov.** 4, 236-248, 2005.

[6] National PBM Drug Monograph Raltegravir (Isentress), December 2007. *www.pbm.va.gov/monograph/Raltegravir.doc* (accessed 20/03, 2009).

[7] Dorr, P., Westby, M., Dobbs, S., Griffin, P., et al. *Maraviroc (UK-427,857), a Potent, Orally Bioavailable, and Selective Small-Molecule Inhibitor of Chemokine Receptor CCR5 with Broad-Spectrum Anti-Human Immunodeficiency Virus Type 1 Activity*. **Antimicrob. Agents. Ch**. 49, 4721-4732, 2005.

[8] Xu, L., Pozniak, A., Wildfire, A., Stanfield-Oakley, S.A., et al. *Emergence and Evolution of Enfuvritide Resistance following Long-Term Therapy involves Heptad Repeat 2 Mutations within gp41*. **Antimicrob. Agents. Ch**. 49, 1113-1119, 2005.

[9] Biswas, P., Tambussi, G., Lazzarin, A. *Access denied? The status of co-receptor inhibition to counter HIV entry*. **Expert. Opin. Pharmaco**. 8, 923-933, 2007.

[10] Del Rio C. *Current concepts in antiretroviral therapy failure*. **Top. HIV. Med.** 14, 102–106.20. (2006)

[11] Baba, M. *Recent status of HIV-1 gene expression inhibitors*. **Antivir. Res**. 71, 301–306, 2006.

[12] Turner, J.J., Ivanova G.D., Verbeure, B., Williams, D., Arzumanov, A.A., Abes, S., Lebleu, B., Gait, M.J. *Cell-penetrating peptide conjugates of peptide nucleic acids (PNA) as inhibitors of HIV-1 Tat-dependent trans-activation in cells*. **Nucl. Acids. Res**. 33, 6837-6849, 2005.

[13] Jayasuriya, H., Lingham, R.B., Graham, P., Quamina, D., Herranz, L., et al. *Durhamycin A, a Potent Inhibitor of HIV Tat Transactivation*. **J. Nat. Prod**. 65, 1091-1095, 2002.

[14] James, J. F. Tat Inhibitors, A New Approach: Interview with Olaf Kutsch, Ph.D. *http://www.aidsnews.org/2005/02/tat-inhibitor.html* (accessed 12/12, 2011).

[15] Kempf, M.C., Jones, J., Heil, M.L., Kutsch, O. *A high-throughput drug screening system for HIV-1 transcription inhibitors.* J. Biomol. Screen. 11, 807-15, 2006.

[16] Kestler, H.W., III., Ringler, D.J., Mori, K., Panicali, D.L. Sehgal, P.K., Daniel, M.D., Desrosiers, R.C. *Importance of the nef gene for maintenance of high virus loads and for development of AIDS*. **Cell**. 65, 651-662, 1991.

[17] Olszewski, A., Sato, K., Aron, Z.D., Cohen, F., Harris, A., et al. *Guanidine alkaloid analogs as inhibitors of HIV-1 Nef interactions with p53, actin and p56^{lck}*. **PNAS**. 101, 14079-14084, 2004.

[18] Daelemans, D., Afonina, E., Nilsson, J., Werner, G., Kjems, J., et al. *A synthetic HIV-1 Rev inhibitor interfering with the CRM1-mediated nuclear export*. **PNAS**. 99, 14440-14445, 2002.

[19] Wang, Z., Burge, C.B. *Splicing regulation: From a parts list of regulatory elements to an integrated splicing code*. **RNA.** 14, 802-813, 2008.

[20] Guttmacher, A.E., Collins, F.S. *Genomic medicine - A primer*. **New. Engl. J. Med**. 347, 1512-1520, 2002.

[21] Rymond, B. *Targeting the spliceosome*. **Nat. Chem. Bio**. 3, 533-535, 2007.

[22] Stoltzfus, C.M., *Regulation of HIV-1 alternative RNA splicing and its role in virus replication*. **Adv. Virus. Res**. 74, 1-40, 2009.

[23] Kotlajich, M. V., Crabb, T. L., & Hertel, K. J. *Spliceosome assembly pathways for different types of alternative splicing converge during commitment to splice site pairing in the A complex*. **Mol. Cell. Biol.** 29, 1072-1082, 2009.

[24] Blencowe, B.J. *Exonic splicing enhancers: mechanism of action, diversity and role in human genetic diseases*. **Trends. Biochem. Sci.** 25, 106-110, 2000.

[25] Bohne, J., Schambach, A., Zychlinski, D. *New Way of Regulating Alternative Splicing in Retroviruses: the Promoter Makes a Difference*. **J. Virol.** 81, 3652-3656, 2007.

[26] Gontarek, R.R., Derse, D. *Interactions among SR proteins, an Exonic Splicing Enhancer, and a Lentivirus Rev Protein Regulate Alternative Splicing*. **Mol. Cell. Biol.** 16, 2325-2331, 1996.

[27] Liu, H-X., Zhang, M., Krainer, A.R. *Identification of functional exonic splicing enhancer motifs recognized by individual SR proteins*. **Genes. Dev**. 12, 1998–2012, 1998.

[28] Schaal, T.D., Maniatis, T. *Selection and characterization of pre-mRNA splicing enhancers: identification of novel SR protein-specific enhancer sequences*. **Mol. Cell. Biol**. 19, 1705–1719, 1999.

[29] Blencowe, B.J., Issner, R., Nickerson, J.A., Sharp, P.A. *A coactivator of pre-mRNA splicing*. **Genes. Dev**. 12, 996–1009, 1998.

[30] Manley, J.L., Krainer, A.R. *A rational nomenclature for serine/arginine-rich protein splicing factors (SR proteins)*. **Genes. Dev**. 24, 1073–1074, 2010.

[31] Zahler, A.M., Damgaard, C.K., Kjems, J., Caputi, M. *SC35 and Heterogeneous nuclear ribonucleoprotein A/B proteins bind to a justapositioned exonic splicing enhancer/exonic splcing silencer element to regulate HIV-1 tat exon 2 splicing*. **J. Biol. Chem.** 279, 10077-10084, 2004.

[32] Han, K., Yeo, G., An, P. Burge, C.B., Grabowski, P.J. *A Combinatorial Code for Splicing UAGG and GGGG Motifs.* **PLoS. Biol.** 843-860, 2005.

[33] Hertel, K.J., Graveley, B. R. *RS domains contact the pre-mRNA throughout spliceosome assembly*. **Trends. Biochem. Sci**. 30, 115–118, 2005.

[34] Zahler, A.M., Lane, W.S., Stolk, J.A., Roth, M.B. *SR proteins: a conserved family of pre-mRNA splicing factors*. **Genes. Dev**. 6, 837-847, 1992.

[35] Lutzelberger, M., Gross, T., Kaufer, N.F. *Srp2, an SR protein family member of fission yeast: in vivo characterization of its modular domains*. **Nucleic. Acids. Res**. 27**,** 2618-2626, 1999.

[36] Shepard, P.J., Hertel, K.J. *The SR protein family*. **Genome. Biol**. 10, 242.1-242.9, 2009.

[37] Graveley, B.R. *Sorting out the complexity of SR protein functions*. **RNA**. 6, 1197-1211, 2000.

[38] Busch, A., Hertel, K.J. *Evolution of SR protein and hnRNP splicing regulatory factors.* **WIREs RNA.** 3, 1-12, 2012.

[39] Cavaloc, Y., Popielarz, M., Fuchs, J.P., Gattoni, R., Stevenin, J. *Characterization and cloning of the human splicing factor 9G8: a novel 35 kDa factor of the serine/arginine protein family*. **EMBO. J**. 13**,** 2639-2649, 1994.

[40] Cáceres, J.F., Misteli, T., Screaton, G.R., Spector, D.L., Krainer, A.R. *Role of the modular domains of SR proteins in subnuclear localization and alternative splicing specificity.* **J. Cell. Biol.** 138**,** 225-238, 1997.

[41] Manley, J.L., Tacke, R. *SR proteins and splicing control*. **Genes. Dev**. 10**,** 1569-1579, 1996.

[42] Fu, X-D. *The superfamily of arginine/serine-rich splicing factors*. **RNA**. 1**,** 663-680, 1995.

[43] Spector, D.L. *Macromolecular domains within the cell nucleus*. **Annu. Rev. Cell. Biol.** 9**,** 265-315, 1993.

[44] Hedley, M.L., Amrein, H., Maniatis, T. *An amino acid sequence motif sufficient for subnuclear localization of an arginine/serine-rich splicing factor.* **PNAS. USA**. 92**,** 11524-11528, 1995.

[45] Jimenez-Garcia, L.F., Spector, D.L. *In vivo evidence that transcription and splicing are coordinated by a recruiting mechanism.* **Cell**. 73**,** 47-59, 1993.

[46] Misteli, T., Caceres, J.F., Spector, D.L. *The dynamics of a pre-mRNA splicing factor in living cells.* **Nature.** 387**,** 523-527, 1997.

[47] Misteli, T., Caceres, J.F., Clement, J.Q., Krainer, A.R., Wilkinson, M.F., Spector, D.L. *Serine phosphorylation of SR proteins is required for their recruitment to sites of transcription in vivo.* **J. Cell. Biol.** 143**,** 297-307, 1998.

[48] Black, D.L. *Mechanisms of alternative pre-messenger RNA splicing.* **Annu. Rev. Biochem.** 72**,** 291-336, 2003.

[49] Mermoud, J.E., Cohen, P., Lamond, A.I. *Ser/Thr-specific protein phosphatases are required for both catalytic steps of pre-mRNA splicing.* **Nucleic. Acids. Res**. 20**,** 5263-5269, 1992.

[50] Mermoud, J.E., Cohen, P.T., Lamond, A.I. *Regulation of mammalian spliceosome assembly by a protein phosphorylation mechanism.* **EMBO. J.** 13**,** 5679-5688, 1994.

[51] Mattaj, I.W. *RNA processing. Splicing in space.* **Nature.** 372**,** 727-728, 1994.

[52] Colwill, K., Pawson, T., Andrews, B., Prasad, J., Manley, J.L., Bell, J.C., Duncan, P.I. *The Clk/Sty protein kinase phosphorylates SR splicing factors and regulates their intranuclear distribution.* **EMBO. J**. 15**,** 265-275, 1996.

[53] Okamoto, Y., Onogi, H., Honda, R., Yasuda, H., Wakabayashi, T., Nimura, Y., Hagiwara, M. *cdc2 kinase-mediated phosphorylation of splicing factor SF2/ASF*. **Biochem. Biophys. Res. Commun**. 249**,** 872-878, 1998.

[54] Soret, J., Tazi, J. *Phosphorylation-dependent control of the pre-mRNA splicing machinery*. **Prog. Mol. Subcell. Biol.** 31**,** 89-126, 2003.

[55] Shen, H., Kan, J.L., Green, M.R. *Arginine-serine-rich domains bound at splicing enhancers contact the branchpoint to promote prespliceosome assembly*. **Mol. Cell.** 13**,** 367-376, 2004.

[56] Shen, H., Green, M.R. *A pathway of sequential arginine-serine-rich domain-splicing signal interactions during mammalian spliceosome assembly*. **Mol. Cell. 16,** 363-373, 2004.

[57] Graveley, B.R., Hertel, K.J., Maniatis, T. *A systematic analysis of the factors that determine the strength of pre- mRNA splicing enhancers.* **EMBO. J.** 17**,** 6747-6756, 1998.

[58] Kanopka, A., Muhlemann, O., Akusjarvi, G. *Inhibition by SR proteins of splicing of a regulated adenovirus pre- mRNA***. Nature.** 381**,** 535-538, 1996.

[59] Cáceres, J.F., Screaton, G.R., Krainer, A.R. *A specific subset of Sr proteins shuttles continuously between the nucleus and the cytoplasm.* **Genes. Dev.** 12**,** 55-66, 1998.

[60] Le Hir, H., Moore, M.J., Maquat, L.E. *Pre-mRNA splicing alters mRNP composition: evidence for stable association of proteins at exon-exon junctions.* **Genes. Dev.** 14**,** 1098-1108, 2000.

[61] Blencowe, B.J., Nickerson, J.A., Issner, R., Penman, S., Sharp, P.A. *Association of nuclear matrix antigens with exon-containing splicing complexes.* **J. Cell. Biol.** 127**,** 593-607, 1994.

[62] Kataoka, N., Bachorik, J.L., Dreyfuss, G. *Transportin-SR, a nuclear import receptor for SR proteins.* **J. Cell. Biol**. 145, 1145–1152, 1999.

[63] Lai, M-C., Lin, R-I., Huang, S-Y., Tsai, C-W., Tarn, W-Y. *A human importin-b family protein, Transportin-SR2, interacts with the phosphorylated RS domain of SR proteins*. **J. Biol. Chem**. 275, 7950–7957, 2000.

[64] Karni, R., de Stanchina, E., Lowe, S.W., Sinha, R., Mu, D., Krainer, A.R. *The gene encoding the splicing factor SF2/ASF is a proto-oncogene*. **Nat. Struct. Mol. Biol**. 14, 185-193, 2007.

[65] Sanford, J.R., Gray, N.K., Beckmann, K., Caceres, J.F. *A novel role for shuttling SR proteins in mRNA translation.* **Genes. Dev.** 18**,** 755-768, 2004.

[66] Michlewski, G., Sanford, J.R., Caceres, J.F. *The splicing factor SF2/ASF regulates translation initiation by enhancing phosphorylation of 4E-BP1*. **Mol. Cell.** 3**,** 179-189, 2008.

[67] Bedard, K.M., Daijogo, S., Semler, B.L. *A nucleo-cytoplasmic SR protein functions in viral IRES-mediated translation initiation.* **EMBO. J.** 26**,** 459-467, 2007.

[68] Swartz, J.E., Bor, Y.C., Misawa, Y., Rekosh, D., Hammarskjold, M.L. *The shuttling SR protein 9G8 plays a role in translation of unspliced mRNA containing a constitutive transport element.* **J. Biol. Chem.** 282**,** 19844-19853, 2007.

[69] Ge, H., Zuo, P., Manley, J. L., *Primary Structure of the Human Splicing Factor ASF Reveals Similarities with Drosophila Regulators*. **Cell**. 66, 373-382, 1991.

[70] Krainer, A. R., Conway, G.C., Kozak, D. *The essential pre-mRNA splicing factor SF2 influences 5′ splice site selection by activating proximal sites*. **Cell**. 62, 35-42, 1991.

[71] Lamond, A. I. *ASF/SF2: a splice site selector*. **TIBS**. 16, 452-453, 1991.

[72] Krainer, A. R., Maniatis, T. *Multiple factors including the small nuclear ribonucleoproteins U1 and U2 are necessary for Pre-mRNA splicing in vitro*. **Cell**. 42, 725-736, 1985.

[73] Krainer, A. R., Conway, G. C., Kozak, D. *Purification and characterization of pre-mRNA splicing factor SF2 from HeLa cells*. **Genes. Dev**. 4, 1158-1171, 1990.

[74] Caceres J. F., Krainer A. R. *Functional analysis of pre-mRNA splicing factor SF2/ASF structural domains*. **EMBO. J**. 12, 4715–4726, 1993.

[75] Zuo P., Manley J. L. *Functional domains of the human splicing factor ASF/SF2*. **EMBO. J**. 12, 4727–4737, 1993.

[76] Tacke R., Manley J. L., *The human splicing factors ASF/SF2 and SC35 possess distinct, functionally significant RNA binding specificities*. **EMBO. J**. 14, 3540–3551, 1995.

[77] Tintaru, A. M., Hautbergue, G. M., Hounslow, A. M., Hung, M., Lian, L., Craven, C. J., Wilson, S. A. *Structural and functional analysis of RNA and TAP binding to SF2/ASF*. **EMBO. J**. 8, 756-762, 2007.

[78] Hagopian, C.J., Ma1, C., Meade, B.R., et al. *Adaptable Molecular Interactions Guide Phosphorylation of the SR Protein ASF/SF2 by SRPK1*. **J. Mol. Biol**. 382, 894-909, 2008.

[79] Aubol, B.E., Chakrabarti, S., Ngo, J., Shaffer, J., Nolen, B., et al. *Processive phosphorylation of alternative splicing factor/splicing factor 2*. **PNAS. USA**. 100, 12601–12606, 2003.

[80] Velazquez-Dones, A., Hagopian, J.C., Ma, C-T., Zhong, X-Y., Zhou, H., et al. *Mass spectrometric and kinetic analysis of ASF/SF2 phosphorylation by SRPK1 and Clk/Sty*. **J. Biol. Chem**. 280, 41761–41768, 2005.

[81] Ngo, J.C., Chakrabarti, S., Ding, J.H., Velazquez-Dones, A., Nolen, B., et al. *Interplay between SRPK and Clk/Sty kinases in phosphorylation of the splicing factor ASF/SF2 is regulated by a docking motif in ASF/SF2*. **Mol. Cell**. 20, 77–89, 2005.

[82] Xiao, S.H., Manley, J.L. *Phosphorylation of the ASF/SF2 RS domain affects both protein-protein and protein-RNA interactions and is necessary for splicing*. **Gene. Dev**. 11, 334–344, 1997.

[83] Choa, S., Hoanga, A., Sinhab, R., Zhongc, X-Y., Fuc, X-D., Krainerb, A.R., Ghosha, G. *Interaction between the RNA binding domains of Ser-Arg splicing factor 1 and U1-70K snRNP protein determines early spliceosome assembly*. **PNAS**. 108, 8233-8238, 2011.

[84] Hanamura, A., Cáceres, J.F., Mayeda, A., Franza, B.R. Jr., Krainer, A.R. *Regulated tissue-specific expression of antagonistic pre-mRNA splicing factors*. **RNA**. 4, 430-444, 1998.

[85] Huang, Y., Gattoni, R., Steitz, J.A. *SR Splicing factors serve as adapter proteins for TAP-dependent mRNA export*. **Mol. Cell**. 11, 837–843, 2003.

[86] Huang, Y., Steitz, J.A. *SRprises along a messenger's journey*. **Mol. Cell**. 17, 613–615, 2005.

[87] Tuduri, S., Crabbe, L., Tourrière, H., Coquelle, A., Pasero1, P. *Does interference between replication and transcription contribute to genomic instability in cancer cells?* **Cell. Cycle**. 9, 1886-1892, 2010.

[88] Li, X., Manley, J.L. *Inactivation of the SR protein splicing factor ASF/SF2 results in genomic instability*. **Cell**. 122, 365–378, 2005.

[89] Cooper, T.A. *Alternative Splicing Regulation Impacts Heart Development.* **Cell**. 120, 1-5, 2005.

[90] Xu, X., Yang, D., Ding, J.H., Wang, W., Chu, P.H., Dalton, N.D., Wang, H.Y., et al. *ASF/SF2-Regulated CaMKIIδ Alternative Splicing Temporally Reprograms Excitation-Contraction Coupling in Cardiac Muscle***. Cell**. 120, 59-72, 2005.

[91] Fischer, D.C., Noack, K., Runnebaum, I.B., Watermann, D.O., Kieback, D.G., Stamm, S., Stickeler, E. *Expression of splicing factors in human ovarian cancer*. **Oncol. Rep**. 11, 1085–1090, 2004.

[92] Ghigna, C., Giordano, S., Shen, H., Benvenuto, F., Castiglioni, F., Comoglio, P.M., Green, M.R., Riva, S., Biamonti, G. *Cell motility is controlled by SF2/ASF through alternative splicing of the Ron protooncogene*. **Mol. Cell**. 20, 881–890, 2005.

[93] Tazi, J., Bakkour, N., Marchand, V., Ayadi, L., Aboufirassi, A., Branlant, C. *Alternative splicing: regulation of HIV-1 multiplication as a target for the therapeutic action*. **FEBS. J**. 277, 867-876, 2010.

[94] Möröy, T., Heyd, F. *The impact of alternative splicing in vivo: mouse models show the way*. **RNA**. 13, 1155–1171, 2007.

[95] Wang, J., Takagaki, Y., Manley, J.L. *Targeted disruption of an essential vertebrate gene: ASF/SF2 is required for cell viability*. **Genes. Dev**. 10, 2588–2599, 1996.

[96] Li, X., Manley, J.L. *Alternative Splicing and Control of Apoptotic DNA Fragmentation*. **Cell. Cycle**. 5, 1286-1288, 2006.

[97] Bakkour, N., Lin, Y.L., Maire, S., et al. *Small-Molecule Inhibition of HIV pre-m-RNA Splicing as a Novel Antiretroviral Therapy to overcome Drug Resistance*. **Plos Pathogens.** 3, 1530-1539, 2007.

[98] Faustino, N.A., Cooper, T.A. *Pre-mRNA splicing and human disease*. **Gene. Dev**. 17, 419-437, 2003.

[99] Moseley, C.T., Mullis, P.E., Prince, M.A., Phillips III, J.A. *An exon splice enhancer mutation causes autosomal dominant GH deficiency*. **J. Clin. Endocrinol. Metab.** 87, 847–852, 2002.

[100] D'Souza, I., Poorkaj, P., Hong, M., Nochlin, D., Lee, V.M., Bird, T.D., and Schellenberg, G.D. *Missense and silent tau gene mutations cause frontotemporal dementia with Parkinsonism-chromosome 17 type, by affecting multiple alternative RNA splicing regulatory elements*. **PNAS.** 96, 5598–5603, 1999.

[101] Narisawa-Saito, M., Kiyono, T. *Basic mechanisms of high-risk human papillomavirus-induced carcinogenesis: roles of E6 and E7 proteins*. **Cancer. Sci**. 98, 1505-1511, 2007.

[102] Berk, A.J. *Recent lessons in gene expression, cell cycle control, and cell biology from adenovirus*. **Oncogene**. 24, 7673-7685, 2005.

[103] Dejardin, J., Bompard-Marechal, G., Audit, M., Hope, T.J., Sitbon, M., et al. *A novel subgenomic murine leukemia virus RNA transcript results from alternative splicing*. **J. Virol**. 74, 3709–3714, 2000.

[104] Yuo, C.Y., Lin, H.H., Chang, Y.S., Yang, W.K., Chang, J.G. *5-(N-ethyl-N-isopropyl)-amiloride enhances SMN2 exon 7 inclusion and protein expression in spinal muscular atrophy cells*. **Ann. Neurol**. 63, 26-34, 2008.

[105] Lefebvre, S., Burglen, L., Reboullet, S., et al. *Identification and characterization of a spinal muscular atrophy-determining gene*. **Cell**. 80, 155–165, 1995.

[106] Wirth, B. *An update of the mutation spectrum of the survival motor neuron gene (SMN1) in autosomal recessive spinal muscular atrophy (SMA).* **Hum. Mutat**. 15, 228 –237, 200.

[107] Monani, U.R., Lorson, C.L., Parsons, D.W., et al. *A single nucleotide difference that alters splicing patterns distinguishes the SMA gene SMN1 from the copy gene SMN2*. **Hum. Mol. Genet**. 8, 1177–1183, 1999.

[108] Lorson, C.L., Hahnen, E., Androphy, E.J., Wirth, B. *A single nucleotide in the SMN gene regulates splicing and is responsible for spinal muscular atrophy*. **PNAS. USA**. 96, 6307–6311, 1999.

[109] Chang, J.G., Hsieh-Li, H.M., Jong, Y.J., et al. *Treatment of spinal muscular atrophy by sodium butyrate*. **PNAS. USA**. 98, 9808 –9813, 2001.

[110] Hahnen, E., Eyupoglu, I.Y., Brichta, L., et al. *In vitro and ex vivo evaluation of second-generation histone deacetylase inhibitors for the treatment of spinal muscular atrophy*. **J. Neurochem**. 98, 193–202, 2006.

[111] Andreassi, C., Jarecki, J., Zhou, J., et al. *Aclarubicin treatment restores SMN levels to cells derived from type I spinal muscular atrophy patients*. **Hum. Mol. Genet**. 10, 2841–2849, 2001.

[112] Zhang, M.L., Lorson, C.L., Androphy, E.J., Zhou, J. *An in vivo reporter system for measuring increased inclusion of exon 7 in SMN2 mRNA: potential therapy of SMA*. **Gene. Ther**. 8, 1532–1538, 2001.

[113] Lunn, M.R., Root, D.E., Martino, A.M., et al. *Indoprofen upregulates the survival motor neuron protein through a cyclooxygenase-independent mechanism*. **Chem. Biol**. 11, 1489 –1493, 2004.

[114] Wolstencroft, E.C., Mattis, V., Bajer, A.A., et al. *A non-sequencespecific requirement for SMN protein activity: the role of aminoglycosides in inducing elevated SMN protein levels*. **Hum. Mol. Genet.** 14, 1199 –1210, 2005.

[115] Solier, S., Lansiaux, A., Logette, E., Wu, J., Soret, J., Tazi, J., Bailly, C., Desoche, L., Solary, E., Corcos, L. *Topoisomerase I and II Inhibitors Control Caspase-2 Pre-Messenger RNA Splicing in Human Cells*. **Mol. Cancer. Res**. 2, 53-61, 2004.

[116] Welch, E.M., Barton, E.R., Zhuo, J., Tomizawa, Y., Friesen, W.J. et al. *PTC124 targets genetic disorders caused by nonsense mutations*. **Nature**. 447, 87-93, 2007.

[117] Anwar, A., Hosoya, T., Leong, K.M., Onogi, H., Okuno, Y., et al. *The Kinase Inhibitory SFV785 Dislocates Dengue Virus Envelope Protein from the Replication Complex and Blocks Virus Assembly*. **PLoS ONE**. 6, e23246, 2011.

[118] Muraki, M., Ohkawara, B., Hosoya, T., Onogi, H., Koizumi, J. *Manipulation of Alternative Splicing by a Newly Developed Inhibitor of Clks*. **J. Biol. Chem**. 279, 24246-24254, 2004.

[119] Fukuhara, T., Hosoya, T., Shimizu, S., Sumi, K., Oshiro, T., et al. *Utilization of host SR protein kinases and RNA-splicing machinery during viral replication*. **PNAS**. 103, 11329-11333, 2006.

[120], J., Bakkour, N., Maire, S., Durand, S., Zekri, L., et al. *Selective modification of alternative splicing by indole derivatives that target serine-arginine-rich protein splicing factors*. **PNAS**. 102, 8764-8769, 2005.

[121] Kuiken, C., Leitner, T., Foley, B. et al. *HIV Sequence Compendium 2008.* **Los Alamos National Laboratory**. Theoretical Biology and Biophysics, Los Alamos, New Mexico. LA-UR 08-03719, 2008.

[122] O'Reilly, M.M., McNally, M.T., Beemon, K.L. *Two strong splice sites and competing suboptimal 3' splice sites involved in alternative splicing of human immunodeficiency virus type 1 RNA*. **Virology.** 213, 373-385, 1995.

[123] Pollard, V.W., Malim, W.H. *The HIV Rev protein.* **Annu. Rev. Microbiol.** 52, 491-532, 1998

[124] Purcell, D.F.J., Martin, M.A. *Alternative Splicing of Human Immunodeficiency Virus Type 1 mRNA Modulates Viral Protein Expression, Replication and Infectivity*. **J. Virology** 67, 6365-6378, 1993.

[125] Kim, S.Y., Byrn, R., Groopman, J., Baltimore, D. *Temporal aspects of DNA and RNA synthesis during human immunodeficiency virus infection: evidence for differential gene expression*. **J. Virol**. 63, 3708–3713, 1989.

[126] Kazmierski, W.M., Kenakin, T.P., Gudmundsson, K.S. *Peptide, Peptidomimetic and Small-molecule Drug Discovery Targeting HIV-1 Host-cell Attachment and Entry through gp120, gp41, CCR5 and CXCR4*. **Chem. Biol. Drug. Des.** 67, 13–26, 2006.

[127] Strebel, K. *Virus–host interactions: role of HIV proteins Vif, Tat, and Rev*. **AIDS**. 17, (suppl 4):S25–S34, 2003.

[128] Stoltzfus, C.M., Madsen, J.M. *Role of Viral Splicing Elements and Cellular RNA Binding Proteins in Regulation of HIV-1 Alternative RNA Splicing*. **Curr. HIV. Res**. 4, 43-55, 2006.

[129] Bilodeau, P.S., Domsic, J. K., Mayeda, A., Krainer, A. R., Stoltzfus, C. M. *RNA Splicing at Human Immunodeficiency Virus Type 1 3' Splice Site A2 Is Regulated by Binding of hnRNP A/B Proteins to an Exonic Splicing Silencer Element*. **J. Virol**. 75, 8487-8497, 2001.

[130] Amendt, B. A., Si, Z. H., Stoltzfus, C. M. *Presence of exon splicing silencers within human immunodeficiency virus type 1 tat exon 2 and tat-rev exon 3: evidence for inhibition mediated by cellular factors*. **Mol. Cell. Biol.** 15, 4606-4615, 1995.

[131] Jacquenet, S., Mereau, A., Bilodeau, P. S., Damier, L., Stoltzfus, C. M., Branlant, C. *A second exon splicing silencer within human immunodeficiency virus type 1 tat exon 2 represses splicing of Tat mRNA and binds protein hnRNP H*. **J. Biol. Chem**. 276, 40464-40475, 2001.

[132] Wentz, M. P., Moore, B. E., Cloyd, M. W., Berget, S. M., Donehower, L. A. *A naturally arising mutation of a potential silencer of exon splicing in human immunodeficiency virus type 1 induces dominant aberrant splicing and arrests virus production*. **J. Virol**. 71, 8542-8551, 1997.

[133] Caputi, M., Zahler, A. M. *SR proteins and hnRNP H regulate the splicing of the HIV-1 tev-specific exon 6D*. **EMBO J**. 21, 845-855, 2002.

[134] Tange, T.O., Damgaard, C.K., Guth, S., Valcarcel, J., Kjems, J. *The hnRNP A1 protein regulates HIV-1 tat splicing via a novel intron silencer element.* **EMBO J**. 20, 5748-5758, 2001.

[135] Asang, C., Hauber, I., Schaal, H. *Insights into the selective activation of alternatively used splice acceptors by the human immunodeficiency virus type-1 bidirectional splicing enhancer*. **Nucleic. Acids. Res**. 36, 1450–1463, 2008.

[136] Marchand, V., Mereau, A., Jacquenet, S., Thomas, D., Mougin, A., Gattoni, R., Stevenin, J., Branlant, C. *A janus splicing regulatory element modulates HIV-1 tat and rev mRNA production by coordination of hnRNP A1 cooperative binding*. **J. Mol. Biol**. 323, 629-652, 2002.

[137] Kammler, S., Otte, M., Hauber, I., Kjems, J., Hauber, J., Schaal, H. *The strength of the HIV-1 3' splice sites affects Rev function*. **Retrovirology**. 3, 89, 2006.

[138] Ge, H., Manley, J.L., *A protein factor, ASF, controls cell-specific alternative splicing of SV40 early pre-mRNA in vitro*. **Cell**. 62, 25-34, 1990.

[139] Jacquenet, S., Decimo, D., Muriaux, D., Darlix, J-L. *Dual effect of the SR proteins ASF/SF2, SC35 and 9G8 on HIV-1 RNA splicing and virion production*. **Retrovirology**. 2, 33, 2005.

[140] Tange, T.O., Kjems, J. *SF2/ASF Binds to a Splicing Enhancer in the Third HIV-1 Tat Exon and Stimulates U2AF Binding Independently of the RS Domain*. **J. Mol. Biol**. 312, 649-662, 2001.

[141] Ropers, D., Ayadi, L., Gattoni, R., Jacquenet, S., Damier, L., Branlant, C., Stévenin, J. *Differential Effects of the SR Proteins 9G8, SC35, ASF/SF2, and SRp40 on the Utilization of the A1 to A5 Splicing Sites of HIV-1 RNA*. **J. Biol. Chem**. 279, 29963-29973, 2004.

[142] Madsen, J.M., Stoltzfus, C.M. *An exonic splicing silencer downstream of 3' splice site A2 is required for efficient human immunodeficiency virus type 1 replication*. **J. Virol**. 79, 10478-10486, 2005.

[143] Burd, C.G., Dreyfuss, G. *RNA binding specificity of hnRNP A1: significance of hnRNP A1 high-affinity binding sites in premRNA splicing*. **EMBO J**. 13, 1197-1204, 1994.

[144] Caputi, M., Freund, M., Kammler, S., Asang, C., Schaal, H. *A Bidirectional SF2/ASF- and SRp40-Dependent Splicing Enhancer Regulates Human Immunodeficiency Virus Type 1 rev, env, vpu, and nef Gene Expression*. **J. Virol**. 78, 6517-6526, 2004.

[145] Staffa, A., Cochrane, A. *Identification of positive and negative splicing regulatory elements within the terminal tat/rev exon of HIV-1*. **Mol. Cell. Biol**. 15, 4597-4605, 1995.

[146] Alvarez, M., Joule, J.A. *Ellipticine, uleine, apparicine, and related alkaloids*. **Alkaloids. Chem. Biol**. 57, 235-272, 2001.

[147] Rivalle, C., Wendling, F., Tambourin, P., Hloste, J.M., Bisagni, E., Cherman, J.C. *Antitumor amino-substituted pyrido[3',4':4,5]pyrrolo[2,3-g]isoquinolines and pyrido[4,3-b]carbazole derivatives: synthesis and evaluation of compounds resulting from new sidechain and heterocycle modifications* **J. Med. Chem.** 26, 181-185, 1983.

[148] Auclair, C. *Multimodal action of antitumor agents on DNA: The ellipticine series* **Arch. Biochem. Biophys.** 259, 1-14, 1987.

[149] Stiborova, M., Rupertova, M., Schmeiser, H.H., Frei, E. *Molecular mechanisms of antineoplastic action of an anticancer drug ellipticine* **Biomed. Pap. Med. Fac. Univ. Palacky Oloumouc. Czech Repub.** 150, 13-23, 2006.

[150] Martinez, R., Chacon-Garcia, L. *The Search of DNA-intercalators as antitumoral drugs: What worked and what did not work* **Curr. Med. Chem.** 12, 127-151, 2005.

[151] Borg, S., Vollinga, R.C., Labarre, M., Payza, K., Terenius, L., Luthman, K. *Design, Synthesis, and Evaluation of Phe-Gly Mimetics: Heterocyclic Building Blocks for Pseudopeptides,* **J. Med. Chem.** 42, 4331-4342, 1999

[152] Andersen, K. E.; Jørgensen, A. S.; Bræstrup, C. *Oxadiazoles as bioisosteric transformations of carboxylic functionalities. Part I*. **Eur. J. Med. Chem**. 29, 393, 1994.

[153] Katritzky, A.R, Shestopalov, A.A., Suzuki, K. *A convenient synthesis of chiral 1,2,4-oxadiazoles from N-protected (α-aminoacyl)benzotriazoles*. **ARKIVOC**. VII, 36-55, 2005.

[154] Wallace, E.M., Lyssikatos, J., Blake, J.F., Seo, J., Yang, H.W., Yeh, T.C., et al. *Potent and selective mitogen-activated protein kinase kinase (MEK) 1,2 inhibitors. 1. 4-(4-bromo-2-fluorophenylamino)-1- methylpyridin-2(1H)-ones*. **J. Med. Chem**. 49, 441-444, 2006.

[155] Huang, H., Hutta, D.A., Hu, H., DesJarlais, R.L., Schubert, C. *Design and synthesis of a pyrido[2,3-d]pyrimidin-5-one class of anti-inflammatory FMS inhibitors*. **Bioorg. Med. Chem. Lett**. 18, 2355–2361, 2008.

[156] Hylden, A.T., Uzelac, E.J., Ostojic, Z., Wu, T., Sacry, K.L., et al. *Cyclization of 5-hexynoic acid to 3-alkoxy-2-cyclohexenone*. **Beilstein J. Org. Chem.** 7, 1323-1326, 2011.

[157] Weast, R. C. In *Handbook of Chemistry and Physics. 60th ed.* CRC Press Inc.: Boca Raton, Florida, 1979; pp 231.

[158] Li, C., Zhu, J., Wu, Z., Hou, J., Li, C., Shao, X., et al. *'Two-point'-bound supramolecular complexes from semi-rigidified dipyridine receptors and zinc porphyrins*. **Tetrahedron.** 62, 6973-6980, 2006.

[159] Hisamatsu, Y., Hasada, K., Amano, F., et al. *Highly Selective Recognition of Adenine Nucleobases by Synthetic Hosts with a Linked Five-Six-Five-Membered Triheteroaromatic Structure and the Application to Potentiometric Sensing of the Adenine Nucleotide*. **Chem. Eur. J.** 12, 7733-7741, 2006.

[160] Soares, O., Barros, D.R., Nogueira, C.W., Stangherlin, E.C., et al. *Copper-Promoted Carbon−Nitrogen Bond Formation with 2-Iodo-selenophene and Amides*. **J. Org. Chem.** 71, 1552-1557, 2006.

[161] Hoegberg, T., Stroem, P., Ebner, M Raemsby, S. *Cyanide as an efficient and mild catalyst in the aminolysis of esters*. **J. Org. Chem**. 52, 2033-2036, 1987.

[162] Benjahad, A., Oumouch, S., Guillemont, J., Pasquier, E., Mabire, D., et al. *Structure–activity relationship in the 3-iodo-4-phenoxypyridinone (IOPY) series: The nature of the C-3 substituent on anti-HIV activity*. **Bioorg. Med. Chem. Lett**. 17, 712–716, 2007.

[163] Nuriev, V.N., Zyk, N.V., Vatsadze, S.V. *The synthetic pathways to a family of pyridine-containing azoles - promising ligands for coordination chemistry*. **ARKIVOC**. IV, 208-224, 2005.

[164] Griffith, D., Zangrando, E., Alessio, E., Marmion, C. *A novel ruthenium nitrosyl complex which also contains a free NO-donor moiety.* **Inorg. Chim, Acta.** 357, 3770-3774, 2004.

[165] Hauser, C. R., Renfrow, W. B., *Benzohydroxamic Acid*. **Org. Syn**. 2, 67, 1943.

[166] Ho, C. Y.; Strobel, E.; Ralbovsky, J.; Galemmo, R. A. J. *Improved Solution- and Solid-Phase Preparation of Hydroxamic Acids from Esters*. **J. Org. Chem**. 70, 4873-4875, 2005.

[167] Ferraris, D.; Duvall, B.; Ko, Y.; Thomas, A.; Rojas, C.; Majer, P.; Hashimoto, K.; Tsukamoto, T. *Synthesis and Biological Evaluation of D-amino Acid Oxidase Inhibitors*. **J. Med. Chem**. 51, 3357-3359, 2008.

[168] Olah, G. A. *Organic Fluorine Compounds. XXVI. Acetoacetyl Fluoride*. **J. Org. Chem**. 26, 225-227, 1961.

[169] El-Faham, A.; Khattab, S. N.; Abdul-Ghani, M. *Tetramethylfluoroformamidinium hexafluorophosphate (TFFH)/benzyltriphenylphosphonium dihydrogen trifluoride (PTF): a unique reagent for the conversion of carboxylic acids to the corresponding alcohols as well as hydroxamic acids*. **ARKIVOC**, xiii, 57-63, 2006.

[170] Sibi, M.P., Hasegawa, H., Ghorpade, *S.R. A Convenient Method for the Conversion of N-Acyloxazolidinones to Hydroxamic Acids*. **Org. Lett**., 4, 3343-3346, 2002**.**

[171] Shaw, A.Y., Chen, Y-R., Tsai, C-H. *Microwave-Assisted Base-Catalyzed Cyclization and Nucleophilic Substitution of O-Azidobenzanilides to Synthesize 1,2-Disubstituted Indazol-3-ones*. **Synthetic. Commun**. 39, 2647-2663, 2009.

[172] Correa, A., Tellitu, I., Domínguez, E., SanMartin, R. *Novel Alternative for the N−N Bond Formation through a PIFA-Mediated Oxidative Cyclization and Its Application to the Synthesis of Indazol-3-ones***. J. Org. Chem**. 71, 3501-3505, 2006.

[173] Majewski, M. *Lithiumdiisopropylamide as ahydridedonor. Reduction of aldehydes.* **Tetrahedron. Lett.** 29, 4057-4060, 1988.

[174] Spicer, J.A., Rewcastle, G.W., Kaufman, M.D., Black, S.L., Plummer, M.S., et al. *4-Anilino-5-carboxamido-2-pyridone Derivatives as Noncompetitive Inhibitors of Mitogen-Activated Protein Kinase Kinase*. **J. Med. Chem**. 50, 5090-5102, 2007.

[175] Wurz, R.P., Pettus, L.H., Xu, S., Henkle, B., Sherman, L., et al. *Part 1: Structure–Activity Relationship (SAR) investigations of fused pyrazoles as potent, selective and orally available inhibitors of p38α mitogen-activated protein kinase*. **Bioorg. Med. Chem. Lett**. 19, 4724-4728, 2009.

[176] Suzuki, M., Morita, Y., Yanagisawa, A., Baker, B.J., Scheuer, P.J., Noyori, R. *Prostaglandin synthesis 15. Synthesis and structural revision of (7E)- and (7Z)-punaglandin 4*. **J. Org. Chem.** 53, 286-295, 1988.

[177] Liddle, S.T., Clegg, W. *Cation-induced structural variations in the alkali metal derivatives of 2-trimethylsilylaminopyridine: synthesis and X-ray structures of complexes for all five metals Li–Cs with 12-crown-4*. **J. Chem. Soc., Dalton Trans.** 402–408, 2001.

[178] Risto, M., Assoud, A., Winter, S.M., Oilunkaniemi, R., Laitinen, R.S., Oakley, R.T. *Heavy Atom Analogues of 1,2,3-Dithiazolylium Salts: Preparation Structures and Redox Chemistry*. **Inorg. Chem**. 47, 10100-10109, 2008.

[179] Smith III, A.B., Visnick, M., Haseltine, J.N., Sprengeler, P.A. *Organometallic reagents in synthesis: A new protocol for construction of the indole nucleus*. **Tetrahedron**. 42, 2957-2969, 1986.

[180] Dehe, D., Munstein, I., Reis, A., Thiel, W.R. *Mild Transition-Metal-Free Amination of Fluoroarenes Catalyzed by Fluoride Ions*. **J. Org. Chem**. 76, 1151–1154, 2011.

[181] Azuma, Y., Morone, M. Nagayama, K, Kawamata, Y., Sato, A. *Synthesis and reactions of 4-shloro-1,2-dihydro-6-methyl-2-oxo-3-pyridinecarbonitrile*. **Het**. 60, 1461-1468, 2003.

[182] Yamada, S., Misono, T., Iwai, Y., Masumizu, A., Akiyama, Y. *New Class of Pyridine Catalyst Having a Conformation Switch System: Asymmetric Acylation of Various sec-Alcohols.* **J. Org. Chem**. 71, 6872-6880, 2006.

[183] Brockman, M.A., Tanzi, G.O, Walker, B.D., Allen, T.M. *Use of a novel GFP reporter cell line to examine replication capacity of CXCR4- and CCR5-tropic HIV-1 by flow cyrometry*. **J Virol. Methods.** 131, 134-142, 2006.

[184] Chen, P., Hubner, W., Spinelli, M.A., Chen, B.K. *Predominant mode of human immunodeficiency virus transfer between T cells is mediated by sustained Env-dependent neutralization-resistant virological synapses.* **J. Virol.** 81, 12582–12595, 2007.

[185] Guava Nexin Annexin V Binding Assay for monitoring induction of apoptosis. *http://www.millipore.com/techpublications/tech1/mk107801* (accessed 12/20, 2011).

[186] Majno, G., Joris, I. *Apoptosis, oncosis, and necrosis: An overview of cell death*. **Am. J. Pathol**. 146, 3-15, 1995.

[187] van Heerde, W.L., de Groot, P.G., Reutelingsperger, C.P. *The complexity of the phospholipid binding protein Annexin V*. **Thromb. Haemostasis**. 73, 172-179, 1995.

[188] Koopman, G., Reutelingsperger, C.P., Kuijten, G.A., Keehnen, R.M., Pals, S.T., van Oers, M.H. *Annexin V for flow cytometric detection of phosphatidylserine expression on B cells undergoing apoptosis*. **Blood**. 84, 1415-1420, 1994.

[189] Martin, S.J., Reutelingsperger, C.E.M., McGahon, A.J., Rader, J.A., van Schieet, R.C.A.A., al. *Early redistribution of plasma membrane phosphatidylserine in a general feature of apoptosis regardless of the initiating stimulus: Inhibition by overexpression of Bcl-2 and Abl*. **J. Exp. Med**. 182, 1545-1556, 1995.

[190] van Engeland, M., Ramaekers, F.C., Schutte, B., Reutelingsperger, C.P. *A novel assay to measure loss of plasma membrane asymmetry during apoptosis of adherent cells in culture*. **Cytometry**. 24, 131-139, 1996.

[191] Schmidt, I., Krall, W.J., Uittenbogaart, C.H., Braun, J., Giorgi, J.V. *Dead cell discrimination with 7-amino-actinomycin D in combination with dual color immunofluorescence in single laser flow cytometry*. **Cytometry**. 13, 204-208, 1992.

[192] Elgazwy, A-S.S.H. The chemistry of isothiazoles. **Tetrahedron**. 59, 7445-7463, 2003.

[193] Strauss, M. *The nitroaromatic group in drug design. Pharmacology and toxicology (for nonpharmacologists).* **Ind. Eng. Chem. Prod. Res. Dev**. 18, 158-166, 1979.

[194] Lachman, A. *Benzophenone oxime*. **Org. Syn. Coll**. 2, 70.

[195] Chen, H., Shi, X., Shen, L. *Synthesis of 5-Fluorosalicylic Acid*. **Nat. Sci. J. Xiangtan University**. 32, 54-56, 2010.

[196] Lepore, S. D., Wiley, M. R. *Use of the Kaiser oxime resin in the solid-phase synthesis of 3-aminobenzisoxazoles*. **J. Org. Chem**. 64, 4547-4550, 1999.

[197] Lefebvre, V., Cailly, T., Fabis, F., Rault, S., *Two-step synthesis of substituted 3-aminoindazoles from 2-bromobenzonitriles*. **J. Org. Chem**. 75, 2730-2732, 2010.

[198] Maris C., Dominguez C., Allain, F.H. *The RNA recognition motif, a plastic RNA-binding platform to regulate post-transcriptional gene expression*. **FEBS. J**. 272**,** 2118–2131, 2005.

[199] Meshorer, E., Bryk, B., Toiber, D., Cohen, J., Podoly, E., Dori, A., Soreq, H. *SC35 promotes sustainable stress-induced alternative splicing of neuronal acetylcholinesterase mRNA*. **Molec. Psych**. 10, 985-997, 2005.

[200] Kielkopf CL, Rodionova NA, Green MR, Burley SK. *A novel peptide recognition mode revealed by the X-ray structure of a core U2AF35/U2AF65 heterodimer*. **Cell**. 106:, 595–605, 2001.

Appendices

A: SRSF1 structural information

Tintaru *et al* investigated the binding properties of RNA and RRM2 using nuclear magnetic resonance spectroscopy and discovered the 'fold' has a lot of homology with typical RRMs, as well as a four-stranded β-sheet packed against two helices.[198] Loop 5, when compared with other RRMs, appeared to have a longer two-stranded β-sheet (**figure 43**).[77]

Separately, Meshorer *et al* compared the RRM of SRSF1 and SRSF2, another SR protein, and discovered strong homology between them with the exception of a cluster of four proline residues in the extended region protruding from the domain (**figure 44**).[199] Within RRMs, a polyproline segment is known as a protein–protein interaction motif necessary during spliceosome assembly.[200] The entire 3D protein structure of SRSF1 has not been determined.

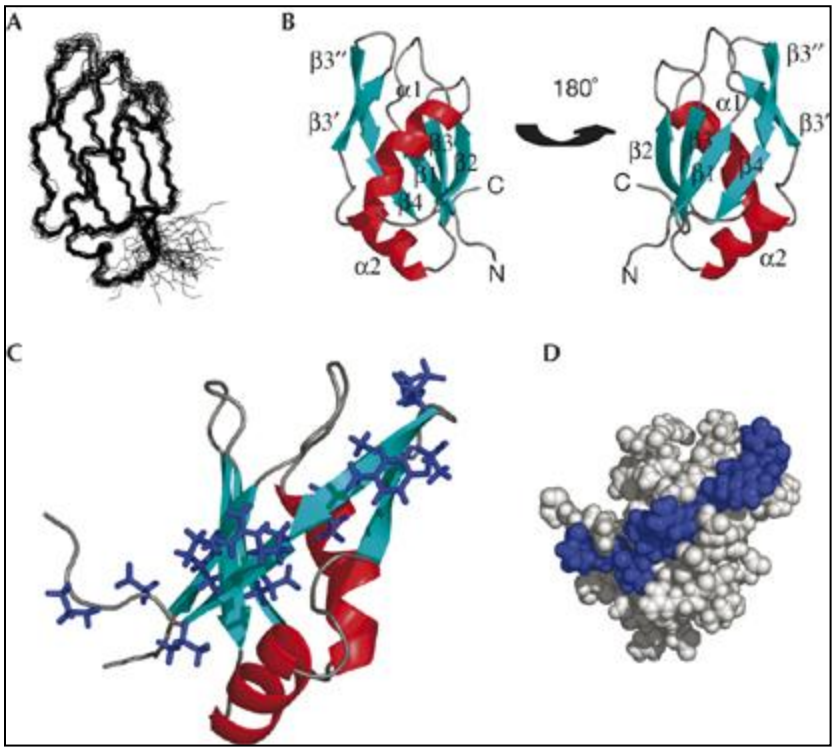

Figure 43. Structure of SRSF1 RNA-recognition motif 2. (A) Superposition of the 20 lowest energy structures of SRSF1 RRM2 (amino acids 107–215). (B) Ribbon representation of SRSF1 RRM2 shown in two orientations. (C) SRPK1 docking motif (blue side chains) highlighted on the RRM2 structure. (D) Space-filled model of RRM2 showing the SRPK1 docking motif in blue. RRM2, RNA-recognition motif 2; SRSF1, splicing factor 2/alternative splicing factor; SRPK1, serine/arginine-rich protein kinase 1. Reprinted by permission from Macmillan Publishers Ltd: EMBO J. "Structural and functional analysis of RNA and TAP binding to SF2/ASF." Tintaru, A. M., et al. 8, p. 757, copyright 2007.

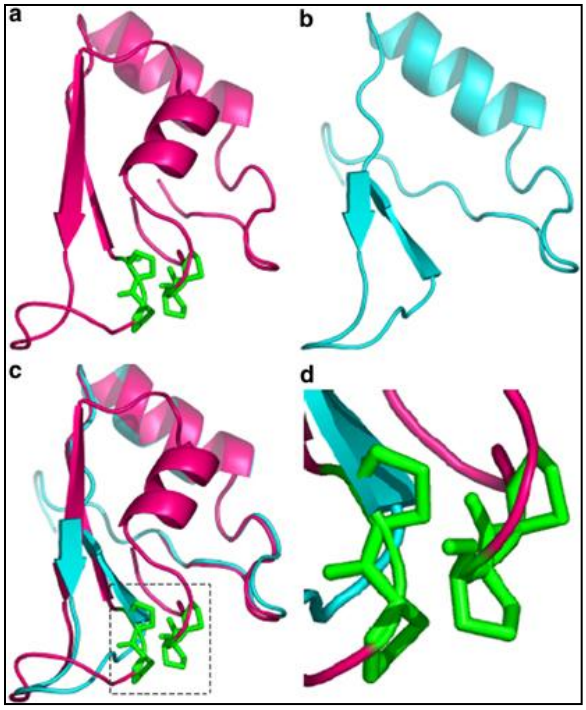

Figure 44. Molecular modeling of SRSF2 and SRSF1 structures. (a) Molecular modeling of SRSF1 structure. (b) Molecular modeling of SRSF2 structure. (c) Superimposition of SRSF1 (red) and SRSF2 (blue) structures. Note the strong similarity, with the exception of the four prolines cluster (green). (d) Enlargement of the proline cluster of SRSF1, shown as dashed square in panel c. Reprinted by permission from Macmillan Publishers Ltd: Molec. Psych. Meshorer, E., et al. SC35 promotes sustainable stress-induced alternative splicing of neuronal acetylcholinesterase mRNA. 10, p. 994, copyright 2005.

B: Duplicate HIV-1 screen of molecules C8 and E5

Table 2: Summary of results for secondary screen of active molecules. The statistics for compounds C8 and E5 using their initial and second HIV-1 test data. The average % inhibition and its standard deviation and the average % of HIV infected cells and its standard deviation were calculated.

plate 1	% of infected cells	% inhibition	Average % inhibition	Standard Deviation
DMSO	51.81			
AZT	7.898	84.75583864	87.48095437	3.853896
C8	15.616	69.85910056	67.31559575	3.597059
E5	18.008	65.24223123	59.59082107	7.992301
plate 2			**Average % inhibition**	**Standard Deviation**
DMSO	35.716			
AZT	3.498	90.20607011	87.48095437	3.853896
C8	12.582	64.77209094	67.31559575	3.597059
E5	16.451	53.93941091	59.59082107	7.992301

	Average % of HIV infected Cells	Standard Deviation
DMSO	43.763	11.38018
AZT	5.698	3.11127
C8	14.099	2.145362
E5	17.2295	1.100965

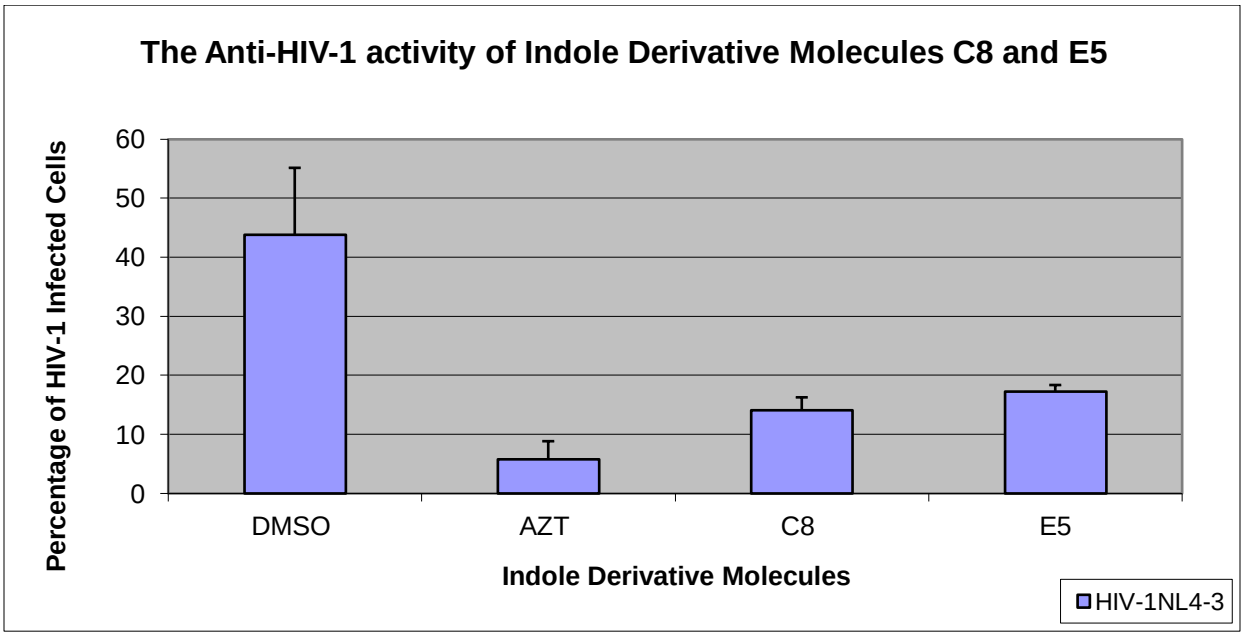

Figure 45: The anti-HIV-1 activity of indole derivative molecules C8 and E5. The average percentage of HIV-1 infected cells of compounds C8 and E5 are compared to the positive and negative controls, AZT and DMSO, respectively.

C: Effect of DMSO on HIV-1 infectivity assay

Table 3: Measure of effect of DMSO on HIV-1 infectivity assay. The percentage of infected cells was measured using different volumes of DMSO.

Amount of DMSO	Percentage of infected cells
NL4-3 only	70.6095
DMSO 50ul	50.6869
DMSO 35ul	57.9112
DMSO 25ul	62.7419
DMSO 12.5ul	69.5048
DMSO 6.25ul	69.6429
DMSO 3ul	69.6869
GXR-5 only	0.0536385

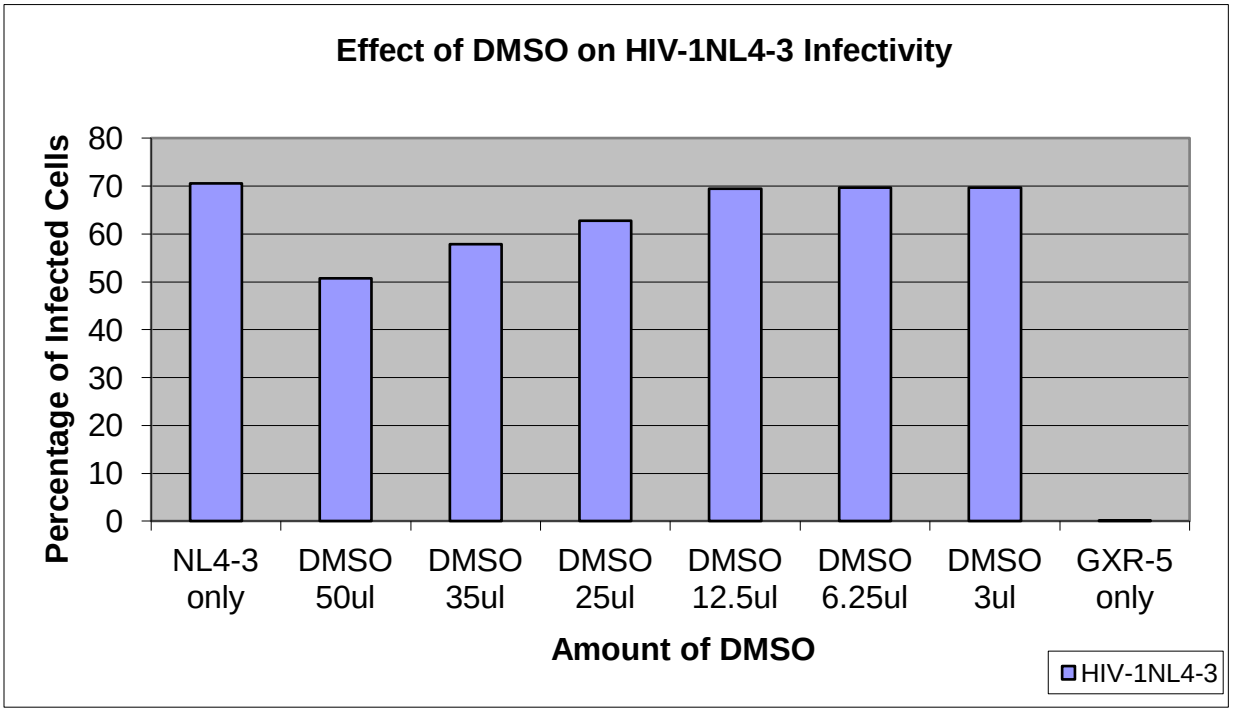

Figure 46: Effect of DMSO on HIV-1NL4-3 infectivity. The percentage of infected cells was measured using different volumes of DMSO and compared to the HIV-1 strain NL4-3.

D: HIV-1 resistant strains profile

E00443_v,
Seq ID: E00443_v

NRTI Resistance Mutations: D67N, T69D, K70R, V75I, F77L, Y115F, F116Y, Q151M, M184V, T215V, K219Q

NNRTI Resistance Mutations: K103N, V108I, K238T

Nucleoside RTI
lamivudine (3TC) High-level resistance
abacavir (ABC) High-level resistance
zidovudine (AZT) High-level resistance
stavudine (D4T) High-level resistance
didanosine (DDI) High-level resistance
emtricitabine (FTC) High-level resistance
tenofovir (TDF) High-level resistance

Non-Nucleoside RTI
delavirdine (DLV) High-level resistance
efavirenz (EFV) High-level resistance
etravirine (ETR) Potential low-level resistance
nevirapine (NVP) High-level resistance

E00435_v
Seq ID: E00435_v

NRTI Resistance Mutations: None
NNRTI Resistance Mutations: K103N

Nucleoside RTI

lamivudine (3TC) Susceptible
abacavir (ABC) Susceptible
zidovudine (AZT) Susceptible
stavudine (D4T) Susceptible
didanosine (DDI) Susceptible
emtricitabine (FTC) Susceptible
tenofovir (TDF) Susceptible

Non-Nucleoside RTI

delavirdine (DLV) High-level resistance
efavirenz (EFV) High-level resistance

etravirine (ETR) Susceptible
nevirapine (NVP) High-level resistance

RT Comments
NNRTI
K103N causes high-level resistance to NVP, DLV, and EFV.

E00476_v
Seq ID: E00476_v

NRTI Resistance Mutations: L74LV, T215DY
NNRTI Resistance Mutations: Y181C

Nucleoside RTI
lamivudine (3TC) Susceptible
abacavir (ABC) Intermediate resistance
zidovudine (AZT) Intermediate resistance
stavudine (D4T) Intermediate resistance
didanosine (DDI) High-level resistance
emtricitabine (FTC) Susceptible
tenofovir (TDF) Low-level resistance

Non-Nucleoside RTI
delavirdine (DLV) High-level resistance
efavirenz (EFV) Intermediate resistance
etravirine (ETR) Intermediate resistance
nevirapine (NVP) High-level resistance

E: HIV-1 dose-response experimental values

Table 4: HAART resistant strain experiment. Experimental values for HIV-1 inhibition experiment using HAART resistant HIV-1 strains (figure 32).

Strain and Compound Added	% HIV-1 Infected Cells
443A-clone DMSO	33.8394
443A-clone 0.1uM AZT	29.4883
443A-clone 1uM AZT	29.9012
443A-clone 2uM AZT	26.4178
443A-clone C8	4.3575
443A-clone E5	15.9588
443A-clone C2	17.905
443A-clone D3	28.5674
476a-clone DMSO	12.0845
476a-clone 0.1uM AZT	5.80613
476a-clone 1uM AZT	5.17092
476a-clone 2uM AZT	4.0431
476a-clone C8	1.69868
476a-clone E5	5.66667
476a-clone C2	6.99957
476a-clone D3	13.4495
435a-clone DMSO	16.0659
435a-clone 0.1uM AZT	5.24706
435a-clone 1uM AZT	3.84658
435a-clone 2uM AZT	4.70451
435a-clone C8	1.82039
435a-clone E5	6.87265
435a-clone C2	8.21966
435a-clone D3	14.5956